The Impact of Glucocorticoids upon the Insulin Sensitivity of Skeletal Muscle

By

Stuart Andrew Morgan

A thesis submitted to The University of Birmingham for the degree of

DOCTOR OF PHILOSOPHY

School of Clinical and Experimental Medicine

College of Medical and Dental Sciences

The University of Birmingham

January 2010

Table of Contents

List of Figures

List of Tables

Abstract

Glucocorticoid (GC) excess is characterised by central obesity, hypertension, proximal myopathy, insulin resistance and in some cases overt type 2 diabetes (T2D). However, the precise molecular mechanisms responsible for these observation have not been defined in detail.

We have shown that GCs reduce the insulin sensitivity of skeletal muscle by impacting upon the insulin signalling cascade at several critical points: IRS1, PI3K and AS160. Furthermore, we have described a novel role of GC, and GCs with insulin, in the regulation of intramyocellular lipid metabolism, which may underpin GC-induced insulin resistance in this tissue.

We have also highlighted the importance of 11β-hydroxysteroid dehydrogenase type 1 (11β-HSD1), which controls local GC availability, as a critical regulator of skeletal muscle insulin sensitivity, and have provided new insight into the insulin sensitizing actions of selective 11β-HSD1 inhibitors.

In summary, these data highlight the importance of GCs, and pre-receptor GC metabolism in the regulation of lipid metabolic pathways and response to insulin stimulation in skeletal muscle.

Abbreviations

4EBP1	Eukaryotic translation initiation factor 4E binding protein-1
11β-HSD1	11beta-hydroxysteroid dehydrogenase type 1
11β-HSD2	11beta-hydroxysteroid dehydrogenase type 2
11DHC	11-dehydrocortocosterone
A	11-dehydrocortocosterone
A1	AstraZeneca's selective 11β-HSD1 inhibitor-1
A2	AstraZeneca's selective 11β-HSD1 inhibitor-2
ACC	Acetyl-CoA carboxylase
ACTH	Adrenocorticotropic hormone
ADP	Adenosine diphosphate
Akt	Protein kinase B
AME	Apparent mineralocorticoid excess syndrome
AMP	Adenosine monophosphate
AMPK	AMP-dependent protein kinase
AS160	Akt substrate of 160kDa
AU	Arbitrary units
ATF	Activating transcription factor
ATGL	Adipose triglyceride lipase
ATP	Adenosine triphosphate
AUC	Area under curve
B	Corticosterone
BSA	Bovine serum albumin
BMI	Body mass index
cAMP	Cyclic adenosine monophosphate
CREBP	cAMP response element-binding protein

CBP	CREB binding protein
cDNA	Complementary deoxyribonucleic acid
CORT	Corticosterone
CPM	Counts per minute
CPT	Carnitine palmitoyltransferase
CRH	Corticotropin-releasing hormone
Ct	Cycle threshold
Cyclo B	Cyclophilin B
DAG	Diacylglycerol
DEX	Dexamethasone
DGAT	Diacylglycerol acyltransferase
DGK-δ	Diacylglycerol kinase-delta
DHEA	Dehydroepiandrosterone
DIO	Diet-induced obese
DMEM	Dulbecco's modified eagle medium
DNA	Deoxyribonucleic acid
DPM	Disintegrations per minute
E	Cortisone
ECL	Enhanced chemiluminescence
ER	Endoplasmic reticulum
ERK	Extracellular signal-regulated kinase
FABP	Fatty acid binding protein
FGF	Fibroblast growth factor
eIF2B	Eukaryotic initiation factor 2B
F	Cortisol
FAS	Fatty acid synthase
FAT/CD36	Long-chain fatty acid transporter

FCS	Foetal calf serum
FFA	Free fatty acids
FOXO	Forkhead transcription factors
G3PDH	Glyceraldehyde-3-phosphate dehydrogenase
G6P	Glucose-6-phosphate
G6Pase	Glucose-6-phosphatase
GC	Glucocorticoid
GE	Glycyrrhetinic acid
Glu	Glucose
GLUT	Glucose transporter
GR	Glucocorticoid receptor
GRE	Glucocorticoid response element
GS	Glycogen synthase
GSK	Glycogen synthase kinase
GTP	Guanosine triphosphate
GTT	Glucose tolerance test
H6PDH	Hexose-6-phosphate dehydrogenase
HOMA	Homeostasis model assessment
HPA	Hypothalamic-pituitary-adrenal axis
HRP	Horse radish peroxidase
HS	Horse serum
HSL	Hormone sensitive lipase
HSP	Heat shock protein
IGF	Insulin-like growth factor
IKKβ	Inhibitor of NF-κB kinase
IL-6	Interleukin-6
IMTG	Intramyocellular triglyceride

Ins	Insulin
InsR	Insulin receptor
IRS	Insulin receptor substrate
IP	Intraperitoneal
JNK	Jun N-terminal kinase
KRB	Kreb’s ringer buffer
LDL	Low-density lipoprotein
LPL	Lipoprotein lipase
MAG	Monoacylglycerol
MAPK	Mitogen-activated protein kinase
MC4R	Melanocortin-4 receptor
MHC	Myosin heavy chain
MODY	Maturity onset diabetes of the young
MR	Mineralocorticoid
MRF	Myogenic regulatory factors
mRNA	Messenger RNA
mTOR	Mammalian target of rapamycin
MuRF	Muscle specific ring finger protein
MyoG	myogenin
NAD	Nicotinamide adenine dinucleotide
NADP	Nicotinamide adenine dinucleotide phosphate
p70S6K	Ribosomal protein S6 kinase
PAGE	Polyacrylamide gel electrophoresis
PAI-1	Plasminogen activator inhibitor-1
PBS	Phosphate buffered saline
PCR	Polymerase chain reaction
PDE3B	Phosphodiesterase-3B

PDK	Pyruvate dehydrogenase kinase
PEPCK	Phosphoenolpyruvatecarboxy kinase
PH	Pleckstrin homology domain
PHLPP	PH-domain leucine-rich repeat protein phosphatase
PI3K	Phosphoinositide 3-kinase
PIP2	Phosphatidylinositol-4,5-bisphosphate
PIP3	Phosphatidylinositol-3,4,5-triphosphate
PKA	Protein kinase A
PKB	Protein kinase B
PKC	Protein kinase C
PMA	Phorbol 12-myristate 13-acetate
PP2A	Protein phosphatase-2A
PPAR	Peroxisome proliferator-activated receptor
PTB	Phosphotyrosine binding domain
PTEN	Phosphatase and tensin homolog
RNA	Ribonucleic acid
rRNA	Ribosomal ribonucleic acid
RT-PCR	Real-time polymerase chain reaction
SCD	Stearoyl-CoA desaturase
SDS	Sodium dodecyl sulfate
SH2	Src homology 2 domain
SH3	Src homology 3 domain
SiRNA	Small interfering ribonucleic acid
SOCS	Suppressor of cytokine signalling
SPT	Serine palmitoyl-CoA transferase
SRC1	Steroid receptor coactivator-1
SREBP1	Sterol regulatory element-binding protein-1

StAR	Steroidogenic acute regulatory protein
T2D	Type 2 diabetes
TAG	Triacylglycerol
TC	Tissue culture
THE	Tetrahydrocortisone
THF	Tetrahydrocortisol
TNFα	Tumour necrosis factor-alpha
TRB3	Tribbles homolog-3
TSC	Tuberous sclerosis complex
TZD	Thiazolidinedione
VLDL	Very low-density lipoprotein
WAT	White adipose tissue
WHO	World health organization

Chapter 1- General Introduction

1.1. Type 2 diabetes – an emerging pandemic

Type 2 diabetes is an endocrine disorder characterised by elevated plasma glucose levels, caused by peripheral insulin resistance. Insulin resistance is defined as the inability of a normal amount of insulin to bring about an adequate response from the liver, adipose and skeletal muscle in terms of stimulating glucose uptake and suppressing glucose production (Yalow & Berson, 1960). Insulin resistance precedes the development of type 2 diabetes, and in this 'pre-diabetic' state the pancreatic β-cells attempt to compensate for peripheral insulin resistance by upregulating insulin secretion to maintain blood glucose levels within the normal range (Efendic et al., 1988). Type 2 diabetes ensues when the levels of insulin secreted by the β-cells fails to keep blood glucose levels under control - leading to the development of hyperglycaemia. Hyperglycaemia in turn leads to glucose toxicity which causes further β-cell dysfunction and impaired insulin secretion - exacerbating the problem (Robertson, Olson & Zhang, 1994).

A study published in 2004 found that the prevalence of type 2 diabetes among all age groups worldwide was 2.5% in the year 2000, and this figure is estimated to rise to 4.4% by 2030 (Wild et al., 2004). The total number of people living with type 2 diabetes is expected to increase from 171 million in 2000 to 366 million by 2030 (Wild et al., 2004). These figures are likely to represent an underestimate. In addition, there is a worrying increase in the number of children and young adults effected with type 2 diabetes (Ehtisham et al., 2004). It appears that increasing levels of obesity, arising from energy-rich diets, and an increasing sedentary lifestyle are driving this global pandemic. However, it is estimated that the

prevalence of diabetes will continue to rise even if obesity levels remain constant (Wild et al., 2004).

Type 2 diabetic subjects have a high standardised mortality ratio (SMR) of 4.47, in age and sex matched populations (SMR= the ratio of observed deaths to expected deaths) (de Marco et al., 1999; Mulnier et al., 2006). As well as increased mortality, there is a dramatic effect upon morbidity. The morbidities associated with type 2 diabetes are wide ranging and include: microvascular complications (damage to small blood vessels) leading in turn to damage to the retina (retinopathy), kidney (nephropathy) and nerves (neuropathy); macrovascular complications (damage to the larger arteries) leading in turn to damage to brain (stroke), heart (coronary heart disease) or to the legs and feet (peripheral vascular disease) (Luan, 2009).

Type 2 diabetes not only has a negative impact upon health, but is also a massive economic burden. For example, figures from the Unites States show that type 2 diabetes accounts for ~$100bn in healthcare expenditure each year. In Britain, the charity Diabetes UK estimated this figure is around £9bn. The associated complications of type 2 diabetes accounts for the majority of this expenditure.

1.2. Genetic and environmental causes of type 2 diabetes

Type 2 diabetes is a polygenic disease caused by the complex interplay between genes and the environment. In most cases the disease is acquired in genetically susceptible individuals. The most important susceptibility gene identified to date is TCF7L2 (Grant et al., 2006). Several type 2 diabetes-associated single nucleotide polymorphisms (SNPs) have been identified in this gene, which encodes a transcription factor involved in secretion of glucagon-like-peptide from the gut - essential for pancreatic β-cell function (da Silva Xavier et al., 2009). TCF7L2 joins a short list of genes associated with type 2 diabetes including: PPARγ (Pro12Ala SNP), which encodes a nuclear receptor primarily involved in adipogenesis (Altshuler et al., 2000); KCNJ11 (Glu23Lys SNP) which encodes a pancreatic β-cell K_{ATP} channel subunit (Gloyn et al., 2003). In addition SNPs in wnt signalling genes are strongly associated with T2D, proposed to play a role in pancreatic development, these include: CCND2, a G1/S phase specific cyclin; SMAD3, a signal transducer and PRICKLE1, a nuclear receptor (Perry et al., 2009). It appears that many of the genetic susceptibilities relate to pancreatic β-cell development and insulin secretion, and work in concert with environmental factors, which includes poor diet, increased sedentary lifestyle and obesity, to trigger the development of type 2 diabetes.

In addition to the multifactorial form of diabetes described above, rarer monogenic forms occur. These are a consequence of a single base pair mutation / exchange and include neonatal diabetes mellitus (Gloyn et al., 2004) and maturity-onset diabetes of the young (MODY) (Pearson et al., 2005). To date, 6 forms of MODY

have been identified, one a consequence of mutated glucokinase (MODY2) and the other forms result from mutations in various transcription factors e.g. HNF-1α, HNF-4α, HNF-1β, IPF-1 and NeuroD (MODY 1,3,4,5,6, respectively) (Gerard, 2005). The severity of this disease varies depending upon the gene mutated e.g. MODY2 has a relatively benign clinical evolution, whereas MODY3 is characterized by severe defects in insulin secretion and hyperglycaemia, progressing quickly to become overt diabetes (Velho et al., 1996).

1.3. Insulin resistance and the metabolic syndrome

The metabolic syndrome (syndrome X) is defined as a cluster of cardiovascular risk factors. In 1988 Dr. Gerald Reaven noticed that people with cardiovascular disease also presented with hypertension, glucose intolerance, hyperinsulinaemia, hypertriglyceridemia and elevated high density lipoprotein (HDL) cholesterol. Raven postulated that insulin resistance was the driving force behind this cluster of cardiovascular risk factors (Reaven, 1988). However, in the preceding years the precise criteria for accurately diagnosing this syndrome has been subject of much controversy, and therefore several organisations have published contrasting definitions.

In 1998, the first set of criteria was published by the World Health Organisation (WHO), based upon the assumption that insulin resistance is the underlying abnormality. Furthermore, this definition requires the presence of two additional risk factors from: central obesity, hypertension, hypertriglyceridemia or

microalbuminuria (Alberti & Zimmet, 1998) (Table1-1). The Adult Treatment Panel (ATP) III criteria was designed to facilitate diagnosis in clinical practice and consequently a measure of insulin sensitivity, which is not normally used in routine practice, was not included. The ATP III guidelines state that metabolic syndrome may be diagnosed when a patient presents with three or more of five identifiable risk factors. These include abdominal obesity, hypertriglyceridemia, hypertension, low HDL cholesterol and fasting hyperglycaemia. Importantly, in the ATP III criteria waist circumference is used to assess central obesity, whereas WHO uses the waist-to-hip ratio (ATPIII, 2001). In 2005, the International Diabetes Federation (IDF) attempted to come up with a unifying set of criteria for diagnosis. The main focus in this definition is central obesity, defined on the basis of waist circumference, and two or more of the following factors: hypertriglyceridemia, reduced HDL cholesterol, hypertension and fasting hyperglycaemia (Lawlor, Smith & Ebrahim, 2006) (Table1-1).

	WHO (insulin resistance plus two others	ATP III (three of the following)	IDF (central obesity plus two others)
Obesity	WHR >0.9 (men WHR >0.85 (women) BMI >30kg/m^2	Waist circ >102cm (m) Waist circ >88cm (w)	Waist circ ≥94cm (m) Waist circ ≥80cm (w)
Hypertriglycerideaemia	≥1.7mmol/L	≥1.7mmol/L	≥1.7mmol/L
Low HDL cholesterol	<0.9mmol/L(m) <1.0mmol/L (w)	<1.036mmol/L(m) <1.295mmol/L (w)	<1.03mmol/L (m) <1.29mmol/L (w)
Hypertension	≥140/90mmHg (or on antihypertensives)	≥130/85mmHg (or on antihypertensives)	≥130/85mmHg (or on antihypertensives)
Fasting hyperglycaemia	IGT, IFG, Insulin resistance, diabetes	≥ 6.1mmol/L	≥ 5.6mmol/L Or type 2 diabetes
Microalbuminuria	Urinary albumin: creatinine ratio 30mg/g, or albumin excretion rate >20μg/min		

Table 1-1 Metabolic syndrome definitions

Insulin resistance has been identified in the majority of people diagnosed with the metabolic syndrome. Therefore, it has been proposed that insulin resistance is the primary abnormality giving rise to: impaired glucose tolerance, dyslipidaemia, hypertension, type 2 diabetes, blood vessel endothelial dysfunction – all of which collectively lead to cardiovascular disease (Reaven, 1988) Moreover, the degree of insulin resistance is positively correlated with the number of features of the syndrome (Cruz et al., 2004), however, others have suggested that vascular endothelial dysfunction causes hypertension, glucose intolerance and insulin resistance (Pinkney et al., 1997). Also, there is evidence that the association between insulin resistance and the other components of the metabolic syndrome is a consequence of them being common outcomes of a state of low grade inflammation (Yudkin et al., 1999). In conclusion, although insulin resistance appears to be integral to the metabolic syndrome, its precise role has not been clarified to date.

1.4. Insulin

Insulin is a peptide hormone synthesised by the pancreatic β-cells. High blood glucose stimulates its release into the blood where it acts on peripheral tissues to increase glucose uptake, suppress hepatic glucose production and prevent lipolysis.

1.4.1. Insulin structure and synthesis

Insulin gene transcription is normally restricted to the pancreatic β-cells within the islets of Langerhans. Insulin mRNA is translated on ribosomes attached to the endoplasmic reticulum (ER) as a single polypeptide precursor called preproinsulin (Figure 1-1). Structurally, preproinsulin consists of four domains: a C-terminal A-chain; an N-terminal B-chain; a connecting region known as the C-peptide; and an N-terminal signal peptide (Sanger, 1959). The signal peptide anchors preproinsulin to the membrane of the ER (Walter & Johnson, 1994). The ER lumen is a highly oxidising environment, which facilitates the formation of two disulphide bridges between the A and B chains of preproinsulin. Cleavage of the signal peptide releases proinsulin into the ER lumen where it is transported to the golgi complex, and subsequent cleavage of the C-peptide yields the mature 5808kDa dipeptide hormone (Patzelt et al., 1978). Insulin is then transported out of the golgi and accumulates in secretary granules in the cytoplasm.

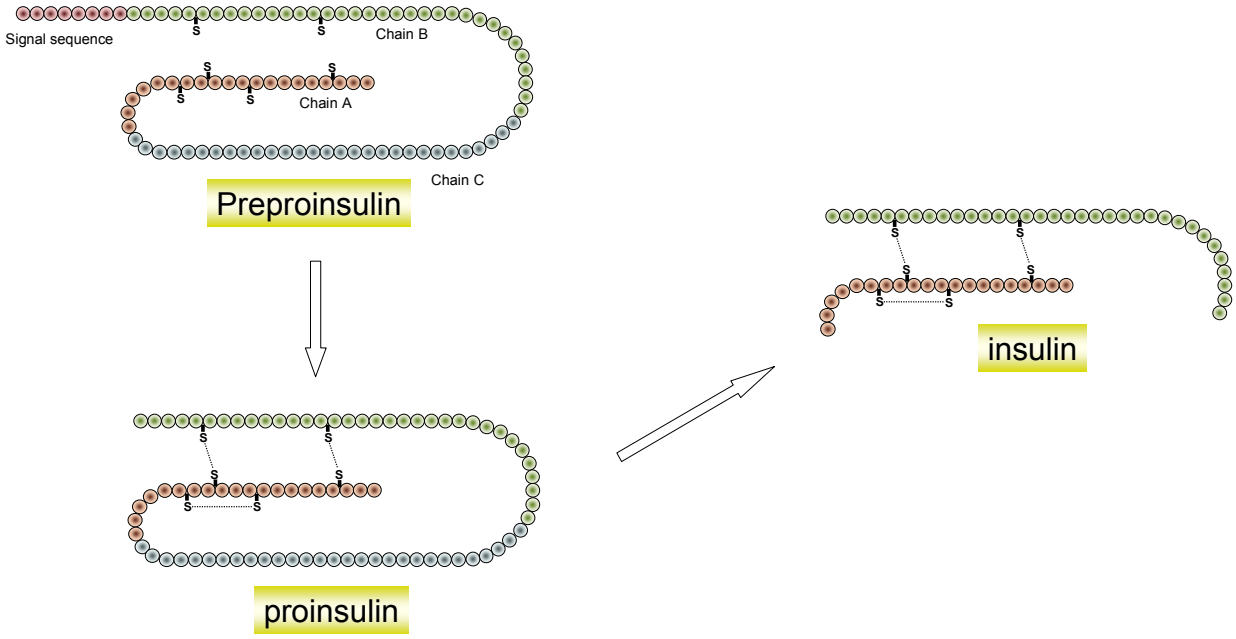

Figure 1-1 The major steps of insulin synthesis in pancreatic β-cells.

1.4.2. Insulin secretion

Insulin secretion is enhanced by a number of stimuli including: glucose (Maske, 1954), amino acids (Floyd et al., 1966) and gastrointestinal hormones such as secretin and glucagon-like peptide-1 (GLP-1) (Chisholm, Young & Lazarus, 1969). Since the primary role of insulin is to control glucose homeostasis, glucose is the most important of these stimuli. Glucose induces a bi-phasic pattern of insulin release from the β-cells. Shortly following glucose stimulation, a transient spike in insulin secretion is observed, this is followed by a more enduring phase of insulin release (Ma et al., 1995). The mechanism by which glucose stimulates insulin secretion is as follows: high circulating glucose diffuses into the β-cells through GLUT2 transporters (Figure 1-2) (Thorens et al., 1988). Within the cytosol, glucose is metabolised through glycolysis generating pyruvate which is further metabolised in the mitochondria generating ATP. The elevated ATP/ADP

ratio induces closure of cell-surface ATP-sensitive K^+ channels - preventing K^+ from leaving the cell, leading to cell membrane depolarization (Ashcroft & Rorsman, 1989; Theler et al., 1992). This in turn leads to an opening of membrane bound voltage-gated Ca^{2+} channels, resulting in an influx of Ca^{2+} into the cytosol (Curry, Bennett & Grodsky, 1968; Theler et al., 1992). The increased cytosolic Ca^{2+} signals exocytosis of storage vesicles containing insulin (Figure 1-2) (Bokvist et al., 1995).

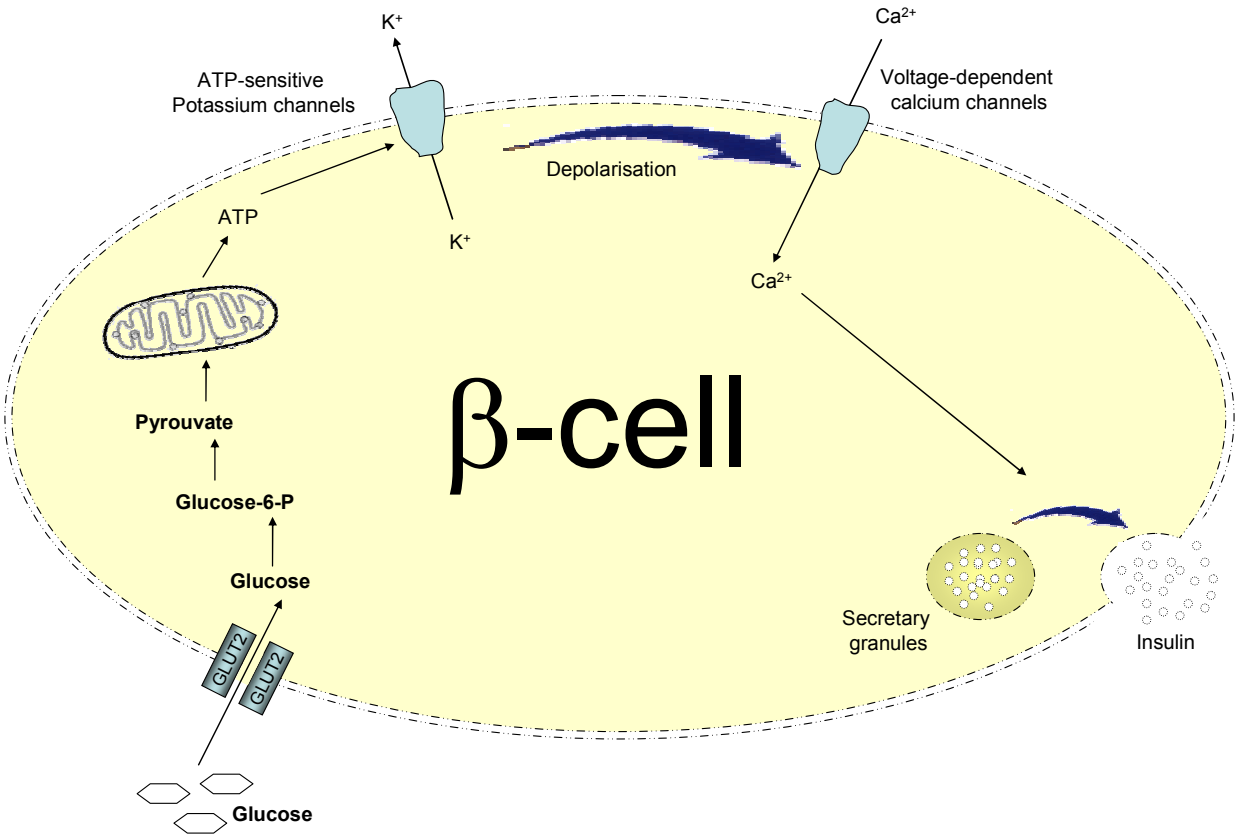

Figure 1-2 Schematic representation of the processes leading to insulin secreting in pancreatic β-cells.

During stress (defined as trauma, sepsis, emotion, starvation) adrenal secretion of GCs and adrenaline increases, which has the action of inhibiting insulin secretion from pancreatic β-cells (Yamazaki, Katada & Ui, 1982).

1.5. Metabolic actions of insulin

Insulin is an anabolic hormone, important during times of nutrient excess; promoting energy storage and decreasing energy release (in the form of glucose from the liver and fatty acids and glycerol from adipose tissue). In the following sections, an overview of the effects of insulin upon metabolism will be addressed - more detailed discussions are dealt with in later sections.

1.5.1. Carbohydrate metabolism

The most important insulin target tissues are the liver, adipose tissue and the skeletal muscle. In the fed state, when circulating glucose levels are elevated, insulin enhances glucose uptake by the adipose tissue and skeletal muscle (Czech & Corvera, 1999). Insulin also upregulates glucose storage, by increasing glycogen synthesis in these tissues (Chiasson et al., 1980; Lawrence, Guinovart & Larner, 1977)

In the fasted state, the liver synthesizes glucose via gluconeogenesis from precursors such as glycerol, lactate and amino acids. Glucose is also liberated by hydrolysis of hepatic glycogen stores. During the transition to the fed state insulin effectively inhibits both hepatic gluconeogenesis and glycogenolysis, consistent

with its role as an anabolic effector (Chiasson et al., 1976).

1.5.2. Protein metabolism

Since insulin signals that energy is abundant, with regards to protein metabolism it acts to increase amino acid uptake from the circulation (Elsas, Albrecht & Rosenberg, 1968), and incorporation into proteins (Proud & Denton, 1997), whilst inhibiting protein breakdown (Tischler et al., 1997). This occurs most notably in tissues where protein content is high, e.g. skeletal muscle.

1.5.3. Lipid metabolism

Insulin promotes lipid storage by increasing lipogenesis - the *de novo* synthesis of fatty acids (Wolfrum et al., 2004; Zhang, Yin & Hillgartner, 2003). *De novo* lipogenesis occurs predominantly in adipose tissue, liver and to a lesser extent in the skeletal muscle. Insulin also enhances uptake of fatty acid (Chabowski et al., 2004), and their esterification with glycerol generating triacylglycrides (TAG) (Dyck, Steinberg & Bonen, 2001). During fasting (in the presence of low insulin), TAG stores are broken down by lipolysis, and the resultant free fatty acids are oxidised in the mitochondria yielding ATP. In addition, some of these TAG-derived fatty acids (particularly from liver) are released into the circulation as lipoproteins, which are utilised as an energy source by other tissues, including the skeletal muscle. During the fed state, insulin inhibits lipolysis (Degerman et al., 1998) and fatty acid oxidation (Park et al., 1995), instead promoting the use of carbohydrates as a source of energy.

1.6. Insulin signalling

1.6.1. Insulin receptor

The actions of insulin are mediated through activation of cell surface receptors, in particular the insulin receptor (InsR), but also the closely related insulin-like growth factor receptor (IGF-IR) (Figure 1-3). InsR mediates metabolic regulation whereas IGF-IR is involved in normal growth and development. Both receptors can bind insulin, however, the binding affinity of IGF-IR for insulin is ~100-fold lower than for its cognate ligand, IGF-I (Andersen et al., 1992). InsR is a disulphide-linked heterotetrameric structure, composed of two identical extracellular α-subunits, and two identical transmembrane β-subunits that have tyrosine kinase activity (Bajaj et al., 1987). Upon binding of insulin to the α-subunits, the receptor undergoes a conformational change leading to activation of the kinase domain resulting in auto-phosphorylation of specific tyrosine residues on the β-subunit (Cann & Kohanski, 1997; Hubbard et al., 1994).

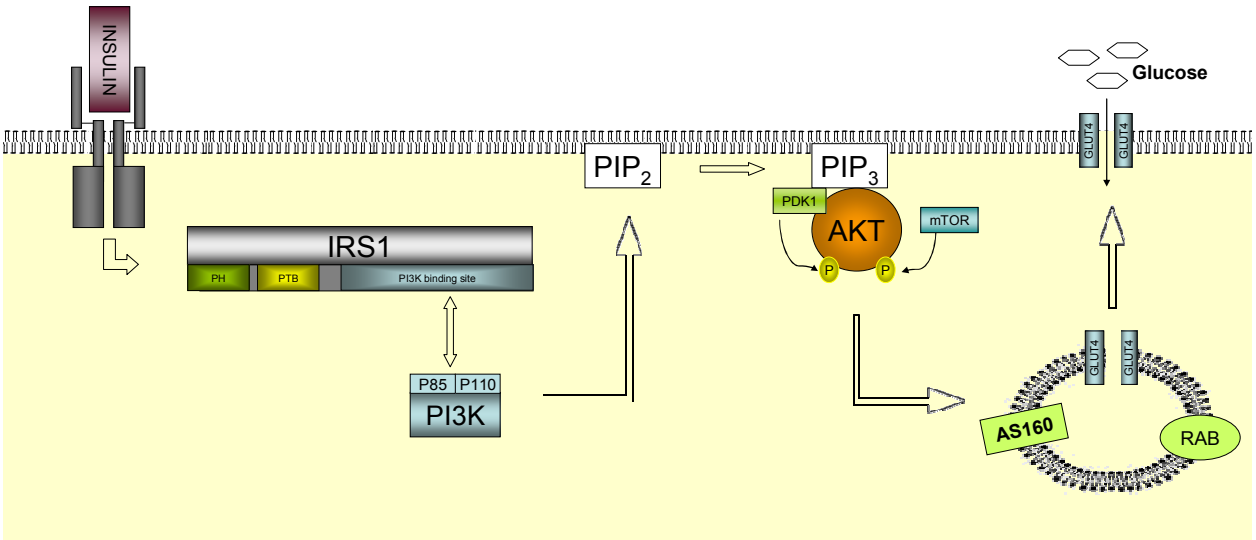

Figure 1-3 The insulin signalling cascade.

1.6.2. Insulin receptor substrates

Upon activation by insulin, the auto-phosphorylated tyrosine residues on InsR act as docking sites for numerous proteins including the family of insulin receptor substrate (IRS) proteins (Figure 1-3). To date, six IRS isoforms have been identified (IRS1-6). IRS1 and IRS2 are ubiquitously expressed, and are most important in mediating metabolic signal transduction (Araki et al., 1994; Fantin et al., 2000; Liu et al., 1999; Withers et al., 1998), whereas the expression of IRS3 is limited to brain and adipocytes (Lavan, Lane & Lienhard, 1997) and IRS4 is expressed primarily in embryonic tissue (Fantin et al., 1998). IRS5 and IRS6 have limited expression and function in signal transduction (Cai et al., 2003). Structurally, IRS proteins share a high degree of homology; each containing an N-terminal pleckstrin-homology (PH) domain for phospholipid binding; a phospho-tyrosine-binding (PTB) domain for docking with phospho-tyrosine sites on activated InsR; and a variable C-terminal region containing numerous tyrosine, threonine and serine phosphorylation sites which confers IRS activity (Sun et al., 1991). The association between IRS1/2 and the activated InsR allows the kinase domain of the receptor to phosphorylate various tyrosine residues within the C-terminal of these proteins (White, Maron & Kahn, 1985). This allows IRS1/2 to act as an adaptor; linking InsR to various src-homology 2 (SH2) domain containing proteins. For example, phosphorylation of IRS1 at tyrosine-612 and 632 (corresponding to 608 and 628 in rodents) is required for full activation of phosphoinositide-3 kinase (PI3K) (Esposito et al., 2001). IRS activating tyrosine phosphorylation is negatively regulated by the phosphatase SHP2; attenuating the metabolic actions of insulin (Myers et al., 1998) (Figure 1-3).

In addition to tyrosine phosphorylation, IRS proteins also undergo serine phosphorylation (Figure 1-4). With over 70 putative serine phosphorylation sites, IRS1 is by far the most characterised isoform. As a general rule, serine phosphorylation inhibits IRS1 function, with increased serine phosphorylation seen in various insulin resistant states. These post translational modifications could be a major contributor to the pathogenesis of insulin resistance (Bouzakri et al., 2006; Corbould et al., 2005). Probably the most characterised of these residues is serine-307 (corresponding to serine 312 in humans), which is located adjacent to the PTB-domain (Figure 1-4). From yeast tri-hybrid assays, it was found that phosphorylation at this site inhibits the InsR / IRS1 interaction, attenuating signal transduction (Aguirre et al., 2000). Other residues associated with inhibiting IRS1 function include serine-612 and serine-632 (corresponding to human serine 616 and serine 636), which are located proximal to the PI3K binding site (Figure 1-4). It is thought that phosphorylation here can preclude the association between PI3K and IRS1, preventing the former from becoming activated (Mothe & Van Obberghen, 1996).

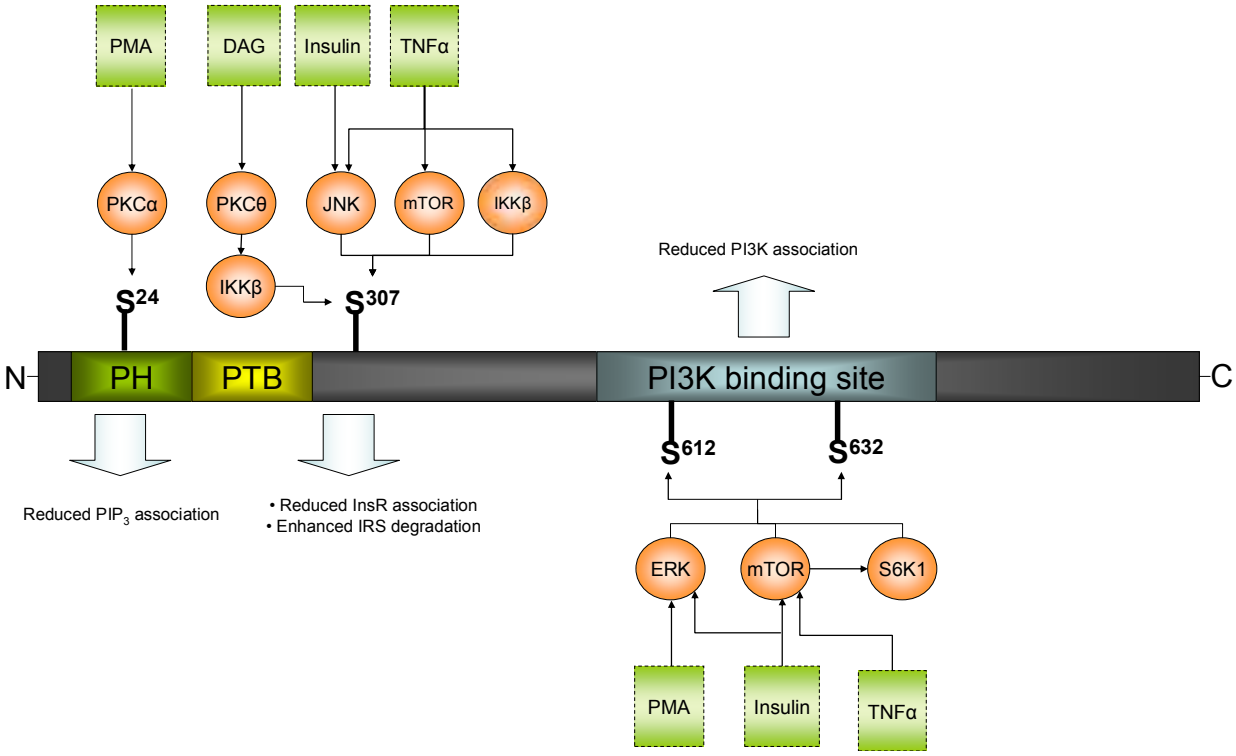

Figure 1-4 The structure of IRS1, highlighting some of the serine phosphorylation residues known to negatively regulate its function. (PH= plextrin homology domain, PTB= phospho-tyrosine tyrosine binding domain, PMA= phorbol 12-myristate 13-acetate, DAG= diacylglycerol)

Numerous kinases have been implicated in mediating inhibitory serine phosphorylation of IRS proteins, and their dysregulation has been implicated in the pathogenesis of insulin resistance (Zick, 2005). These include Jun kinase (JNK) (Aguirre et al., 2000), inhibitor of nuclear factor κB (NF-κB) kinase-β (IKKβ) (Gao et al., 2002), p70S6K (S6K1) (Harrington et al., 2004), the mammalian target of rapamycin (mTOR) (Ozes et al., 2001), extracellular signal-regulated kinase (ERK) (Bouzakri et al., 2003) and certain protein kinase C (PKC) isoforms (Yu et al., 2002).

In addition to regulation of IRS activity by phosphorylation, levels of IRS proteins are regulated at the level of mRNA transcription and protein stability. For example, insulin can inhibit IRS2 expression, as a negative feedback mechanism (Hirashima et al., 2003). Furthermore, the induction of suppressor of cytokine signalling-1 and -3 (SOCS1, -3) enhances ubiquitination of IRS1 and IRS2, targeting them for proteosomal degradation (Rui et al., 2002).

Although there is a high degree of homology between IRS1 and IRS2, studies from animal knockout models have shown that they serve complementary, rather than identical roles in insulin signalling. $IRS1^{-/-}$ mice are markedly insulin resistant, due to defective insulin action, primarily in the skeletal muscle. These mice also present with growth retardation, due to IGF-I resistance (Araki et al., 1994). Similarly, $IRS2^{-/-}$ mice are resistant to the actions of insulin, reportedly with the greatest defects in insulin signalling in the liver. However, unlike the $IRS1^{-/-}$ mice, $IRS2^{-/-}$ mice have defects in pancreatic β-cells development, rendering these mice unable to compensate for the peripheral insulin resistance by increasing insulin secretion - eventually leading to a type 2 diabetic state. By contrast, the $IRS1^{-/-}$ mice can maintain lifelong hyperinsulinaemia (Withers et al., 1998).

1.6.3. Phosphoinositide 3-kinase

The PI3K enzyme is a heterodimer composed of a catalytic subunit ~110kDa (p110) and an SH2 domain containing regulatory subunit ~85kDa (p85). Binding of the regulatory subunit to the catalytic subunit allosterically inhibits its catalytic function (Yu et al., 1998). Only when the SH2 domain of the regulatory subunit binds with phosphorylated tyrosine sites on IRS is this inhibition relieved (Myers et al., 1992). Furthermore, binding of PI3K to IRS brings it into close proximity with its substrate, the membrane lipid phosphatidylinositol-3,4-diphosphate, which it subsequently phosphorylates at the 5' position, generating phosphatidylinositol-3,4,5-trisphosphate (PIP_3). The formation of this second messenger allows for the activation of PH-domain containing proteins, such as PKB/akt (Alessi et al., 1997). Negative regulation of insulin signalling can occur at the level of PIP_3, by the phosphatases PTEN which dephosphorylate and inactivate PIP_3 (Maehama & Dixon, 1999). Furthermore, the stoichiometry of the regulatory subunit to the heterodimer allows for competition for binding IRS proteins (Mauvais-Jarvis et al., 2002).

1.6.4. Protein Kinase B

There are three members of the mammalian protein kinase B (PKB) family: PKBα, PKBβ and PKBγ (akt1, akt2 and akt3, respectively). All isoforms share three conserved functional domains: an N-terminal PH-domain; a central serine/threonine kinase domain; and a regulatory domain at the C-terminal. Generation of PIP_3 by PI3K is necessary for the multi-step activation of PKB/akt (Hanada, Feng & Hemmings, 2004). The PH-domain of PKB/akt binds PIP_3,

allowing for its recruitment to the plasma membrane from the cytosol, where it subsequently undergoes phosphorylation at threonine-308 (located within the kinase activation loop) by another PH-domain containing serine/threonine kinase, PDK1 (Alessi et al., 1997; Stephens et al., 1998). Phosphorylation at serine-473 (within the regulatory domain) by the mammalian target of rapamycin (mTOR) complex, leads to full activation (Sarbassov et al., 2005) - allowing PKB/akt to phosphorylate numerous targets at the plasma membrane, cytosol and in the nucleus. PKB/akt activity is negatively regulated by the protein phosphatase-2A (PP2A), and the PH-domain leucine-rich repeat protein phosphatase (PHLPP), both effectively dephosphorylate PKB/akt when the activating stimuli has been removed (Gao, Furnari & Newton, 2005; Millward, Zolnierowicz & Hemmings, 1999).

1.6.4.1. Protein kinase B and glucose uptake

One of the central roles of activated PKB/akt is to increase glucose transport into the cell. Under basal conditions, the GLUT4 glucose transporters reside in cytosolic storage vesicles containing rab GTPases, which are required for the cytoskeletal rearrangement necessary to target these vesicles to the plasma membrane. Also present in these vesicles is the rab-GTPase-activating protein AS160 (which stands for akt substrate of 160kDa), that effectively inhibits the rab GTPases, maintaining them in an inactive, GDP-bound form. Upon insulin stimulation, activated PKB/akt directly phosphorylates AS160, resulting in its association with the cytosolic scaffold protein 14-3-3. AS160 is subsequently removed from the storage vesicles, sequestered to 14-3-3 in the cytosol, relieving

the inhibition upon the rab GTPases and allowing the GLUT4 storage vesicles to be targeted to the plasma membrane - increasing glucose transport into the cell (Ramm et al., 2006; Sano et al., 2003). In addition, there is evidence that insulin-stimulated glucose uptake can occur by a pathway independent of PKB/akt, involving PI3K-induced activation of atypical protein kinase C (PKC) isoforms (PKCλ/ζ) (Farese, 2002; Standaert et al., 2001), however, the precise molecular mechanism by which this pathway enhances insulin-stimulated glucose uptake is not clear.

1.6.4.2. Protein kinase B and enzymic activation

PKB/akt directly regulates the activity of a number of metabolic enzymes. For example, glycogen synthase (GS), a key enzyme involved in glycogen synthesis is negatively regulated by glycogen synthase kinase (GSK) which, in the presence of low insulin, phosphorylates GS, maintaining it in an inactive state. Under insulin-stimulating conditions, PKB/akt phosphorylates GSK resulting in its deactivation, which relieves the inhibition upon GS, and subsequently increasing glycogen synthesis (Sutherland, Leighton & Cohen, 1993). In addition, PKB/akt mediated suppression of GSK activity enhances protein synthesis by decreasing the GSK-induced inhibitory phosphorylation of the eukaryotic initiation factor 2B (elF2B) (Welsh & Proud, 1993). PKB/akt also activates protein synthesis by a separate mechanism involving phosphorylation and inhibition of tuberous sclerosis complex-2 (TSC2) (Potter, Pedraza & Xu, 2002). Since the TSC1/2 complex inhibits mTOR, PKB/akt effectively activates mTOR which goes on to enhance protein translation by phosphorylating S6-kinase and the eukaryotic

translation initiation factor 4E binding protein-1 (4EBP1) (Miron, Lasko & Sonenberg, 2003).

1.6.4.3. Protein kinase B and secondary messaging

PKB/akt can modulate the activity of some metabolic enzymes through controlling the levels of second messengers in the cell, particularly cyclic AMP (cAMP). In the presence of low insulin, cytosolic cAMP levels are high, activating protein kinase A (PKA), which in turn activates serine/threonine LKB by phosphorylation. AMP-dependent protein kinase (AMPK) is subsequently activated by LKB, and goes on to phosphorylate acetyl-CoA carboxylase (ACC), inhibiting its activity. ACC catalyses the rate limiting step of lipogenesis, and its reaction products (malonyl-CoA) suppress β-oxidation. Consequently, inhibition of ACC promotes the use of fatty acids as fuel over their storage. In the presence of high insulin, PKB/akt phosphorylates and activates phosphodiesterase-3B (PDE3B), which hydrolyses cAMP to inactive 5'AMP (Kitamura et al., 1999), relieving the AMPK-induced inhibition on ACC, resulting in fatty acid storage being favoured over oxidation. In addition to this role, activated PKA phosphorylates and activates phosphorylase kinase (PK), which in turn activates glycogen phosphorylase resulting in mobilisation of glycogen stores (Mehrani & Storey, 1993). The insulin-induced inhibition of PKA blocks this effect.

1.6.4.4. Protein kinase B and transcriptional regulation

PKB/akt can regulate the expression of a number of metabolic enzymes by controlling the activity of key transcription factors. The activities of several of the winged helix or forkhead (FOX) family are regulated by insulin (Tran et al., 2003). For example, in the presence of low insulin, FOXO1 activates the gluconeogenic enzymes: phosphoenolpyrouvate (PEPCK) and glucose-6-phosphatase (G6Pase) in the liver (Barthel et al., 2001; Hall et al., 2000; Puigserver et al., 2003). Similarly, FOX2A increases the transcription of genes involved in hepatic fasting metabolism (ketogenesis and fatty acid oxidation) (Wolfrum et al., 2004). In the presence of insulin, activated PKB/akt phosphorylates these transcription factors preventing their nuclear localisation, instead sequestering them to the cytosol and thus terminating the fasting metabolic program (Wolfrum et al., 2004). Insulin also enhances the expression of activating transcription factor 4 (ATF4, also known as CREB2), which co-ordinately increases the transcription of genes involved in amino acid biosynthesis and transport (Adams, 2007).

In summary, the insulin signalling cascade is a complex network of membrane receptors, adaptor proteins and kinases which are both positively and negatively regulated through post-translational phosphorylation events. Numerous factors have been implicated in the pathogenesis of insulin resistance including: factors secreted by adipose tissue (e.g. TNFα and IL-6) and the intracellular accumulation of lipid metabolites (e.g. diacylglycerides (DAG) and ceramides). These agents impinge upon insulin signalling by activating ‘stress kinases’ which go on to directly phosphorylate components of the insulin signalling cascade.

1.7. Glucocorticoid structure, synthesis and action

1.7.1. Adrenal glands

The adrenal glands (also known as the suprarenal glands) are bilateral structures located above the kidneys (Figure 1-5). They are surrounded by a capsule of adipose and fibrous tissue. Each gland is separated into two distinct structures; an inner structure called the medulla, and an outer structure called the cortex. The cortex constitutes 90% of the weight of the adrenal gland and can be sub-divided into 3 distinct zones: the zona reticularis (ZR), located next to the medulla; the zona fasciculata (ZF), located in the centre of the cortex; and the zona glomerulosa (ZG), located beneath the capsule (Figure 1-5). Blood is supplied to the adrenal glands by the inferior phrenic artery, renal artery and the aorta, giving this gland one of the highest blood supplies per gram of tissue. Blood from the adrenals drains into vena cava and renal vein (Arlt & Stewart, 2005; Larsen et al., 2003).

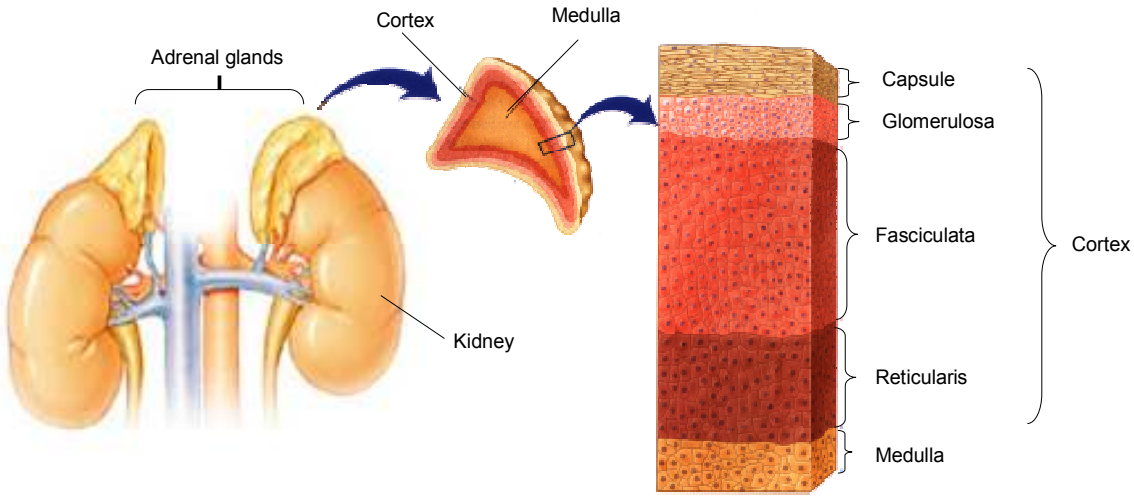

Figure 1-5 The Adrenal glands are positioned above the kidneys and are divided into two distinct structures, the adrenal cortex and the adrenal medulla. The cortex is further divided into three distinct zones; the glomerulosa, fasciculata and reticularis.

1.7.2. Structure of adrenal steroids

One of the major roles of the adrenal gland is the synthesis and secretion of steroids. All steroids are synthesized from the precursor cholesterol, and share a common basic structure; three cyclohexane rings fused to a cyclopentane ring (Figure 1-6). The chemical properties of these molecules are dependent upon the number of carbons atoms and side groups bonded to the basic four ring structure. There are 5 main groups of steroid produced by the adrenal gland, identified by the number of carbon atoms they contain. For example, androgens and progestogens both have 19 carbons; estrogens have 18 carbons; mineralocorticoids and GCs have 21 carbons (Arlt & Stewart, 2005).

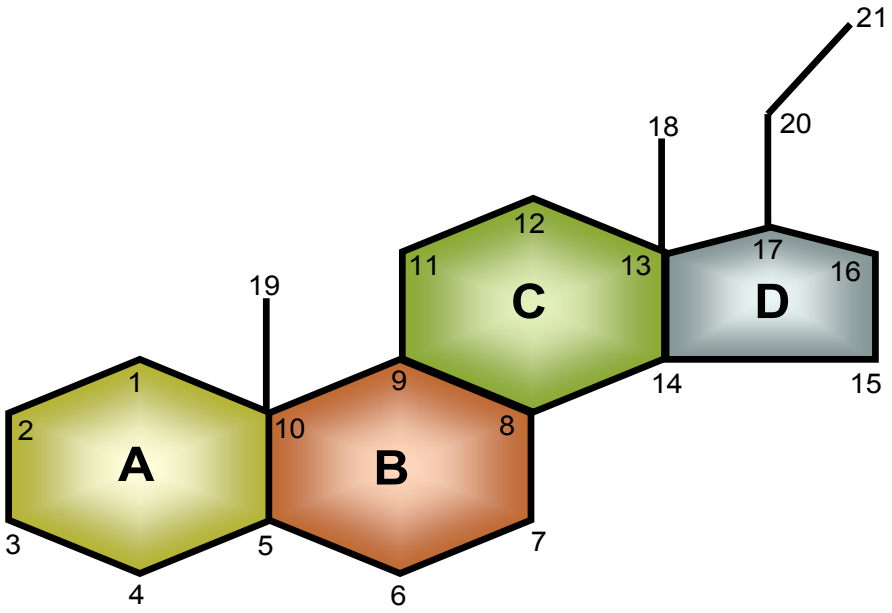

Figure 1-6 Standard structure and nomenclature of adrenal steroids. The numbers designate the carbon atoms and letters designate the rings.

1.7.3. Steroidogenesis

All adrenal steroids are synthesized from the precursor cholesterol in the cortex. The predominant source of cholesterol is through the uptake of low density lipoproteins (LDL) from the circulation. Adrenal tissue expresses specific cell surface receptors that bind and internalise circulating LDL, by receptor-mediated endocytosis. Once in the cytosol, the LDL is hydrolysed, liberating free cholesterol. Cholesterol can also be synthesized *de novo* within the cortex by the enzyme acetyl coenzyme A (acetyl-CoA) (Arlt & Stewart, 2005; Larsen et al., 2003).

The three zones of the cortex have distinct enzymic profiles, allowing them to specialise to the synthesis of specific steroids. The first step of steroidogenesis takes place in all zones, and involves the transport of cholesterol, from the cytosol, to the inner mitochondrial membrane, where it is subsequently converted to pregnenolone by cytochrome P450scc. The zona glomerulosa is specialised for synthesising mineralocorticoids, due to the high expression of aldosterone synthase (P450c18) in this zone. This enzyme is not expressed in either the zona fasciculata nor the zona reticularis, consequently these zones are unable to synthesize aldosterone (Figure 1-7) (Arlt & Stewart, 2005). By contrast, the zona fasciculata and zona reticularis express P450c17, which is absent from the zona glomerulosa. This enzyme has both 17α-hydrolylase and 17,20-lyase activity, the latter being dependent upon the availability of the flavoprotein cytochrome b_5. In the zona fasciculata, the 17α-hydrolylase activity of P450c17 predominates, generating 17-OH-pregnenolone; a prerequisite for GC synthesis in this zone

(Figure 1-7). In the zona reticularis, the comparatively high expression of cytochrome b_5 allows P450c17 to carry out 17,20-lyase activity, which is necessary for the generation of the adrenal androgen precursors, dehydroepiandrosterone (DHEA) and androstenedione in this zone (Figure 1-7) (Arlt & Stewart, 2005; Larsen et al., 2003).

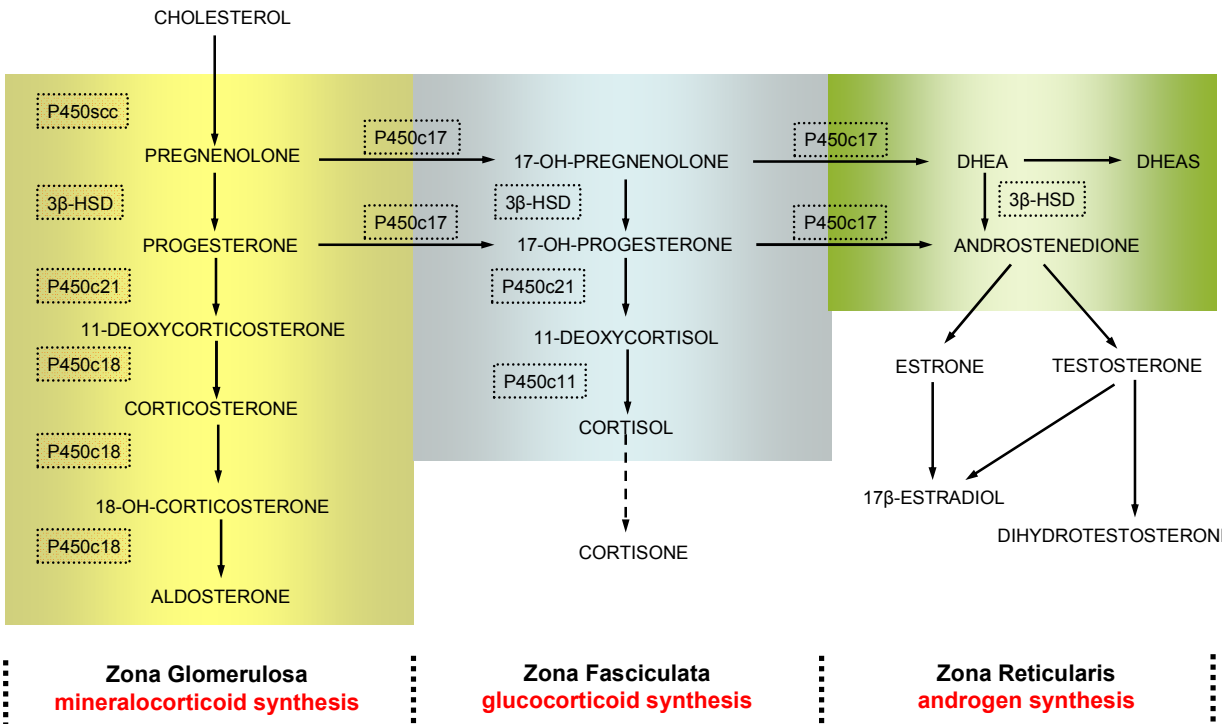

Figure 1-7 The 3 zones of the adrenal cortex have distinct enzymic profiles - allowing for the synthesis of specific steroids in each zone.

1.7.4. Cortisol synthesis

The active GC, cortisol, is synthesized in the zona fasciculata. The first step of cortisol synthesis is the conversion of cholesterol to pregnenolone within the mitochondria, and involves hydroxylation and side chain cleavage at C20 by P450scc. Pregnenolone is released from the mitochondria, and subsequently converted to 17-OH-progesterone by one of two possible pathways. In the predominant pathway, pregnenolone is firstly converted to progesterone in the cytosol by 3β-HSD, by a reaction involving isomerisation of the double bond at C5 and dehydrogenation of the 3-OH group. P450c17 then converts progesterone to 17-OH-progesterone by hydroxylation of C17 using its 17α-hydroxylase activity, and cleavage of the 2 carbon side chain at C17 using its 17,20-lyase activity. The alternative pathway for 17-OH-progesterone synthesis utilises the same enzymes, however, P450c17 first converts pregnenolone to 17-OH-pregnenolone, which in turn is converted to 17-OH-progesterone by the actions of 3β-HSD. The next step in cortisol biosynthesis is the conversion of 17-OH-progesterone to 11-deoxycortisol by 21-hydroxylase (P450c21), in a reaction that involves hydroxylation of C21. The last step takes place in the mitochondria, and involves the conversion of 11-deoxycortisol to cortisol by the enzyme 11β-hydroxylase (P450c11) (Arlt & Stewart, 2005; Larsen et al., 2003).

1.7.5. The hypothalamic-pituitary-adrenal axis

GC secretion is controlled by the hypothalamic-pituitary-adrenal (HPA) axis (Figure 1-8). Neural stimuli from the brain drive the hypothalamus to secrete corticotrophin releasing hormone (CRH) into the hypophyseal portal vein, where it travels to the anterior pituitary and binds to the type I CRH receptors. This in turn stimulates the release of adrenocorticorticotrophic hormone (ACTH) from the anterior pituitary into the circulation, where it acts on the adrenal gland increasing cortisol secretion. A negative feedback system is in place whereby cortisol can inhibit the release and synthesis of CRH and ACTH.

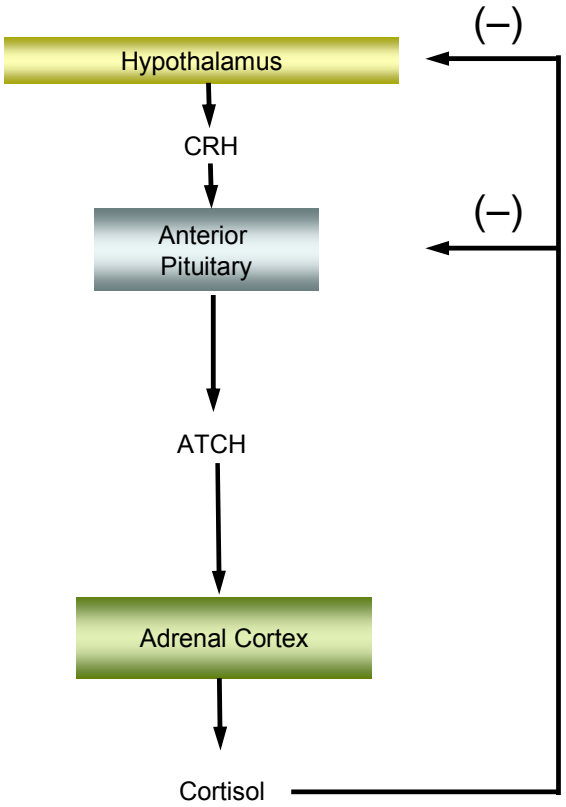

Figure 1-8 The hypothalamic-pituitary-adrenal (HPA) axis. A negative feed back mechanism is in place whereby cortisol inhibits its own release.

ACTH secretion varies on a pulsatile basis, with peaks at approximately 30 minute intervals. Furthermore, ACTH levels vary throughout a 24 hour cycle, in a pattern known as the circadian rhythm. As a consequence, cortisol secretion is also pulsatile, and follows the circadian rhythm with levels peaking just before waking, followed by a slow decline through the day reaching a nadir during the first few hours of sleep. The mechanism for how ACTH is released in the circadian rhythm is currently unknown. In response to stress (defined as trauma, sepsis, emotion, starvation), ACTH levels can increase independently of the circadian rhythm, which in turn drives an increase in cortisol secretion (Becker et al., 2001; Larsen et al., 2003).

1.7.6. Regulation of cortisol secretion and synthesis

ACTH is the principle regulator of cortisol synthesis and secretion. It is capable of eliciting both acute and chronic effects on steroidogenesis, through binding G protein-coupled melanocortin-2 receptors (MC2R) expressed on the adrenal cortex cell surface (Catalano, Stuve & Ramachandran, 1986). Activation of MC2R triggers the cytosolic accumulation of cyclic-AMP (cAMP), which in turn activates cAMP-dependent protein kinase A (PKA) (Cooke, 1999; Rae et al., 1979). Cholesterol esterase is activated by PKA, enhancing the release of free cholesterol from intracellular stores (Boyd & Trzeciak, 1973; Cook et al., 1982). The rate limiting step of steroidogenesis is the transport of cholesterol from the cytoplasm to the inner mitochondrial membrane, for its conversion to pregnenolone by P450scc. This step is mediated by steroidogenesis acute regulatory protein, StAR. ACTH-induced activation of PKA enhances cholesterol

uptake into the mitochondria by increasing StAR mRNA expression (Clark et al., 1995), RNA stability (Ariyoshi et al., 1998), translation (Clark et al., 1995) and phosphorylation (Clark, Ranganathan & Combs, 2000). In addition, prolonged ACTH exposure enhances the expression the steroidogenic genes: P450scc, P450c17, P250c21 and P450c11 - enhancing steroidogenesis (Chu & Kimura, 1973; Simpson & Waterman, 1988; Waterman & Bischof, 1997). ATCH can also increase the synthesis of LDL receptors (Larsen et al., 2003)

1.7.7. Glucocorticoid action

In the circulation, 90% of cortisol is bound to the α_2-globulin, cortisol binding globulin (CBG) and albumin (Hammond, 1990). This reduces the bioactivity of cortisol, leaving the unbound fraction (10%) free to diffuse across cell membranes to exert its effect. Interestingly, serum CBG levels have been found to correlate negatively with BMI, waist-to-hip ratio and HOMA-IR (an index of insulin resistance) (Fernandez-Real et al., 2002; Ousova et al., 2004). Once in the cytosol, the predominant actions of cortisol are through the glucocorticoid receptor (GR), which regulates the transcription of specific genes. The GR is a member of steroid hormone receptor family, which are ligand-activated nuclear receptors. All members of this family share a common structure, consisting of a C-terminal ligand binding domain, a DNA binding domain and an N-terminal transactivation domain (Giguere et al. 1986). The GR shuttles between the cytoplasm and nucleus upon ligand binding. In its unbound form, the GR is localised to the cytosol where it forms a heterocomplex with 2 molecules of heat shock protein-90 (hsp90), stoichiometric amounts of heat shock protein-70

(hsp70), p23 and immunophilin (Pratt, 1998; Pratt & Toft, 1997) (Figure 1-9). The association between GR and hsp90 opens the hydrophobic steroid-binding cleft within the GR, allowing access by the steroid ligand (Stancato et al., 1996). Upon steroid binding, the hsp-immunophilin complex dissociates and the liganded GR rapidly translocates into the nucleus where it interacts with positive / negative GC responsive elements (GREs) within the DNA of gene targets - activating / repressing gene transcription (Figure 1-9) (Adcock, 2000; Schaaf & Cidlowski, 2002).

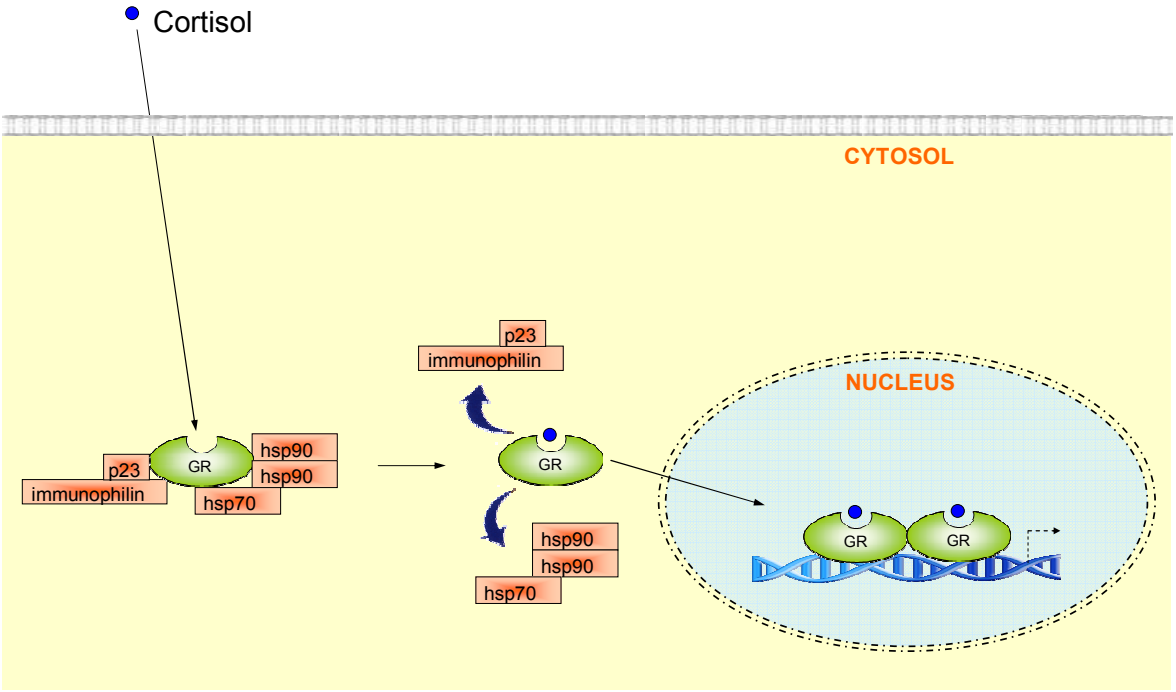

Figure 1-9 The mechanism of GC action. Upon steroid binding, the GR dissociates from its protein complex, translocates into the nucleus and modulates gene transcription.

Structurally, the GR can be organised into 3 functional domains: an N-terminal domain, a DNA-binding domain and a ligand-binding domain (Figure 1-10) (Kumar & Thompson, 2005). The DNA-binding domain is composed of two highly

conserved zinc fingers, located centrally within the amino acid sequence. The first zinc finger is primarily responsible for site specific GR-DNA binding, since amino acid residues located in this region make specific interactions with bases located within the GRE (Hard et al., 1990; Luisi et al., 1991). The second zinc finger functions to stabilise GR-DNA interactions, and also plays a role in homodimerisation at the GRE (Hard et al., 1990; Luisi et al., 1991). Much of the GRs transcriptional activity is dependant upon the AF1 activation region, located within the N-terminal domain. AF1 has been shown to associate with a number of transcriptional co-activators and co-repressors including: TFIIB, CBP and SRC1 (Kumar et al., 2004; Kumar, Serrette & Thompson, 2005). In addition to its role in binding steroid-ligands and chaperones, the ligand-binding domain also has an activation subdomain (AF2) which, like AF1, binds co-activators and co-repressors including SRC1 (Giguere et al., 1986; Kucera et al., 2002).

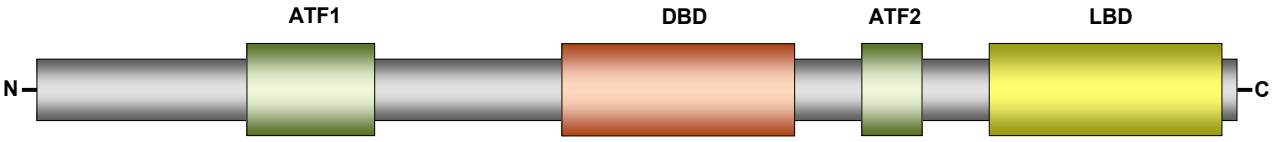

Figure 1-10 The GC receptor domain structure. (DBD= DNA binding domain, LBD= ligand binding domain).

In addition to regulating the transcription of genes which have GREs, the GR can also regulate transcription of genes that do not posses these elements: by interact with, and regulating the activity of, transcription factors bound to their own response element (Rogatsky et al., 2003).

The primary changes in gene transcription meditated by the GR can be either positive or negative, and can take place in as little as 15 minutes following GC exposure (Ringold et al., 1977). In addition, the GR can elicit secondary events whereby the expression of GC responsive genes can modulate the expression or activity of other proteins.

The GR gene is subject to alternative splicing at the first and last exons. The most abundant spliced variants are GRα and GRβ (Lu & Cidlowski, 2004). GRα has a high affinity for GCs, and is expressed ubiquitously, whereas GRβ has a very low affinity for GCs, limited tissue distribution, and may act as a dominant negative regulator of GRα activation (Giguere et al., 1986; Lu & Cidlowski, 2004).

Some GC effects have been reported to occur within minutes, and are insensitive to transcriptional inhibition (Croxtall, Choudhury & Flower, 2000; Croxtall et al., 2002; Liu et al., 2005). There is evidence that these non-genomic GC effects are, at least partly, mediated by a membrane bound GR (Chen, Watson & Gametchu, 1999; Gametchu, Watson & Wu, 1993). Reported non-genomic effects include activation of the insulin signalling components PI3K and PKB/akt (Hafezi-Moghadam et al., 2002). The precise signalling events leading to these effects has not been fully elucidated, but are thought involve caveolin-1 (Matthews et al., 2008).

1.7.8. Metabolic actions of glucocorticoids

Acutely, GCs are released as part of the response to stress, for the purpose of dampening down many of the responses to illness, as well as resetting metabolism to favour release of substrates for oxidative metabolism. However, chronically, the effects of high levels of GCs are less beneficial, enhancing muscle wasting, visceral adipose accumulation and lipid accumulation within the liver (Becker et al., 2001).

1.7.8.1. Carbohydrate metabolism

GCs have catabolic effects, some of which oppose the anabolic actions of insulin. Therefore, under conditions of GC excess, there is a decrease in peripheral insulin sensitivity (particularly of the skeletal muscle), leading to hyperglycaemia (Rizza, Mandarino & Gerich, 1982). Furthermore, GCs increase hepatic *de novo* glucose production - further contributing to the hyperglycaemic state (Kraus-Friedmann, 1984). Insulin secretion by the pancreatic β-cells is attenuated when GC sensitivity is increased through transgenic GR expression (Lambillotte, Gilon & Henquin, 1997). In the liver, GCs may work in concert with insulin to enhance hepatic glycogen synthesis and deposition - protection against long term starvation (Steiner, Rauda & Williams, 1961).

1.7.8.2. Protein metabolism

GCs have catabolic / anti-anabolic effects upon protein metabolism in adipose tissue, bone and the lymphoid tissue (Becker et al., 2001), however, since skeletal muscle accounts for ~40% of the body mass, and is extremely protein rich, the effects of GC excess upon protein metabolism in this tissue are perhaps most relevant. It has been demonstrated that GC excess induces muscle atrophy (Schacke, Docke & Asadullah, 2002) by enhancing protein breakdown (Bodine et al., 2001), decreasing protein synthesis (Ma et al., 2003) and increasing amino acids conversion to glutamine (Falduto, Hickson & Young, 1989). The net result is elevated plasma free amino acid levels - providing substrate for glucose synthesis by gluconeogenesis in the liver.

1.7.8.3. Lipid metabolism

In the liver, GCs stimulate the production of very low density lipoprotein (VLDL) particles, enhance *de novo* synthesis of triacylglycerides (TAG) (Taskinen et al., 1983), while decreasing the utilisation of stored TAG for VLDL production (Dolinsky et al., 2004). The effect of GCs in adipose tissue differs depending on the depot. Notably, GCs enhance pre-adipocyte differentiation (Gaillard et al., 1991) and TAG accumulation (Samra et al., 1998) - resulting in central obesity. Furthermore, GCs enhance lipolysis, leading to elevated circulating free fatty acid levels (Slavin, Ong & Kern, 1994). The action of GCs upon lipid metabolism within the skeletal muscle will be discussed in detail in section 1.12.4.

1.7.9. Glucocorticoid metabolism

Cortisol has a circulating half life of between 70 and 120 minutes (Peterson et al., 1955). The major site of cortisol metabolism is the liver, but the kidney has also been found to inactivate cortisol to cortisone by 11β-HSD2. In the liver, both cortisol and cortisone are reduced at the C4-C5 double bond by 5β-reductase, and hydroxylated at the 3-oxo group by 3α-hydroxysteroid dehydrogenase forming 5β-tetrahydrocortisol (5β-THF) and tetrahydrocortisone (THE), respectively (Figure 1-11) (Okuda & Okuda, 1984). The alternative reduction of the C4-C5 double bond of cortisol by 5α-reductace generates allo-THF, however, the 5β-THF metabolite predominates (Russell & Wilson, 1994). Approximately 50% of secreted cortisol appears in the urine as THF, allo-THF and THE conjugated to glucuronic acid (Larsen et al., 2003). Alternatively, further reduction of THF and THE, at the 20-oxo group, by 20α-HSD or 20β-HSD generates cortols and cortolones respectively (Figure 1-11) (Shackleton, 1993). These metabolites account for 25% of the secreted cortisol. The remaining cortisol is secreted as C19 steroids (10%), Cortolic / cortolonic acids (10%) and unconjugated steroids (5%) (Larsen et al., 2003).

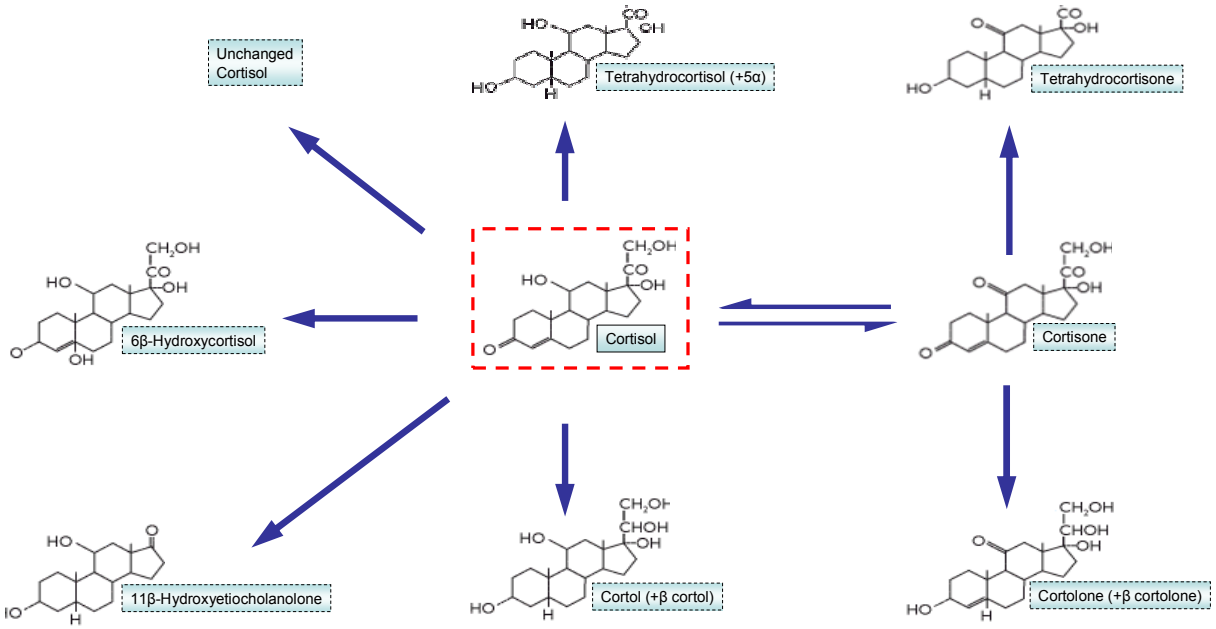

Figure 1-11 The major metabolites of cortisol.

Total urinary GC metabolites give an indication of adrenal cortisol secretion. Using a deuterated cortisol tracer, adrenal cortisol secretion rates were estimated at approximately 10 mg/day (Esteban et al., 1991).

1.7.10. 11β-HSD and pre-receptor GC metabolism

The interconversion between cortisol and its inactive metabolite, cortisone, are carried out by: 11β-HSD1 and -2. These isozymes are members of the short-chain alcohol dehydrogenase family, and contain regions that allow cofactor binding and tethering to the ER membrane. They are products of separate genes. The ratio of urinary THF to THE is a predictor of the interconversion of cortisol and cortisone by 11β-HSDs.

1.7.10.1. 11β-hydroxysteroid dehydrogenase type 1

The HSD11B1 gene is located on chromosome 1q32.2 and encodes a 34kDa glycosylated enzyme. It was first purified from rat liver, and initially thought to have only dehydrogenase activity - deactivating cortisol (Lakshmi & Monder, 1988). However, later studies utilising intact cells, including hepatocytes (Jamieson et al., 1995), adipocytes (Bujalska, Kumar & Stewart, 1997), lung cells (Hundertmark et al., 1995) and skeletal myocytes (Jang et al., 2006), have demonstrated that 11β-HSD1 is predominantly an oxo-reductase - activating cortisol, unless cells are disrupted (Figure 1-12). This is supported by the higher affinity of 11β-HSD1 for cortisone (Km= 0.3μM), compared with cortisol (Km= 2.1μM) (Stewart, Murry & Mason, 1994). 11β-HSD1 is tethered to the ER-membrane, with the catalytic domain located within the lumen of the ER (Ozols, 1995). A high concentration of NADPH, within the ER lumen, is thought to be responsible for maintaining the activity of 11β-HSD1 in the oxo-reductase direction. Hexose-6-phosphate dehydrogenase (H6PDH) is also present within the ER lumen, and is physically associated with 11β-HSD1. This enzyme generates a high concentration of NADPH within the ER lumen using the substrates NADP and Glucose-6-phosphate (Figure 1-12) (Bujalska et al., 2005). Evidence that the presence of this enzyme is essential for the directionality of 11β-HSD1 is found from the H6PDH null mice, where liver and adipose 11β-HSD1 activity switches to the dehydrogenase direction (Bujalska et al., 2005; Lavery et al., 2006). HSD11B1 is widely expressed throughout the body in many tissues, including: the liver, adipose tissue, skeletal muscle and brain (Jang et al., 2006; Ricketts et al., 1998)

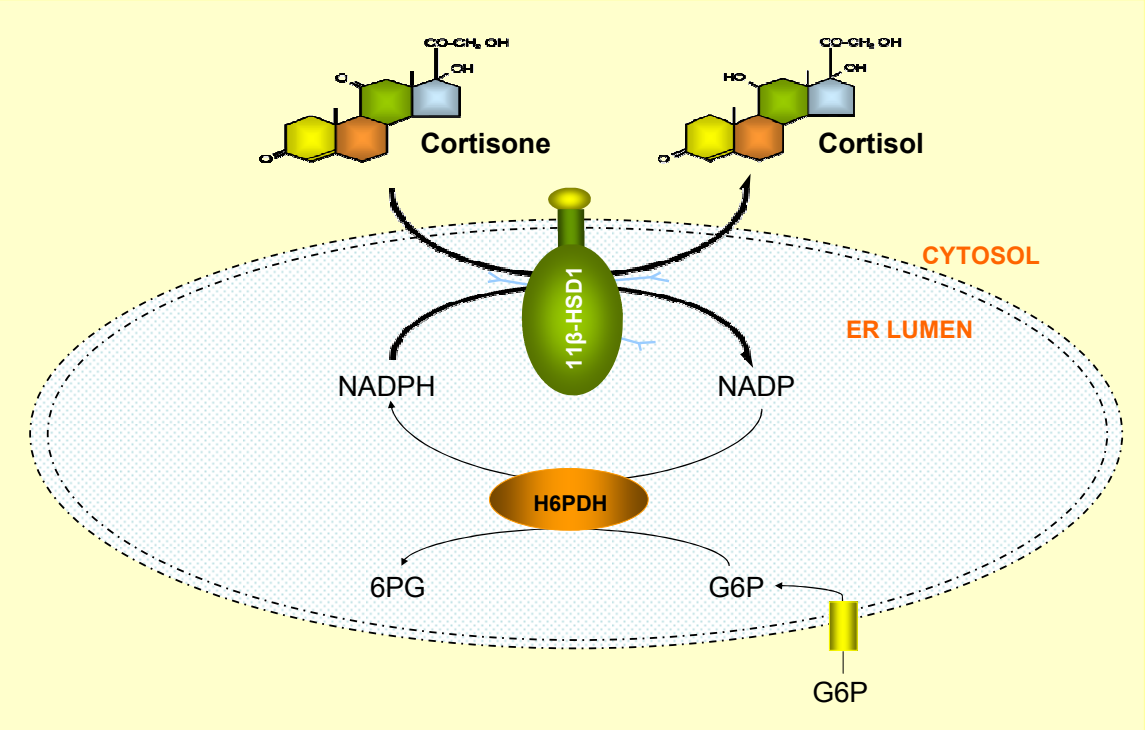

Figure 1-12 Pre-receptor regulation of GC generation. In skeletal muscle, liver and adipose 11β-HSD1 acts as an oxo-reductase. This directionality is conferred by the catalytic products of H6PDH.

1.7.10.2. 11β-hydroxysteroid dehydrogenase type 2

The HSD11B2 gene is located on chromosome 16q22 and encodes a 44kDa dehydrogenase which catalyses the NAD^+ dependent inactivation of cortisol to cortisone. Unlike the type 1 isozyme, the type 2 form has more limited tissue distribution; expressed predominantly in mineralocorticoid target tissues such as the colon (Whorwood, Ricketts & Stewart, 1994) and the kidney (Whorwood et al., 1995). The role of 11β-HSD2 in these tissues is to provide protection against the mineralocorticoid receptor (MR) being activated by cortisol, which has the same affinity for the MR as it does for the GR (Arriza et al., 1987; Edwards et al., 1988). Mutations in the HSD11B2 gene result in a condition called apparent

mineralocorticoid excess (AME). In this condition, activation of the MR by GCs results in hypertension and renal sodium retention (Palermo et al., 1996; Stewart et al., 1996). 11β-HSD2 has also been detected in the placenta, and is thought to protect the foetus from maternal GC exposure (Brown et al., 1996). In pregnancies presenting with intrauterine growth restriction, reduced placental 11β-HSD2 expression has been detected (Shams et al., 1998). 11β-HSD2, like the type 1 isozyme, is anchored to the ER membranes, however, its catalytic domain is orientated towards the cytosol (Odermatt et al., 1999).

In summary, the 11β-HSD isozymes catalyse the interconversion of inactive and active GCs, and thus play an integral role in controlling GR activation. Therefore, the tissue specific expression and activity of 11β-HSD1, 11β-HSD2, H6PDH and the GR all impact upon the GC response elicited in that tissue.

1.8. Skeletal muscle

Skeletal muscle is a major component of the human body, accounting for ~40% of the total body mass. Its purpose is to provide support and movement to the skeleton and perform numerous vital metabolic functions. In this section, aspects of skeletal muscle development, morphology and function will be discussed.

1.8.1. Skeletal muscle embryology

In vertebrates, skeletal muscle development starts during early embryogenesis. With the exception of the craniofacial muscles, all skeletal muscles are derived from the somite, which is a transient condensation of mesodermal cells (Christ & Ordahl, 1995). The dorsal part of the somite responds to signals from the adjacent dorsal neural tube and notochord, forming the dermomyotome. Cells in this tissue continue to divide but are prevented from differentiating by signals released from the surface ectoderm and lateral plate (Amthor, Christ & Patel, 1999; Pourquie et al., 1996). The formation of the dorsomedial lip of the dermomyotome leads to the migration of cells under the dermomyotome giving rise to a sheet of differentiated skeletal myocytes called the myotome, which subsequently form the axial skeletal muscles (Cinnamon et al., 2001; Ordahl et al., 2001). Formation of skeletal muscles in the appendages starts with the migration of cells from the lateral dermomyotome into the limbs, where they are exposed to local signals inducing a program of skeletal muscle differentiation (Daston et al., 1996; Tremblay et al., 1998).

1.8.2. Skeletal myocyte differentiation

During embryo development, entry of progenitor cells into myogenesis is controlled by the expression of the paired box transcription factors (pax3 and -7). The expression of these markers occurs when the muscle progenitor cells are still proliferating (Relaix et al., 2005), and have important roles in regulating the migration of these cells to the limbs (particularly pax3) (Daston et al., 1996), as well as ensuring cell survival (both pax3 and -7) (Borycki et al., 1999). Double knockout of Pax3 and -7 in the mouse embryo results in major developmental defects of the skeletal muscle (Relaix et al., 2005). These genes appear to act upstream of, or in parallel with, basic helix-loop-helix domain-containing myogenic regulatory factors (MRFs) which include; myogenic differentiation 1 (MyoD), myogenic factor 5 (Myf5) and myogenin (Myog) (Tajbakhsh et al., 1997). MRFs are late markers of the committed myogenic lineage, and are responsible for regulating the expression of muscle specific proteins. For example, MyoD triggers the expression of the contractile proteins: myosin heavy and light chains (Seward et al., 2001) and creatine kinase - essential for regulating anaerobic respiration within the muscle (Lassar et al., 1989). In addition, MyoD expression forces exit from the cell-cycle by upregulating the cyclin-dependent kinase inhibitor $p21^{Waf/Cip1}$ (Figure 1-13) (Halevy et al., 1995).

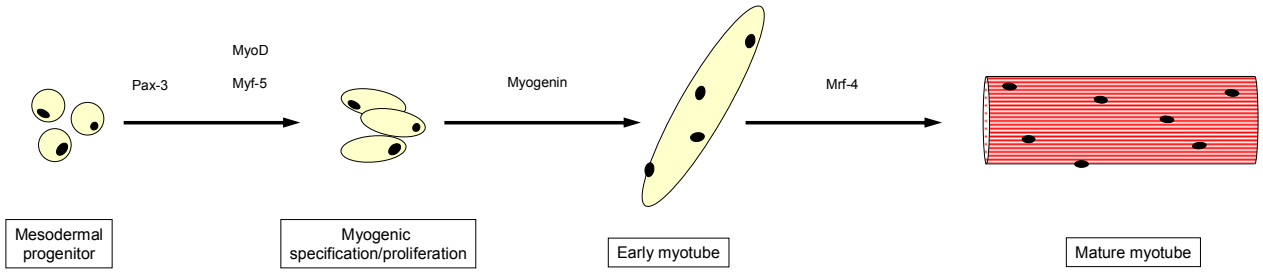

Figure 1-13 Myogenesis involves the formation of multinucleated myotubes that express characteristic contractile proteins.

A key feature of terminally differentiated myocytes is the presence of multiple nuclei per cell. Each nucleus originated from separate myoblasts which fused together to form single, elongated, cylindrical cells referred to as myotubes which, for reasons discussed above, no longer have a proliferative capacity. Also present amongst terminally differentiated myotubes, located around the basal lamina, is a source of myogenic progenitor cells (also known as satellite cells) - essential for growth and regeneration of postnatal skeletal muscle (Moss & Leblond, 1971). In the healthy adult skeletal muscle, these cells are mitotically quiescent, however, in response to various stimuli, including: exercise and injury, they become activated, undergoing multiple rounds of cell division generating a pool of cells that ultimately fuse to form new muscle.

1.8.3. Hormonal regulation of skeletal muscle development

The process of muscle development is complex, with many factors influencing both satellite cell proliferation and differentiation. One such example is IGF-I, which is synthesised by skeletal myocytes and the liver. This ligand acts in an autocrine, paracrine and endocrine fashion through the IGF-IR, expressed on the

cell surface of skeletal muscle. Initially, IGF-I signals myocyte proliferation, whilst inhibiting differentiation, but this pattern is reversed at a later time point by an IGF-I induced upregulation of the MRFs (Engert, Berglund & Rosenthal, 1996). It is well documented that exercise can increases IGF-I secretion from liver and muscle - increasing skeletal muscle mass (Czerwinski, Martin & Bechtel, 1994; Greig et al., 2006). Like IGF-I, IGF-II impacts upon skeletal muscle differentiation, with expression and secretion increasing prior to myoblast fusion (Florini et al., 1991).

Myostatin, a recently identified member of the TGF-β superfamily, is synthesized and secreted by the skeletal myocytes, and has been found to have a negative impact upon satellite cell activation, proliferation and differentiation (McCroskery et al., 2003; McFarland et al., 2007). Its role is exemplified by its knockout in Belgian Blue cattle, where a substantial increase in skeletal muscle mass is observed (Grobet et al., 1997).

Other factors associated with regulating myocyte development include: fibroblast growth factor-1 and -2 (FGF1, -2) which are synthesized and secreted by the skeletal muscle and enhances proliferation in response to muscle damage (Hannon et al., 1996). Also, muscle derived hepatocyte growth factor (HGF) has been found in the extracellular matrix of the skeletal muscle (Tatsumi & Allen, 2004), capable of inducing satellite cell activation in response to muscle injury (Tatsumi et al., 1998).

In addition to peptide hormones, certain endogenous steroids such as androgens and oestrogens impact upon myocyte development. For example, high testosterone levels are observed in males *in utero*, which greatly increases skeletal muscle mass - accounting for increased muscle strength in turn (Fink et al., 2006). Similarly, post-menopausal women on estrogen replacement therapy have greater skeletal muscle mass (Sipila & Poutamo, 2003). Like the peptide hormones described above, steroids are thought to mediate their effect by targeting the satellite cells (Nnodim, 2001).

1.8.4. Skeletal muscle physiology

As discussed above, myogenesis results in the formation of multinuclear cells called myotubes (also known as myofibres) (Figure 1-14). These cells can range in length from a hundred microns in diameter and a few millimetres in length, to hundreds of microns in diameter and several centimetres in length. Each myofibre expresses the contractile proteins myosin and actin which are incorporated into long filaments, organised into repeating units called sarcomeres (Figure 1-14). Sarcomeres in series are referred to as myofibrils, and give skeletal muscle a striated appearance. Multiple myofibres lie in parallel, linked by connective tissue (Brooks, 2003).

Force is generated in skeletal muscle through the actions of the myosin filaments moving against filaments of actin (Figure 1-14). Briefly, ATP binding to the catalytic domain of the myosin motor head induces a conformational change, leading to dissociation of myosin from actin. ATP is subsequently hydrolysed,

inducing a further conformational change allowing the myosin motor head to bind actin at a different location along the filament - forming the “cross-bridge”. Inorganic phosphate release results in a conformational change - inducing the “power-stroke” causing the myosin filament to slide longitudinally with respect to the actin filament (Geeves & Holmes, 1999).

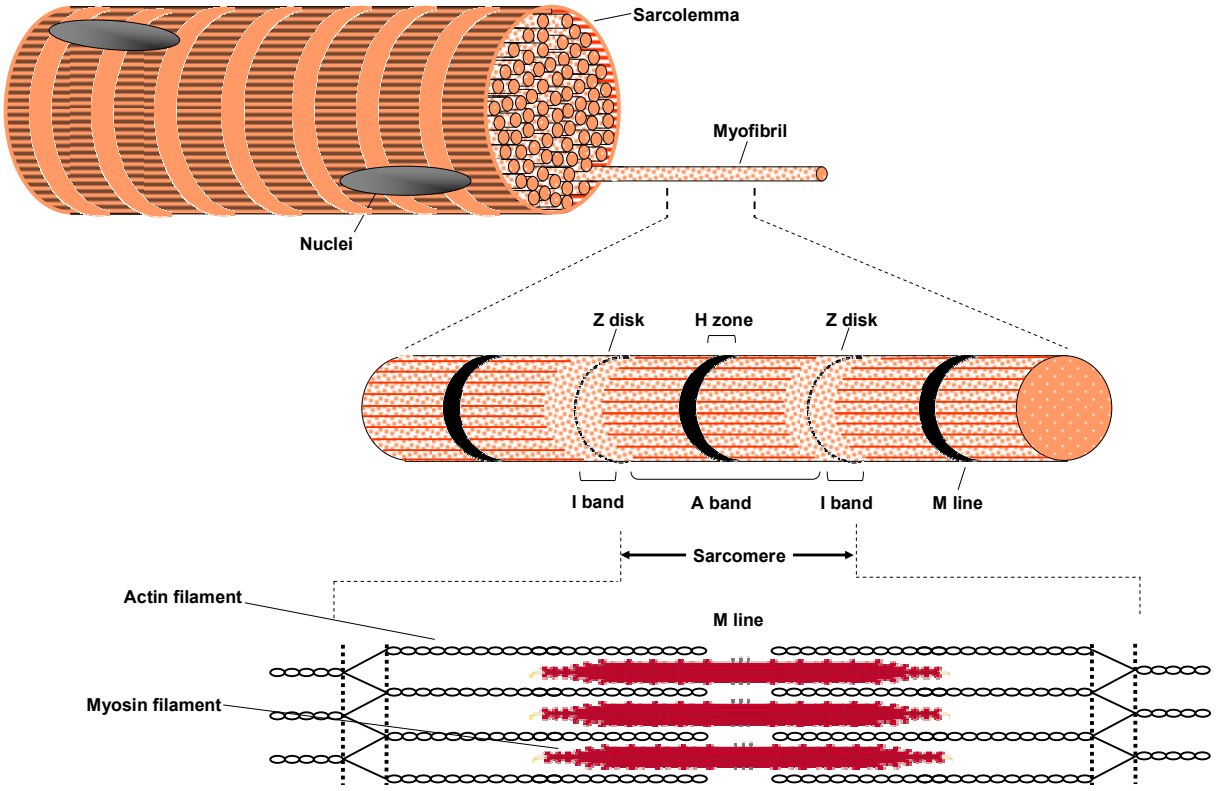

Figure 1-14 The structure of skeletal muscle. Skeletal muscle is composed of muscle fibres which express contractile proteins organised into myofibrils.

A unique feature of skeletal muscle is its fibre type heterogeneity, which allows for different functional capabilities (Table 1-2). There are two main types of muscle fibre; Type I (oxidative, slow-twitch) fibres, and type IIa / IIb / IIx (glycolytic, fast-twitch) fibres (Bottinelli & Reggiani, 2000). Type I fibres express slow myosin heavy chain (MHC) isoforms, that give these fibres slow contractible properties

and high resistance to fatigue. These fibres generate energy by oxidising fatty acids, and have high levels of intramyocellular TAG (Bottinelli & Reggiani, 2000). Type II fibres exist in three forms; type IIa, type IIb and type IIx. All express fast MHC isoforms giving these fibres a fast contraction velocity, but fatigue relatively quickly when compared to type I fibers. Type IIa and IIx fibres generate energy from fatty acid oxidation and glycolysis, whereas type IIb fibres are solely glycolytic (Bottinelli & Reggiani, 2000). Most muscle beds are a mixture of both type I and type II fibres, but their relative composition varies according to the action of that muscle. Exercise can influence MHC expression and thus induce fibre type switching from type IIb to type IIa and type I fibres (Jarvis et al., 1996; Olson & Williams, 2000).

Fiber Type	Type I fibers	Type IIa fibers	Type IIx fibers	Type IIb fibers
Contraction time	Slow	Moderately Fast	Fast	Very fast
Size of motor neuron	Small	Medium	Large	Very large
Resistance to fatigue	High	Fairly high	Intermediate	Low
Activity Used for	Aerobic	Long-term anaerobic	Short-term anaerobic	Short-term anaerobic
Max. duration of use	Hours	<30 minutes	<5 minutes	<1 minute
Power produced	Low	Medium	High	Very high
Mitochondrial density	High	High	Medium	Low
Capillary density	High	Intermediate	Low	Low
Oxidative capacity	High	High	Intermediate	Low
Glycolytic capacity	Low	High	High	High
Major storage fuel	Triglycerides	Creatine phosphate, glycogen	Creatine phosphate, glycogen	Creatine phosphate, glycogen
Myosin heavy chain	MYH7	MYH2	MYH1	MYH4

Table 1-2 Comparison between the different skeletal muscle fibre types.

1.9. Lipid metabolism in the skeletal muscle

1.9.1. Fatty acid oxidation (β-oxidation)

In the fasted state, fee fatty acids are sequentially broken down in the mitochondria by a process called β-oxidation and the break down products are subsequently used to generate ATP by oxidative-phosphorylation (Figure 1-15). Transport of fatty acids (in the form of acyl-CoAs) across the outer mitochondrial membrane is the rate limiting step of β-oxidation. Carnitine palmitoyltransferase-1 (CPT-I) facilitates this transport, by conjugating the fatty acyl groups with carnitine, releasing free CoA into the cytosol. Acyl-carnitine is then free to cross the outer mitochondrial membrane to the inter-membrane space (Fritz & Yue, 1963). Subsequent transport across the inner mitochondrial membrane is facilitated by carnitine-acylcarnitine translocase (CAT) (Murthy & Pande, 1984). Acyl-carnitine is then converted back to acyl-CoA by inner membranes bound carnitine palmitoyltransferase II (CPT-II), leaving the free carnitine to cycle back to the cytosol. Once in the mitochondrial matrix, acyl-CoA is broken down by multiple rounds of a 4 reaction process. Each round, two cabons are cleaved from acyl-CoA, producing acetyl-CoA and 1 molecule of NADH and $FADH_2$ respectively. This process continues until all but two carbons of the original acyl chain remain (Rasmussen & Wolfe, 1999). The NADH and $FADH_2$ generated are utilised as reducing power to generate a proton electrochemical gradient across the inner mitochondrial membrane. Dissipation of this gradient through the inner membrane bound ATP-synthase allows for coupling of ADP to inorganic phosphate (Pi) generating ATP (oxidative phosphorylation). Furthermore, the

multiple acetyl-CoA molecules generated by oxidation of acyl-CoA enter the tricarboxylic acid (TCA) cycle in the mitochondrial matrix - generating more reducing power and consequently more ATP molecules.

1.9.1.1. Regulation of β-oxidation

The rate limiting step of β-oxidation; the transport of acyl-CoA across the outer mitochondrial membranes, is inhibited by the catalytic product of acetyl-CoA carboxylase-2 (ACC2) – malonyl-CoA (Abu-Elheiga et al., 2001). ACC2 is phosphorylated and inhibited by AMPK, and since the latter is activated by a low ATP/ADP ratio, β-oxidation is tightly regulated by the energy status of the cell (Carling et al., 1989; Yeh, Lee & Kim, 1980) . Furthermore, there is evidence that GCs regulate β-oxidation, however, their effect varies depending upon the tissue exposed. For example, GCs appear to inhibit β-oxidation in the liver (Letteron et al., 1997), whereas in the skeletal muscle GCs are reported to stimulate β-oxidation (Salehzadeh et al., 2009).

1.9.2. Lipolysis

Within the cytosol of muscle cells, located adjacent to the mitochondria, are stored lipids in the form of TAG (intramyocellular triacylglycerides, IMTG) which, during exercise or fasting, are broken down, liberating free fatty acids that are subsequently used to generate ATP by β-oxidation (Figure 1-15). The most studied lipolytic enzyme expressed in skeletal muscle is hormone sensitive lipase (HSL) (Langfort et al., 2000; Langfort et al., 1999; Watt, Heigenhauser & Spriet,

2003). This enzyme is capable of cleaving fatty acids from both TAG and diacylglycerides (DAG), but acts predominantly upon the latter, generating monoacylglycerides (MAG) (Haemmerle et al., 2002). The remaining fatty acid is cleaved from MAG by monoacylglyceride lipase (MAGL), releasing glycerol (Karlsson et al., 1997). Type I muscle fibres also highly express adipose triglyceride lipase (ATGL) which hydrolyses TAG generating DAG and a fatty acid (Jocken et al., 2008; Villena et al., 2004).

1.9.2.1. Regulation of lipolysis

The rate of lipolysis within the skeletal muscle is regulated primarily at the level of HSL. Adrenaline has a stimulatory effect upon lipolysis by activating the β-adrenergic receptor (Langfort et al., 1999). This results in activation of adenylate cyclase; increases cytosolic cAMP levels - resulting in PKA activation. PKA is known to phosphorylate and activate HSL. By contrast, insulin has anti-lipolytic action, by activating PDE3B resulting in a reduction of cytosolic cAMP levels leading to reduced PKA activation (Enoksson et al., 1998). Muscle contraction increases lipolysis by activating HSL by a pathway involving protein kinase C (PKC) and extracellular signal-related kinase (ERK) activation (Donsmark et al., 2003). The role of AMPK in the regulation of lipolysis is controversial. For example, exercise induced activation of AMPK mediates inhibitory phosphorylation of HSL, preventing its activation by adrenergic stimulation (Watt et al., 2004). This was supported by a study where AMPK was made constitutively active in a rat skeletal muscle cell line, inhibiting HSL function (Watt et al., 2006). However, in isolated rat soleus muscles undergoing contraction,

variable HSL activation was observed in the face of constant AMPK activation (Donsmark et al., 2004).

Lipolysis is increased by GCs in adipose tissue and the liver, consistent with its role as a catabolic effector (Divakaran & Friedmann, 1976; Senft et al., 1968; Xu et al., 2009). The proposed mechanism is thought to involve a GC-mediated downregulation of PDE3B, thus increasing cytosolic cAMP levels (Senft et al., 1968). Furthermore, GCs have also been found to upregulate the expression of both HSL and ATGL in adipose tissue (Xu et al., 2009). In human skeletal muscle, GC infusion also has a stimulatory effect upon lipolysis. In addition, co-infusion of both GCs and growth hormone has an additive stimulatory impact upon lipolytic rates in this tissue (Djurhuus et al., 2004). Although it is not clear how GCs increase intramyocellular lipolysis, a downregulation of PDE3B following GC treatment has been identified in skeletal muscle (Senft et al., 1968)

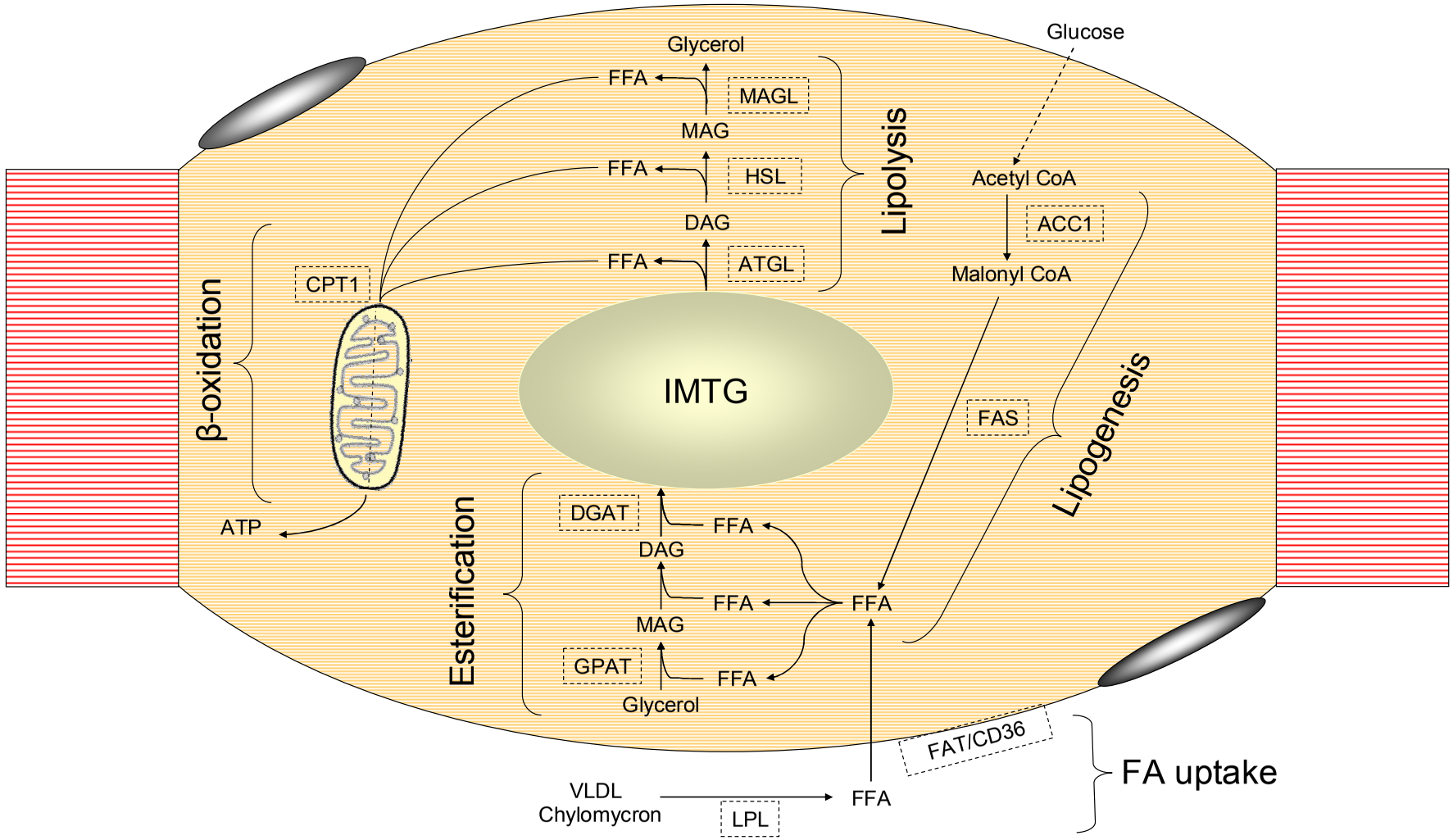

Figure 1-15 Lipid metabolism within the skeletal muscle. (IMTG- intramyocellular triglycerides, MAG= monoacylglycerides, DAG= diacylglycerides, FFA= free fatty acids, VLDL= very low dencity lipoproteins)

1.9.3. Fatty acid uptake

The predominant source of skeletal muscle fatty acids is through uptake of liver / diet derived fatty acids from the circulation (Figure 1-15). The liver synthesises fatty acids by *de novo* lipogenesis, which are subsequently esterified into TAG and packaged, along with cholesteryl esters, phospholipids and apolipoproteins, into very low density lipoproteins (VLDL). In the fasted state, the liver releases VLDL into the circulation where the constituent fatty acids are used by the skeletal muscle as a fuel (Gibbons et al., 2004). In addition, another source of fatty acids is from the intake of dietary lipids. These are absorbed into intestinal mucosal cells (enterocytes) where they are packaged with cholesteryl esters, phospholipids and apolipoproteins to form chylomicrons which are subsequently released into the circulation (Mu & Hoy, 2004). Neither VLDL nor chylomicrons can cross the plasma membrane of skeletal myocytes, however, hydrolysis of these particles by lipo-protein lipase (LPL) liberates free fatty acids which can enter the cell (Bickerton et al., 2007). Skeletal muscle secretes LPL, which attaches to chains of heparin sulphate on endothelial cells within the vascular space of the skeletal muscle (Kiens et al., 2004; Scow, Blanchette-Mackie & Smith, 1976). Once released by LPL, free fatty acids can enter the muscle cells by simple diffusion across the plasma membrane or via the fatty acid transporter FAT/CD36 (Bonen, Miskovic & Kiens, 1999). Skeletal muscle also expresses fatty acid binding proteins (FABP) which facilitate fatty acid uptake and intracellular transport (Binas et al., 2003). The predominant FABP isoform expressed in the skeletal muscle is FABP3 (Fischer et al., 2006). Fatty acids absorbed from the circulation are either esterified with glycerol and stored as TAG (when energy

demands are low), or enter β-oxidation and used to generate ATP (when energy demands are high).

1.9.3.1. Regulation of fatty acid uptake

Insulin enhances fatty acid uptake into skeletal muscle by increasing expression of the FAT/CD36 transporter (Corpeleijn et al., 2008; Dyck et al., 2001). Similarly, muscle contraction increases fatty acid uptake by upregulating LPL (Kiens et al., 1989), FABP and increasing membrane localisation of FAT/CD36 (Bonen et al., 2000). However, the main mechanism by which exercise enhances fatty acid uptake into the skeletal muscle is via increased muscle capillary blood flow, allowing for increased LPL-mediated lipolysis. The effect of GCs upon skeletal muscle fatty acid uptake has not been investigated to date, however, GCs have been found to increase fatty acid uptake in adipocytes by upregulating LPL expression (Ashby & Robinson, 1980).

1.9.4. Fatty acid esterification

The predominant source of intramyocellular TAG is through esterification of fatty acids taken up from the circulation (Figure 1-15). Esterification involves the conjugation of three fatty acids to a single glycerol-3-phosphate molecule, but intramyocellular hydrolysis of IMTG is also a source. Glycerol-3-phosphate can be generated from the precursors: lactate, pyruvate, alanine or TCA-cycle intermediates by glyceroneogenesis, which accounts for ~60% of the synthesized glycerol-6-phosphate (Nye, Hanson & Kalhan, 2008). The remaining ~40% of

skeletal muscle glycerol-3-phosphate come from glycolysis. An additional, yet minor source of glycerol-3-phosphate is via uptake of plasma glycerol (Coppack et al., 1999) and subsequent phosphorylation by glycerol kinase (GlK) (Newsholme & Taylor, 1969; Seltzer et al., 1989). The main enzymes involved in fatty acid esterification are: glycerol-3-phosphate acyltransferase (GPAT), which catalyses the addition of the first fatty acid to glycerol-3-phosphate; and diacylglycerol acyltransferase (DGAT), which mediates addition of a fatty acid at the third position.

1.9.4.1. Regulation of esterification

AMPK has been found to phosphorylate and inhibit GPAT - linking the rate of TAG synthesis to the energy status of the cell (Muoio et al., 1999). By contrast, insulin upregulates TAG synthesis by increasing GPAT expression (Gonzalez-Baro, Lewin & Coleman, 2007). Furthermore, exercise upregulates sterol regulatory element-binding protein 1 (SREBP-1), which in turn upregulates DGAT - enhancing esterification (Ikeda et al., 2002).

1.9.5. *De novo* lipogenesis

De novo lipogenesis is the process by which simple sugars, such as glucose, are converted to fatty acids which are subsequently esterified to glycerol-3-phosphate (Figure 1-15). Although *de novo* lipogenesis is not thought to be a major contributor to intramyocellular lipid stores under normal conditions, it is thought to occur under hyperglycaemic conditions (Aas et al., 2004; Baltzan et al., 1962;

Gaster & Beck-Nielsen, 2006; Guillet-Deniau et al., 2004). The principle building blocks for fatty acid synthesis are acetyl-CoA, produced in the mitochondria from the metabolism of fatty acids, pyruvate, ketone bodies and certain amino acids. Many of the lipogenic enzymes are located in the cytosol, consequently, acetyl-CoA is converted to citrate allowing for its transport across the mitochondrial membrane, where it is subsequently converted back to acetyl-CoA by citrate lyase in the cytosol (Haralambie, 1977). The first and rate limiting step of *de novo* lipogenesis is the ATP-dependent conversion of acetyl-CoA to malonyl-CoA, catalyzed by acetyl-CoA carboxylase 1 (ACC1) (Lane, Moss & Polakis, 1974). Fatty acid synthase (FAS) then condenses malonyl-CoA with acetyl-CoA, by a series of reactions leading to the formation of acyl-CoA. Subsequent reactions between newly synthesized malonyl-CoA molecules and the growing acyl-CoA chain eventually result in the formation of the fatty acid palmitate (16 carbons) (Smith, Witkowski & Joshi, 2003).

1.9.5.1. Regulation of de novo lipogenesis

De novo lipogenesis within the skeletal muscle is induced in an SREBP-dependent manner by glucose: through upregulation of FAS and ACC1 (Guillet-Deniau et al., 2004); by insulin: through upregulation of FAS and citrate lyase (Guillet-Deniau et al., 2002); and by muscle contraction: through upregulation of ACC1 (Ikeda et al., 2002). Furthermore, GCs have been found to augment the stimulatory actions of insulin upon lipogenesis in adipose tissue by upregulating FAS expression and activity (Wang et al., 2004).

1.10. Lipotoxicity and insulin resistance in the skeletal muscle

1.10.1. Intramyocellular triglycerides

Lipotoxicity is the aberrant accumulation of IMTG and other lipid species within the skeletal muscle, resulting in chronic cellular dysfunction. IMTG turnover is a measure of the balance between TAG synthesis and degradation; both are influenced by β-oxidation rates and plasma fatty acid availability. High levels of IMTGs are associated with insulin resistance and type 2 diabetes (Koyama et al., 1997; Pan et al., 1997; van Loon et al., 2004), however, endurance athletes also have an increased IMTG content whilst maintaining a high sensitivity to insulin, suggesting that a build up of IMTG per se, does not cause insulin resistance (Pruchnic et al., 2004; Tarnopolsky et al., 2007; van Loon et al., 2004). Recently, it has been proposed that the accumulation of lipid intermediates, such as long-chain fatty acyl-CoAs, DAGs and ceramides, derived from IMTG stores, are actually the species responsible for inducing the insulin resistance. Since endurance athletes are thought to have a higher IMTG turnover, accumulation of these harmful metabolites is avoided. By contrast, in insulin resistant subjects, the defects in lipid metabolism are partly attributed to a reduction in mitochondrial number and function (Kelley et al., 2002). This results in diminished / incomplete oxidation of fatty acids, contributing to the accumulation of insulin resistance-inducing lipid intermediates (Figure 1-16) (Muoio & Koves, 2007). Multiple factors have been associated with mitochondrial dysfunction, including: age, poor diet, lack of exercise as well as polymorphisms in the mitochondrial biosynthesis regulator PGC-1α (Phielix & Mensink, 2008). In this section, the consequences of

elevated intramyocellular long-chain fatty acyl-CoAs, DAG and ceramide levels upon the insulin sensitivity of skeletal muscle will be discussed.

1.10.2. Long-chain fatty acyl-CoA

Elevated intracellular long-chain fatty acyl-CoA are associated with insulin resistance (Chalkley et al., 1998; Chen et al., 1992; Oakes et al., 1997b). Intracellular fatty acyl-CoAs are derived from the hydrolysis of IMTG stores, or taken up from the circulation. Rat soleus muscles incubated with fatty acids have reduced insulin-stimulated glycogen synthesis and glucose uptake (Thompson et al., 2000). Also, high-fat fed rats, fasted overnight or exercised, have reduced intracellular fatty acyl-CoA levels, and improved insulin sensitivity (Oakes et al., 1997a). To date, it is unclear if / how long-chain fatty acyl-CoAs mediate these effects, although direct inhibition of hexokinase (HK) has been proposed as a potential mechanism, decreasing glucose flux (Tippett & Neet, 1982). However, it is likely that the elevated intracellular long-chain fatty acyl-CoAs levels seen in states of insulin resistance are merely a marker of increased DAG / ceramides accumulation.

1.10.3. Diacylglycerides

Accumulation of intracellular DAG is also linked to insulin resistance (Figure 1-16) (Montell et al., 2001; Saha et al., 1994; Yu et al., 2002). DAG can be generated from multiple sources, including: hydrolysis of phospholipids by phospholipase C and D (PLC, PLD), esterification of two fatty acids with glycerol-3-phosphate and

hydrolysis of IMTG by ATGL. The latter two routes are likely to be the most predominant source of intramyocellular DAG. DAG levels have also been found to be negatively regulated by diacylglycerol kinase-δ (DGK-δ), which phosphorylates DAG forming phosphatidic acid. Interestingly, DGK-δ is downregulated in type 2 diabetes (Chibalin et al., 2008). Regulation of fatty acid saturation also impacts upon DAG levels, since saturated fatty acids (e.g. palmitate) are preferentially incorporated into DAG, rather than TAG (Pickersgill et al., 2007). This is exemplified by inhibition of stearoyl-CoA desaturase-1 (SCD-1) (a key enzyme involved formation of monounsaturated fatty acids), resulting in reduced insulin sensitivity (Pinnamaneni et al., 2006).

Within the cell, DAG has an important role as a second messenger through its ability to activate PKC. The PKC family consists of ~12 isozymes, derived from multiple genes by alternative splicing (Nishizuka, 1988). There are three PKC subclasses: classical (cPKCα, βI, βII, γ), which are DAG, Ca^{2+} and phospholipid dependent; novel (nPKCδ, θ, ε, η) which are DAG and phospholipid dependent; and atypical (aPKCζ, λ), which are independent of DAG, Ca^{2+} and phospholipids (Newton, 1995). PKC activation involves their translocation to the plasma membrane where they phosphorylate numerous targets. In the skeletal muscle extracted from high fat fed rats, an increased proportion of PKCθ, PKCε and PKCδ localised at the plasma membrane was observed, correlating with the elevated intracellular DAG levels (Heydrick et al., 1991). Increased membrane localisation of PKCθ has been found in lipid infused rats, which was associated with enhanced inhibitory serine-307 phosphorylation of IRS1, and reduced IRS1-associated PI3K activity (Figure 1-16) (Yu et al., 2002). PKCθ is further implicated

in DAG-induced insulin resistance from the PKCθ$^{-/-}$ mice, which are markedly insulin sensitive compared to control mice following lipid infusion (Kim et al., 2004). In humans, lipid infusion increased DAG accumulation and PKCβII and PKCθ membrane localisation within the skeletal muscle (Itani et al., 2002).

1.10.4. Ceramides

Ceramides are a family of lipid species that function as signalling molecules. Within the cell they signal apoptosis and inhibit cell division (Haimovitz-Friedman, Kolesnick & Fuks, 1997). Ceramide accumulation has been reported in the skeletal muscle of insulin resistant animals (Figure 1-16) (Turinsky, O'Sullivan & Bayly, 1990), obese insulin resistant humans (Adams et al., 2004) and lipid infused humans (Straczkowski et al., 2004). Accumulation of ceramides could be a consequence of sphingomyelin hydrolysis (a plasma membrane constituent), catalysed by sphingomyelinase (Hannun & Obeid, 2002). Alternatively, ceramides can be generated from two fatty acids and a serine in four enzymic steps (Merrill & Jones, 1990). The first step is rate limiting, catalysed by serine palmitoyltransferase (SPT), which specifically requires a saturated fatty acid as substrate. Increased saturated fatty acid uptake by the skeletal muscle, or inhibition of SCD-1 enhance ceramide levels (as well as DAG levels, as discussed above) (Pickersgill et al., 2007; Pinnamaneni et al., 2006).

The mechanism by which ceramides induce insulin resistance is via activation of PP2A, which dephosphorylates and inactivates PKB/akt (Stratford et al., 2004). Furthermore, ceramides have been found to activate PKCζ, which phosphorylates

PKB/akt within the PH-domain - preventing PIP_3 association at the plasma membrane (Figure 1-16) (Hajduch et al., 2001; Powell et al., 2003).

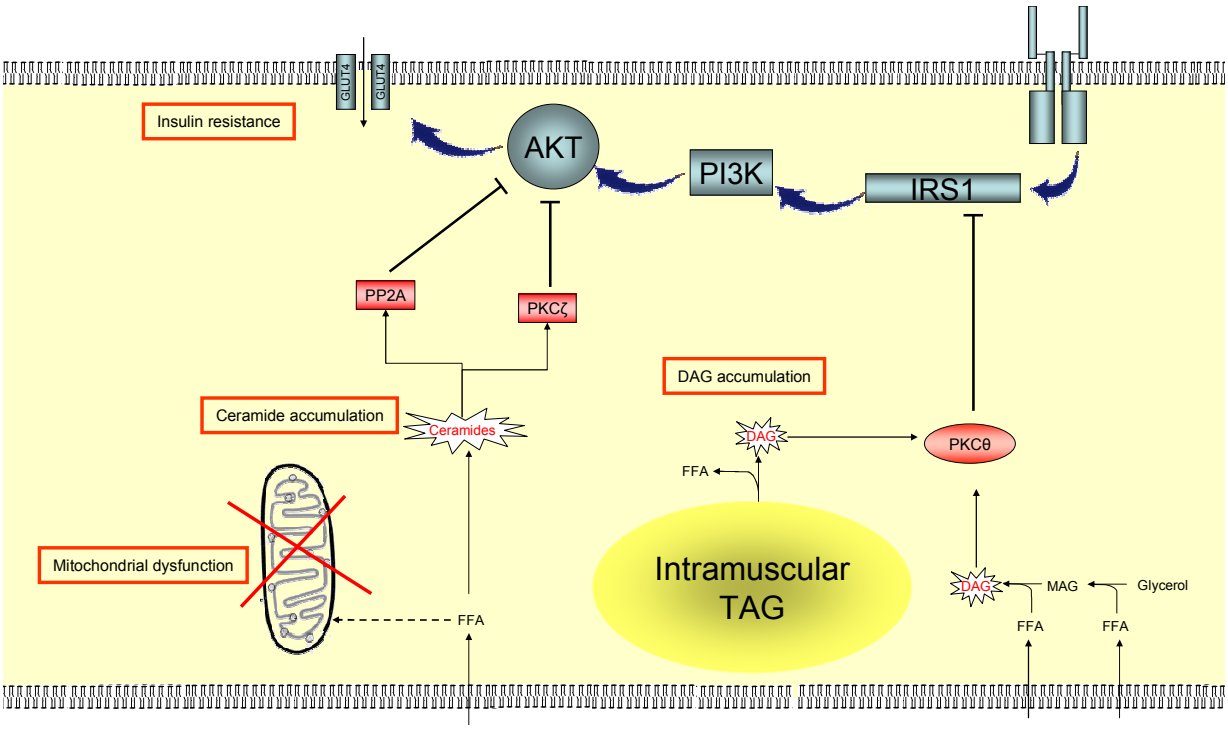

Figure 1-16 Lipotoxicity within the skeletal muscle. Aberrant accumulation of DAG and ceramides contribute to insulin resistance.

1.11. Skeletal muscle and adipose tissue crosstalk

Adipose tissue is key endocrine organ that is central to whole-body metabolic homeostasis. Adipose tissue secretes a large number of factors known collectively as adipokines, which regulate numerous processes ranging from inflammation to insulin sensitivity and appetite. Altered production of adipokines contributes to the association between obesity and type 2 diabetes. Importantly, many of these secreted factors impact upon the insulin sensitivity of the skeletal muscle, and consequently play an important role in the pathogenesis of insulin resistance and type 2 diabetes (Figure 1-17). In this section, the mechanisms by which some of these adipokines modulate the insulin sensitivity of skeletal muscle will be discussed.

1.11.1. Adiponectin

Adiponectin (also known as AdipoQ) has recently emerged as a key adipokine. It acts as an insulin sensitizer / mimetic and has additional, anti-atherogenic, anti-inflammatory and cardioprotective properties (Whitehead et al., 2006). In contrast to the majority of adipokines, circulating levels of adiponectin are decreased in obese (Arita et al., 1999) and type 2 diabetic humans (Hotta et al., 2000). Adiponectin has been found to have a beneficial effect upon lipid metabolism within the skeletal muscle, by increasing fatty acid oxidation and thus reducing IMTG content in both mice (Fruebis et al., 2001) and humans (Thamer et al., 2002). These beneficial effects are thought to be mediated via increased transcriptional activity of PPARα, which in turn leads to increased expression of

target genes including: CPT1, which catalyses the rate limiting step of β-oxidation (Yoon et al., 2006). Consequently, a reduction in adiponectin levels contributes to elevated IMTG levels, which are strongly correlated with reduced insulin sensitivity, as discussed in section 1.10.1.

1.11.2. Resistin

The role of resistin in the metabolic syndrome has been the subject of much controversy. In mice, resistin levels are elevated in obesity (Rajala et al., 2004), and have also been associated with insulin resistance when overexpressed (Satoh et al., 2004). Moreover, resistin knockout mice are insulin sensitive (Banerjee et al., 2004), however, resistin expression differs between rodents and humans. In rodents, resistin is expressed in white adipose tissue, whereas in humans it appears to be limited to mononuclear cells (Savage et al., 2001). Further inconsistencies have been found with human association studies. For example, some have shown that high resistin levels are associated with obesity and insulin resistance (Osawa et al., 2008), whereas others have not (Kielstein et al., 2003). In rodent skeletal muscle, resistin decreased insulin stimulated glucose uptake (Jorgensen et al., 2009; Moon et al., 2003). However, although resistin appears to mediate insulin sensitivity in rodent adipocytes (Steppan et al., 2005) and hepatocytes (Liu et al., 2008) by upregulating SOCS3, this does not appear to be its mechanism of action in skeletal muscle (Jorgensen et al., 2009).

1.11.3. Pro-inflammatory cytokines

Systemic inflammation is thought to have a role in the pathogenesis of insulin resistance, since markers of inflammation are elevated in obese and insulin resistant subjects. Many of these pro-inflammatory cytokines are derived from the adipose tissue.

1.11.3.1. Tumour necrosis factor-α

Expression of TNFα in adipose tissue is increased in obese and insulin resistant subjects (Hotamisligil et al., 1995) (Hotamisligil, Shargill & Spiegelman, 1993). Serum levels of TNFα are also increased in obesity (Olszanecka-Glinianowicz et al., 2004) and type 2 diabetes (Spranger et al., 2003; Zinman et al., 1999), however, this is not a consistent finding (Ho et al., 2005). At a cellular level, TNFα is thought to activate several key kinases associated with insulin resistance in the skeletal muscle, including: IKKβ (Jiang et al., 2003) and cJUN (Aguirre et al., 2000) both of which are involved in inhibitory serine phosphorylation of IRS1. Furthermore, TNFα upregulates sphingomyelinase which hydrolyses sphingomyelin located within the plasma membrane, generating ceramides – also contributing to reduced insulin sensitivity (see section 1.10.4) (Murase et al., 1998). TNFα has been linked with muscle wasting by inhibiting myoblast differentiation (Szalay, Razga & Duda, 1997) and enhancing protein degradation (Garcia-Martinez et al., 1993).

1.11.3.2. Interleukin factor-6 (IL-6)

Adipose derived circulating levels of IL-6 are increased in obese and insulin resistant subjects (Kern et al., 2001; Spranger et al., 2003). Following weight loss, circulating levels of IL-6 are reduced (Bastard et al., 2000). Cell culture experiments using human primary myotubes found IL-6 to induce insulin resistance by upregulating SOCS3 (Rieusset et al., 2004).

The adipokines discussed here represent a handful of a growing list secreted from adipose tissue. Other adipokines, whose aberrant expression and circulating levels potentially impact upon the insulin sensitivity of the skeletal muscle include: PAI-1 (Alessi et al., 2000), vaspin (Youn et al., 2008) and leptin (Mohiti, Talebi & Afkhami-Ardekani, 2009).

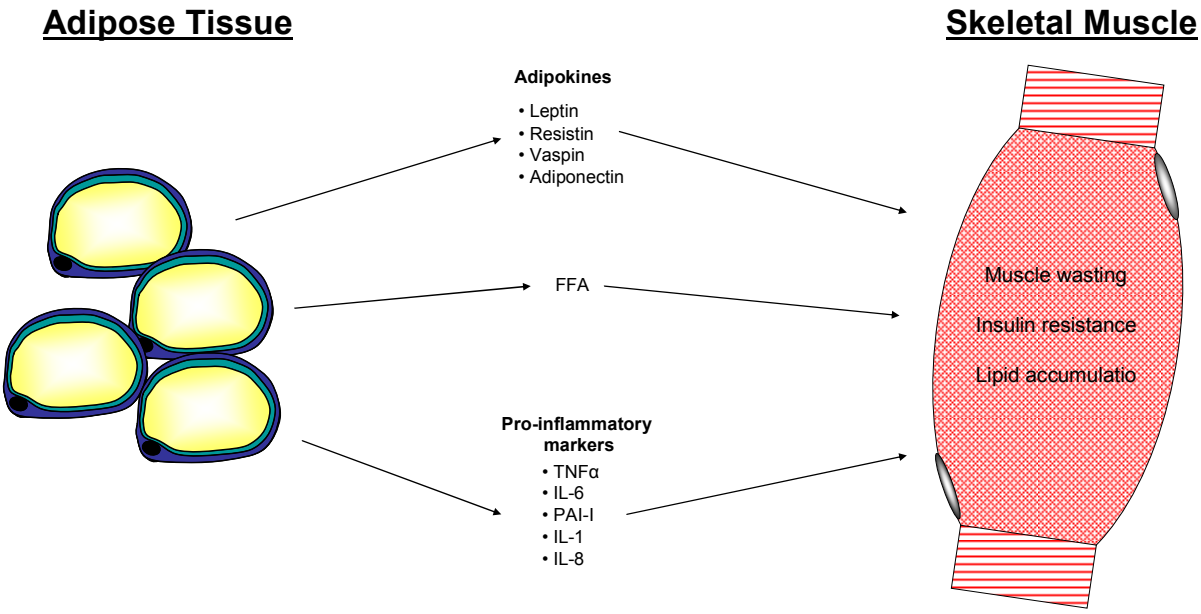

Figure 1-17 Tissue crosstalk between adipose tissue and the skeletal muscle.

1.12. GCs, atrophy & insulin resistance in skeletal muscle

1.12.1. Glucocorticoid excess

The classical example of GC excess, Cushing's disease, was first described by Harvey Cushing in 1912. This relatively uncommon disease is caused by a pituitary tumour secreting ACTH, which in turn, drives increased cortisol secretion from the adrenal (Cushing, 1913). By contrast, the more prevalent Cushing's syndrome typically arises as a result of an adrenal tumour - driving ectopic cortisol release. Alternatively, aberrant ACTH secretion from anywhere other than the pituitary (e.g. lung tumour), can also result in this condition, however, the most common cause is GC therapy. An estimated 0.3% of the population are taking prescribed high dose GCs (>7.5mg daily) to benefit from their immunosuppressive anti-inflammatory properties (van Staa et al., 2000).

The elevated circulating cortisol in patients with Cushing's disease/syndrome result in a wide range of pathologies, such as: increased visceral adipose mass, skin thinning, hypertension, muscle wasting and insulin resistance - ultimately leading to type 2 diabetes. Metabolic syndrome, which affects 1 in 5 adults (Ford, Giles & Dietz, 2002), shares many similarities to Cushing's syndrome/disease. These include central obesity, glucose intolerance, insulin resistance, type 2 diabetes and increased cardiac risk of mortality (Friedman et al., 1996). Due to these similarities, there has been much interest into the role GCs play in the pathology of insulin resistance and type 2 diabetes.

1.12.2. Glucocorticoids and skeletal muscle atrophy

GCs are required for the activation of muscle protein degradation in several muscle atrophy models (May, Kelly & Mitch, 1986; Mitch et al., 1999; Wing & Goldberg, 1993). Skeletal muscle proteolysis is partly regulated by the IRS1–associated PI3K/Akt axis. Under insulin / IGF1 stimulation, activation of this axis leads to PKB/akt-induced phosphorylation and inhibition of the forkhead family of transcription factors (e.g. FOXO1), which are required for the transcription of proteolytic genes, such as the E3 ubiquitin ligase, atrogin-1 (Sandri et al., 2004). Under conditions whereby the activity of the IRS1–associated PI3K/Akt axis is reduced, FOXO1 becomes dephosphorylated and activated, resulting in increased atrogin-1 transcription and consequently enhanced protein breakdown (Sandri et al., 2004). It has recently been shown that activated GR competes with IRS1 for binding PI3K; enhancing FOXO1 activation, leading to increased proteolysis. This represents a non-genomic action of GCs (Hu et al., 2009). FOXO3 also regulates the expression of key atrophy genes, including atrogin-1, and also enhances autophagy (the degradation of cellular components through the lysosomal machinery). The activity of FOXO3, like FOXO1, is inhibited is by akt phosphorylation (Zhao et al., 2008).

GCs have also been shown to increase skeletal muscle proteolysis by upregulating the expression of another E3 ubiquitin ligase, muscle specific ring finger-1 (MuRF1) (Waddell et al., 2008), a gene upregulated in several atrophy conditions (Gomes et al., 2001; Lecker et al., 2004). In contrast to the above, the actions of GCs upon MuRF1 expression are via the association between

activated GR and a GRE located within the MuRF1 promoter. As with atrogin-1, transcriptional activation is dependent upon activated FOXO1. Furthermore, IGF1 has been found to overcome the GC-induced increase in MuRF1 expression, which correlates with loss of FOXO1 binding to the promoter (Waddell et al., 2008).

1.12.3. Glucocorticoids & the insulin signalling cascade

As discussed above, GC excess induces whole body insulin resistance. However, since skeletal muscle accounts for ~80% of glucose disposal, under insulin stimulating conditions, it is inferred to be a major site of GC-induced insulin resistance (DeFronzo et al., 1981). The interaction between GC and the insulin signalling cascade in skeletal muscle has only been examined in a small number of studies, which have offered varying explanations for the induction of insulin resistance. Chronic GC treatment decreases insulin-stimulated glucose uptake and GLUT4 translocation in skeletal muscle, without reducing the total content of GLUT4 (Dimitriadis et al., 1997; Haber & Weinstein, 1992). This suggests that the defect in insulin signalling lies upstream of GLUT4. Many studies have shown that GC exposure reduces insulin stimulated PKB/akt phosphorylation (Ruzzin, Wagman & Jensen, 2005), however, this is not a consistent finding (Rojas, Hirata & Saad, 2003). Similarly, IRS1 protein content and tyrosine phosphorylation appear to be reduced in skeletal muscle following GC treatment (Giorgino & Smith, 1995; Rojas et al., 2003), as is IRS1-associated PI3K activity (Giorgino et al., 1997; Giorgino & Smith, 1995; Hu et al., 2009; Rojas et al., 2003; Saad et al., 1993). By contrast, InsR levels and autophosphorylation are reproducibly

unaffected by GC exposure in skeletal muscle (Block & Buse, 1989; Leighton et al., 1987; Saad et al., 1993), suggesting the defect lies downstream of the receptor. In summary, although it is clear that GC have an inhibitory effect upon the insulin signalling cascade in skeletal muscle, the precise molecular mechanism underpinning these observations is unclear.

1.12.4. Lipotoxicity and glucocorticoids

GCs have been linked with the accumulation of insulin resistance inducing lipid metabolites within the skeletal muscle. High fat fed mice treated with the synthetic GC, dexamethasone, have increased IMTG and DAG levels within skeletal muscle. The precise mechanisms by which GCs induce these changes are unclear, but the authors speculated that they may exacerbate the lipid exchange between adipose tissue and skeletal muscle. These mice were also insulin resistant, which may attributed to the elevated DAG levels - inducing PKC activation (Gounarides et al., 2008). In support of this hypothesis, GCs activate conventional PKC isoforms (PKCα, and β) in rodent adipocytes, and their inhibition (with use of a conventional PKC selective inhibitor) reversed the dexamethasone induced insulin resistance in these cells (Kajita et al., 2000; Kajita et al., 2001). GCs have also been found to enhance *de novo* ceramides synthesis in the skeletal muscle by upregulating SPT (Holland et al., 2007).

1.13. 11β-HSD1 and insulin resistance

1.13.1. 11β-HSD1 activity and expression in insulin resistance

11β-HSD1 is expressed and is biologically active in human skeletal muscle (Jang et al., 2006). Elevated 11β-HSD1 has been described in rodent skeletal muscle in models of diabetes (Zhang et al., 2009), and in myotubes isolated from patients with insulin resistance and type 2 diabetes (Abdallah, Beck-Nielsen & Gaster, 2005; Whorwood et al., 2002), however, this is not a consistent finding (Jang et al., 2007) and its precise contribution to metabolic and muscle phenotype is still to be clarified.

1.13.2. Genetics of 11β-HSD1 and insulin resistance

As discussed in section 1.2, epidemiologic and family studies have demonstrated that there is a moderate genetic influence on the development on insulin resistance. With respect to the HSD11B1 gene, one study conducted in children has found that an intronic single nucleotide polymorphism is associated with insulin resistance (Gelernter-Yaniv et al., 2003).

1.14. 11β-HSD animal models

1.14.1. 11β-HSD1 knockout

Whole body knockout of 11β-HSD1 in mice has a beneficial metabolic phenotype. 11β-HSD1 null mice are insulin sensitive; resisting hyperglycaemia-induced by stress (Kotelevtsev et al., 1997), and are protected from type 2 diabetes when fed on a high fat diet (Morton et al., 2004). Much of the research as to why these mice are insulin sensitive has focussed upon the liver and adipose. Hepatic gluconeogenesis is attenuated in the fasted state (Kotelevtsev et al., 1997), and basal and insulin stimulated glucose uptake is increased in the adipose tissue (Morton et al., 2004). However, the metabolic impact of 11β-HSD1 knockout in skeletal muscle has not been explored.

The 11β-HSD1 knockout mice are further protected from the accumulation of visceral fat when fed on a high fat diet (Morton et al., 2004). Interestingly, these mice have a higher adrenal secretion of corticosterone, which is attributed to adrenal hyperplasia (Kotelevtsev et al., 1997).

1.14.2. Hexose-6-phosphate dehydrogenase knockout

As described in section 1.7.10.1, H6PDH generates NADPH, which confers the directionality of 11β-HSD1. In the H6PDH knockout mouse, 11β-HSD1 switches to a dehydrogenase - inactivating corticosterone to 11-dehydrocorticosterone (Bujalska et al., 2008; Lavery et al., 2006). These mice have a reduced ability to store lipid in adipose tissue, and serum fatty acid levels remained unchanged

upon fasting (Bujalska et al., 2008). The insulin sensitivity of these mice is improved, with increased insulin-stimulated glucose uptake in skeletal muscle beds enriched with type IIb fibres (extensor digitorum longus). By contrast, no impact upon glucose uptake of type I fibre rich muscle beds is observed (soleus) (Rogoff et al., 2007). It is unclear whether this is a consequence of GC insensitivity, or loss of other actions of H6PDH. The most striking observation is that H6PDH null mice have severe muscle myopathy. The reduced NADPH within the sarcoplasmic reticulum (SR) alters the NADPH/NADP ratio, altering the redox balance in this environment. This has a knock-on effect upon the folding of proteins in the SR, leading to activation of the unfolded protein response (UPR) pathway. Once activated, large vacuoles are formed within the type IIb fibres, which are thought to be abnormally large SR. This is followed by fibre type switching from type IIb fibres to type I fibres - accounting for the muscle myopathy (Lavery et al., 2008).

1.14.3. 11β-HSD as a therapeutic target

11β-HSD1 has been considered an attractive therapeutic target for a number of years. Human studies using the non-specific 11β-HSD inhibitor, carbenoxolone, have proved useful as proof of concept experiments, but because this compound also inhibits 11β-HSD2 (resulting in mineralocorticoid excess), carbenoxolone cannot be used therapeutically. Therefore, a number of pharmaceutical companies have developed selective 11-βHSD1 inhibitors. Published data on the metabolic impact of these compounds is predominately from rodent studies. The effects of selective 11β-HSD1 inhibition has been explored in primates and more

recently human clinical trials, although the latter is in a preliminary abstract stage (findings summarised in Figure 1-18).

The first selective inhibitor to be described was a benzene sulphonamide, BVT2733, which has a 200-fold greater selectivity for inhibiting 11β-HSD1 than 11β-HSD2 (Barf et al., 2002). This compound, when administered to rodents for 4 days, reduced fasting free fatty acid (19%), cholesterol (15%) and TAG (17%) levels, and also decreased total body weight (5%), when compared to vehicle treated animals. However, a decrease in food intake was observed (10%) which may have conferred improved metabolic function. In addition, insulin sensitivity and glucose tolerance were improved, with reductions in fasting glucose and insulin levels (Alberts et al., 2003). Hepatic gluconeogenesis was reduced by ~60% (Alberts et al., 2002; Alberts et al., 2003). In a separate study, the effectiveness of BVT2733 was compared to thiazolidinedione (TZD) compounds (PPAR agonists are currently in use as a treatment for type 2 diabetes in humans) in diabetic mice and, at the highest dose, was found to decrease blood glucose to similar levels to that induced by rosiglitazone (PPARγ agonist) (Sundbom et al., 2008). Although BVT2733 is highly effective at inhibiting rodent 11β-HSD1 (IC_{50} 96nM), it is far less effective at inhibiting the human isozyme (IC_{50} of 3341nM) (Barf et al., 2002).

An adamantyl triazole compound developed by Merck, inhibitor 544, has been tested in several rodent models (Hermanowski-Vosatka et al., 2005). When administered to diet-induced obese (DIO) mice for 11 days, reductions in fasting glucose, insulin, TAG, cholesterol and body weight were observed. Similarly,

when administered to mouse model of type 2 diabetes there were reductions in fasting glucose, insulin, glycogen, TAG, free fatty acids and an improvement in glucose tolerance. Interestingly, in mice with targeted deletion of apolipoproteins E, inhibitor 544 reduced atherosclerotic plaque formation - known to be the key clinical consequence of metabolic syndrome (Hermanowski-Vosatka et al., 2005).

The metabolic impact of another selective 11β-HSD1 inhibitor, 4-heteroarylbicycol[2.2.2]octyltriazole (Compound A), has recently been studied in rats fed on a high fat, high sucrose diet. Following a 3 week treatment with Compound A, there was a decrease in fasting serum TAG and free fatty acid levels without altering glucose and insulin levels. Food intake and body weight were unaffected at this dose. The lipid content of the liver and brown adipose tissue was decreased. Fatty acid uptake and β-oxidation rates were elevated in oxidative tissues including the skeletal muscle (Berthiaume et al., 2007a; Berthiaume et al., 2007b). More recently, Compound A has been used in combination with a TZD compound (rosiglitazone) and was found to further decrease hepatic steatosis and serum TAG levels compared to TZD treatment alone (Berthiaume et al., 2009).

To date, all published reports on the metabolic impact of 11β-HSD inhibition in humans are from the non-selective compound carbenoxolone. When administered to healthy individuals, improvements in whole body insulin sensitivity is observed (Walker et al., 1995). Carbenoxolone has also been administered to patients with type 2 diabetes, and was found to decrease glucose production, principally through decreasing glycogenolysis, with no apparent effect

on gluconeogenesis. Circulating cholesterol levels were also reduced by this compound (Andrews, Rooyackers & Walker, 2003). Although carbenoxolone has been shown to access liver and subcutaneous adipose tissue (Tomlinson et al., 2007), it is unknown whether this compound can inhibit local cortisol availability within the skeletal muscle. Furthermore, the use of carbenoxolone has limited therapeutic potential because of its inhibition of 11β-HSD2 which can lead to hypertension, hypokalemia and fluid retention (mineralocorticoid excess).

Recently, data has begun to emerge from selective 11β-HSD1 inhibitor studies in primates and humans. Compound PF-915275 selectively inhibits 11β-HSD1 in both monkeys and humans, as measured from urinary steroid metabolites and from prednisolone conversion studies (a synthetic analog of cortisone that can be distinguished from the endogenous substrate cortisone, enabling a direct measure of substrate to product conversion) (Bhat et al., 2008; Courtney et al., 2008). Following an 8 hour treatment with this compound, primates were found to have decreased fasting insulin levels. To date, there have been no formal, peer reviewed, reports in the literature regarding the effect of selective inhibitors in humans. However, some data has been published in abstract form including a compound developed by Incite (INCB13739), which is currently in phase IIb clinical trials. In phase IIa, type 2 diabetic subjects were orally administered INCB13739 or placebo for 28 days. Insulin sensitivity was assessed via hyperinsulinaemic, euglycaemic and pancreatic clamps and showed that the inhibitor improved hepatic insulin sensitivity and, more importantly, increased peripheral insulin stimulated glucose uptake. Other beneficial effects of this drug include; reduced plasma cholesterol and LDL levels. INCB13739 has recently

been administered to type 2 diabetic patients where glucose levels were not adequately controlled by the standard metformin treatment. After 12 weeks on a combination of both drugs, the INCB13739 treatment group had lower HbA1c and total cholesterol levels, compared to the metformin alone - suggesting beneficial effects on both carbohydrate and lipid metabolism. Importantly, this study demonstrated that after twelve weeks of treatment the compound was still well tolerated (http://www.incyte.com/drugs_product_pipeline.html).

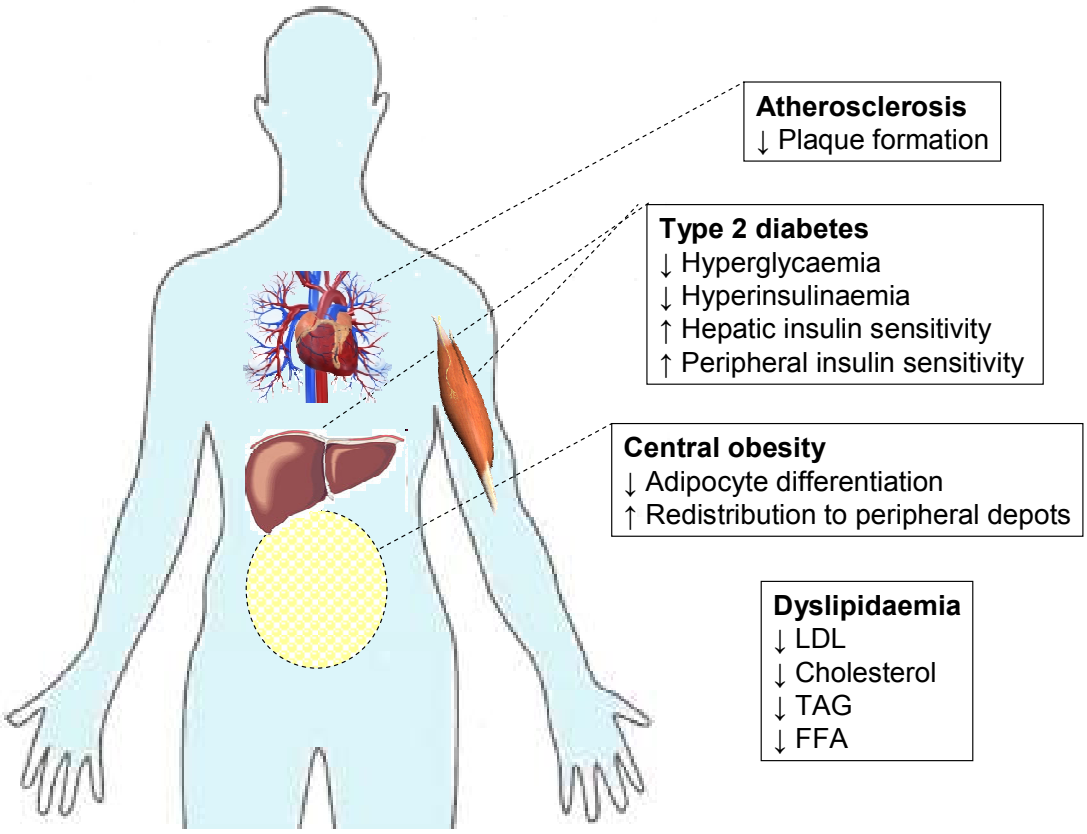

Figure 1-18 Data generated using rodents, along with human clinical studies suggest that selective 11β-HSD1 inhibitors have a beneficial metabolic impact.

1.15. Unanswered questions

The rationale for this work is based upon the phenotype of GC excess. It is clear that GCs induce insulin resistance, and since skeletal muscle accounts for ~80% of glucose disposal, under insulin stimulating conditions, it is likely skeletal muscle is the major site of GC action in this respect. However, the precise molecular mechanism underpinning GC-induced insulin resistance in skeletal muscle is unknown. Recently, the accumulation of intramyocellular lipid metabolites has been linked with reduced insulin sensitivity in skeletal muscle, and although GC have been shown to regulate lipid metabolism in other tissues, their precise role in regulating these pathways in skeletal muscle is yet to be fully elucidated. Furthermore, 11β-HSD1 is of great interest as a therapeutic target in the treatment of type 2 diabetes, however, the role of this enzyme in the insulin sensitivity of skeletal muscle has not been firmly established.

1.16. Aims

- Characterise the expression of the insulin signalling cascade, and genes involved in regulating GC response across myocyte differentiation (**Chapter 3**).

- Characterise the impact of GCs upon the insulin signalling cascade and glucose uptake in skeletal muscle using rodent and human cell lines (**Chapters 4, 5, 6 and 7**).

- Determine the role of 11β-HSD1 and pre-receptor GC metabolism in the regulation of insulin signalling in rodent skeletal muscle *in vitro* and *in vivo* *(**Chapters 5 & 6**)*.

- Identify the role of GCs in the regulation of intramyocellular lipid metabolism (**Chapters 4 & 6**).

Chapter 2 - General Methods

The procedures described in this chapter were commonly used in this thesis. Methods specific to individual chapters are found in the methods section of those particular chapters. Unless otherwise stated, all reagents were purchased from Sigma Aldrich, Dorset, UK.

2.1. C2C12 cell culture

2.1.1. C2C12 cell line

The C2C12 cell line is a well established model of both skeletal muscle proliferation and differentiation. Originally generated by serial passage of myoblasts, cultured from the thigh muscles of C2H mice 70 h following a crush injury (Yaffe & Saxel, 1977). A subclone of these myoblasts was selected for its ability to differentiate rapidly and express characteristic muscle proteins (Blau et al., 1985).

2.1.2. Proliferation

Cryofrozen C2C12 myoblasts were purchased from ECACC (Salisbury, UK) and maintained in 75cm^3 TC flasks (Corning, Surrey, UK) in 12mL of Dulbecco's modified eagle medium (DMEM) (PAA, Somerset, UK), supplemented with 10% foetal calf serum (FCS), at 37°C under a 5% CO_2 atmosphere. At 60-70% confluence, cells were trypsinised, and re-seeded into fresh flasks. Prior to experiments being performed, cells were trypsinised and subcultured into 12-well TC plates (Corning, Surrey, UK), and cultured until 60-70% confluent. Proliferation media was replaced every 48 h.

2.1.3. Differentiation

Once myoblasts reached 60-70% confluence, differentiation was initiated by replacing proliferation media with DMEM, supplemented with 5% horse serum.

Differentiation media was replaced every 48 h. After 8 days, myoblasts had fused to form multinucleated myotubes (Figure 2-1).

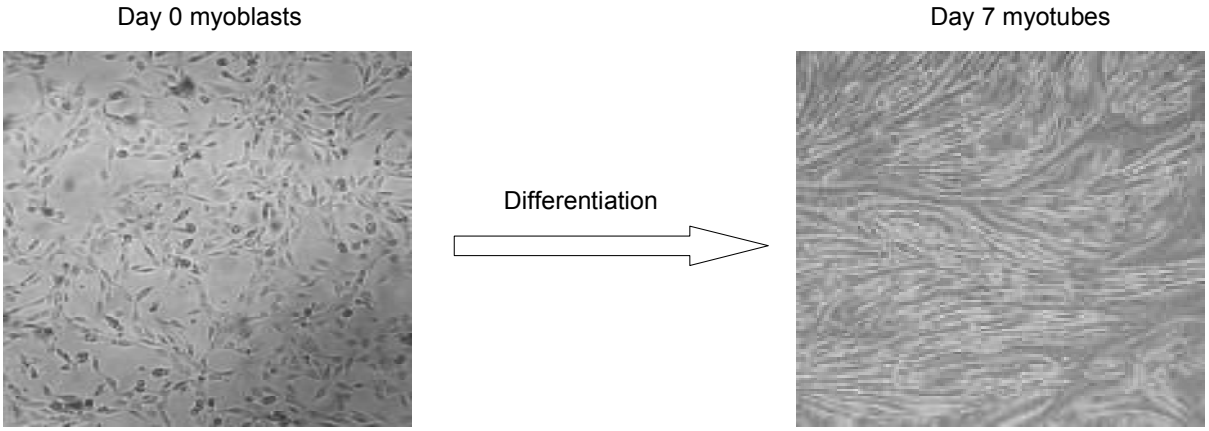

Figure 2-1 C2C12 cells were differentiated in chemically defined media for 8 days, forming multinucleated myotubes.

2.1.4. Freezing down

Cells to be frozen down were grown in 75cm^3 TC flasks until 60-70% confluence. Cells were trypsinised, and then resuspended in 10mL of proliferation media, before being centrifuged at 1000 g for 10 mins. Media was aspirated and the cell pellet resuspended in 3mL of FCS supplemented with 10% DMSO. The cell mixture was then aliquoted into 1.5mL cryovials and slowly cooled to -80°C at a rate of 1°C/min, in a cryofreezing chamber (Nalgene, Hereford, UK) containing isopropanol. Cells were transferred to liquid nitrogen for long-term storage.

2.2. Human primary skeletal muscle cell culture

2.2.1. Promocell skeletal muscle cells

Primary human myoblasts were obtained from Promocell (Heidelberg, Germany). The Myoblasts were isolated from the M. gluteus maximus muscle of a healthy 31 year old woman, according to promocell referenced procedures, and frozen in serum free cryopreservation media. These cells are not transformed, and have a limited prolferative / differentiative lifespan.

2.2.2. Proliferation

Myoblasts were initially seeded at $5x10^3$ cells/cm^3 in a $25cm^3$ TC flask (Corning, Surrey, UK), in 6mL of skeletal muscle growth media (Promocell, Heidelberg, Germany). Cells were maintained at 37°C under a 5% CO_2 atmosphere. At 60-70% confluence cells were washed with HEPES buffered saline (Promocell, Heidelberg, Germany) before trypsinisation. A trypsin neutralising solution (Promocell, Heidelberg, Germany) was added before suspending the cells in growth media and reseeding them into fresh flasks. Prior to the experiment, cells were trypsinised and subcultured into 12-well TC plates (Corning, Surrey, UK) and cultured until 60-70% confluent. Proliferation media was replaced every 48 h.

2.2.3. Differentiation

At 60-70% confluence, cells were transferred to Promocell serum free media, supplemented with 10µg/ml insulin and 2% horse serum. Differentiation media

was replaced every 48 h. After 7 days, myoblasts had fused to form multinucleated myotubes (Figure 2-2). For all experiments, no cells were used at a passage greater than 7.

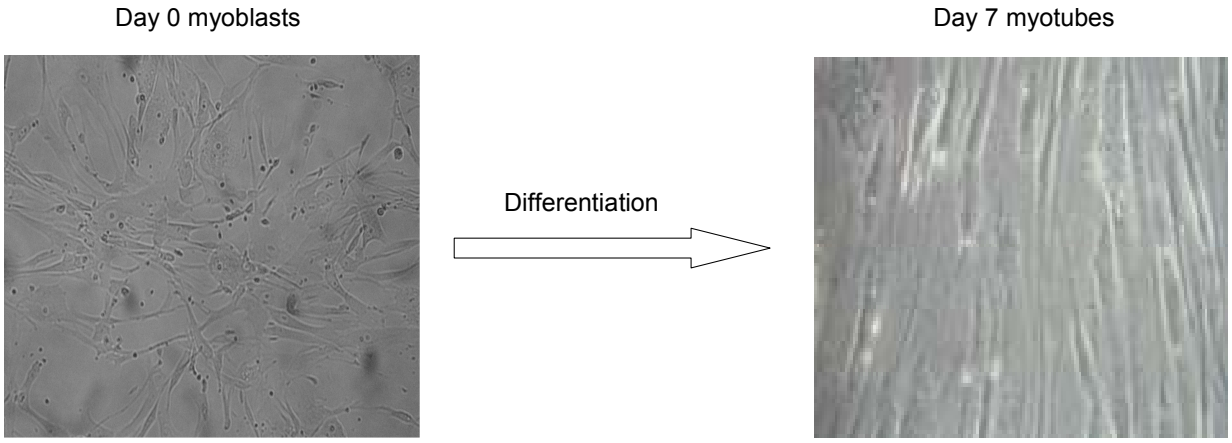

Figure 2-2 Human primary myocytes were differentiated in chemically defined media for 7 days forming multinucleated myotubes.

2.2.4. Freezing down

Cells to be frozen down were grown in 75cm^3 TC flasks, until 60-70% confluence. Cells were trypsinised, as described above, then resuspended in 10mL proliferation media before being spun 1000 g for 10 mins. Media was aspirated, and the cell pellet resuspended in 3mL of cryo serum free media (Promocell, Heidelberg, Germany). Cell mixture was aliquoted into 1.5mL cryovials and slowly cooled to -80°C at a rate of 1°C/min, in a cryo freezing chamber (Nalgene, Hereford, UK) containing isopropanol. Cells were transferred to liquid nitrogen for long-term storage.

2.3. Glucose transport assay

2.3.1. Principles

Glucose transport assays allow a functional readout of insulin action upon the cell, through uptake of a radiolabelled glucose tracer (Liu et al., 2001). The effect of a specific treatment, on both basal and insulin stimulated glucose uptake, can be assessed by incubating cells with a fixed concentration of glucose combined with a radiolabelled traced in the presence and absence of insulin. After uptake, the amount of radiolabelled glucose trace taken into the cells can be measured by scintillation counting. 2-deoxy-D-[glucose] is used as it is not metabolised beyond 2-deoxy-D-[glucose]-6-phosphate - thus it accumulates in the cells.

2.3.2. Method

Treatments were carried out in 24-well TC plates (Corning, Surrey, UK). At the end of the treatment, cells were washed 3 times with warm PBS then incubated with 0.9mL krebs ringer buffer (KRB, 4.7mM KCl, 136mM NaCl, 1.25mM $CaCl_2$, 1.25mM $MgSO_4$ and 10mM sodium phosphate buffer at pH 7.4) containing treatments at 37°C for 10 mins under a 5% CO_2 atmosphere. Insulin was added (80nM final concentration), and cells incubated at 37°C for 20 mins under a 5% CO_2 atmosphere. Glucose uptake was initiated by addition of 0.1mL of KRB containing 6mM glucose combined with 37MBq/L of 2-deoxy-D-[^{3}H-glucose] (GE Healthcare, Bucks, UK) as a tracer. After incubation at 37°C for 60 mins under a 5% CO_2 atmosphere, glucose uptake was terminated by removal of culture media. Cells were washed 3 times with ice cold PBS and lysed by addition of

0.1ml of 1M NaOH for 30 mins. A 15µl aliquot was taken for protein quantification (see section 2.6.2) before each well was neutralised by addition of 85µl of 1M HCl. The cell lysates were combined with scintillation fluid (PerkinElmer, Bucks, UK), and counted using a Wallac 1414 liquid scintillation counter (PerkinElmer, Bucks, UK)

2.4. 11β-HSD1 enzyme activity assay

2.4.1. Principles

This technique allows for the measurement of the interconversion between the rodent inactive 11-dehydrocorticosterone (A) and active corticosterone (B), by 11β-HSD1 [this technique was also used to measure the interconversion between human cortisone (E) and cortisol (F)]. This protocol was carried out on both monolayers of intake cells and whole tissue explants.

2.4.2. Method

2.4.2.1. Monolayer of cells

Confluent rodent cell monolayers were washed once with PBS, then incubated with serum free media containing 100nM of either 11-DHC enriched with 20000cpm/reaction ^{3}H-11DHC (for synthesis see below) or corticosterone enriched by 20000cpm/reaction of ^{3}H-corticosterone (GE Healthcare, Bucks, UK). If human cell monolayers were used, then cells were washed as described above

but alternatively incubated with 100nM of either cortisone, enriched with 20000cpm/reaction ^{3}H-corticone (GE Healthcare, Bucks, UK), or cortisol, enriched by 20000cpm/reaction of ^{3}H-cortisol (GE Healthcare, Bucks, UK). Incubations were carried out at 37°C under a 5% CO_2 atmosphere for 2 - 24 h, depending on the cell type. Media was then transferred to glass test tubes and 6mL of dichloromethane was added. The cells were retained in 100µL of PBS and stored at -80°C for protein quantification (see section 2.6.2). Steroids were extracted from media by vortexing the tubes for 20 secs. Aqueous and organic phases were separated by centrifugation at 1000 g for 10 mins. The aqueous phase was aspirated and the organic phase containing the steroids was evaporated at 55°C using an air blowing sample concentrator (Techne, New Jersey, US). Steroids were resuspended in 55µl of dichloromethane and spotted onto a silica coated thin layer chromatography plate (Thermofisher, Surrey, UK) using a Pasteur pipette, followed by 2µl of non-radiolabelled 11DHC/corticosterone or cortisone/cortisol (10mM in ethanol). Each spot was separated by at least 1.5cm from adjacent samples, and 2cm from the bottom of the plate. Steroids were then separated by thin layer chromatography (TLC) using 200mL of cholorform:ethanol (92:8) as the mobile phase for 2.5 h. Radioactivity of the separated ^{3}H-11DHC/^{3}H-corticosterone or ^{3}H-corticone/^{3}H-cortisol was measured using a Bioscan 200 imaging scanner (LabLogic, Sheffield, UK). Finally, to assign the radioactivity peaks with the correct steroids, the plates were placed under UV light to visualise the position of the cold standards. See Figure 2-3 for an example of typical Bioscan traces. Percentage conversion was calculated using region counts for the individual peaks. Enzyme activity was expressed in pmoles of steroid converted per mg of protein per hour (pmol/mg/h).

2.4.2.2. *Mouse tissue explants*

Fresh tissue explants were chopped to ~20mg/well and the above protocol was followed. Activity expressed as pmoles of steroid converted per mg of tissue per hour (pmol/mg/h).

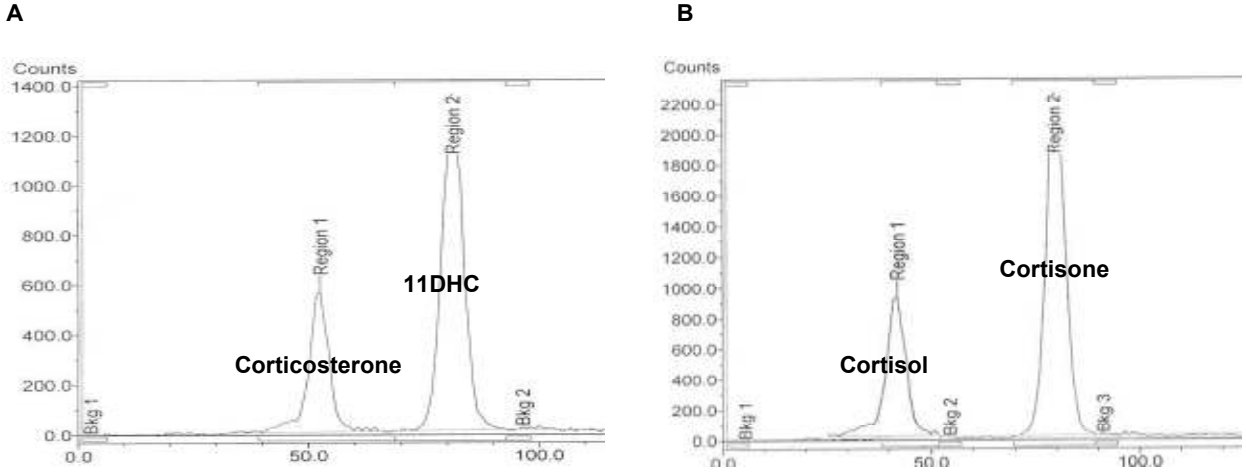

Figure 2-3 Representative Bioscan traces for 11β-HSD1 oxo-reductase activity in mouse C2C12 myotubes (A) and human primary myotubes (B).

2.4.3. Production of ^{3}H-11DHC

Unlike tritiated cortisone (^{3}H-corticone), tritiated 11-dehydrocorticosterone (^{3}H-11DHC) is not commercially available; consequently tritiated corticosterone (^{3}H-corticosterone) (GE Healthcare, Bucks, UK) was used to generate ^{3}H-11DHC. In glass test tubes, 20µl of ^{3}H-corticosterone (1mCi/mL) was incubated with 250µg of homogenised mouse placenta, in 500µl of 0.1M phosphate buffer, pH7.4, with 500µM NAD^{+}. Conversion was carried out overnight in a shaking water bath at 37°C. Steroids were extracted by addition of 6mL of dichloromethane and vortexing the tubes for 20 secs. Aqueous and organic phases were separated by centrifugation at 1000 g for 10 mins. The aqueous phase was aspirated and the

organic phase, containing the steroids, was evaporated at 55°C using an air blowing sample concentrator (Techne, New Jersey, US). Steroids were resuspended in 55µl of dichloromethane and spotted onto a silica coated thin layer chromatography plate (Thermofisher, Surrey, UK) using a Pasteur pipette. Steroids were then separated by thin layer chromatography using 200mL of cholorform:ethanol (92:8) as the mobile phase for 2.5 h. To establish position of ^{3}H-11DHC, the silica plates were read using a Bioscan 200 imaging scanner (LabLogic, Sheffield, UK). The silica at the ^{3}H-11DHC position was scraped into a glass test tube, and eluted in 300µL of ethanol overnight at 4°C. The eluted ^{3}H-11DHC and silica were separated by centrifugation at 100 g for 5 mins. Radioactivity of ^{3}H-11DHC was determined by separating 5µL of stock by thin layer chromatography, and number of counts determined using the Bioscan 200 imaging scanner. Stock was then diluted in ethanol to give ~1000 counts/µL.

2.5. Protein Extraction

2.5.1. Principles

The extraction of soluble proteins from cell monolayers or whole tissue was carried out using a cell lysis buffer containing protease inhibitors and detergent. Insoluble cell debris, such as membrane lipids, was removed by centrifugation.

2.5.2. Method

2.5.2.1. Monolayer of cells

Monolayers of cells were placed on ice and washed with cold PBS. For cells grown 12-well plates, 40µl of RIPA buffer (1mM EDTA, 150mM NaCl, 0.25% SDS, 1% NP40, 50mM Tris pH 7.4, supplemented with protease inhibitor cocktail (Roche, Sussex, UK) and phosphatase inhibitor (Thermofisher, Surrey, UK)), was added per well, into which the cells were scraped using a 1mL syringe plunger. Cell lysates were then transferred to eppendorf tubes and incubated at -80°C for 20 mins. The lysates were then thawed out on ice and centrifuged at 14,000 g for 15 mins at 4°C. The supernatant containing soluble proteins was transferred to fresh eppendorf tubes and stored at -80°C prior to assessment of protein concentrations (see below).

2.5.2.2. Mouse tissue explants

Mouse tissue was quickly harvested and snap frozen using liquid nitrogen. Samples were then transferred to -80°C until required. Proteins were extracted by homogenising ~ 20mg of tissue in 1.5mL of RIPA buffer using a mechanical homogeniser. Cell lysates were then incubated at -80°C for 20 mins, thawed out on ice, then centrifuged at 14,000 g for 15 mins at 4°C. The supernatants containing soluble proteins was transferred to fresh eppendorf tubes and stored at -80°C prior to assessment of protein concentrations (see below).

2.6. Measuring protein concentration

2.6.1. Principles

Total protein concentration from both cell monolayers and tissue explants was assessed using the BioRad RC DC protein assay (BioRad, Herts, UK). The assay is based on the Lowry method, but has been modified to be reducing agent compatible (*RC*) as well as detergent compatible (*DC*). The protein to be quantified initially reacts with the copper in an alkaline copper tartrate solution. Folin then reacts with the copper treated protein subsequently leading to the generation of various reduced folin species all of which have a characteristic blue colour and absorb maximally at 750nM and minimally at 405nM.

2.6.2. Method

Protein assays were carried out according to the protocol provided by manufacturer (BioRad, Herts, UK). Firstly, 5µL of sample protein or protein standards was added per well of a 96-well plate in duplicate. The protein standards were made by dissolving bovine serum albumin (BSA) in RIPA buffer and serially diluted to generate the following concentrations: 0, 0.5, 1, 2, 4, 6mg/mL (Figure 2-4). 25µL of an alkaline copper tartrate solution (solution A) was added to each well followed by 200µL of a folin solution. The assay was incubated at room temperature for 10 mins prior to absorbance being read at 690nM on a vector3 1420 multilable counter (PerkinElmer, Bucks, UK).

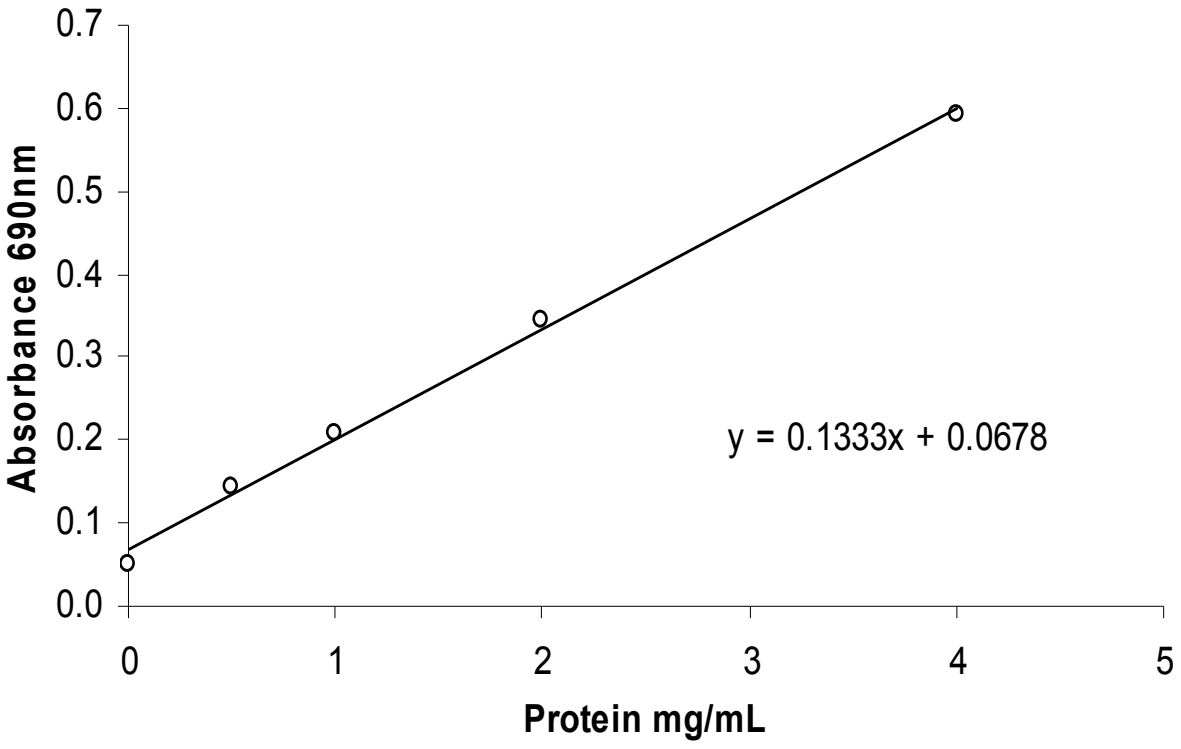

Figure 2-4 Representative BSA protein standard curve for the BioRad RC DC protein assay.

2.7. Immunoblotting

2.7.1. Principles

Immunoblotting allows the measurement of relative amounts of a specific protein in a mixed protein sample (Towbin, Staehelin & Gordon, 1979). Proteins are boiled in a strong reducing agent which removes all secondary and tertiary structures and gives them a uniform negative charge. SDS-PAGE electrophoresis is then employed to separate the proteins according to molecular mass. Since the proteins are negatively charged they are pulled through the gel towards the anode at a speed that is dependent upon their size - small proteins migrate fast and large proteins migrate slowly. The separated proteins are then transferred to a membrane, usually polyvinylidene diflorise (PVDF) or nitrocellulose using electrical current. Since these membranes strongly bind proteins they will also bind to any antibodies that they are exposed to. To prevent this non-specific binding the membrane is incubated in a blocking solution containing a generic protein such as milk or BSA. The next step involves probing the membrane with a primary antibody that specifically recognises the protein of interest, followed by incubation with a secondary antibody that is directed against the primary antibody. The secondary antibody is conjugated to horseradish peroxidase (HRP) which, in the presence of hydrogen peroxide, catalyses a reaction involving the oxidation of luminol. Upon oxidation of luminol, an iridescent blue light is produced which is proportional to the amount of protein hybridised to the antibody on the membrane. The reaction is captured on photographic film.

2.7.2. Method

Between 20-30µg of protein was mixed with an appropriate volume of 5 x loading buffer, and boiled for 5 mins. Samples were loaded into a 4-20% gradient SDS-PAGE gel (BioRad, Herts, UK) and run at 200V for 1 h - 1 h 30 mins. Transfer of proteins to nitrocellulose membrane (GE Healthcare, Bucks, UK) was conducted at 140mA for 1-2 h, depending on the size of the protein of interest. Efficient transfer was assessed by incubating the membrane in Ponceau stain with agitation for 60 secs, and then rinsed with water to allow visualisation of the protein bands. Electrophoresis and protein transfer was carried out in BioRad mini protein 3 apparatus (BioRad, Herts, UK). Membranes were blocked in 10mL of blocking buffer (5% milk or BSA) for 1 h at room temperature with constant agitation, then incubated with primary antibody overnight at 4°C on an orbital shaker. Membranes were washed with 100mL of washing buffer 3 times for 15 mins. Secondary antibody incubation was conducted at room temperature with constant agitation. The membrane was then washed with 100mL of washing buffer 3 times for 15 mins. Bound antibody was detected using Enhanced Chemluminescence (ECL, GE Healthcare, Bucks, UK) The reaction mixture was set up by combining substrate A with substrate B at a 50:50 ratio (final volume: 1mL per membrane). Following equilibration for 5 mins, 1mL was added per membrane and left to incubate for 2 mins before the membrane was placed between two plastic sheets in a photo cassette. Photographic film (PerkinElmer, Surrey, UK) was placed over the membrane in the dark and exposed for 30 secs to 3 h, then developed on Compact X4 automatic film processor (Xograph Imaging Systems, Gloustershire, UK). Membranes were routinely stripped to

remove bound primary/secondary antibodies by incubating the membrane in stripping buffer (2% SDS, 100mM β-mercaptoethanol, 50mM Tris, pH 6.8) at 50°C for 1 h with gentle agitation. Membranes were then washed with 100mL of washing buffer 3 times for 15 mins before being reprobed with a different primary antibody. Immunoblots were evaluated by integrating densitometry using GeneSnap and GeneTool (Chemigenius Gel Documenting System, Syngene, Cambridge, UK). Equal loading was confirmed by reprobing the membrane with anti-β-actin antibody conjugated to HRP and visualized as described above.

2.8. RNA extraction

2.8.1. Principles

RNA is extracted from cultured cell monolayers or tissue explants using a single step procedure developed by Chomczynski (Chomczynski & Sacchi, 1987). This is achieved by homogenizing tissue or lysis of cultured cells in TRI reagent. This solution contains phenol and guanidine thiocyanate, and immediately and effectively inhibits RNase activity. The addition of chloroform, followed by centrifugation, results in the formation of three phases. RNA is present exclusively in the aqueous phase, and is subsequently precipitated with isopropanol.

2.8.2. Method

For cultured cell monolayers: media was removed and cells washed in PBS before 1mL of TRI reagent (Sigma-Aldrich, Dorset, UK) was added per well (for a 12-well plate) and incubated at room temperature for 5 mins using a mechanical homogeniser. For tissue explants: ~20mg of tissue was homogenized in 1.5mL of TRI reagent then incubated at room temperature for 5 min. For both cultured cell monolayers and tissue explants, cell lysates in TRI reagent were transferred to eppendorfs tubes. 200µL of chloroform was added and tubes were shaken vigorously for 30 sec, before incubation at room temperature for 15 mins. The mixture was centrifuged at 10,000 g for 15 min at 4˚C. The RNA contained within the aqueous phase was transferred to a fresh eppendorf tube and 200µL of isopropanol was added. The tubes were inverted 4 times then incubated at room temperature for 15 mins. RNA was pelletted by centrifugation at 10,000 g for 15 min at 4˚C. The supernatant was aspirated and the RNA pellet was washed with 75% ethanol, centrifuged and ethanol was removed by aspiration. The RNA pellet was air dried then resuspended in 50µL of nuclease free water.

2.8.3. RNA quantification

The quantity of RNA was measured using NanoDrop ND-1000 UV-Vis Spectrophotometer (Thermofisher, Surrey, UK). The absorbance of 2µl of RNA at 260nm and 280nm was determined where 1 OD_{260} = 40µg/mL of RNA and the OD_{260}/OD_{280} ratio indicates the RNA purity. Only OD_{260}/OD_{280} ratios in the range of 1.8- 2 were used. All measurements were made with respect to a blank consisting of the nuclease free water in which the RNA was suspended.

In addition, the integrity of the RNA was assessed by electrophoresis on a 1% agarose gel containing 0.15µg/mL ethidium bromide. The RNA separates down the gel according to its molecular mass and the resultant bands were visualized under UV light. Intact RNA shows two sharp bands corresponding to the highly abundant 28S and 18S rRNA.

2.8.4. DNase treatment

10µg of RNA was further purified by removal of any contaminating genomic DNA by incubation at 30°C with DNase I enzyme (Ambion, Warrington, UK).

2.9. Reverse transcription of RNA

2.9.1. Principles

Reverse transcription (RT) is the process of converting single stranded RNA to complementary DNA (cDNA), using RNA-dependent DNA polymerase. Initially the extracted RNA is heated to denature secondary structure which allows the random hexomers to anneal to the RNA template. The reverse transcription process is initiated by increasing the temperature further, allowing the RNA-bound primers to be extended generating a complementary DNA copy of the RNA template. Lastly, the reaction is heated to a high temperature to inactivate the enzyme and terminate the reaction.

2.9.2. Method

All RT reactions were carried out using Applied Biosystems High-Capacity Reverse Transcription Kit (Applied Biosystems, Warrington, UK). The reagents listed in the table below were combined in an eppendorf tube to generate a 2x RT master mix.

Component	Volume (µl) per sample
10X RT Buffer	2
25X dNTP mix (100mM)	0.8
10X Random Hexomers	2
MultiScribe Reverse Transcriptase	1
RNase inhibitor	1
Nuclease-free H_2O	3.2
TOTAL VOLUME	**10**

1µg of RNA was diluted with nuclease free water to a volume of 10µl before 10µl of 2x RT master mix was added giving a final volume of 20µl. Samples were loaded onto a thermal cycler (Applied Biosystems, Warrington, UK) and incubated at 25°C for 10 mins followed by 48°C for 30 mins and finally 95°C for 5 mins to terminate the reaction.

2.10. Conventional Polymerase Chain Reaction (PCR)

2.10.1. Principle

Regions of DNA or cDNA can be amplified using oligonucleotide primers that are complementary to the 3' and 5' ends of this region. High temperature is used to denature double stranded DNA which is then cooled to allow the oligonucleotides primers to anneal. When the temperature is increased to the optimal catalytic temperature for taq polymerase, these oligonucleotides are extended to generate complementary DNA strands. Subsequent repeated rounds of denaturation, oligonucleotide annealing and DNA synthesis allow the amount of product to increases exponentially until production plateaus due to limiting nucleotides availability and/or low taq concentration. Conventional PCR, although not used for experimentation, was used to check the integrity of cDNA prior to RT-PCR.

2.10.2. Method

All conventional PCRs were carried out using Promega reagents (Promega, Southampton, UK). In a 20µl reaction, the following components were added: reaction buffer (final concentration 1x), MgCl (1-2.5mM), deoxy-dNTPs (0.5µM), Taq polymerase (0.05U/µl) forward and reverse primers (0.6µM) and 100µg of cDNA. Samples were incubated in a thermal cycler at 95°C for 5 mins then cycled 30 times at 95°C for 30 secs, 60°C for 30 secs and 72°C for 1 min. Finally, samples were incubated at 72°C for 7 mins.

2.11. Relative quantitative (Real-time) polymerase chain reaction

2.11.1. Principles

Real-time PCR or relative quantitative PCR is a technique used to monitor the progress of a PCR reaction in real-time. Using oligonucleotide primers that are complementary to the 5' and 3' ends of a region of interest, cDNA can be amplified by PCR. The presence of an oligonucleotide probe complementary to a sequence downstream of one of the primers allows quantification of the target transcript by fluorescence (Figure 2-5). This probe is chemically synthesized with a fluorescent reporter dye at the 5' end and a quencher dye at the 3' end. Since the quencher dye is in close proximity to the fluorescent reporter dye it reduces the fluorescence emitted by the latter through a process called fluorescence resonance energy transfer (FRET). During the primer elongation step of the PCR reaction the probe bound downstream from one of the primers is cleaved due to the 5'- 3' exonuclease activity of taq DNA polymerase. Removal of the probe allows primer extension to continue and amplification of the sequence of interest, it does not inhibit the PCR process. Cleavage of the probe separates the quencher dye from the reporter dye, increasing the fluorescence emitted by the latter (Figure 2-5). Fluorescence intensity is proportional to the amount of PCR product produced. The point at which the target sequence is detected is called the cycle threshold (Ct). This threshold is set to the exponential phase of the amplification for the most accurate reading. The higher the target sequence copy number within the original cDNA sample the lower the cycle number at which fluorescence is observed. Real-time PCR is a relative measure of gene

expression, therefore, the Ct of the target genes is compared to the Ct of a house keeping gene with constant expression levels. This is calculated by subtracting the Ct of the house keeping gene from the Ct of the target gene, the resultant value is known as the ΔCt. The greater the ΔCt, the greater the change in gene expression due to treatment.

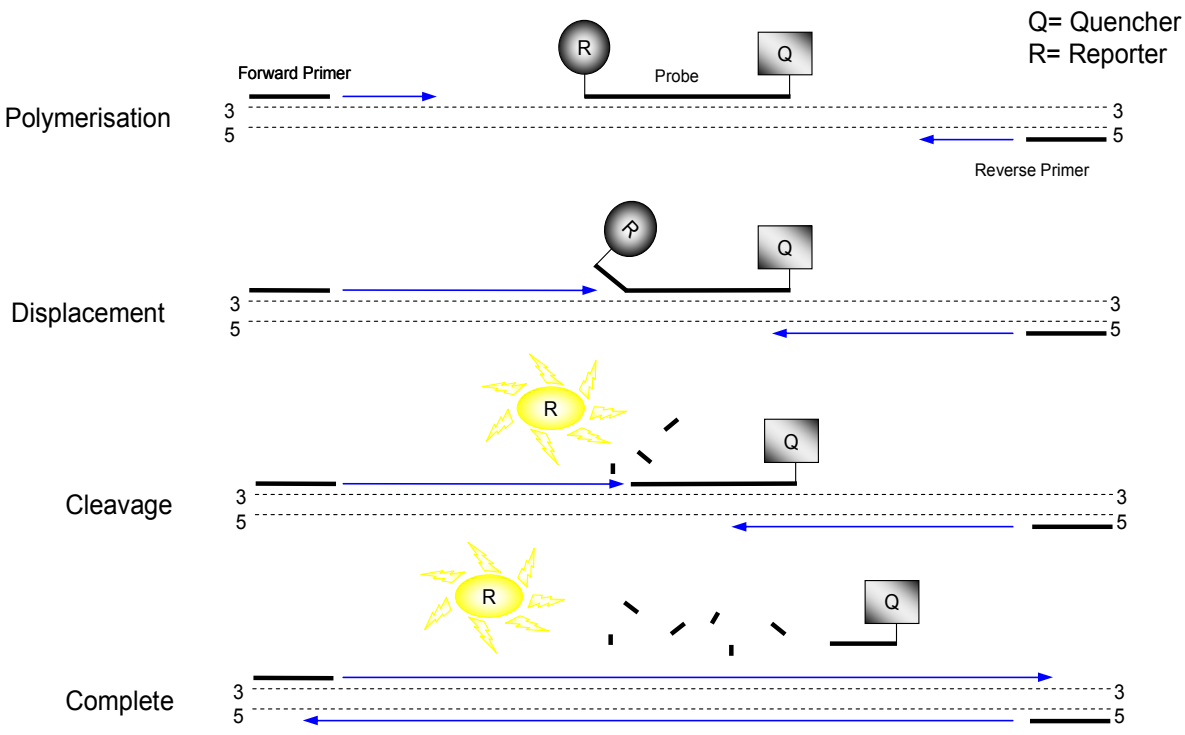

Figure 2-5 Schematic representation of real-time PCR. Separation of reporter dye from the quencher allows detection of fluorescence.

2.11.2. Method

Real-time PCR was carried out using Applied Biosystems reagents and expression assays (Applied Biosystems, Warrington, UK), unless otherwise stated. Target gene expression was normalised against the 18s rRNA house keeping gene and these measurements were carried out in separate wells from target gene expression measurements (singleplex). All reactions were carried out in duplicate in 96-well plates (Applied Biosystems, Warrington, UK). For the 18S house keeping gene, the following components were combined per well: 10µl of 2x MasterMix, 18S forward and reverse primers and vic labelled probe (final concentration 25nM each), 100ng of cDNA and nuclease free water to a final volume of 20µl. For the gene of interest, the following components were combined per well: 10µl of 2x MasterMix, 1µl of 20x expression assay, 100ng of cDNA and nuclease free water to a total volume of 20µl. Plates were sealed with clear adhesive film (Applied Biosystems, Warrington, UK) and run on a 7500 real-time PCR system (Applied Biosystems, Warrington, UK). Data was expressed as Ct values (threshold set within the exponential part of the PCR amplification curve and above the baseline value*), a*nd used to calculate ΔCt [Ct of gene of interest - Ct of 18S house keeping gene]. All data was expressed as arbitrary units [AU = $1000x2^{-\Delta Ct}$]. *Fold change* was calculated using the $2^{-\Delta\Delta Ct}$ method.

2.12. Custom taqman real-time PCR arrays

2.12.1. Principles

Taqman custom arrays work by same the principles as standard real-time PCR (see section 2.11.2), but differ in the fact that a greater number of target genes that can be assayed simultaneously on the same plate. This is a faster and more cost effective way of analysing expression of multiple gene targets.

2.12.2. Method

Taqman custom arrays were purchased from Applied Biosystems (Applied Biosystems, Warrington, UK). Each array consisted of 384-well plates preloaded with 48 custom gene expression assays (including 3 house keeping genes) organised into channels to allow a maximum of 8 unique samples to be assayed simultaneously. 50µl of 2x Taqman Universal PCR MasterMix (Applied Biosystems, Warrington, UK) was mixed with 500µg of cDNA and nuclease free water to give a final volume of 100µl. Samples were loaded into the fill reservoirs at the end of each channel and distributed into the reaction wells by centrifugation twice at 331 g for 1 min with an up/down ramp rate of 9. Centrifugation was carried out in a Heraeus centrifuge and bucket (DJB Labcare, Bucks, UK). The array was sealed to isolate the wells using a low density array sealer (Applied Biosystems, Warrington, UK) and run on a 7900HT fast real-time system (Applied Biosystems, Warrington, UK). Data was expressed as Ct values (threshold set within the exponential part of the PCR amplification curve and above the baseline value), and used to calculate ΔCt [Ct of gene of interest - Ct of house keeping

gene]. *Fold change* was calculated using the $2^{-\Delta\Delta Ct}$ method. Results were validated with standard taqman RT-PCR.

2.13. Short interfering RNA (siRNA)

2.13.1. Principles

Short interfering RNA (siRNA) or RNA interference is a technique used to knockdown the expression of a specific gene by targeting its transcribed mRNA species. SiRNA oligonucleotides are around 20-25 nucleotides in length and are complementary to the mRNA product of the gene of interest. Since these oligonucleotides are large and negatively charged they cannot pass through the cell membrane into the cytosol unfacilitated. This problem can be overcome by using a lipid based delivery system, which works because positive surface charges on the liposomes interacts with the nucleic acids of the siRNA species and the cell membrane, allowing for fusion of the liposome/nucleic acids (transfection complex) with the negatively charged cell membrane. The transfection complex can then enter the cell through endocytosis. Once inside the cell, the siRNA oligonucleotides assemble into endoribonuclease-containing complexes known as RNA-induced silencing complexes (RISCs). The siRNA strands subsequently guide the RISCs to the target mRNA molecules. Cleavage of cognate RNA takes place near the middle of the region bound by the siRNA strand.

2.13.2. Method

Predesigned short-interfering oligonucleotide (siRNA) sequences directed against genes of interest were purchased from Dharmacon (Thermofisher, Surrey, UK), each contains 4 different oligonucleotide sequences directed against separate regions of the target gene (ON-TARGETplus, SMARTpool). The lyophilised siRNA was resuspended in 1X siRNA buffer (Thermofisher, Surrey, UK) to a stock concentration of 20μM then aliquoted and stored at -80°C until required. C2C12 myocytes were initially seeded at $5x10^4$cells/mL in 12-well TC-plates and incubated overnight at 37°C with 5% CO_2. On the day of the experiment, stock siRNA was diluted in 1X siRNA buffer to a concentration of 5μM then further diluted in serum free medium (final volume 100μL/well) and incubated at room temperature for 5 mins. In a separate tube, a lipid based transfection reagent, DharmaFECT3 (Thermofisher, Surrey, UK), (5μl/well) was combined with serum free media (95μL/well) and incubated for 5 mins at room temperature. Both siRNA and DharmaFECT3 were combined (final volume 200μL/well), mixed then incubated at room temperature for 20 mins. 800μL/well of complete media (containing serum) was then added (giving a final siRNA concentration of 100nM) and introduced onto the cells. Experimental controls, run in parallel, included: no treatment, negative control (non-targeting siRNA, 100nM), mock transfection (DharmaFECT3 without siRNA) and a positive control (siRNA directed against a highly expressed house keeping gene; cyclophilin B [ON-TARGETplus, SMARTPool, 100nM]).

2.14. Acetyl-CoA Carboxylase (ACC) assay

2.14.1. Principles

De novo lipogenesis involves the conversion of acetyl-CoA to free fatty acids. The first and rate limiting step of this pathway is the conversion of acetyl-CoA to malonyl-CoA and is catalysed by acetyl-CoA carboxylase (ACC). Malonyl-CoA is subsequently converted to fatty acids by fatty acid synthase (FAS). This assay measures the accumulation of a 1-[^{14}C]-acetic acid tracer. The acetate is first converted to acetyl-CoA by acetyl-CoA synthase before entering *de novo* lipogenesis. After incubation, cellular lipids are extracted, and retained radioactivity is measured by scintillation counting.

2.14.2. Method

C2C12 myocytes were cultured and treated in 24-well TC places and differentiated into myotubes. Cells were incubated with 500µL of serum free media with 0.12µCi/L 1-[^{14}C]-acetic acid (GE Healthcare, Bucks, UK) with unlabelled sodium acetate to a final concentration of 10µM acetate, with treatments and with or without insulin. The cells were incubated at 37°C for 4 h. Cells were then washed 3 x with ice cold PBS, scraped into 250µL of PBS then transferred into glass tubes. To extract the lipid fraction, 5mL of Folch solvent was added and shaken vigorously for 20 secs. 1mL of water was added and shaken vigorously for 20 secs. Phases were separated by centrifugation at 300 g for 5 mins. The upper aqueous phase was removed by aspiration, and lower fraction transferred to a 5mL scintillation tube and evaporated until dry using a sample

dryer (Techne, New Jersey, US). Once dry, 5mL of scintillation cocktail was added (PerkinElmer, Bucks, UK) and samples were counted using a Wallac 1414 Liquid Scintillation Counter (PerkinElmer, Bucks, UK).

2.15. β-oxidation assay

2.15.1. Principles

β-oxidation is the pathway by which fatty acids are sequentially broken down in the mitochondria, generating acyl-CoA molecules which enter the TCA cycle ultimately leading to increased ATP production. This assay involves incubating cells with a tritiated fatty acid tracer and measuring the accumulation of tritiated water, released during each round of the oxidation process. After incubation, the tritiated water is extracted and radioactivity measured by scintillation counting.

2.15.2. Method

C2C12 myocytes were cultured and treated in 24-well TC places and differentiated into myotubes. Cells were incubated with 500µL of serum free media containing 0.1 mmol/L palmitate (9,10-[^{3}H]palmitate (5µCi/mL) (GE Healthcare, Bucks, UK), 2% BSA and treatments for 24 h. After incubation, the media was retained and precipitated twice with equal volumes of 10% trichloroacetic acid to remove excess labelled palmitate. The supernatants (≈0.5mL) were extracted by addition of 2.5mL of methanol:chloroform (2:1) and 1mL of 2mol/L KCl:HCl, followed by centrifugation at 3000 g for 5 min. Aqueous

phase (0.5mL) was then added to scintillation cocktail (PerkinElmer, Bucks, UK), and samples were counted using a Wallac 1414 Liquid Scintillation Counter (PerkinElmer, Bucks, UK).

Chapter 3 - Characterisation of the Insulin Signalling Cascade and Genes Involved in Regulating the GC Response Across Skeletal Myocyte Differentiation

3.1. Introduction

Skeletal muscle is a major component of the human body, accounting for ~40% of the total body mass. Its purpose is to provide support and movement to the skeleton, but also has numerous vital metabolic functions. The formation of mature muscle fibres is dependent upon the fusion of multiple proliferative myoblasts to form long multinucleated myotubes, which express characteristic contractile proteins. Although the relative abundance of unfused myoblasts compared with differentiated myotubes is relatively low in adult skeletal muscle, the comparative insulin sensitivity of these two cell populations has not been explored in detail.

The insulin signalling cascade has multiple roles within differentiating skeletal myocytes, governed by IGF-I/IGF-II as well as insulin; signalling both proliferation and differentiation through the IGF-I receptor (Engert et al., 1996), as well as glucose uptake through the insulin receptor. Little is know with regards to the gene expression of these signalling components across myocyte differentiation; during a time when the role of the cascade switches from signalling myoblast proliferation/differentiation to predominately signalling glucose uptake when myotube formation is complete.

The aim of this chapter is to compare the insulin sensitivity of undifferentiated myoblasts with that of differentiated myotubes, and characterise the gene expression of the insulin signalling cascade and genes involved in regulating GC

response across myocyte differentiation.

3.2. Strategy of Research

Using cultured C2C12 myocytes as a skeletal muscle model, the insulin sensitivity of undifferentiated myoblasts and differentiated myotubes was assessed by measuring uptake of a radiolabelled glucose tracer in presence and absence of insulin.

Gene expression of the insulin signalling cascade, 11β-HSD1 and genes involved in regulating GC responses were assessed in C2C12 myoblasts and myotubes using real-time PCR.

Functional 11β-HSD1 activity was assessed in C2C12 myoblasts and myotubes by measuring the conversion of a radiolabelled GC tracer.

3.3. Methods

3.3.1. C2C12 cell culture

Proliferating C2C12 myoblasts were cultured in DMEM supplemented with 10% FCS and seeded into 12-well TC plates. At 60-70% confluence differentiation was initiated by replacing proliferation media with DMEM supplemented with 5% horse serum and differentiated for 8 days (Figure 3-1). Prior to treatment, cells were incubated in DMEM free from additives for 4 h.

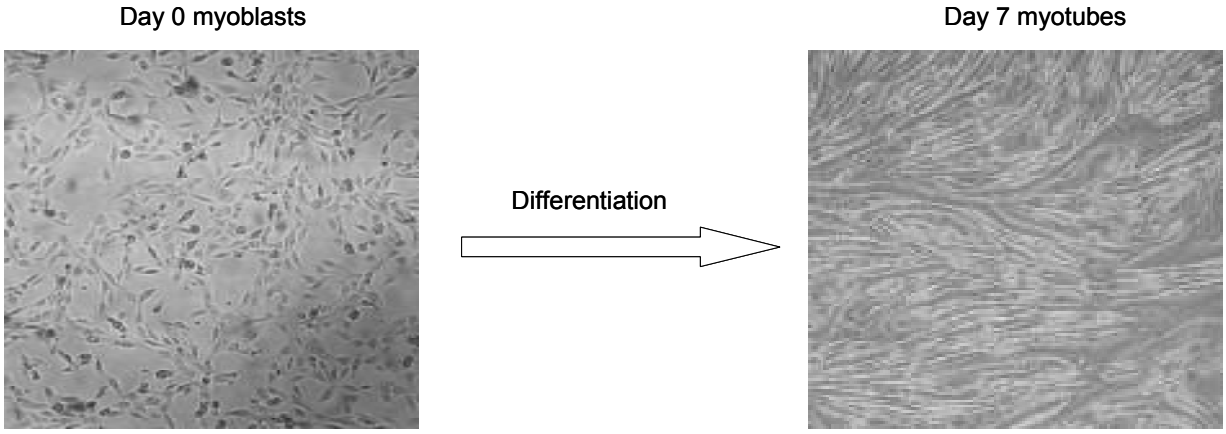

Figure 3-1 Murine C2C12 myocytes differentiated in chemically defined media for 8 days forming multinucleated myotubes

3.3.2. 11β-HSD1 activity assay

C2C12 myoblasts (at approx. 70% confluence) and differentiated myotubes were incubated with 100nM 11DHC or corticosterone supplemented with a tritiated tracer for 2 h. Steroids were then extracted using dichloromethane, separated using a mobile phase consisting of ethanol/chloroform (8:92) by thin layer chromatography, and scanned using a Bioscan 200 imaging scanner (LabLogic,

Sheffield, UK). Total protein levels were assayed using a commercially available kit (BioRad, Herts, UK), and activity expressed as pmol corticosterone/11DHC generated per mg of protein per hour.

3.3.3. RNA extraction

Total RNA was extracted using Tri-reagent system, concentration determined spectrophotometrically at OD_{260} and integrity assessed by agarose gel electrophoresis. For reverse transcription (see section 2.9.2) 1µg of RNA was used.

3.3.4. Real-time PCR

InsR, IRS1, IRS2, PI3K(p110), PI3K(p85), PKBα/akt1, PKBβ/akt2, GLUT4, AS160, 11β-HSD1, H6PDH, GRα, α-actin and myogenin mRNA levels were determined using an ABI 7500 sequence detection system (Applied Biosystems, Warrington, UK). Reactions were performed in singleplex as described in section 2.11.2, and normalised against the 18s rRNA house keeping gene. Primers and probes and for all genes were supplied by Applied Biosystems as pre-mixed ‘assay on demands’ (Applied Biosystems, Warrington, UK).

3.3.5. Glucose uptake assay

Glucose transport was assessed by measuring uptake of a radiolabelled glucose tracer as described previously (Liu et al., 2001) and as described in section 2.3.2. C2C12 myoblasts were grown to approx. 70% confluence or differentiated as described above then incubated in serum free DMEM for 4 h. Cells were washed 3 times with PBS then transferred to 0.9mL of KRB and incubated for 10 mins. Cells were spiked with 0.5µg/mL insulin for 20 mins prior to the addition of 0.1mL KRB containing 6mM glucose combined with 37MBq/L of 2-deoxy-D-[3H-glucose] (GE Healthcare, Bucks, UK) as a tracer. Radioactivity retained by cells was determined by scintillation counting. Glucose uptake was expressed as radioactivity retained by the cells in presence and absence of insulin. This assay was optimised as described in Figure 3-2 and Figure 3-3.

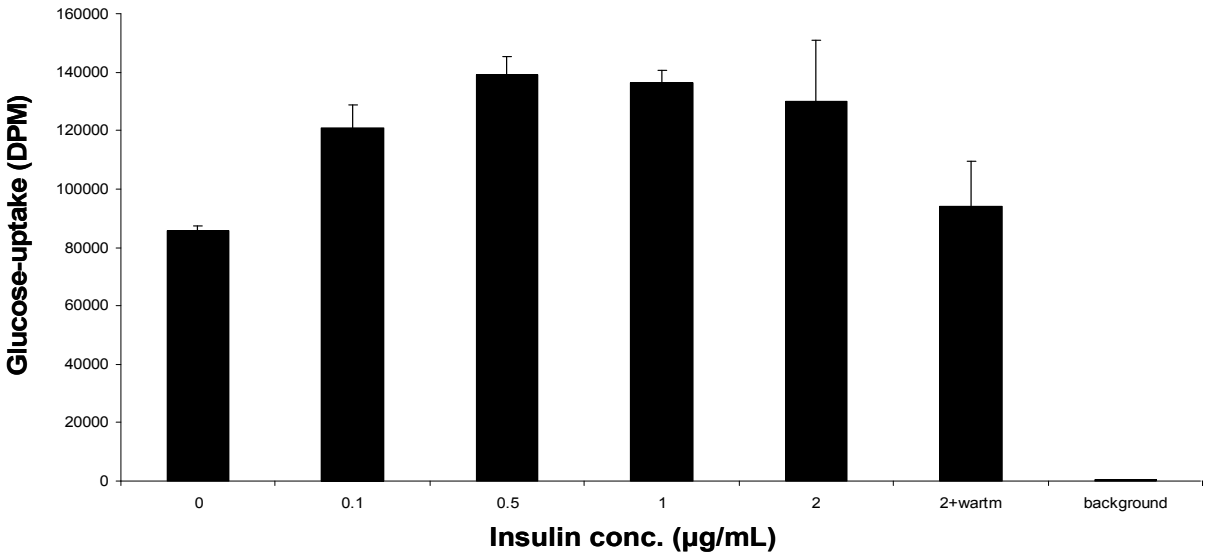

Figure 3-2 Preliminary glucose uptake assays to identify the optimal insulin concentration to achieve maximal insulin-stimulated glucose uptake in C2C12 myotubes. Insulin stimulation = 20 mins, incubation in the presence of glucose tracer = 60 mins. Wortmannin = PI3K inhibitor. (background= wells containing no cells)

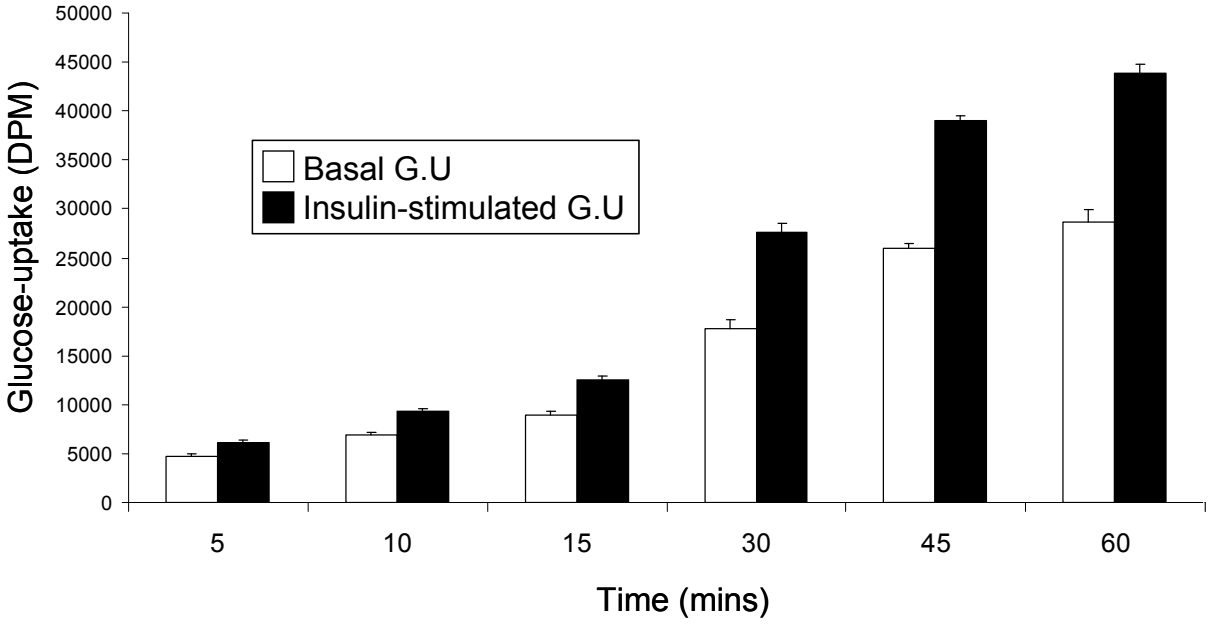

Figure 3-3 Preliminary glucose uptake assay to identify the optimal glucose exposure time to achieve maximal insulin-stimulated glucose uptake. Insulin conc. = 0.5µg/mL, 20 mins.

3.3.6. Statistical analysis

Where data were normally distributed, unpaired student t-tests were used to compare single treatments to control using SigmaStat 3.1 (Systat Software, CA, US). If normality tests failed, non-parametric tests were used. One way ANOVA on ranks, was used to compare multiple treatments, doses or times using SigmaStat 3.1. Statistical analysis on PCR data was performed on mean ΔCt values.

3.4. Results

After myocyte differentiation, there was a decrease in the mRNA expression of the key insulin signalling cascade components: IRS1 (18.6±3.1 vs. 8.7±0.7, $p<0.01$), IRS2 (27.6±1.2 vs. 0.34±0.06AU, $p<0.001$) and AS160 (9.2±3.6 vs. 0.12±0.02AU, $p<0.001$) (Table 3-1). By contrast, there was an increase in the expression of the catalytic subunit of PI3K (p110) (0.070±0.002 vs. 0.32±0.04AU, $p<0.0001$) and GLUT4 (1.1±0.2 vs. 2.3±0.3AU, $p< 0.01$), with no significant change in the gene expression of InsR, the regulatory subunit of PI3K (p85), PKBα/akt1 or PKBβ/akt2. The transition from myoblasts to myotubes also saw an increase in the expression of genes involved in regulating GC metabolism: 11β-HSD1 (5.2±0.6 vs. 32.9±2.9, $p<0.001$), H6PDH (0.03±0.01 vs. 0.10±0.01AU, $p<0.01$) and GRα (0.92±0.19 vs. 4.0±0.8AU, $p<0.001$). Myocyte differentiation was confirmed by the increase in the expression of α-actin (0.20±0.01 vs. 1.4±0.1AU, $p<0.05$) and myogenin (0.070±0.001 vs. 2.1±0.2AU, $p<0.01$); markers of myotubes formation.

		mRNA expression (AU ± SE)		
	Gene	**Myoblasts**	**Myotubes**	**p-value**
Insulin Signalling Cascade	InsR	5.0 ± 0.5	4.4 ± 0.4	0.486
	IRS1	18.6 ± 3.1	8.7 ± 0.7	0.007
	IRS2	27.6 ± 1.2	0.34 ± 0.06	0.000149
	PI3K (p85)	2.4 ± 0.3	1.4 ± 0.2	0.430
	PI3K (p110)	0.070 ± 0.002	0.32 ± 0.04	< 0.0001
	PKBα/akt1	63.2 ± 6.2	45.2 ± 5.4	0.080
	PKBβ/akt2	1.1 ± 0.2	1.5 ± 0.3	0.430
	AS160	9.2 ± 3.6	0.12 ± 0.02	0.000103
	GLUT4	1.1 ± 0.2	2.3 ± 0.3	0.010
Glucocorticoid Metabolism and Action	11β-HSD1	5.2 ± 0.6	32.9 ± 2.9	0.001
	H6PDH	0.03 ± 0.01	0.10 ± 0.01	0.001
	GRα	0.92 ± 0.19	4.0 ± 0.8	0.00059
Myocyte Differentiation	α-ACTIN	0.20 ± 0.01	1.4 ± 0.1	0.011
	MYOGENIN	0.070 ± 0.001	2.1 ± 0.2	0.001

Table 3-1 mRNA expression of key components of the insulin signalling cascade and GC metabolism in C2C12 myocytes across differentiation, measured using real-time PCR. Data are the mean values from n=5 experiments and expressed as arbitrary units (AU)±S.E.

11β-HSD1 activity was detected in both in C2C12 myoblasts and myotubes (Figure 3-4). Activity was bidirectional, but oxo-reductase activity predominated. Furthermore, oxo-reductase activity increased 13-fold after myocyte differentiation (7.8±1.9 vs. 103.4±22.5pmol/mg/h, p<0.05).

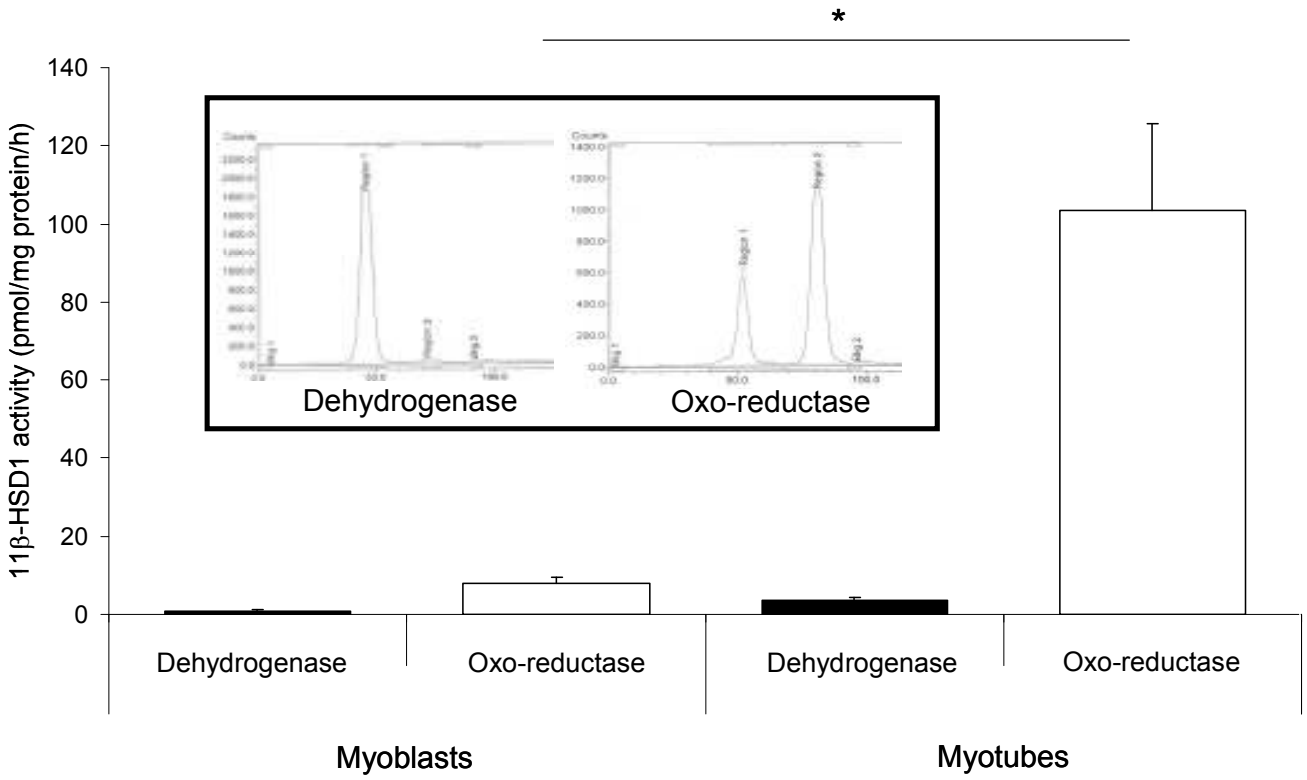

*Figure 3-4 11β-HSD1 activity (oxo-reductase and dehydrogenase) in C2C12 myoblasts and myotubes. (Data shown are the mean±s.e. of n=4 experiments, with representative activity traces inserted, * p<0.05).*

Tritiated glucose uptake was assessed across C2C12 myocyte differentiation (Figure 3-5). Basal glucose uptake increased 22-fold in the transition from myoblasts to myotubes (0.72±0.01 vs. 15.7±2.9dpmx10^4, p<0.05). Insulin stimulation increased total glucose uptake in both myoblasts (0.72±0.01 vs. 1.80±0.02dpmx10^4, p<0.001) and myotubes (15.7±2.9 vs. 21.8±3.6dpmx10^4, p<0.05). In addition, insulin stimulated glucose uptake (glucose uptake in

presence of insulin - glucose uptake in absence of insulin) increased 5.6-fold across myocyte differentiation (1.20±0.03 vs. 6.10±0.78dpmx$10^{4,}$ $p<0.05$).

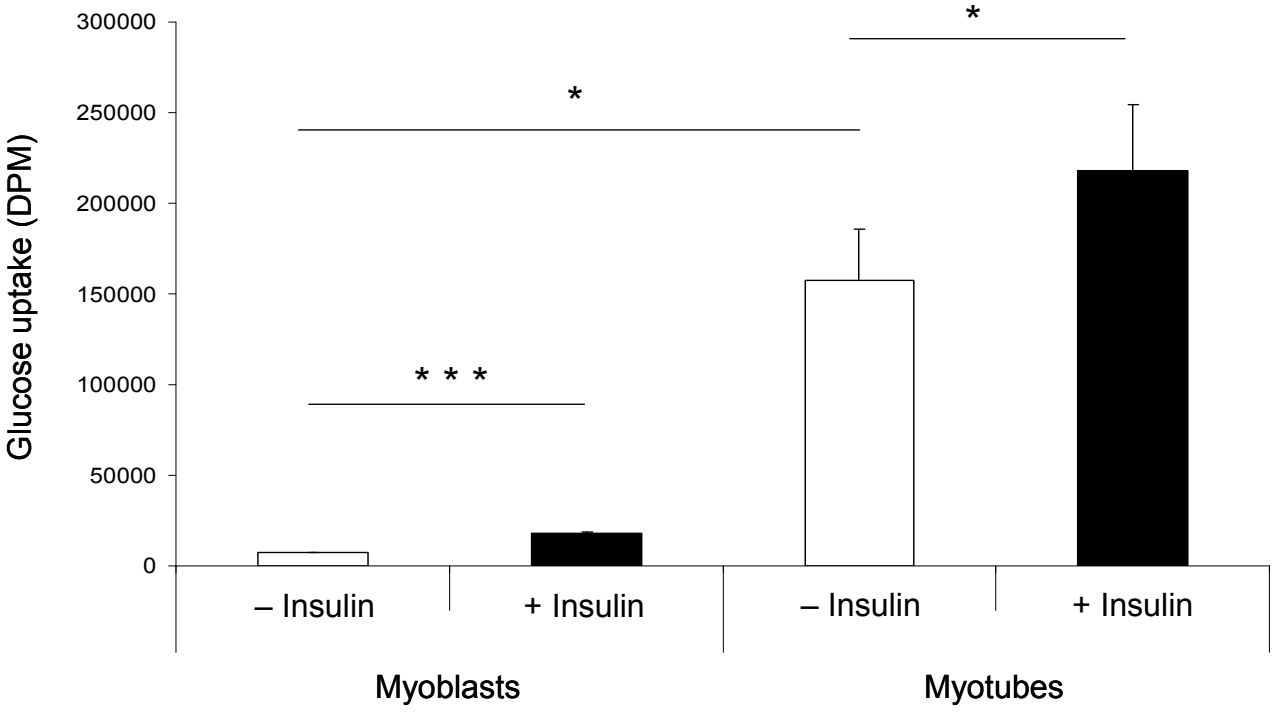

Figure 3-5 Tritiated glucose uptake in C2C12 myoblasts and myotubes with and without insulin (0.5µg/mL, 20 mins). (p<0.05; *** p<0.001)*

3.5. Discussion

During skeletal myocyte differentiation, IGF-I/IGF-II are synthesized and secreted by differentiating myoblasts and act autocrine and paracrine by associating with the IGF-I receptors. Subsequent stimulation of the IRS/PI3K axis enhances the activity of the mitogen-activated protein kinase (MAPK) family, namely extracellular signal-regulated kinase-1 and -2 (ERK-1 and -2), which regulate myocyte proliferation/differentiation (Engert et al., 1996). We have shown that across myocyte differentiation there is a downregulation in IRS1 and IRS2 mRNA expression. The reason for this downregulation is unclear, however, IRS proteins have recently been shown to activate cell-cycle progression in an IGF-I dependent manner by translocating into the nucleus where they are necessary for cyclin D1 promoter activation (Wu, Chen & Baserga, 2008). The observed decrease in expression of these proteins may simply reflect the fact that differentiated myotubes no longer undergo cell division, and thus do not require this transactivation function.

Further downstream in the insulin signalling cascade, an increase in the expression of the catalytic subunit of PI3K (p110) with respect to its regulatory subunit (p85) was observed across myocyte differentiation. Due to the competition for binding IRS1 between the p85 monomers and the catalytically active p85-p110 heterodimer (Giorgino et al., 1997), this stoichiometric change is predicted to have an insulin sensitising effect. Similarly, the insulin dependent glucose transporter (GLUT4) was expressed 2-fold higher in the differentiated myotubes. Both these gene expression changes could explain the enhanced

glucose uptake of the myotubes compared with the myoblasts.

.

In addition to assessing mRNA expression levels of key proteins in the insulin signalling cascade, we also analysed the expression of genes involved in regulating GC action across myocyte differentiation. The expression of 11β-HSD1, H6PDH and GRα increased in the transition from myoblasts to myotubes. Furthermore, oxo-reductase activity of 11β-HSD1 (which generates active GC) also increased, amplifying local GC availability. These results are consistent with previously published work (Aubry & Odermatt, 2009). Taken together, these data indicate that GCs, generated within the skeletal myocytes, could be integral to promoting and maintaining differentiation of these cells. Indeed, there is evidence in support of this from experiments done previously within our group whereby antagonism of the GC receptor by RU38486, introduced into the differentiation media, abolished all C2C12 myotube formation (personal communication, Mark Sherlock). Similar results were achieved by selectively inhibiting 11β-HSD1 during differentiation (personal communication, Mark Sherlock). Adding further support, treatment of C2C12 myocytes with DEX significantly enhances the expression of Myog, Myod1, Myf5 and MRF4, demonstrating that GC regulate the expression of key myogenic cell differentiation-related genes (Nishimura et al., 2008). However, retinoic acid (RA) induced downregulation of 11β-HSD1 expression has been shown to be without effect upon myotube formation (Aubry & Odermatt, 2009).

Interestingly, the expression of many of the insulin signalling cascade genes appear to be GC regulated, as demonstrated in Chapter 4, thus it is tempting to

speculate that some of the expression changes discussed in this chapter could, at least in part, be a consequence of enhanced activation of the GR as myocytes differentiate.

Chapter 4 - Impact of the Synthetic Glucocorticoid Dexamethasone Upon the Insulin Signalling Cascade and Lipid Metabolism in Skeletal Muscle

4.1. Introduction

The pathophysiological effects of excess GCs are well described and impact upon almost all organ systems within the body. This is highlighted by patients with endogenous or exogenous GC excess, Cushing's syndrome which is characterised by central obesity, hypertension, proximal myopathy, insulin resistance and in some cases overt type 2 diabetes (T2DM) (Wajchenberg et al., 1984). In addition, it is estimated that up to 0.3% of the population are taking prescribed high dose GCs (>7.5mg daily) (van Staa et al., 2000), and their side effects represent a considerable clinical burden (for both patient and clinician).

GCs induce whole body insulin resistance in both animal models and humans as measured by hyperinsulinaemic euglycaemic clamps (Larsson & Ahren, 1996). However, the precise molecular mechanisms that underpin this observation have not been defined in detail. It is likely that reduced whole body insulin sensitivity is the additive effect of metabolic events in different organ systems. For instance, in the liver, GC exposure increases glucose output and decreases glucose utilisation contributing to insulin resistance (Guillaume-Gentil, Assimacopoulos-Jeannet & Jeanrenaud, 1993). Furthermore, short-term cortisol treatment of healthy individuals was found to impair the ability of glucose to suppress its own production (Nielsen et al., 2004). In adipose tissue, some have observed a GC-induced decrease in insulin-stimulated glucose uptake (Sakoda et al., 2000), but this is not a consistent observation (Gathercole et al., 2007). Since skeletal muscle accounts for at least 80% of the glucose disposal under, insulin-stimulating conditions (DeFronzo et al., 1981), the effects of GCs in this tissue

could be the major contributor to whole body insulin resistance. Indeed, a number of studies have demonstrated that GC directly inhibit insulin-stimulated glucose uptake in skeletal muscle (DiabetologiaWagman & Jensen, 2005; Dimitriadis et al., 1997; Guillaume-Gentil et al., 1993; Venkatesan et al., 1996).

Following binding of insulin to its cell surface receptor, a complex signalling cascade is initiated, as discussed in detail in section 1.6. Briefly, the metabolic actions of insulin occur through the IRS1/PI3K axis (Giorgetti et al., 1993). This results in activation of PKB/akt, which subsequently phosphorylates AS160 allowing GLUT4 storage vesicles to be trafficked to the plasma membrane - increasing uptake of glucose into the cell (Larance et al., 2005).

The molecular mechanisms underpinning insulin resistance are complex and variable, however, many studies have focussed on the role of IRS1 as a critical regulatory point of the insulin signalling cascade. IRS1 has more than 70 putative serine/threonine phosphorylation sites which have the dual function of both positively and negatively regulating insulin signal transduction. Phosphorylation of IRS1 at serine-307 negatively regulates insulin signalling by inhibiting insulin-stimulated tyrosine phosphorylation, and IRS1-associated PI3K activity, potentially through disruption of the protein–protein interaction between IRS1 and the insulin receptor (Aguirre et al., 2000; Aguirre et al., 2002). Intracellular accumulation of DAG is associated with enhanced phosphorylation at this site through activation of PKCθ - highlighting a close link between intramyocellular lipid metabolism and the insulin signalling cascade (Gao et al., 2004; Yu et al., 2002), however, activation of numerous kinases, including: Jun kinase (JNK)

(Aguirre et al., 2000), inhibitor of nuclear factor κB (NF-κB) kinase-β (IKKβ) (Gao et al., 2002), p70S6K (S6K1) (Harrington et al., 2004), the mammalian target of rapamycin (mTOR) (Ozes et al., 2001) and extracellular signal-regulated kinase (ERK) (Bouzakri et al., 2003) have been linked with phosphorylation at this site (Aguirre et al., 2000; Carlson, White & Rondinone, 2004). More recently, phosphorylation of IRS1 at serine-24 has been identified as being important in regulating lipid binding and intracellular localization of IRS1 (Nawaratne et al., 2006).

The interaction between GCs and the insulin signalling cascade in skeletal muscle has only been examined in a small number of studies, which have offered varying explanations for the induction of insulin resistance (Giorgino et al., 1993; Giorgino et al., 1997; Giorgino & Smith, 1995; Rojas et al., 2003; Ruzzin et al., 2005; Saad et al., 1993). We have therefore characterized the impact of the synthetic GC, dexamethasone (Dex), upon the insulin signalling cascade in rodent skeletal muscle. In addition, since there is a strong link between dysregulated intramyocellular lipid metabolism and reduced insulin sensitivity, the impact of DEX upon these metabolic pathways has also been investigated.

4.2. Strategy of research

Using cultured C2C12 myocytes as a skeletal muscle model, the functional impact of the synthetic GC, DEX, upon insulin sensitivity was addressed by measuring uptake of a radiolabelled glucose tracer in presence and absence of insulin.

The impact of GCs upon the gene expression of the insulin signalling cascade, genes involved in glucocorticoid metabolism/action and genes regulating lipid metabolism in C2C12 myocytes was assessed using real-time PCR.

Western blot analysis was employed to analyse the impact of GCs upon protein levels / phosphorylation status of the insulin signalling cascade components in C2C12 myocytes.

The functional impact of GCs, and GCs with insulin upon the rate of *de novo* lipogenesis was assessed in C2C12 myotubes by measuring the intracellular accumulation of a radiolabelled acetic acid tracer.

The functional impact of GCs, and GCs with insulin upon the rate of β-oxidation was assessed in C2C12 myotubes by measuring the release of radiolabelled water following treatment with a radiolabelled palmitic acid tracer.

4.3. Methods

4.3.1. C2C12 cell culture

Proliferating C2C12 myoblasts were cultured in DMEM supplemented with 10% FCS and seeded into 12-well TC plates. At 60-70% confluence, differentiation was initiated by replacing proliferation media with DMEM supplemented with 5% horse serum, and differentiated for 8 days (Figure 3-1). Prior to treatment, cells were incubated in DMEM without additives for 4 h.

4.3.2. Generation of C2C12s stably expressing rIRS1

C2C12 cells stably expressing myc-his-tagged IRS1 were generated by retroviral mediated gene transfer (Pear et al., 1993). Briefly, subconfluent BOSC23 packaging cells were transfected with pBabePuro-rIRS1mychis plasmids, and conditioned media was collected 48 h later. This was passed through a 0.45-μm filter, supplemented with 16μg/ml of polybrene, and used to infect proliferating C2C12 myocytes. Drug selection with 4μg/ml puromycin was initiated 2 days later. After a week in drug selection, stable cell lines were confirmed by western blot analysis and expanded. (This protocol was carried out by Jazwinder Sethi, University of Cambridge)

4.3.3. Cell treatments

In all cell culture experiments investigating insulin signalling cascade protein expression/phosphorylation status, media was spiked with human insulin (50nM) for the final 15 mins of the treatment period. In experiments using the GR antagonist, RU38486, cells were pre-treated with RU38486 (10μM) for 10 mins before adding DEX (1μM) in DMEM media. In experiments using C2C12 stably overexpressing IRS1, phorbol-12-myristate-13-acetate (PMA) was used at 1μM. Cells were treated for 24 h.

4.3.4. RNA extraction

Total RNA was extracted using Tri-reagent system, concentration determined spectrophotometrically at OD_{260} and integrity assessed by agarose gel electrophoresis. For reverse transcription (see section 2.9.2) 1μg of RNA was used.

4.3.5. Real-time PCR

InsR, IRS1, IRS2, PI3K(p110), PI3K(p85), PKBα/akt1, PKBβ/akt2, GLUT4, AS160, 11β-HSD1, H6PDH, GRα, LPL, HSL, ATGL, FAS, ACC1, ACC2, GPAT, DGAT and PDK4 mRNA levels were determined using an ABI 7500 sequence detection system (Applied Biosystems, Warrington, UK). Reactions were performed in singleplex as described in section 2.11.2, and normalised against the 18s rRNA house keeping gene. Primers and probes and for all genes were supplied by Applied Biosystems as pre-mixed ‘assay on demands’ (Applied

Biosystems, Warrington, UK).

4.3.6. Generation of anti-pSer24 IRS1 antibody

The generation of anti-pSer24-IRS1 was commissioned from Cambridge Research Biochemicals Ltd. (Cambridge, UK). Briefly, rabbit antisera were generated against the following N-terminally, keyhole limpet hemocyanin-conjugated phosphopeptide: [C]YLRKPKS(p)MHKRFF. The phosphoreactive serum was then affinity purified on a Thiopropyl Sepharose 6B column derivatized with nonphosphorylated antigen. The unbound antiserum was then passed down a Thiopropyl Sepharose 6B column derivatized with the phosphorylated peptide. The resulting triethylamine eluate retained significant phosphospecific immunoreactivity on peptide-coated ELISA plates and was used in western blot analysis as described below. (This protocol was carried out by Jazwinder Sethi, University of Cambridge)

4.3.7. Immunoblotting

Proteins were extracted from cell lysates, and concentration determined as described in section 2.6.2. For IRS1, p-IRS1, IRS2 and AS160 40µg of protein was resolved on 8% SDS-PAGE gels. For PKB/akt and p-PKB/akt, 20µg of protein was resolved on 12.5% SDS-PAGE gels. Proteins were transferred to nitrocellulose membranes (for IRS1, p-IRS1, IRS2 and AS160, proteins transferred at 140mA for 2 h, for PKB/akt and p-PKB/akt proteins transferred at 140mA for 1 h). Primary (anti-IRS1, anti-pSer307 IRS1, anti-IRS2 and anti-AS160 were purchased from Upstate, Dundee, UK, anti-PKB/akt and anti-pSer473 PKB/akt [recognizing isoforms 1 and 2] were purchased from R&D Systems,

Abingdon, UK and anti-pTyr608 was purchased from Biosource, Nivelles, Belgium) and secondary antibodies (Dako, Glostrop, UK) were used at a dilution of 1/1000. Membranes were re-probed for β-actin and primary and secondary antibodies used at a dilution of 1/5000 (Abcam, Cambridge, UK). Bands were visualised using ECL detection kit (GE Healthcare, Bucks, UK) and quantified with Genesnap by Syngene (Cambridge, UK). The ratio of p-IRS1 to β-actin was normalised to the ratio of IRS1 to β-actin.

4.3.8. Glucose uptake as a measure of insulin resistance

Glucose transport was assessed by measuring uptake of a radiolabelled glucose tracer as described previously (Liu et al., 2001), and as described in section 2.3.2. Cells were pre-treated with 10μM RU38486 for 10 mins prior to addition of 1μM DEX, and treated for 24 h. Cells were washed 3 times with PBS then transferred to 0.9mL of KRB containing same treatments and incubated for 10 mins. Cells were spiked with 0.5μg/mL insulin for 20 mins, prior to the addition of 0.1mL KRB containing 6mM glucose combined with 37MBq/L of 2-deoxy-D-[^{3}H-glucose] (GE Healthcare, Bucks, UK) as a tracer. Radioactivity retained by cells was determined by scintillation counting. For all treatments, glucose uptake was expressed as radioactivity retained by the cells in presence and absence of insulin.

4.3.9. Acetyl-CoA Carboxylase (ACC) assay

ACC activity was measured by the uptake of 1-[^{14}C]-acetic acid into the cellular lipid components of C2C12 myotubes as described in section 2.14. Cells were cultured in 24-well plates and at 60-70% confluence differentiated into myotubes in chemically defined media. Cells were incubated in serum free media for 4 h and then treated with either low dose DEX (5nM), high dose DEX (500nM) or no treatment for 24 h. In addition, treatments took place in the presence / absence of insulin (5nM). Cells were then incubated with 500µL of serum free media supplemented with 0.12µCi/L 1-[^{14}C]-acetic acid (GE Healthcare, Bucks, UK) and unlabelled sodium acetate - to a final concentration of 10µM acetate (with same treatments). The cells were incubated at 37°C for 4 h and then washed 3x with ice cold PBS, scraped into 250µL of PBS and then transferred into glass tubes. To extract the lipid fraction, 5mL of Folch solvent was added and shaken vigorously for 20 secs. 1mL of water was added and shaken vigorously for 20 secs. Phases were separated by centrifugation at 300 g for 5 mins. The upper aqueous phase was removed by aspiration, and lower fraction transferred to a 5mL scintillation tube and evaporated until dry using a sample dryer (Techne, New Jersey, US). Once dry, 5mL of scintillation cocktail was added (PerkinElmer, Bucks, UK), and samples were counted using a Wallac 1414 liquid scintillation counter (PerkinElmer, Bucks, UK).

4.3.10. β-oxidation assay

C2C12 myocytes were cultured and treated in 24-well TC places and, at 60-70% confluence, differentiated into myotubes using chemically defined media. Cells were incubated in serum free media for 4 h before incubation with 500μL of serum free media containing 0.1 mmol/L palmitate (9,10-[^{3}H]palmitate (5μCi/mL) (GE Healthcare, Bucks, UK), 2% BSA and DEX (5nM or 500nM) with or without insulin (5nM) for 24 h. After incubation, the media was retained, and precipitated twice with equal volumes of 10% trichloroacetic acid, to remove excess labelled palmitate. The supernatants (≈0.5mL) were extracted by addition of 2.5mL of methanol:chloroform (2:1) and 1mL of 2mol/L KCl:HCl, followed by centrifugation at 3000 g for 5 min. Aqueous phase (0.5mL) was then added to scintillation cocktail (PerkinElmer, Bucks, UK), and samples were counted using a Wallac 1414 liquid scintillation counter (PerkinElmer, Bucks, UK).

4.3.11. Statistical analysis

Where data were normally distributed, unpaired student t-tests were used to compare single treatments to control using SigmaStat 3.1 (Systat Software, CA, US). If normality tests failed, non-parametric tests were used. One way or two way ANOVA on ranks was used to compare multiple treatments, doses or times using SigmaStat 3.1. Statistical analysis on PCR data was performed on mean ΔCt values.

4.4. Results

4.4.1. Insulin sensitivity of undifferentiated myoblasts

Treatment of undifferentiated C2C12 myoblasts with DEX (1μM, 24h) was without effect upon both basal (Figure 4-1A) and insulin-stimulated glucose uptake (Figure 4-1B).

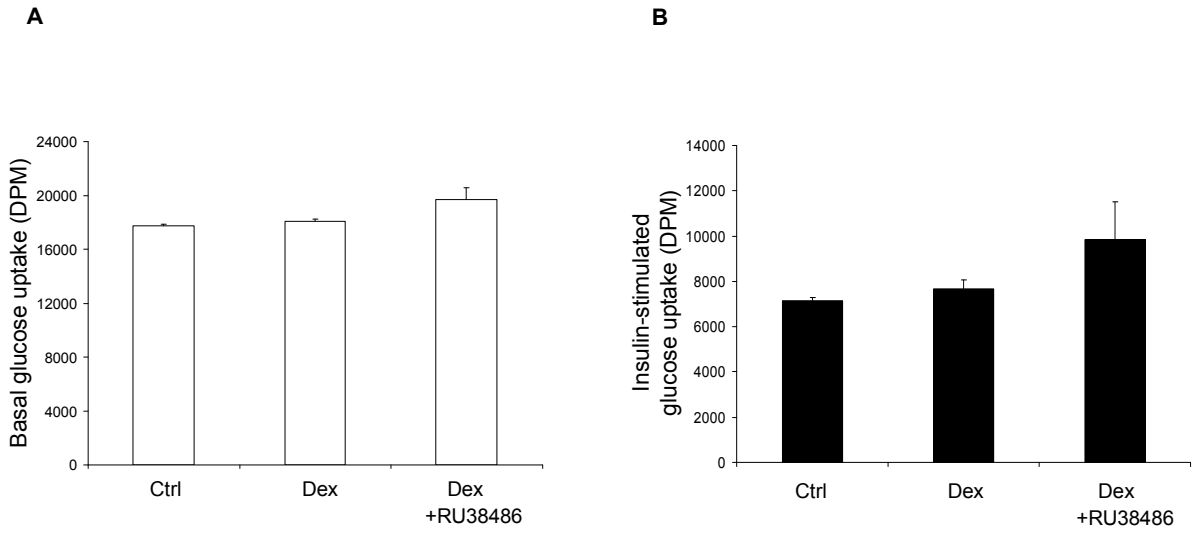

Figure 4-1 DEX (1μM, 24 h) had no effect upon basal (A) or insulin-stimulated glucose uptake (B) in undifferentiated C2C12 myoblasts. Insulin-stimulated glucose uptake = glucose uptake with insulin (0.5μg/mL, 20 mins) minus glucose uptake in the absence of insulin. (DEX=dexamethasone, Ctrl=control).

In undifferentiated C2C12 myoblasts, DEX (1μM, 24h) decreased mRNA expression of IRS1 (18.6±3.1 vs. 9.6±0.9AU, $p<0.05$), an effect that was blocked by the GR antagonist RU38486 (Table 4-1). In contrast, IRS2 and PKBβ/akt2 mRNA expression was increased by DEX. RU38486 blocked the DEX-induced increase in IRS2 expression. DEX treatment increased the expression of 11β-HSD1 (5.2±0.6 vs. 11.0±1.1AU, $p<0.05$) and H6PDH (0.03±0.01 vs. 1.95±0.11AU, $p<0.001$). RU38486 blocked the effect of DEX upon H6PDH

expression, but was without effect upon 11β-HSD1 expression (Table 4-1).

In undifferentiated C2C12 myoblasts, DEX decreased IRS1 total protein (0.5-fold, $p<0.05$), which was reversed by RU38486. However, DEX did not alter the relative activation state of IRS1, as shown by a parallel reduction in serine-307 phosphorylation (Figure 4-2)

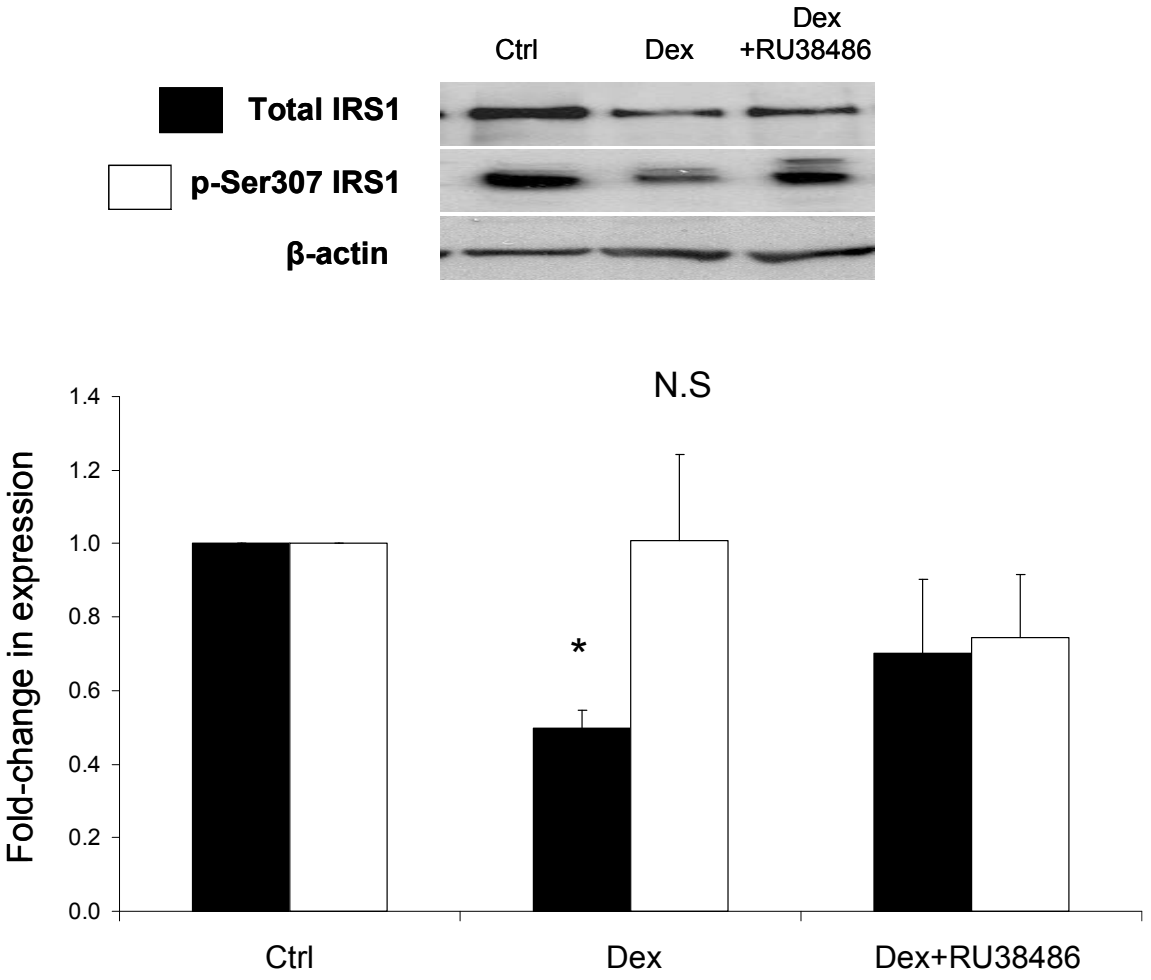

Figure 4-2 DEX treatment (1μM, 24 h) of undifferentiated C2C12 myoblasts decreases IRS1 total protein expression, an effect reversed by co-incubation with the GR antagonist RU38486 (10μM). IRS1 inactivating serine-307 phosphorylation was unchanged following DEX treatment. Cells were spiked with insulin (50nM) for the last 15 mins of treatment. Data presented are the mean of n=6 experiments with representative western blots inserted above. Bands quantified relative to β-actin as internal loading control and the ratio of p-IRS1 to β-actin was normalised to the ratio of IRS1 to β-actin. (p<0.05 vs. control; † p<0.05, vs. DEX) (DEX=dexamethasone, Ctrl=control, N.S=not significant*

		mRNA expression (AU ± SE)					
		Myoblasts			Myotubes		
	Gene	Control	Dex	Dex+RU38486	Control	Dex	Dex+RU38486
Insulin Signalling cascade	InsR	5.0 ± 0.5	8.1 ± 0.3 [a]	6.5 ± 0.8	4.4 ± 0.4	6.1 ± 0.5 [b]	5.4 ± 0.5
	IRS1	18.6 ± 3.1	9.5 ± 0.9 [a]	15.1 ± 2.9 [d]	8.7 ± 0.7	4.5 ± 0.4 [a]	7.5 ± 0.7 [d]
	IRS2	27.6 ± 1.2	47.8 ± 1.2 [a]	47.1 ± 3.4 [d]	0.34 ± 0.06	0.54 ± 0.03 [a]	0.54 ± 0.11
	PI3K (p85)	2.4 ± 0.3	3.2 ± 0.4	3.8 ± 0.5	1.4 ± 0.2	2.2 ± 0.2 [a]	2.2 ± 0.1
	PI3K (p110)	0.070 ± 0.002	0.060 ± 0.002	0.090 ± 0.002	0.32 ± 0.04	0.21 ± 0.03 [b]	0.31 ± 0.07
	PKBα/akt1	63.2 ± 6.2	78.5 ± 1.8	57.7 ± 9.7	45.2 ± 5.4	44.4 ± 2.8	45.1 ± 3.4
	PKBβ/akt2	1.1 ± 0.2	1.8 ± 0.1 [a]	1.3 ± 0.3	1.5 ± 0.3	2.3 ± 0.1 [a]	1.9 ± 0.3
	AS160	9.2 ± 3.6	14.5 ± 3.1	12.8 ± 1.0	0.12 ± 0.02	0.23 ± 0.02 [a]	0.12 ± 0.01 [d]
	GLUT4	1.1 ± 0.2	2.2 ± 0.7	0.4 ± 0.1	2.3 ± 0.3	13.1 ± 1.5 [c]	3.7 ± 0.4 [e]
Glucocorticoid Metabolism and action	11β-HSD1	5.2 ± 0.6	11.0 ± 1.1 [a]	11.2 ± 1.4	32.9 ± 2.9	27.6 ± 2.7 [a]	35.6 ± 3.6
	H6PDH	0.03 ± 0.01	1.95 ± 0.11 [c]	0.10 ± 0.01 [f]	0.10 ± 0.01	1.30 ± 0.07 [c]	0.18 ± 0.02 [f]
	GRα	0.92 ± 0.19	0.69 ± 0.32	1.53 ± 0.15	4.0 ± 0.8	1.8 ± 0.2 [a]	4.5 ± 1.1 [d]

Table 4-1 mRNA expression of key components of the insulin signalling cascade and GC metabolism in C2C12 myoblasts and myotubes, measured using real-time PCR following treatment with Dex (1μM, 24 h) with or without the GR antagonist, RU38486 (10μM). Data are the mean values from n=5 experiments, and expressed as arbitrary units (AU)±S.E. ([a] p<0.05, [b] p<0.01 and [c] p<0.001 vs. control; [d] p<0.05, [e] p<0.01 and [f] p<0.001 vs. Dex).

4.4.2. Insulin sensitivity of differentiated myotubes

In contrast to the undifferentiated myoblasts, DEX decreased insulin-stimulated glucose uptake (5.7±0.1 vs. 4.7±0.4dpmx10^4, $p<0.05$, n=5) in differentiated C2C12 myotubes, an effect recovered by co-incubation with RU38486 (Figure 4-3B). Basal glucose uptake was also reduced following DEX treatment (1.6±0.25 vs. 1.3±0.08dpm dpmx10^5, $p<0.05$, n=5, Figure 4-3A).

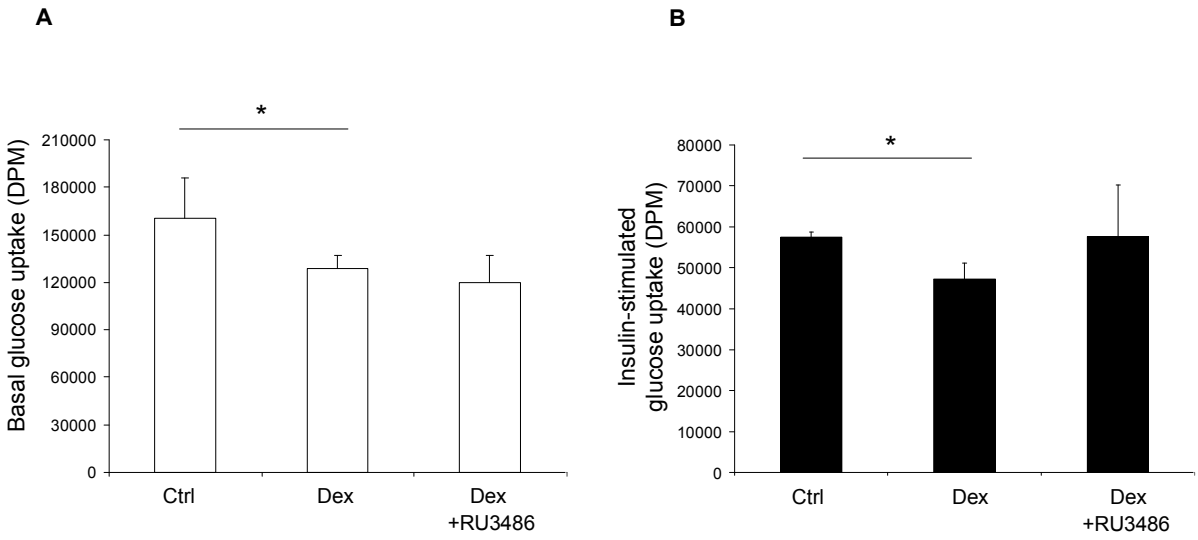

Figure 4-3 DEX (1μM, 24 h) decreased basal (A) and insulin-stimulated glucose uptake (B) in differentiated C2C12 myotubes. RU38486 (10μM) recovered the effect of DEX upon insulin-stimulated glucose uptake. Insulin-stimulated glucose uptake = glucose uptake with insulin (0.5μg/mL, 20 mins) minus glucose uptake in the absence of insulin. (DEX=dexamethasone, Ctrl=control).

In differentiated C2C12 myotubes, DEX (1μM, 24 h) decreased mRNA expression of IRS1 (8.7±0.7 vs. 4.5±0.4AU, $p<0.05$, n=5), an effect that was blocked by the GR antagonist RU38486 (Table 4-1). In contrast, InsR, PKBβ/akt2, AS160 and GLUT4 expression all increased. However, only the effect of DEX upon GLUT4 and AS160 expression was reversed with RU38486. DEX treatment had

contrasting effects upon the expression of the PI3K subunits; increasing p85 (regulatory subunit) expression (1.4±0.2 vs. 2.2±0.2AU, $p<0.05$) and decreasing p110 (catalytic subunit) expression (0.32±0.04 vs. 0.21±0.03AU, $p<0.01$). Whilst DEX treatment did not alter 11β-HSD1 expression, H6PDH expression increased (0.1±0.01 vs. 1.3±0.07AU, $p<0.001$) and this was blocked by co-incubation with RU38486 (0.18±0.02AU, $p<0.001$ vs. DEX). Decreased GRα expression was observed with DEX treatment (4.0±0.8 vs. 1.8±0.2AU, $p<0.05$), which was blocked by RU38486 (4.5±1.1AU, $p<0.05$ vs. DEX). Absolute mRNA expression levels following DEX treatment with and without the GR antagonist RU38486 are presented in Table 4-1.

In differentiated C2C12 myotubes, treatment with DEX decreased IRS1 total protein expression (0.4-fold, $p<0.05$), which was recovered by co-incubation with RU38486 (Figure 4-4). Activating tyrosine-608 phosphorylation of IRS1 was unchanged with DEX treatment (Figure 4-4), however, inactivating serine-307 phosphorylation (3.3-fold, $p<0.05$) was enhanced, and this was blocked by RU38486 (Figure 4-4).

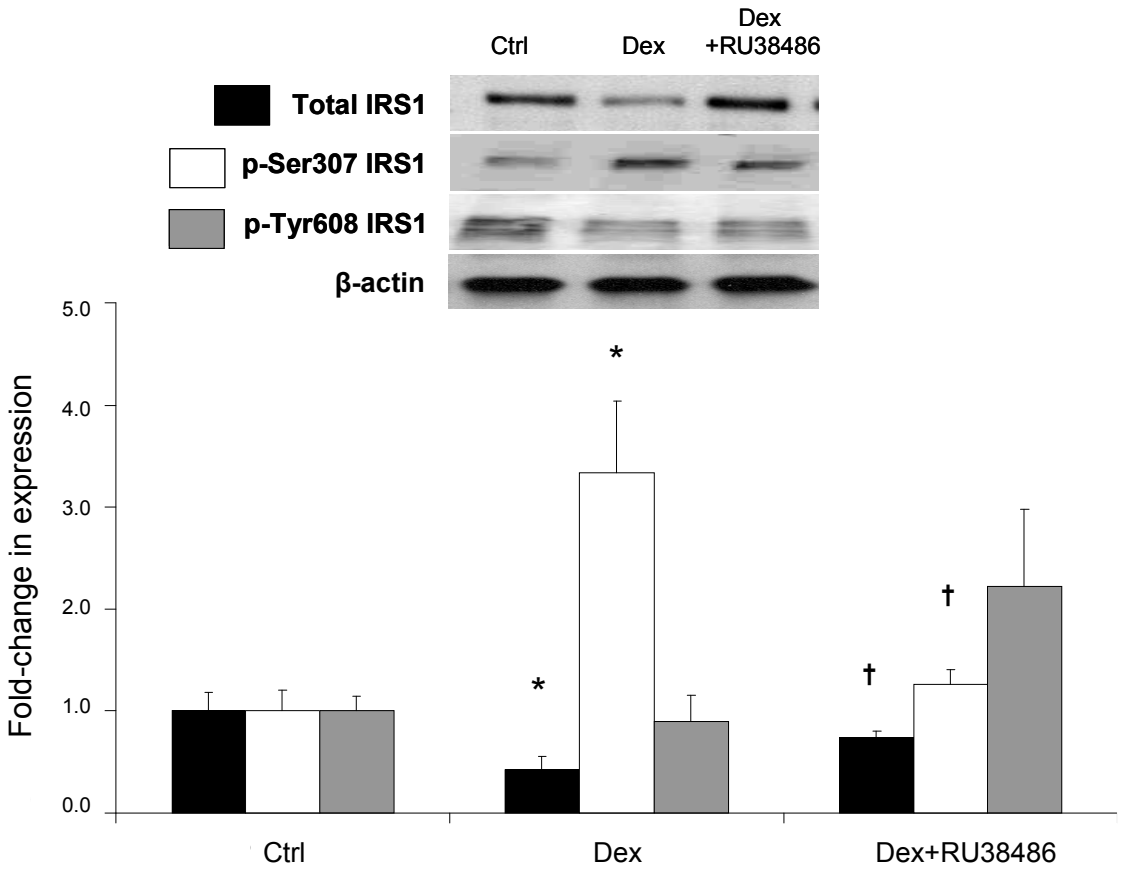

Figure 4-4 DEX treatment (1μM, 24 h) of differentiated C2C12 myotubes decreases IRS1 total protein expression, increases inhibitory serine-307 phosphorylation of IRS1 but does not change activating tyrosine-608 phosphorylation. These effects are blocked by co-incubation with the GR antagonist RU38486 (10μM). Cells were spiked with insulin (50nM) for the last 15 mins of treatment. Data presented are the mean of n=4-6 experiments with representative western blots inserted above. Bands quantified relative to β-actin as internal loading control and the ratio of p-IRS1 to β-actin was normalised to the ratio of IRS1 to β-actin. (p<0.05 vs. control; † p<0.05, vs. DEX) (DEX=dexamethasone, Ctrl=control)*

Phosphorylation of IRS1 at serine-24 has been linked to the pathogenesis of insulin resistance. We therefore examined the effect of DEX on C2C12 myobubes stably over expressing IRS1 (Nawaratne et al., 2006). Whilst DEX also increased serine-307 phosphorylation in this model, there was no impact upon serine-24 phosphorylation (Figure 4-5).

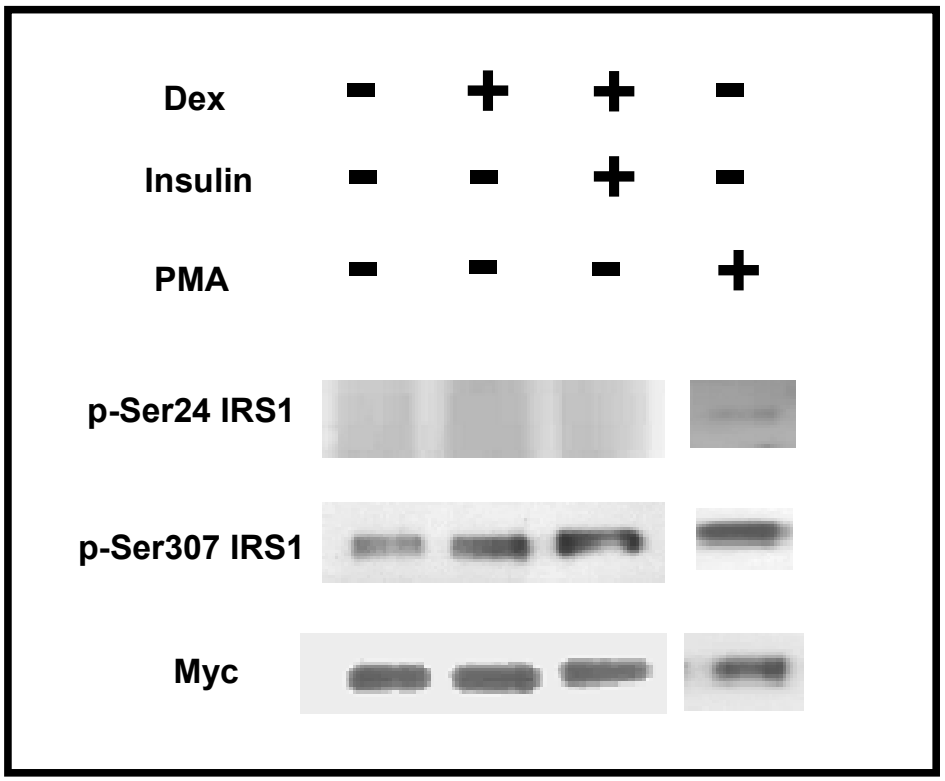

Figure 4-5 C2C12 myocytes stably over-expressing IRS1 were differentiated into myotubes and treated with DEX (1μM, 24 h) resulting in an increase in inhibitory IRS1 serine-307 phosphorylation, but not inhibitory serine-24 phosphorylation (Experiments carried out in collaboration with Jaswinder Sethi, University of Cambridge). (DEX=dexamethasone, PMA= phorbol-12-myristate-13-acetate).

In differentiated C2C12 myotubes, DEX increased total IRS2 protein expression (1.7-fold, $p<0.001$) (Figure 4-6). Further downstream, PKB/akt protein expression did not change with DEX treatment, but activating serine-473 phosphorylation decreased (0.5-fold, $p<0.05$) (Figure 4-7). DEX increased AS160 total protein levels 1.5-fold ($p<0.05$), which was blocked by co-incubation with RU38486 (Figure 4-8)

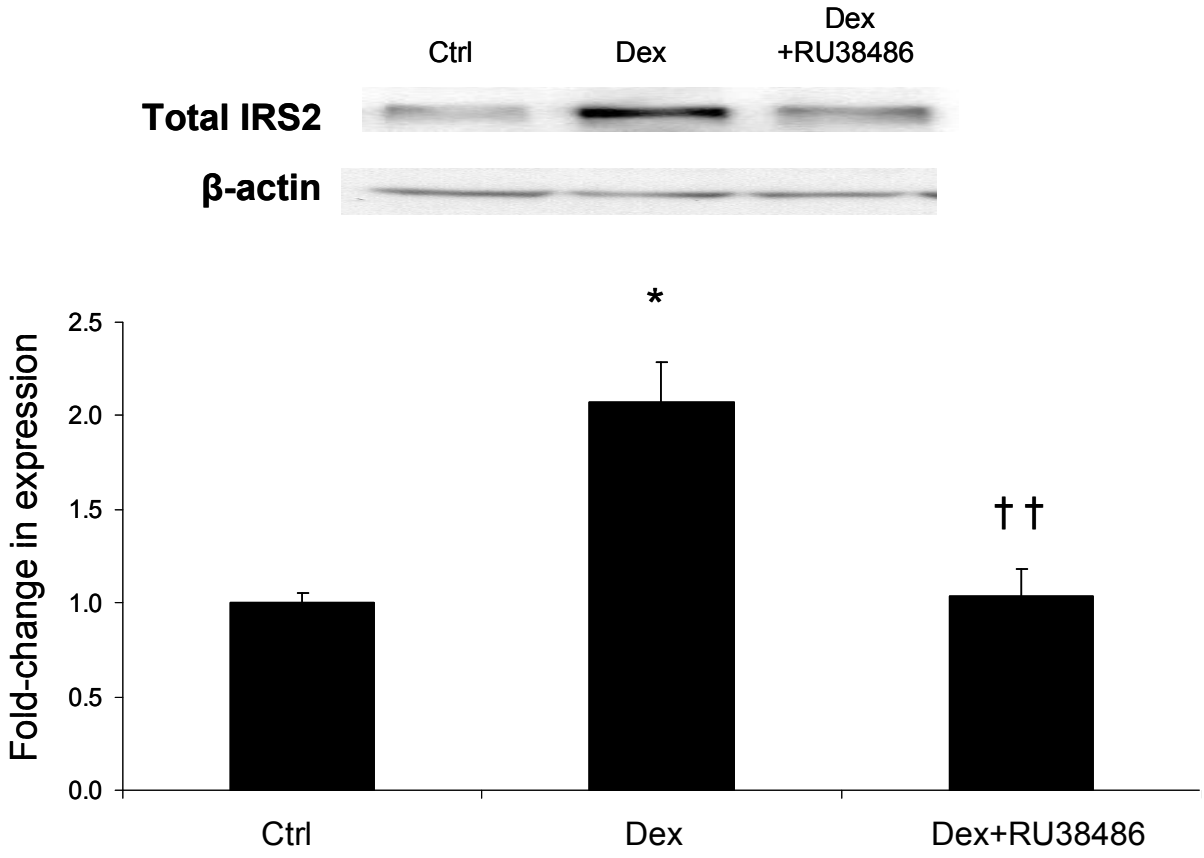

Figure 4-6 Total IRS2 protein expression increase following DEX treatment (1μM, 24 h) and was reversed with RU38486 (10μM) in differentiated C2C12 myotubes. Data presented are the mean of n=4 experiments with representative western blots inserted above. Bands quantified relative to β-actin as internal loading control. (p<0.05 vs control, †† p<0.01 vs. DEX) (DEX=dexamethasone, Ctrl=control).*

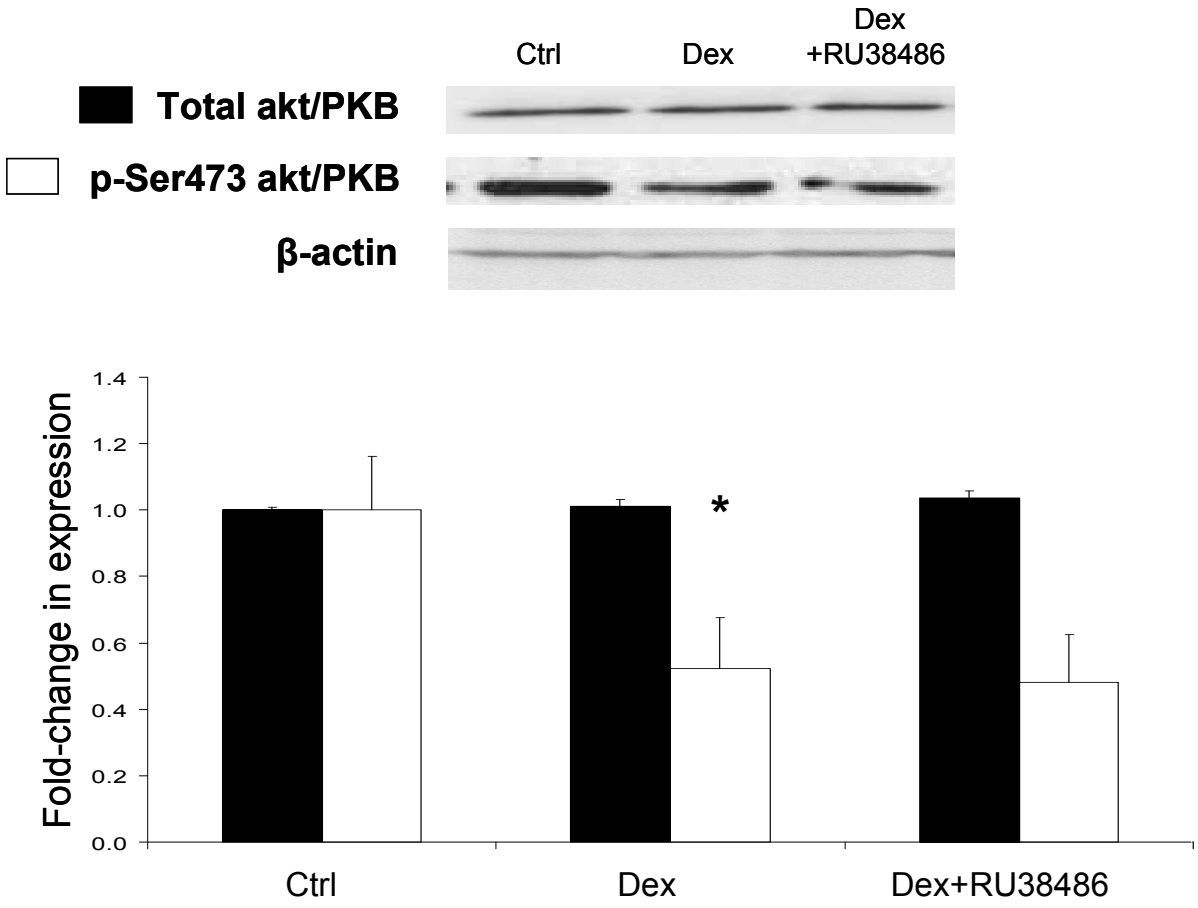

Figure 4-7 DEX treatment (1μM, 24 h) of C2C12 myotubes did not alter PKB/akt expression, whilst activating serine-473 phosphorylation was decreases but not recovered by co-incubation with RU38486 (10μM). Data presented are the mean of n=4 experiments with representative western blots inserted above. Bands quantified relative to β-actin as internal loading control (p<0.05 vs control) (DEX=dexamethasone, Ctrl=control)*

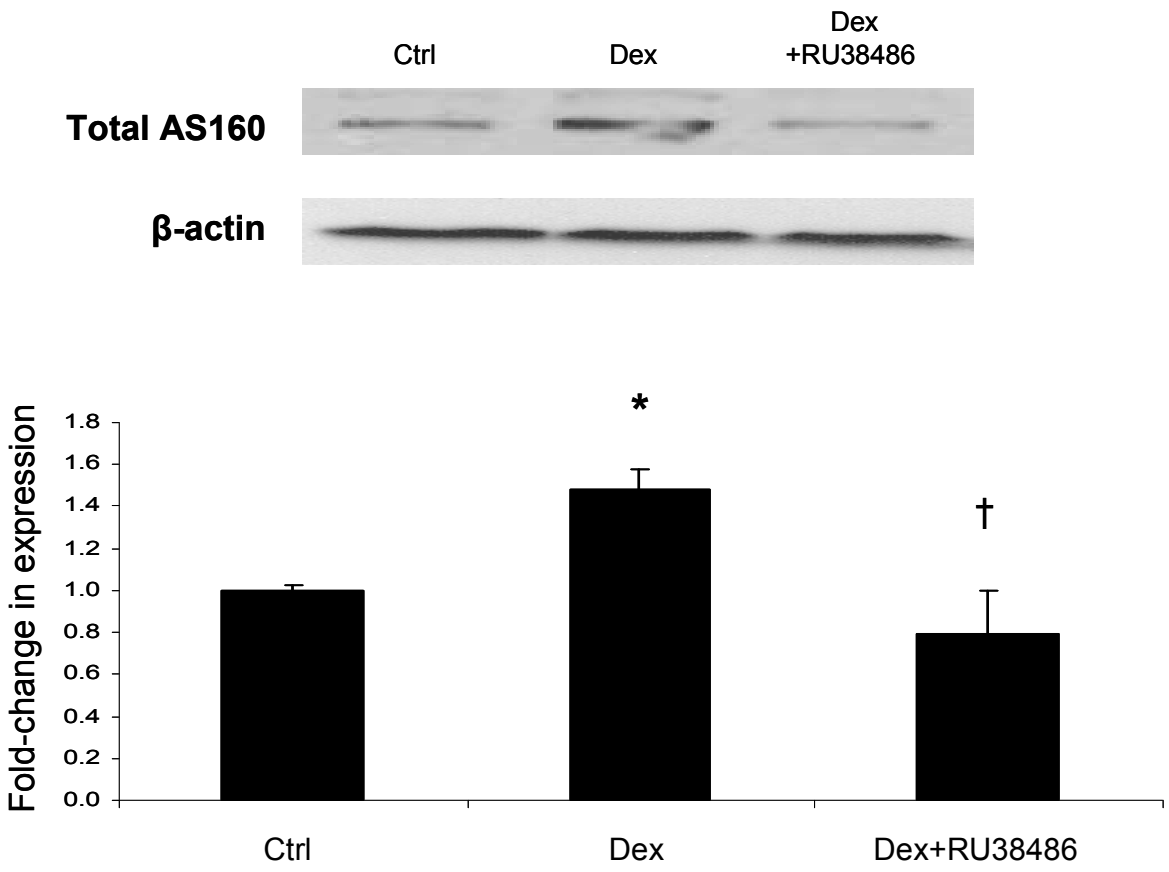

Figure 4-8 Total AS160 protein expression increase following DEX treatment (1μM, 24 h) and was reversed with RU38486 (10μM) in differentiated C2C12 myotubes. Data presented are the mean of n=3 experiments with representative western blots inserted above. Bands quantified relative to β-actin as internal loading control (p<0.05 vs control; † p<0.05 vs. DEX) (DEX=dexamethasone, Ctrl=control).*

Defects in intramyocellular lipid metabolism have been linked with insulin resistance. Table 4-2 highlights the effects of DEX upon the expression of genes involved in key lipid metabolic pathways in differentiated C2C12 myotubes in the absence of insulin. LPL expression decreased following DEX treatment (0.88±0.13 vs. 0.65±0.08AU, $p<0.05$), reversed by RU38486. Similarly, FAS and ACC1, both key lipogenic genes, were decreased by DEX (1.90±0.18 vs. 1.25±0.15AU, $p<0.01$; 1.03±0.09 vs. 0.83±0.06AU, $p<0.05$ respectively) (Table 4-2, Figure 4-9). The effect of DEX upon FAS expression was the only change reversed by RU38486. By contrast, ACC2 expression was unaltered by DEX.

DEX increased the expression of the lipolytic gene ATGL (0.65±0.05 vs. 0.97±0.13AU, p<0.05), which was blocked by co-incubation with RU38486 (Table 4-2, Figure 4-9). A decrease in the expression of the gene which catalyses the first and committed step of the fatty acid esterification pathway, GPAT, was observed following DEX treatment (0.56±0.06 vs. 0.35±0.03AU, p<0.05), and reversed by RU38486 (Table 4-2, Figure 4-9). PDK4 phosphorylates and deactivates pyruvate dehydrogenase which catalyses the multi-step conversion of pyruvate (generated mainly from glucose) to acetyl-CoA (which subsequently enters the TCA cycle and used to generate ATP), thus this enzyme is a key metabolic switch between glucose and lipid metabolism. DEX treatment increased the expression of PDK4 (0.66±0.08 vs. 7.36±1.11AU, P<0.001), which was blocked when co-incubated with RU38486 (Table 4-2, Figure 4-9).

		mRNA expression (AU ± SE)		
	Gene	Control	Dex	Dex+RU38486
Lipid metabolism	LPL	0.88 ± 0.13	0.65 ± 0.08 [a]	0.99 ± 0.16 [d]
	ATGL	0.65 ± 0.05	0.97 ± 0.13 [a]	0.57 ± 0.13 [d]
	HSL	0.08 ± 0.008	0.12 ± 0.03	0.10 ± 0.02
	FAS	1.90 ± 0.18	1.25 ± 0.15 [b]	2.50 ± 0.48 [d]
	ACC1	1.03 ± 0.09	0.83 ± 0.06 [a]	0.97 ± 0.19
	ACC2	0.010 ± 0.002	0.010 ± 0.001	0.013 ± 0.003
	GPAT	0.56 ± 0.06	0.35 ± 0.03 [a]	0.43 ± 0.08
	DGAT	0.94 ± 0.12	1.35 ± 0.03	1.43 ± 0.29
	PDK4	0.66 ± 0.08	7.36 ± 1.11 [c]	1.49 ± 0.24 [e]

Table 4-2 mRNA expression of genes involved in key lipid metabolic pathways in differentiated C2C12 myotubes, measured using real-time PCR following treatment with DEX (1μM, 24 h) with or without the GR antagonist, RU38486 (10μM). Cells were treated in the absence of insulin. Data are the mean values from n=7 experiments and expressed as arbitrary units (AU)±S.E. ([a] p<0.05, [b] p<0.01 and [c] p<0.001 vs. control; [d] p<0.05, [e] p<0.01 and [f] p<0.001 vs. DEX).

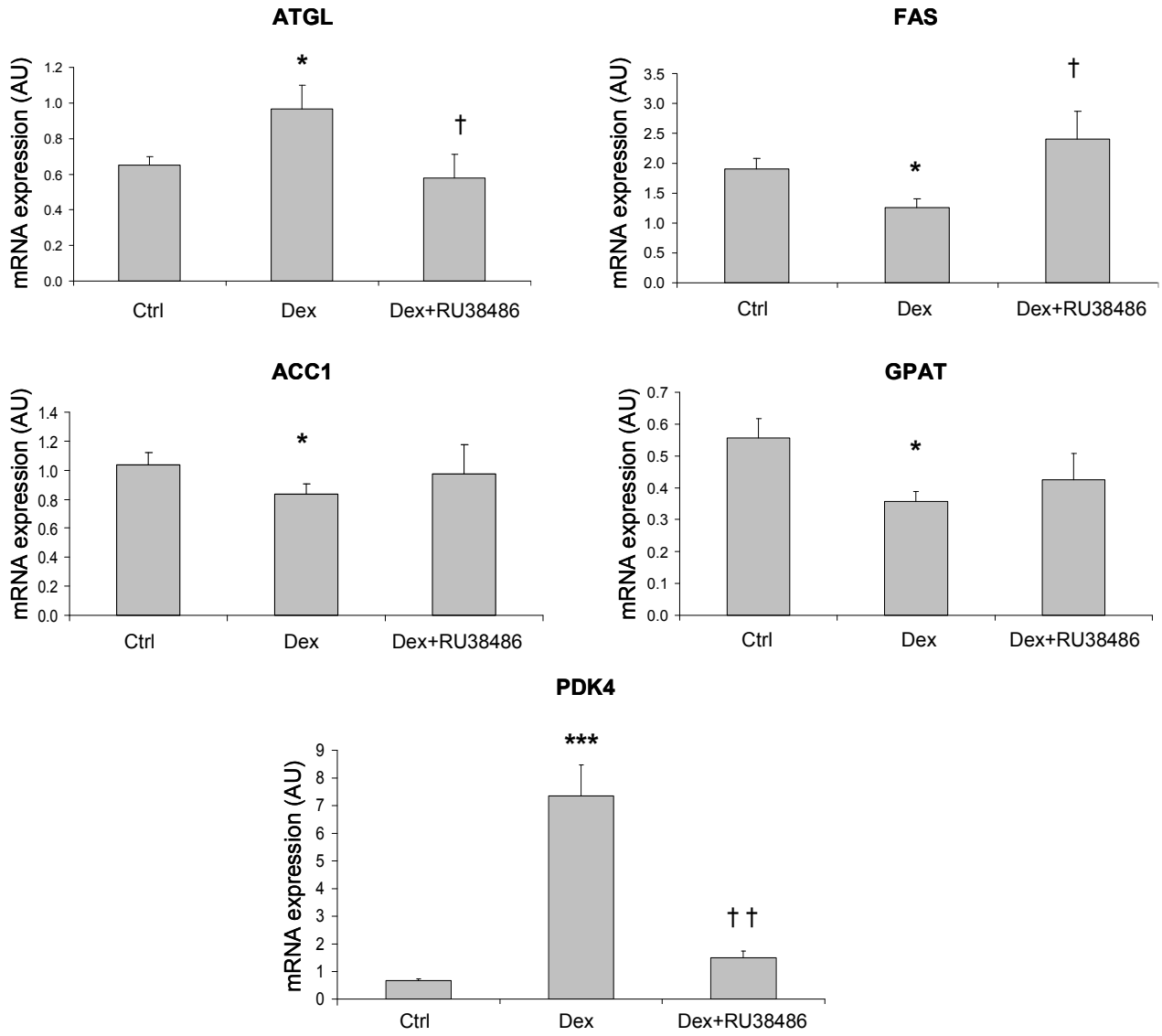

Figure 4-9 mRNA expression of genes involved in key lipid metabolic pathways in differentiated C2C12 myotubes (graphical representation of selected genes taken from Table 4-2), measured using real-time PCR following treatment with DEX (1μM, 24 h) with or without the GR antagonist, RU38486 (10μM). Cells were treated in the absence of insulin. Data are the mean values from n=7 experiments and expressed as arbitrary units (AU)±S.E. (p<0.05, *** p< 0.001 vs control; † p<0.05, †† p<0.01 vs. DEX) (DEX=dexamethasone, Ctrl=control).*

Endorsing the results from Table 4-2, *de novo* lipogenesis in C2C12 myotubes was decreased by DEX in a concentration dependent manner (2.9±0.04 vs. 1.9±0.03 [5nM] vs. 1.3±0.02dpmx10^4 [500nM], $p<0.05$) (Figure 4-10). In the presence of insulin (5nM), low dose DEX was without effect upon *de novo* lipogenesis (3.1±0.05 vs. 3.2±0.06dpmx10^4 [5nM], p=ns) (Figure 4-10), whereas high dose DEX reduce lipogenesis (3.1±0.05 vs. 2.2±0.02dpmx10^4 [500nM], $p<0.05$).

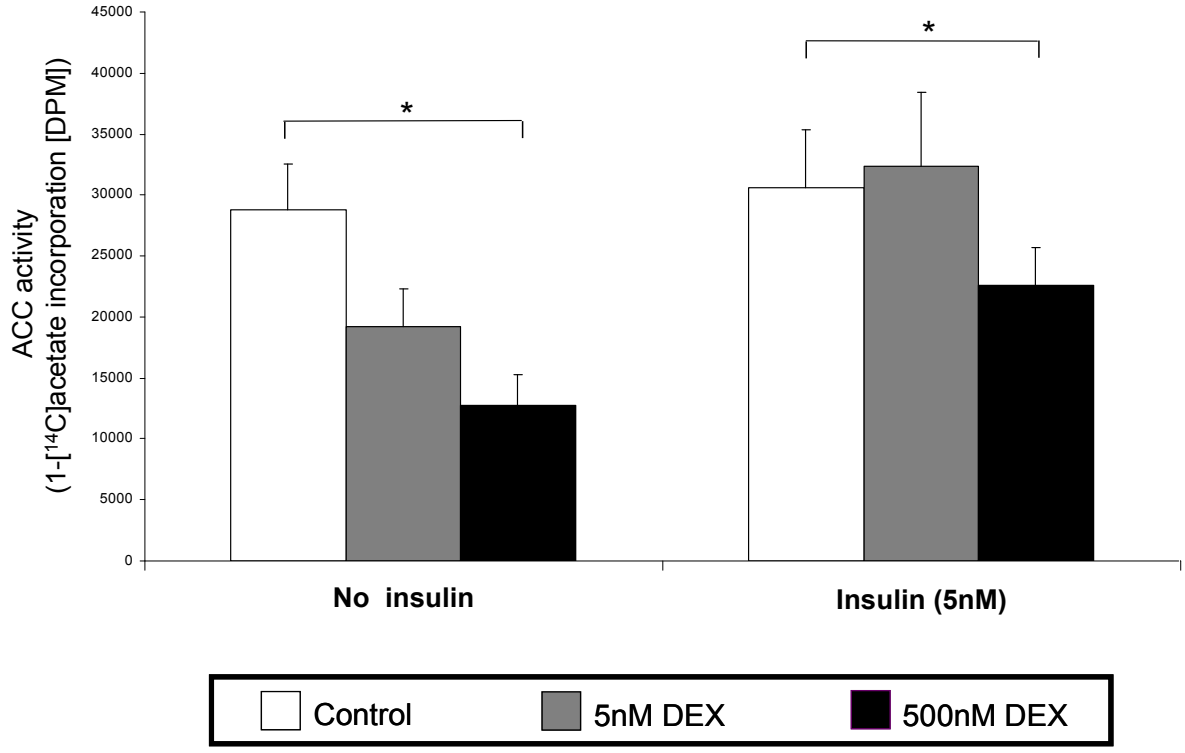

Figure 4-10. The effect of DEX (5nM, 500nM) upon the rate of de novo lipogenesis (ACC activity) in the presence/absence of insulin (5nM) in C2C12 myotubes. (p<0.05, comparison indicated by the brackets)*

DEX conversely increased the rate of β-oxidation in these cells (25.8±2.1 vs. 27.7±2.9 [5nM] vs. 28.9±3.1dpmx10^4 [500nM], $p<0.05$) (Figure 4-11). In the presence of insulin (5nM), β-oxidation was decreased by DEX in a concentration dependent manner (25.2±2.0 vs. 23.5±2.9 [5nM] vs. 21.9±2.1dpmx10^4 [500nM], $p<0.01$) (Figure 4-11).

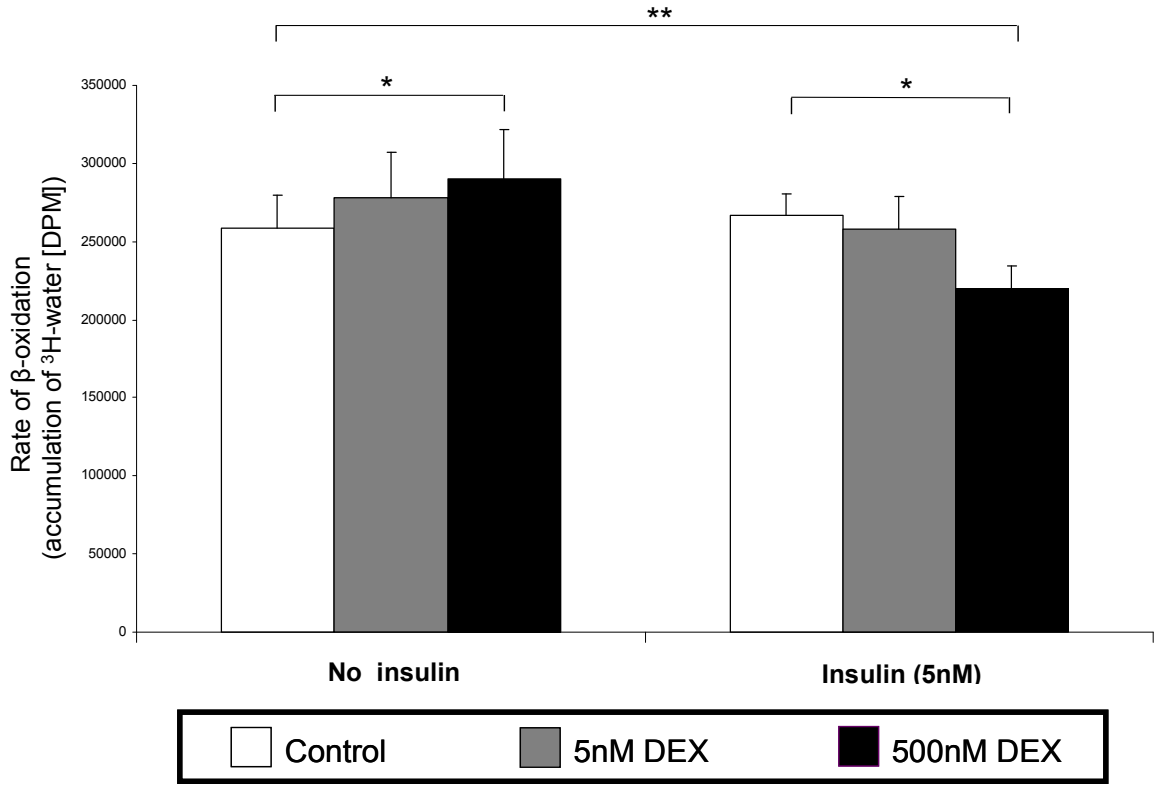

Figure 4-11 The effect of DEX (5nM, 500nM) upon the rate of β-oxidation in the presence/absence of insulin (5nM) in C2C12 myotubes. (p<0.05, ** p<0.01, comparison indicated by the brackets)*

4.5. Discussion

Our data show that the synthetic GC, DEX, impairs insulin signalling at multiple levels, importantly decreasing total IRS1 protein expression and increasing inhibitory IRS1 serine-307 phosphorylation. This increase in serine phosphorylation leads to a decrease in the affinity of IRS1 for the insulin receptor and increases IRS1 degradation (Aguirre et al., 2000; Aguirre et al., 2002), and may contribute to the decrease in IRS1 total protein expression that we observed. The pivotal role of IRS1 in skeletal muscle insulin signalling is highlighted by IRS1 knock-out mice (Araki et al., 1994; Kido et al., 2000; Withers et al., 1998) which develop marked insulin resistance. Serine phosphorylation of IRS1 at numerous residues has been implicated in the development of insulin resistance (Mussig et al., 2005; Nawaratne et al., 2006; Waraich et al., 2008; Werner et al., 2004). Specifically, serine-307 phosphorylation has been implicated in various models, as a negative regulator of IRS1 function. Inflammatory cytokines including TNFα and C-reactive peptide increase serine-307 phosphorylation (D'Alessandris et al., 2007) (de Alvaro et al., 2004), and insulin itself has similar effects (Danielsson, Nystrom & Stralfors, 2006; Gual et al., 2003). Serine-307 is phosphorylated following FFA exposure and PKCθ is believed to have a critical role in this process (Gao et al., 2004; Yu et al., 2002). With enhanced serine-307 phosphorylation one would expect to see a decrease in activating tyrosine phosphorylation of IRS1. However, we saw no change in tyrosine phosphorylation following GC treatment. The explanation for this observation is unclear, but may reflect the fact that serine-307 is located within the binding region of the phosphatase PTP1B, and thus the GC-induced phosphorylation at this site may

preclude this phosphatase from associating with IRS1 (Paz et al., 1999). Alternatively, phosphorylation of serine-307 could induce translocation of IRS1 (Heller-Harrison, Morin & Czech, 1995) away from the relevant phosphatases. Another residue on IRS1 associated with inhibiting insulin signalling is serine-24, located within the membranes lipid binding PH-domain. Phosphorylation at this site is proposed prevent IRS1 from associating with membrane lipids in the vicinity of the insulin receptor, and thus participating in signal transduction (Nawaratne et al., 2006). PKCθ does not contribute to phorbol-12-myristate-13-acetate induced serine-24 phosphorylation, but instead is dependent upon PKCα activation (Nawaratne et al., 2006). We observed no regulation of serine-24 phosphorylation by GCs suggesting that phosphorylation at these two sites is via distinct mechanisms.

Other studies have also highlighted the pivotal role of IRS1 in GC-induced insulin resistance. The results of these studies do show some discrepancy, for example some, but not all have shown decreased activating tyrosine phosphorylation of IRS1 (Giorgino et al., 1993; Rojas et al., 2003; Saad et al., 1993). Others have reported changes in the insulin receptor expression and activation, PI3K activity and expression, and IRS2 expression and phosphorylation (Giorgino et al., 1997; Giorgino & Smith, 1995; Saad et al., 1993). The explanation for these inconsistencies is not entirely clear, but may reflect differences between rats and mice, differing cell models and specific investigative protocols. One particular study looking at the effects of GCs upon the insulin signalling cascade in cultured primary rat myoblasts found no regulation of IRS1 serine-307 phosphorylation following treatment with DEX (Brown et al., 2007), however, the effect of DEX

upon differentiated primary rat myotubes was not explored in this study. Consistent with this finding, we also observed no regulation of IRS1 serine-307 phosphorylation in undifferentiated C2C12 myoblasts following DEX treatment, suggesting that GC-induced IRS1 serine-307 phosphorylation may only occur when myoblasts have fused to form mature differentiated myotubes. In support of this, we observed no change in insulin-stimulated glucose uptake with DEX in undifferentiated cells, whereas insulin-stimulated glucose uptake was reduced in the myotubes; consistent with the induction of insulin resistance in the latter. On the basis of this evidence, combined with the low 11β-HSD1 expression and activity we observed in the myoblasts, we chose to concentrate our study exclusively on the differentiated myotubes from there on.

Downstream of IRS1, we observed altered expression of the subunits comprising PI3K. DEX upregulated the mRNA levels of the regulatory subunit (p85) while downregulating the catalytic subunit (p110). If this translates to protein stociometry this altered subunit ratio could contribute to a state of insulin resistance, since the regulatory subunit is in competition for binding IRS1 with the catalytically active heterodimer. This effect of GCs upon the insulin signalling cascade has been reported previously in L6 myoblasts (Giorgino et al., 1997).

As discussed in the introduction, the role of PI3K is to generate the second messenger of the insulin signalling cascade; PI-3,4,5-P_3, recruiting PKB/akt to the plasma membrane where it is subsequently activated. We observed a decrease in PKB/akt activating serine-473 phosphorylation following DEX treatment, we therefore propose that this may be a direct consequence of enhanced IRS1

inactivation, along with potentially altered PI3K subunit stoichiometry.

AS160 is a recently identified protein with Rab-GTPase activity that, under basal conditions, is resident in GLUT4 containing vesicles, and limits the GTP availability that is necessarily for vesicle translocation to the cell membrane to permit glucose entry. Upon phosphorylation by PKB/akt, AS160 dissociates from the vesicle and thus allows GTP to bind to Rab proteins and vesicle translocation to the cell membrane can then occur (Larance et al., 2005; Sano et al., 2003). Whilst regulation of AS160 phosphorylation at differing sites by growth factors, including IGF-1 and EGF, has been described (Geraghty et al., 2007), GC regulation has not been explored. Our data show that GCs increase both AS160 protein and mRNA expression in a GR dependent mechanism. Since there is no change in PKB/akt mRNA or protein levels, the GC-induced upregulation of AS160 could play an inhibitory role in insulin stimulated glucose uptake. These observations are interesting and point towards a separate mechanism of regulation, rather than simply a down-stream consequence of decreased IRS1/PI3K activation.

Whilst the net effect of GCs is to induce insulin resistance, we did observe an increase in IRS2 mRNA and protein expression. Moreover, InsR and GLUT4 mRNA expression increased. It is possible that this represents a compensatory mechanism to preserve insulin sensitivity; adjusting for the inhibition of signalling through IRS1/PI3K/AS160. However, overall the effect of GC exposure is to limit insulin stimulated glucose uptake.

Basal glucose uptake is also decreased with GC exposure in differentiated myotubes, consistent with previously published finding (Salehzadeh et al., 2009). This is likely to represent a mechanism independent of GCs effects upon the insulin signalling cascade. One possible explanation could be linked to the increase in PDK4 expression we observed following DEX treatment. PDK4 phosphorylates the pyruvate dehydrogenase complex, resulting in its deactivation - inhibiting glucose flux and thus favouring fatty acid utilisation as a fuel. Indeed, GCs have been found to enhance fatty acid oxidation rates in cultured human primary myotubes in support of this (Salehzadeh et al., 2009).

Defects in intramyocellular lipid metabolism have been linked to insulin resistance (Consitt, Bell & Houmard, 2009), however, the effects of GCs upon these metabolic pathways in skeletal muscle have not been investigated in detail. Classically, GCs oppose the actions of insulin; acting to increase catabolism, but in the case of *de novo* lipogenesis, there is evidence that GCs act with insulin as an anabolic effector (Wang et al., 2004; Williams & Berdanier, 1982). In our experiments using C2C12 myotubes, the effects of DEX treatment upon lipid metabolism, in the absence of insulin, was in keeping with GCs known catabolic role. For example, we observed decreases in the mRNA levels of lipogenic genes, as well as genes involved in fat esterification, and importantly *de novo* lipogenic rates were reduced in a dose dependent manner following DEX treatment. This suggests that GC alone act to decrease intramyocellular lipid accumulation. In addition, the expression of key lipolytic genes were upregulated following DEX exposure - increasing intramyocellular free fatty acid availability, and in addition, may also afford increases in intramyocellular DAG levels, which

have been linked with PKCθ activation resulting in enhanced IRS1 serine-307 phosphorylation (Yu et al., 2002). The possibility that the mechanism of GC-induced IRS1 serine-307 phosphorylation is through enhanced DAG-sensitive PKC activation, is investigated in later chapters.

The rate of β-oxidation was increased in C2C12 myotubes following DEX treatment, which is consistent with the observed increase in PDK4 expression, i.e. suggesting a shift from glucose metabolism to lipid metabolism. Collectively, these data show that mimicking in the fasted state (in the absence of insulin), GCs promote fatty acid release over their storage, and mediate metabolic switching from glucose to free fatty acids as a fuel. By contrast, coincubation of DEX with insulin blocked the DEX-induced decrease in *de novo* lipogenesis at lower DEX concentrations. Although we have shown that the impact of GC upon *de novo* lipogenesis differs depending on whether insulin is present, we have not endorsed observations made in other tissues that GC work in concert with insulin to enhance *de novo lipogenesis*. Interestingly, when DEX was coincubated with insulin, the rate of β-oxidation was decreased, suggesting that in the fed state, there is a concerted action of GCs and insulin to reduce fatty acid utilisation - potentially contributing to the accumulation of IMTGs which have been identified as a marker of insulin resistance.

In addition to investigating the effects of GC upon the insulin signalling cascade and lipid metabolic pathways, we also studied their effects upon genes involved in GC metabolism and action. The observed decrease in GRα expression with DEX treatment could represent a negative feedback mechanism, limiting the genomic

effects of GCs following chronic GRα activation. H6PDH controls NADPH availability, an essential cofactor for 11β-HSD1 oxo-reductase activity. The 13-fold increase in H6PDH expression we observed following treatment with DEX could drive increased 11β-HSD1 activity. In support of this others in our lab have demonstrated elevated 11β-HSD1 oxo-reductase activity in C2C12 myotubes following DEX treatment (Mark Sherlock, personal communication).

In summary, we have identified a novel action of GCs upon the insulin signalling cascade in skeletal muscle, by decreasing IRS1 total protein and increasing inhibitory serine-307 phosphorylation. This, in concert with potentially altered PI3K subunit stoichiometry along with increased AS160 expression leads to decreased activation of the insulin signalling cascade - reducing insulin-stimulated glucose uptake. Furthermore, we have shown that GCs impact upon intramyocellular lipid metabolism, which may underpin GC-induced insulin resistance.

Chapter 5 - Pre-receptor Glucocorticoid Metabolism and Regulation of Insulin Signalling in Skeletal Muscle

5.1. Introduction

Excess circulating GC levels, as seen in Cushing's syndrome, result in increased adiposity, skeletal myopathy and insulin resistance (van Staa et al., 2000; Wajchenberg et al., 1984). As discussed in chapter 4, the synthetic GC, DEX, enhances inhibitory serine-307 phosphorylation of IRS1, resulting in insulin resistance in C2C12 skeletal myotubes. Enhanced serine-312 phosphorylation (corresponding to rodent serine-307) has been linked with insulin resistance in humans (Bouzakri et al., 2006; Corbould et al., 2005; Seow et al., 2007). However, in patients with type 2 diabetes and insulin resistant obese subjects, circulating GC levels are not elevated. In key insulin target tissues including liver, adipose and skeletal muscle, GC availability to bind and activate the GR is controlled by 11β-HSD1. 11β-HSD1 is an endo-lumenal enzyme that inter-converts inactive (cortisone in humans and 11-dehydrocorticosterone in rodents) and active GCs (cortisol in humans and corticosterone in rodents) (Tomlinson et al., 2004). Critically, the directionality of 11β-HSD1 activity is cofactor (NADPH) dependent, which is supplied by a tightly associated endo-lumenal enzyme, H6PDH. Decreases in H6PDH expression / activity results in a switching of 11β-HSD1 activity from an oxo-reductase to a dehydrogenase (Bujalska et al., 2005; Lavery et al., 2006). Despite this bidirectional potential, the predominant direction of activity in liver, adipose and skeletal muscle is oxo-reductase - generating active GCs (cortisol / corticosterone) and thus amplifying local GC availability (Bujalska et al., 1997; Jamieson et al., 2000; Whorwood et al., 2001). The contribution of pre-receptor GC metabolism to the insulin sensitivity of skeletal

muscle is unknown. 11β-HSD1 knockout mice are relatively insulin sensitive (Morton et al., 2001) and, as discussed in section 1.14.3, selective inhibitors of 11β-HSD1 improve lipid profiles, glucose tolerance and insulin sensitivity and have considerable potential as therapeutic agents (Alberts et al., 2002; Alberts et al., 2003; Berthiaume et al., 2007a; Hermanowski-Vosatka et al., 2005). However, the molecular mechanisms that underpin these observations remain to be defined. In this chapter, we have characterised the expression and activity of 11β-HSD1 in rodent and human skeletal muscle, and determined the functional impact of selective 11β-HSD1 inhibition upon insulin signalling.

5.2. Strategy of research

Expression of 11β-HSD1, and genes involved in regulating GC response were measured in C2C12 myotubes and rodent tissue explants using real-time PCR.

Functional 11β-HSD1 activity was assessed in C2C12 myotubes, rodent skeletal muscle explants and human primary myotubes by measuring the conversion of a radiolabelled inactive GC tracer.

Western blot analysis was employed to assess the impact of pharmacological inhibition of 11β-HSD1 (using non-specific 11β-HSD inhibitor glycyrrhetinic acid as well as AstraZeneca's selective 11β-HSD1 compound, A1) upon the insulin signalling cascade protein levels / phosphorylation status in C2C12 myotubes.

5.3. Methods

5.3.1. C2C12 cell culture

Proliferating C2C12 myoblasts were cultured in DMEM supplemented with 10% FCS and seeded into 12-well TC plates. At 60-70% confluence, differentiation was initiated by replacing proliferation media with DMEM, supplemented with 5% horse serum and differentiated for 8 days (Figure 3-1). Prior to treatment, cells were incubated in DMEM free from additives for 4 h.

5.3.2. Primary human myocyte cell culture

Primary human myoblasts were obtained from Promocell (Heidelberg, Germany). Myoblasts were cultured to 60-70% confluence, as per the manufactures guidelines using the supplied media. Once confluent, media was changed to a chemically defined media (Promocell, Germany), supplemented with 2% horse serum and cells differentiated into myotubes for 7 days (Figure 5-1). Following differentiation, cells were incubated with serum free media for 4 h prior to treatment.

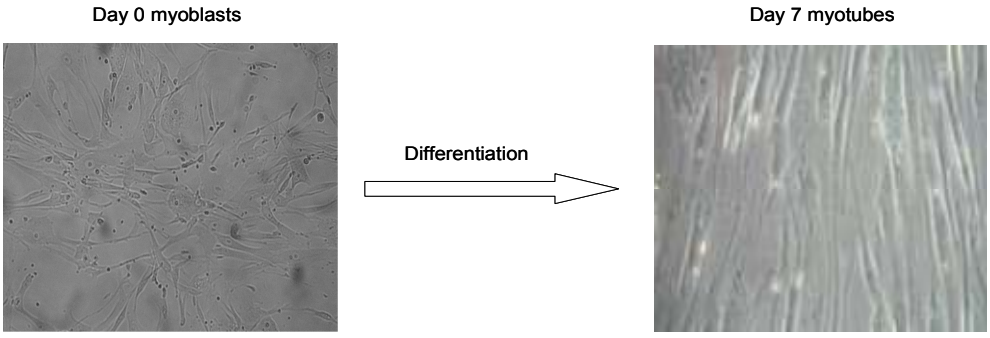

Figure 5-1. Human primary myocytes were differentiated in chemically defined media for 7 days forming multinucleated myotubes.

5.3.3. Immunocytochemistry staining for myotubes formation

Since we had not previously used Promocell's human primary myocytes, we (in conjunction with AstraZeneca) carried out quantitative immunocytochemistry staining in order to identify the optimal conditions for maximal myotube formation. Human primary myoblasts were grown to 60-70% confluence in 24-well TC plates (Corning, Surrey, UK) and differentiated for 7-days in chemically defined media with variable constituents. Following differentiation, media was removed and cells fixed by incubation in 4% paraformaldehyde for 15 mins at room temperature. Cells were washed 3 times with PBS then blocked with PBS supplemented with 3% BSA for 1 h. Blocking solution was removed and replaced with fresh blocking solution supplemented with the primary antibodies and incubated for 1 h 30 mins. The primary antibodies used were; anti-myosin slow and anti-myosin fast (Sigma Aldrich, Dorset, UK), at a dilution of 1/1000 and 1/250 respectively. Cells were washed 3 times with PBS then incubated with alexa-488-labelled secondary antibody (Invitrogen, Paisley, UK), at a dilution of 1/300 in blocking solution for 40 mins. Nuclei were stained by the addition of 2µg/ml hoescht dye 3342 (Invitrogen, Paisley, UK) in PBS and incubated in the dark for 10 mins. Cells were washed 3 times with PBS then fluorescence read on ImageXpress ultra imaging system (Molecular Devices, Pennsylvania, US). Analysis was performed using MetaXpress software (molecular Devices, Pennsylvania, US) (Figure 5-2)

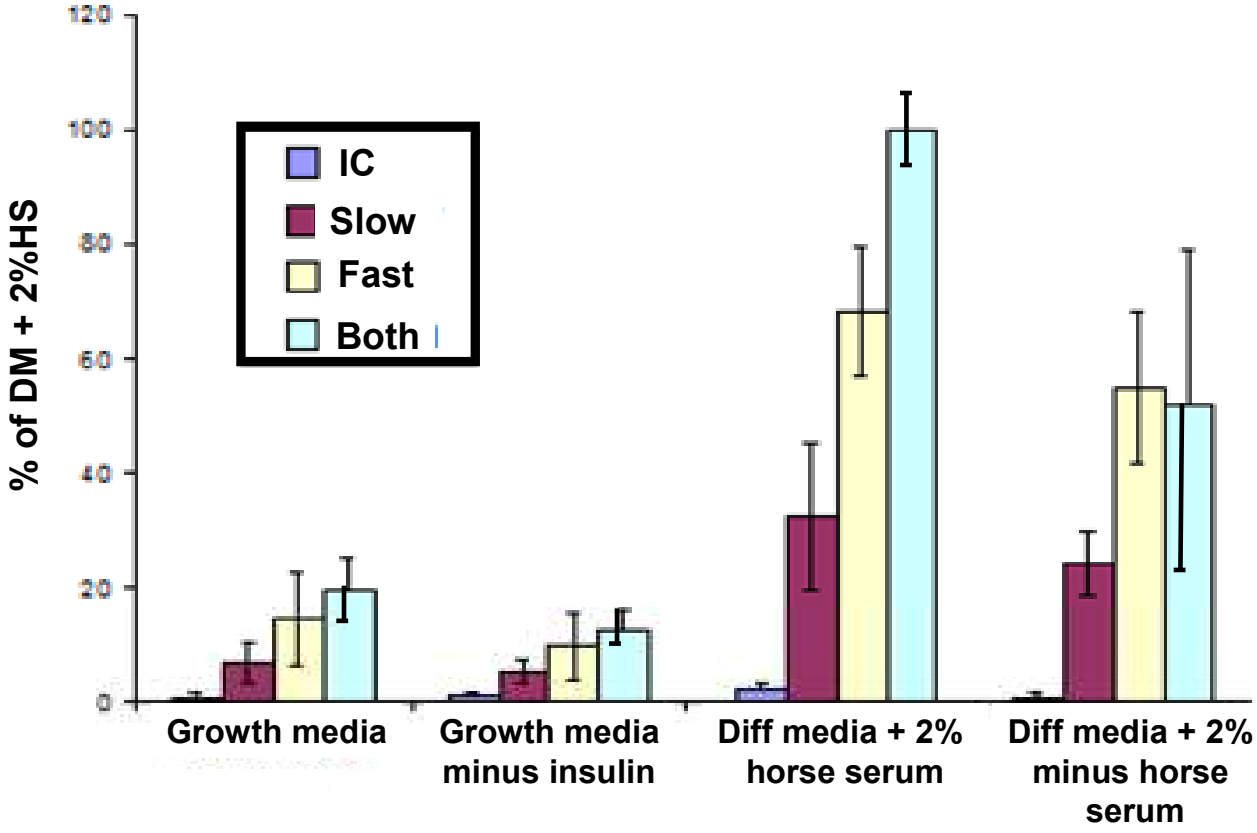

Figure 5-2 Quantitative immunocytochemistry staining for slow and fast twitch muscle fibres for the purpose of optimising differentiation media constituents (n=5). Experiments performed by Wendy Tomlinson (AstraZeneca). (IC= internal control; incubation with PBS 3% BSA minus primary antibody)

5.3.4. Cell treatments

In all cell culture experiments investigating insulin signalling cascade protein expression / phosphorylation status, media was spiked with human insulin (50nM) for the final 15 mins of the treatment period. In experiments using the 11β-HSD inhibitors, GE or A1, cells / tissue explants were pre-treated with the inhibitor for 1 h prior to the addition of the steroids. Treatments were made up in serum free DMEM media.

5.3.5. 11β-HSD1 selective inhibitor

AstraZeneca's selective 11β-HSD1 inhibitor, A1, was used in both mouse and human cell culture experiments. A1 has an IC_{50} for human recombinant 11β-HSD1 of 0.3nM, for rat: 637nM, for mouse: 33nM and for human 11β-HSD2: >15μM (personal communication AstraZeneca).

5.3.6. Rodent protocol

Male C57BL/6 mice (6-8 weeks of ages) were housed in standard conditions on a 12 h / 12 h light-dark cycle with access to standard rodent chow and water *ad libitum.* All procedures were carried out in accordance with the UK Animals (Scientific Procedures) Act, 1986. On the day of experiment mice were sacrificed by cervical dislocation then adipose tissue, liver tissue and femoral quadricept muscles were removed and snap-frozen in liquid nitrogen for characterisation of mRNA expression. For measurement of 11β-HSD1 activity: freshly harvested tissue was transferred directly to the assay.

5.3.7. 11β-HSD1 activity assay

Intact cells (grown in 12-well TC plates) and tissue explants (roughly 20mg) were incubated with 100nM 11DHC or cortisone supplemented with a tritiated tracer. For C2C12 myotubes and tissue explants steroid incubation took place for 2 h, whereas human primary myotubes were incubated for 24 h. Steroids were then extracted using dichloromethane, separated using a mobile phase consisting of ethanol/chloroform (8:92) by thin layer chromatography, and scanned using a

Bioscan 200 Imaging Scanner (LabLogic, Sheffield, UK). For intact cells protein levels were assayed using a commercially available kit (BioRad, Herts, UK), and activity expressed as pmol corticosterone/cortisol generated per mg of protein per hour. For tissue explants activity expressed as pmol corticosterone generated per mg of tissue per hour.

5.3.8. RNA extraction

Total RNA was extracted using Tri-reagent system, concentration determined spectrophotometrically at OD_{260} and integrity assessed by agarose gel electrophoresis. For reverse transcription (see section 2.9.2) 1µg of RNA was used.

5.3.9. Real-time PCR

11β-HSD1, H6PDH and GRα mRNA levels were determined using an ABI 7500 sequence detection system (Applied Biosystems, Warrington, UK). Reactions were performed in singleplex as described in section 2.11, and normalised against the 18s rRNA house keeping gene. Primers and probes and for all genes were supplied by Applied Biosystems as pre-mixed ‘assay on demands’ (Applied Biosystems, Warrington, UK).

5.3.10. Immunoblotting

Proteins were extracted from cell lysates and concentration determined as described in section 2.6.2. For IRS1, and p-IRS1, 40µg of protein was resolved on 8% SDS-PAGE gels. For PKB/akt and p-PKB/akt, 20µg of protein was resolved on 12.5% SDS-PAGE gels. Proteins were transferred to nitrocellulose membranes (for IRS1, p-IRS1, proteins transferred at 140mA for 2 h, for PKB/akt and p-PKB/akt proteins transferred at 140mA for 1 h). Primary (anti-IRS1 and anti-pSer307 were purchased from Upstate, Dundee, UK, anti-PKB/akt and anti-pThr308 PKB/akt [recognizing isoforms 1 and 2] were purchased from R&D Systems, Abingdon, UK) and secondary antibodies (Dako, Glostrop, UK) were used at a dilution of 1/1000. Membranes were re-probed for β-actin and primary and secondary antibodies used at a dilution of 1/5000 (Abcam, Cambridge, UK). Bands were visualised using ECL detection kit (GE Healthcare, Bucks, UK), and quantified with Genesnap by Syngene (Cambridge, UK). The ratio of p-IRS1 to β-actin was normalised to the ratio of IRS1 to β-actin.

5.3.11. Statistical analysis

Where data were normally distributed, unpaired student t-tests were used to compare single treatments to control using SigmaStat 3.1 (Systat Software, CA, US). If normality tests failed, non-parametric tests were used. One way ANOVA on ranks was used to compare multiple treatments, doses or times using SigmaStat 3.1. Statistical analysis on PCR data was performed on mean ΔCt values.

5.4. Results

5.4.1. 11β-HSD1 in rodent and human skeletal muscle

11β-HSD1 mRNA was highly expressed in C2C12 cells. Expression was also detected in whole mouse tissue explants of quadriceps muscle, although levels were lower than those seen in liver and adipose tissue.

	mRNA expression (AU ± SE)			
Gene	**C2C12**	**Quadriceps**	**Liver**	**Adipose**
11β-HSD1	32.9 ± 2.9	0.29 ± 0.03	18.40 ± 1.96	1.26 ± 0.14
H6PDH	0.10 ± 0.02	0.10 ± 0.01	0.12 ±0.005	0.11 ± 0.001
GRα	0.56 ± 0.02	5.67 ±0.29	3.33 ± 0.36	3.90 ± 0.68

Table 5-1 Comparative mRNA expression of 11β-HSD1, GRα and H6PDH in mouse skeletal muscle and C2C12 myotubes. Expression in mouse liver and adipose tissue are provided as a quantitative reference. Data are expressed as arbitrary units (A.U.±S.E), n=3-5 experiments)

In all systems examined (C2C12 myocytes, human primary cultures and whole tissue explants from mouse), functional 11β-HSD1 activity was demonstrated. Activity was bi-directional, however, oxo-reductase activity, generating active cortisol or corticosterone predominated (Figure 5-3). In addition, in rodent quadriceps explants, activity was decreased following co-incubation with the non-selective 11β-HSD inhibitor, glycyrrhetinic acid (GE, 1μM, 2 h) (114.0±5.7 vs. 44.6±11.1 pmol/g/h, $p<0.05$).

A1 is a selective 11β-HSD1 inhibitor provided by AstraZeneca. A1 has an IC_{50} for human recombinant 11β-HSD1 of 0.3nM, 637nM for rat and 33nM for mouse. Treatment with A1 (1μM, 24 h), significantly decreased oxo-reductase activity in rodent quadriceps whole tissue explants, differentiated C2C12 myotubes, and primary cultures of differentiated human skeletal myotubes (Figure 5-3).

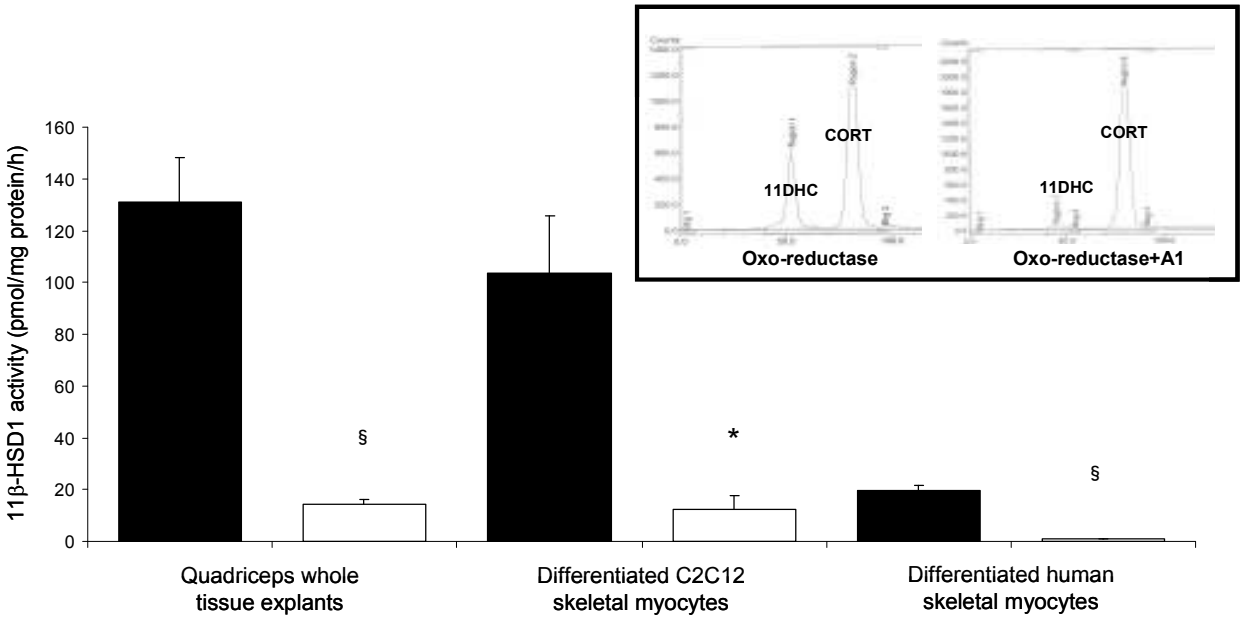

Figure 5-3 The selective 11β-HSD1 inhibitor, A1 (1μM, 24 h), decreases oxo-reductase activity in mouse whole tissue quadriceps explants, differentiated C2C12 skeletal myotubes and differentiated human primary myotubes. (Data shown are the mean±s.e. of n=3-6 experiments with representative activity traces inserted (p<0.05, § p<0.005).*

5.4.2. Functional impact of 11β-HSD1 inhibition in skeletal muscle

In order to determine whether our observations with synthetic GCs were applicable in a physiological context, further experiments were performed using the active endogenous rodent GC corticosterone (CORT). Consistent with our observations using DEX, CORT caused a concentration and time dependent decrease in IRS1 total protein expression (Dose: 1.0 (control) vs. 0.59-fold (100nM), $p<0.01$, 0.47-fold (250nM), $p<0.05$, 0.44-fold (500nM), $p<0.01$, 0.38-fold (1000nM), $p<0.01$; Time: 1.0 (control) vs. 0.19±0.04 (48 h), $p<0.05$, (Figure 5-4A and B). This was accompanied by a concentration- (1.0 (control) vs. 2.80-fold (250nM), $p<0.01$, 3.99-fold (500nM), $p<0.01$, 4.37-fold (1000nM), $p<0.001$) (Figure 5-4A) and time- (1.0 (control) vs. 3.0±0.08 (48 h), $p<0.05$) (Figure 5-4B) dependent increase in serine-307 phosphorylation.

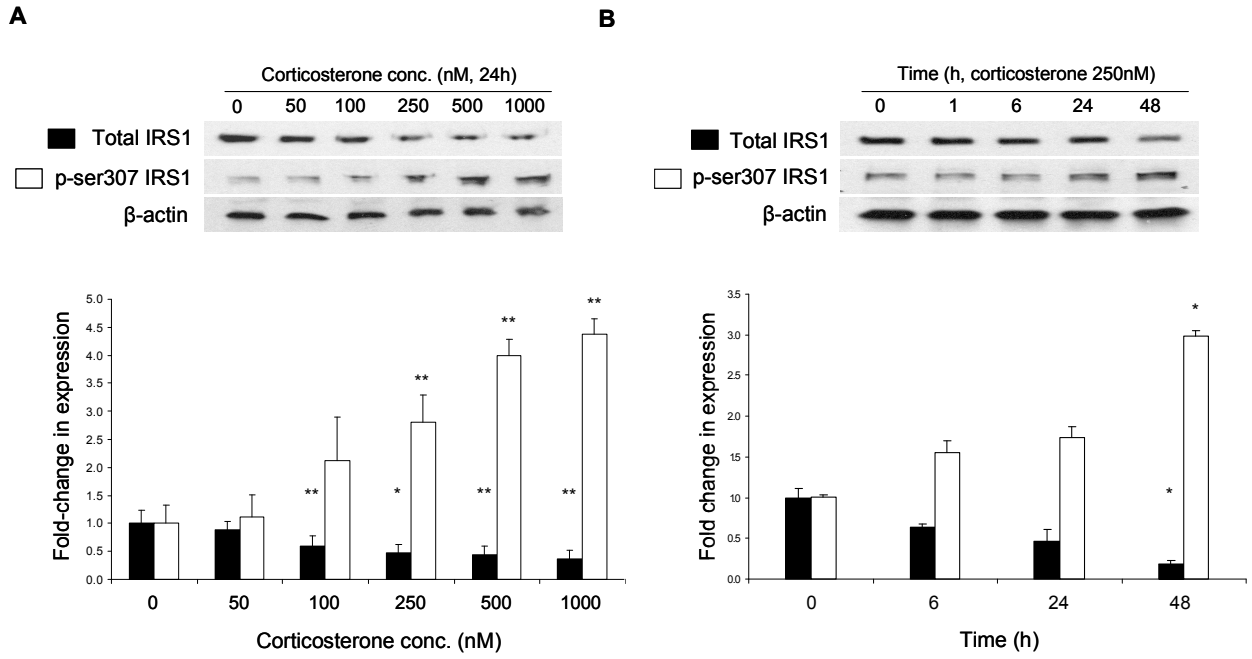

Figure 5-4 The endogenous rodent glucocorticoid, corticosterone (CORT) induces a dose (A) and time (B) dependent decrease in total IRS1 protein expression and increase in serine-307 phosphorylation in C2C12 myotubes. Data presented are the mean of n=4-6 experiments with representative western blots inserted above. Bands quantified relative to β-actin as internal loading control and the ratio of p-IRS1 to β-actin was normalised to the ratio of IRS1 to β-actin (p<0.05, ** p<0.01 vs. control).*

Paralleling our observations with CORT, 11DHC (250nM, 24 h) decreased IRS1 total protein (0.5-fold, $p<0.05$) expression and increased serine-307 phosphorylation (2.0-fold, $p<0.05$) in C2C12 cells (Figure 5-5). Co-incubation with the non-selective 11-βHSD inhibitor GE (2.5μM, 24 h) decreased 11DHC-induced serine-307 phosphorylation to levels seen in control untreated cells (1.1-fold, $p=0.56$ vs. control) (Figure 5-5A). GE treatment alone was without effect (data not shown). Similarly, observations with the selective 11β-HSD1 inhibitor, A1 (2.5μM, 24h), mirrored those with GE, completely blocking the effects of 11DHC to decreases total IRS1 expression and increase serine-307 phosphorylation (Figure 5-5B).

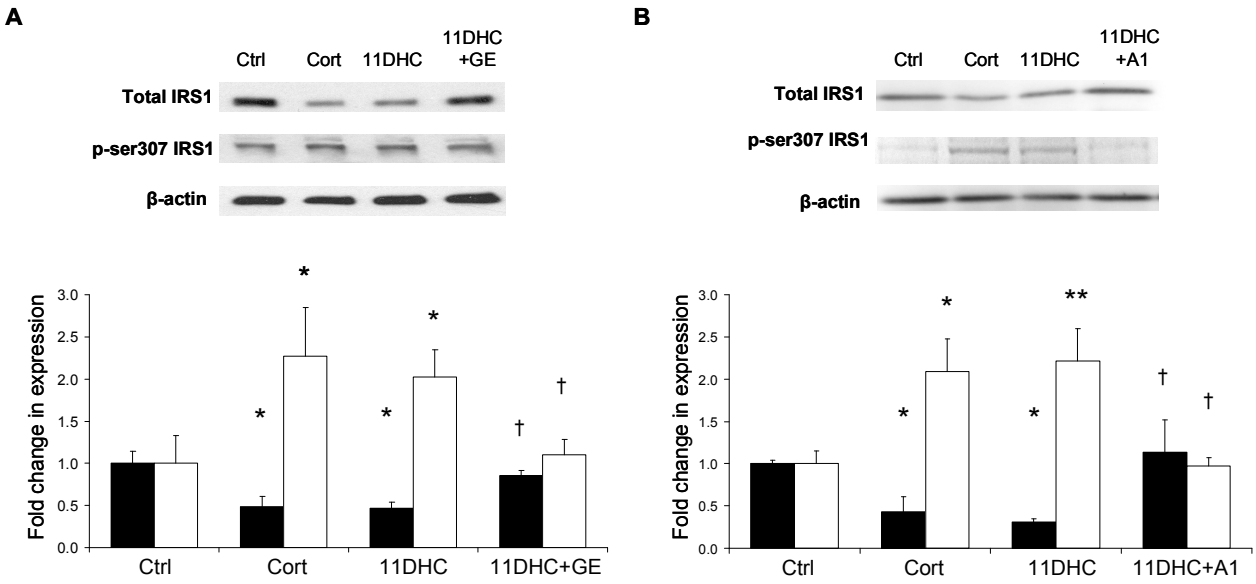

Figure 5-5 Both corticosterone (CORT) and 11-dehydrocorticosterone (11DHC) decrease IRS1 expression and increase serine-307 phosphorylation in C2C12 myotubes. The activity of 11DHC is dependent upon its activation to CORT by 11β-HSD1. Inhibition of 11β-HSD1 using glycerrhetinic acid (GE) (A) or the selective 11β-HSD1 inhibitor, A1 (B) reverses the effect of 11DHC upon IRS1 expression and phosphorylation. Data presented are the mean of n=6 experiments with representative western blots inserted. Bands quantified relative to β-actin as internal loading control and the ratio of p-IRS1 to β-actin was normalised to the ratio of IRS1 to β-actin. (p<0.05, ** p<0.01 vs. control, † p<0.05 vs. 11DHC) (Ctrl=control).*

Extending these findings, in primary cultures of human skeletal muscle, treatment with cortisone (250nM, 24 h) decreased insulin-stimulated threonine-308 phosphorylation of PKB/akt, without altering total PKB/akt protein expression. These observations were completely abolished following co-incubation with A1 (Figure 5-6).

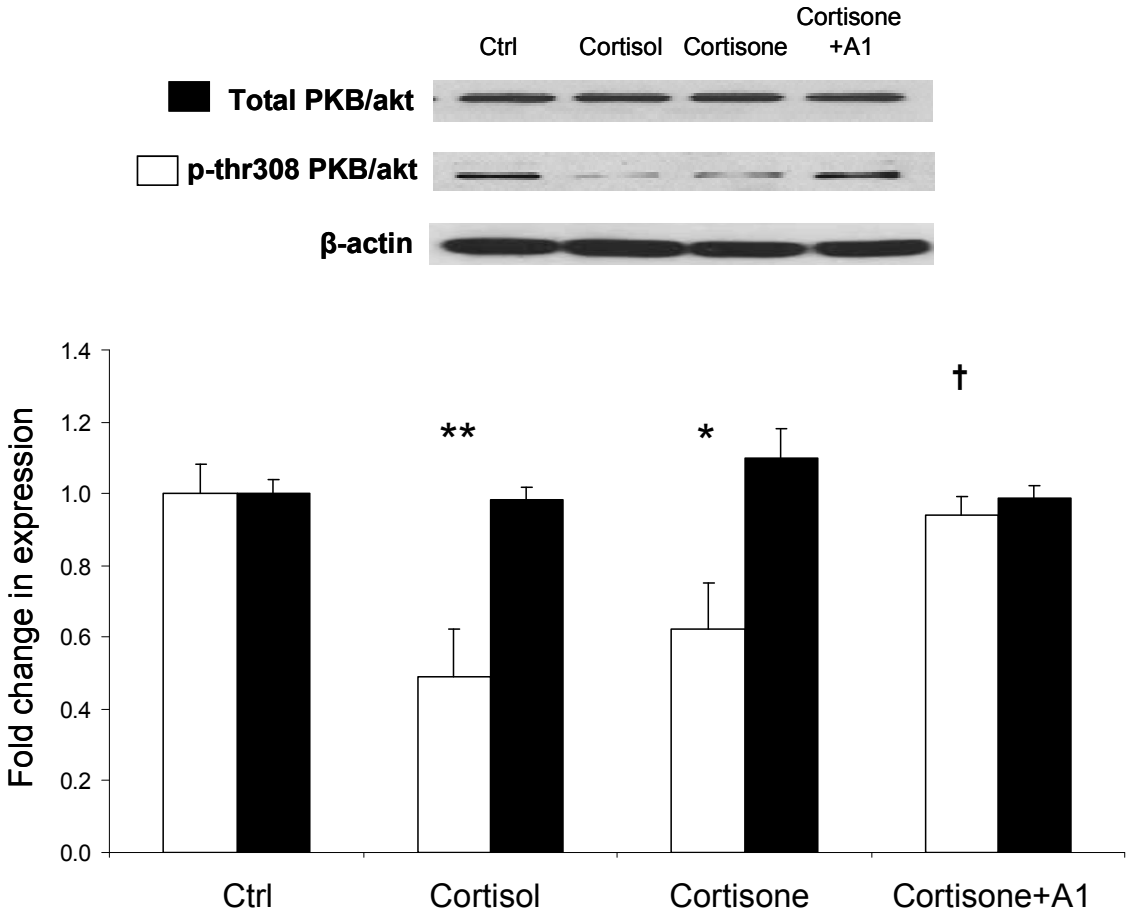

Figure 5-6 Both cortisol and cortisone decrease PKB/akt threonine-308 phosphorylation in insulin-stimulation human primary myotubes. No effect was observed with total PKB/akt levels. The activity of cortisone is dependent upon its activation to cortisol by 11β-HSD1. Inhibition of 11β-HSD1 using the selective 11β-HSD1 inhibitor, A1 reverses the effect of cortisone upon PKB/akt phosphorylation. Data presented are the mean of n=4 experiments with representative western blots inserted (p<0.05, ** p<0.01 vs. control, † p<0.05 vs. cortisone) (Ctrl=control).*

5.5. Discussion

In this chapter we have confirmed that, in agreement with our finding with the synthetic GC, the mouse physiological GC mediates inhibitory effects upon the insulin signalling cascade by decreasing IRS1 total protein and increasing inhibitory IRS1 serine-307 phosphorylation in C2C12 myotubes. In addition, we have clearly shown expression and activity of 11β-HSD1 in both human and rodent cell skeletal muscle culture models as well as rodent muscle explants, consistent with previously published findings (Jang et al., 2006). Activity is predominantly oxo-reductase, generating active GC, and is blocked by selective and non-selective 11β-HSD1 inhibitors. Our use of primary human skeletal myocytes, purchased from Promocell, has allowed us to demonstrate the relevance of this enzyme in human skeletal muscle. However, due to the high cost of using these cells, it has only been feasible to carry out a limited number of experiments.

Our rationale for investigating the role of this enzyme in the insulin sensitivity of skeletal muscle comes from a limited number of rodent studies. For example, over-expression of 11β-HSD1 has been described in rodent skeletal muscle in models of diabetes (Zhang et al., 2009), and myotubes isolated from patients with insulin resistance and type 2 diabetes (Abdallah et al., 2005; Whorwood et al., 2002). However, this is not a consistent finding (Jang et al., 2007). Furthermore, selective 11-βHSD1 inhibitors, currently in development, have insulin sensitising effects, as discussed in section 1.14.3 (Alberts et al., 2002; Alberts et al., 2003; Bhat et al., 2008; Hermanowski-Vosatka et al., 2005). These studies, along with

encouraging preliminary data from human clinical trials, have shown that 11β-HSD1 has considerable therapeutic potential. However the precise contribution to the metabolic and muscle phenotype is still to be clarified.

In our studies, we have shown that selective 11β-HSD1 inhibition restores IRS1 protein levels to that seen in control but also decreases inhibitory serine-307 phosphorylation, while further downstream enhances PKB/akt activation. This may therefore represent an important insulin sensitizing action of selective 11β-HSD1 inhibitors. In light of these results, we will further our studies into the role of this enzyme, and its selective inhibition, upon skeletal muscle insulin sensitivity using whole rodent studies.

Chapter 6 - The Impact of Selective 11β-HSD1 Inhibition upon Insulin Sensitivity and Lipid Metabolism *in vivo*

6.1. Introduction

As discussed in chapter 5, selective 11β-HSD1 inhibitors, which are currently in development, limit local GC availability and improve glucose tolerance, lipid profiles and insulin sensitivity in rodents, primates (Alberts et al., 2002; Alberts et al., 2003; Berthiaume et al., 2007a; Hermanowski-Vosatka et al., 2005) and, as indicated from the preliminary results of phase IIa and IIb clinical trials, humans. However, the precise molecular mechanism underpinning these beneficial effects is not clear. In chapter 5, we showed that skeletal muscle is a true pharmacological target of these inhibitors, and that selective inhibition of this enzyme reverses GC-induced inactivation of IRS1 which could, in part, explain the insulin sensitising effects of these compounds. In this chapter, we attempted to endorse these cell culture findings *in vivo*. In addition, since we demonstrated that many of the genes involved in intramyocellular lipid metabolism are GC regulated (these include: ACC1, FAS, ATGL, HSL, GPAT and PDK4, chapter 4), we assessed the impact of selective 11β-HSD1 inhibition upon the expression of these genes, many of which are implicated in the accumulation of insulin resistance-inducing lipid intermediates (DAGs, ceramides and fatty acids).

6.2. Strategy of research

The effect of pre-receptor GC metabolism upon lipid metabolic gene expression was assessed in C2C12 myotubes, using the selective 11β-HSD1 inhibitor (AstraZeneca's compound, A1).

Using C57Bl6 mice, the effect of selective 11β-HSD1 inhibition (using AstraZeneca's compound, A2) upon food intake, glucose tolerance and insulin sensitivity was measured.

Using cortisone conditioned KK/Ta Jcl mice, the impact of selective 11β-HSD1 inhibition (using AstraZeneca's compound, A2), upon the mRNA levels of genes of the insulin signalling cascade and genes involved in intramyocellular lipid metabolism, was assessed using genecard analysis and selected results were validated using real-time PCR. Furthermore, total protein levels / phosphorylation status of the insulin signalling cascade components were studied using western blot.

6.3. Materials and methods

6.3.1. C2C12 cell culture

Proliferating C2C12 myoblasts were cultured in DMEM supplemented with 10% FCS and seeded into 12-well TC plates. At 60-70% confluence differentiation was initiated by replacing proliferation media with DMEM supplemented with 5% horse serum and differentiated for 8 days (Figure 3-1). Prior to treatment, cells were incubated in DMEM free from additives for 4 h.

6.3.2. Cell treatments

In cell culture experiments investigating the expression of genes involved in lipid metabolism, cells were treated with CORT (250nM, 24 h). In addition, cells were treated with 11-DHC (250nM, 24 h) with or without the selective 11β-HSD1 inhibitor, A1 (2.5μM, 24 h). Cells were pre-treated with A1 for 10 mins prior to the addition of 11-DHC.

6.3.3. 11β-HSD1 selective inhibitors

AstraZeneca's selective 11β-HSD1 inhibitor, A2, was used in preference over A1 in all rodent *in vivo* protocols because the former has a lower IC_{50} for mouse 11β-HSD1 (26nM vs. 33nM). Moreover, screening carried out at AstraZeneca showed that A2 has a better pharmacodynamic profile *in vivo* compared with A1.

6.3.4. Mouse protocols

The selective 11β-HSD1 inhibitor, A2, was used in 2 separate mouse protocols. All experimental procedures were conducted in accordance with the Animal Scientific Procedures Act 1986, Animal Welfare Act 2006 and local guidelines (at AstraZeneca). Firstly, male C57Bl6 mice (6 weeks of age) were maintained for 20 weeks on a diet comprising 48kcal% fat and 10kcal% fructose (Special Diets Services, Witham, UK). Mice were housed with a standard light cycle (6am on 6pm off) and A2 was administered (20mg/kg b.i.d) by oral gavage for 28 days and compared against vehicle-control and pair-fed, vehicle treated animals. Food intake was assessed over the 28-day period and prior to animal sacrifice, after a 12 h fast, an OGTT was performed. This experiment was performed at AstraZeneca by David Laber. AstraZeneca have granted us permission to use data derived from these experiments in this thesis.

6.3.5. Oral glucose tolerance test (OGTT)

C57Bl6 mice were fasted from 8pm until 8am before glucose (2g/kg) was administered via oral gavage. Plasma glucose levels were assessed from tail vein nicks using a hand-held glucometer (Roche, Sussex, UK) prior to glucose administration (fasting levels) and at 20, 60, 90 and 120 mins post glucose injection. In addition, 25μL of blood was extracted from the tail veins at the same time points, for determination of plasma insulin levels using a commercially available assay (Crystal Chem, Illinois, US). The areas under the curves (AUCs) were calculated using trapezoidal integration. This experiment was performed at AstraZeneca by David Laber. AstraZeneca have granted us permission to use

data derived from these experiments in this thesis.

6.3.6. HOMA Index

Insulin sensitivity was estimated using homeostatic model assessment (HOMA) index which was calculated using the equation below:

$$\text{insulin sensitivity} = \frac{\text{fasting glucose (mmols/L) X fasting insulin (ng/mL)}}{\mathbf{1.0}}$$

6.3.7. Insulin Elisa

Following the extraction of blood from tail vein nicks using heparin coated capillary tubes, the plasma was separated by centrifugation at 1000 g for 10 mins. Supernatant containing the plasma was then transferred to cryo-vial and stored at -80°C until required. Plasma insulin levels were measured using a commercially available kit (Crystal Chem, Illinois, US). 5µL plasma was diluted in 95µL of sample diluting buffer per well of a 96-well plate, and incubated for 2 h at 4°C. All measurements were run in triplicate. Samples were then washed 5x with the wash buffer before 100µl anti-insulin enzyme conjugate was dispensed per well. The plate was then incubated for 30 mins at room temperature. Each well was then washed 7x with wash buffer before 100µl enzyme substrate solution was added per well, and incubated at room temperature for 40 mins. The reaction was terminated by the addition of 100µl/per well of the enzyme reaction stop solution. The absorbance at 450nm and 630nm was determined on a vector3 1420 multilable counter (PerkinElmer, Bucks, UK). A_{450nm} was then subtracted from

A_{630nm} and used to calculate the insulin concentration using a standard curve. This assay was performed at AstraZeneca by David Laber. AstraZeneca have granted us permission to use data derived from these experiments in this thesis.

6.3.8. Slow release GC pellet implantation

Separately, the impact of A2 upon skeletal muscle gene and protein expression in an additional hyperglycemic model was determined (male KK/Ta Jcl mice aged 7 weeks, CLEA Japan Inc., Tokyo, Japan). This study was run at AstraZeneca in parallel with the C57Bl6 mice experiments. Animals had free access to water and irradiated RM3 (E) diet composed of 11.5Kcal% fat, 27Kcal% protein and 62Kcal% carbohydrate (Special Diets Services). Compound A2 (20mg/kg) or vehicle (10ml/kg) was administered by oral gavage at 08:00 and 20:00 hours for 4 consecutive days. Following the administration of the 3rd dose of A2, mice were anaesthetised by inhalation of 2-3% v/v isoflurane (vaporised by oxygen at 1.6 litre/minute flow rate) and a 5mg slow-release cortisone pellet (approximately 8mg/kg/day in a 29g mouse) was implanted subcutaneously in the lateral aspect of the neck (Innovative Research of America, Sarasota, USA). On day 4, 1-2 h after the 7th oral dose of A2, a rising-dose carbon dioxide concentration was used to humanely terminate mice and femoral quadriceps muscles were removed and snap-frozen in liquid nitrogen. Pellet implantation, A2 administration and animal sacrifice were carried out by David Laber at AstraZeneca, however, I was present during these procedures. I was responsible for harvesting the skeletal muscle from these mice following sacrifice, and any further experimentation carried out on this tissue was done solely by me. AstraZeneca have granted us permission to

use data derived from these experiments in this thesis.

6.3.9. Genecard analysis

Taqman 348-well custom arrays were purchased from Applied Biosystems containing 45 custom genes and 3 house keeping genes. 500ng of cDNA was mixed with taqman universal PCR master mix (Applied Biosystems) and the array was run on an ABI 7900HT Fast Real-Time PCR System (Applied Biosystems). Data were obtained as Ct values which were normalised against 18s rRNA house keeping gene and fold changes calculated as described in section 2.12.2. Results were validated with standard Taqman RT-PCR.

6.3.10. Real-time PCR

Taqman RT-PCR was carried out on an ABI 7500 sequence detection system (Applied Biosystems, Warrington, UK). Reactions were performed in singleplex as described in section 2.11.2, and normalised against the 18s rRNA house keeping gene. Primers and probes and for all genes were supplied by Applied Biosystems as pre-mixed ‘assay on demands’ (Applied Biosystems, Warrington, UK).

6.3.11. Immunoblotting

Proteins were extracted from femoral quadriceps muscles and concentration determined as described in section 2.6.2. For IRS1, and p-IRS1, 40µg of protein was resolved on 8% SDS-PAGE gels. For PKB/akt and p-PKB/akt, 20µg of protein was resolved on 12.5% SDS-PAGE gels. Proteins were transferred to nitrocellulose membranes (for IRS1, p-IRS1 proteins transferred at 140mA for 2 h, for PKB/akt and p-PKB/akt proteins transferred at 140mA for 1 h). Primary (anti-IRS1 and anti-pSer307 were purchased from Upstate, Dundee, UK, anti-PKB/akt and anti-pThr308 PKB/akt [recognizing isoforms 1 and 2] were purchased from R&D Systems, Abingdon, UK) and secondary antibodies (Dako, Glostrop, UK) were used at a dilution of 1/1000. Membranes were re-probed for β-actin and primary and secondary antibodies used at a dilution of 1/5000 (Abcam, Cambridge, UK). Bands were visualised using ECL detection kit (GE Healthcare, Bucks, UK).

6.3.12. Statistical analysis

Where data were normally distributed, unpaired student t-tests were used to compare single treatments to control using SigmaStat 3.1 (Systat Software, CA, US). If normality tests failed, non-parametric tests were used. One way ANOVA on ranks was used to compare multiple treatments, doses or times using SigmaStat 3.1. Statistical analysis on PCR data was performed on mean ΔCt values.

6.4. Results

6.4.1. Impact of A1 upon lipid metabolism in C2C12 myotubes

To study the effects of selective 11β-HSD1 inhibition upon muscle lipid metabolism, C2C12 myotubes were treated with endogenous GCs in the presence of the selective 11β-HSD1 inhibitor, A1. In agreement with the effects of DEX (chapter 4), both CORT and 11DHC increased the mRNA expression of the key lipolytic genes ATGL (Ctrl vs. CORT: 0.46±0.05 vs. 1.01±0.04AU, $p<0.01$; Ctrl vs. 11DHC: 0.46±0.05 vs. 1.05±0.02AU, $p<0.05$) and HSL (Ctrl vs. CORT: 0.046±0.005 vs. 0.100±0.012AU, $p<0.05$; Ctrl vs. 11DHC: 0.046±0.005 vs. 0.086±0.013AU, $p<0.05$) (Table 6-1). In both cases, the effects of 11DHC were reversed by co-incubation with A1. The expression of FAS and ACC1 was downregulated by 11DHC only (2.73±0.50 vs. 1.99±0.15AU, $p<0.05$; 0.36±0.18 vs. 0.29±0.15AU, $p<0.05$ respectively). GPAT expression was downregulated by CORT (0.40±0.01 vs. 0.25±0.01AU, $p<0.05$) and 11DHC (0.40±0.01 vs. 0.28±0.02AU, $p<0.05$). The effects of the latter were reversed by A1. As with DEX, the expression of DGAT did not change with either CORT or 11DHC. Other genes analysed include: stearoyl-CoA desaturase 1 and -2 (SCD1, -2) (which catalysing the addition of double bonds into unsaturated fatty acids), neither of which appeared to be GC regulated. The expression of PPARα, PPARβ/δ and PPARγ, key transcription factors integral to transcription control of many lipid metabolic genes, was also analysed. With the exception of PPARβ/δ, the expression of these genes was either very low (PPARα) or undetected (PPARγ). Both CORT and 11DHC was without effect upon LPL expression.

		mRNA expression (AU ± SE)			
	Gene	Control	Corticosterone	11-dehydrocorticosterone	11-dehydrocorticosterone + A1
Lipid metabolism	LPL	0.61 ± 0.37	0.84 ± 0.20	0.85 ± 0.19	0.96 ± 0.27
	ATGL	0.46 ± 0.05	1.01 ± 0.04 [b]	1.05 ± 0.02 [a]	0.86 ± 0.01 [a]
	HSL	0.046 ± 0.005	0.100 ± 0.012 [a]	0.086 ± 0.013 [a]	0.063 ± 0.009 [a]
	FAS	2.73 ± 0.50	2.24 ± 0.14	1.99 ± 0.15 [a]	3.63 ± 0.62 [d]
	ACC1	0.36 ± 0.18	0.32 ± 0.16	0.29 ± 0.15 [a]	0.35 ± 0.18
	ACC2	0.008 ± 0.002	0.016 ± 0.003	0.012 ± 0.003	0.015 ± 0.005
	GPAT	0.40 ± 0.01	0.25 ± 0.01 [a]	0.28 ± 0.02 [a]	0.46 ± 0.01 [d]
	DGAT	0.63 ± 0.01	0.71 ± 0.04	0.69 ± 0.07	0.82± 0.01
	SCD1	12.6 ± 3.2	16.2 ± 2.5	15.7 ± 2.5	15.6 ± 4.4
	SCD2	12.1 ± 2.4	11.4 ± 1.3	10.5 ± 1.2	11.0 ± 2.3
	PPARα	0.0014 ± 0.0004	0.0042 ± 0.0001 [b]	0.0043 ± 0.0008 [b]	0.0039 ± 0.0013 [a]
	PPARβ/δ	0.34 ± 0.09	0.45 ± 0.09	0.47± 0.09 [b]	0.39 ± 0.10

Table 6-1 mRNA expression of genes involved in key lipid metabolic pathways in differentiated C2C12 myotubes, measured using real-time PCR following treatment with CORT (250nM, 24 h) or 11DHC (250nM, 24 h) with or without selective 11β-HSD1 inhibitor, A1 (2.5μM). Cells were treated in the absence of insulin. Data are the mean values from n=7 experiments and expressed as arbitrary units (AU)±S.E. ([a] p<0.05, [b] p<0.01 and [c] p<0.001 vs. control; [d] p<0.05 vs. 11DHC).

6.4.2. Mouse in vivo studies with inhibitor A2

Food intake, glucose tolerance and insulin sensitivity: Food intake decreased within the first 48 h in the A2 treated animals in comparison with vehicle-treated controls, however, by day 4 and for the remainder of the 28 day protocol, food intake did not differ between the groups (day 4: 15.5±0.4 vs. 16.5±0.4 kcal/day (A2 treated vs. vehicle treated), p=N.S) (Figure 6-1).

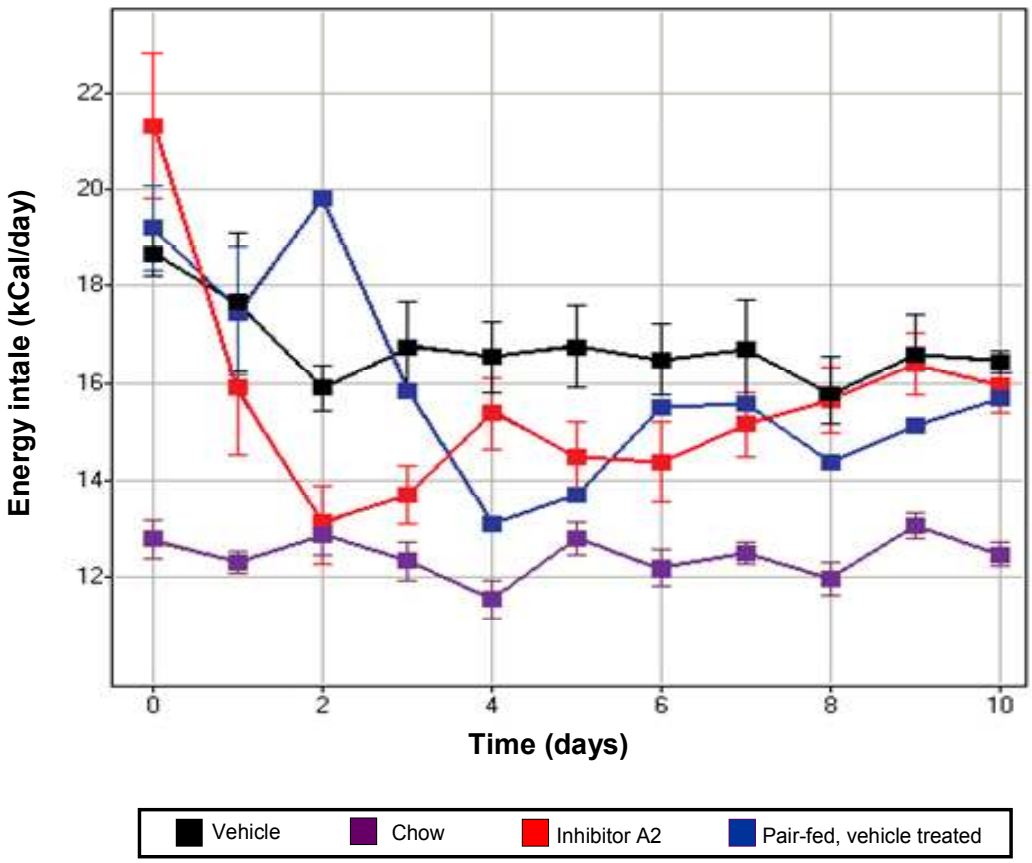

Figure 6-1 C57Bl6 mice treated with selective 11β-HSD1 inhibitor, A2, initially had reduced food intake compared to vehicle treated mice. Levels normalized by day 4 and remained constant and non-significant compared to vehicle treated mice for the duration of the treatment (28 days).

At day 28, fasting blood glucose and insulin levels were lower in the A2 treated animals compared to both vehicle treated and pair-fed controls (glucose: 6.8±0.3 vs. 7.4±0.35 vs. 7.7±0.3mmol/L, $p<0.05$; insulin: 0.60±0.10 vs. 0.82±0.14 vs. 0.91±0.11ng/mL, $p<0.05$, A2 vs. vehicle vs. pair-fed vehicle) (Figure 6-2A and B). Glucose levels across an OGTT (area under curve, AUC) did not change significantly (22.4±0.46 vs. 24.2±0.42 vs. 22.9±0.45mmol/L.h (A2 vs. vehicle vs. pair-fed vehicle), p=NS) (Figure 6-2C). By contrast, insulin secretion was lower (AUC) (2.29±0.23 vs. 2.95±0.37 vs. 2.94±0.21ng/mL.h (A2 vs. vehicle vs. pair-fed vehicle), $p<0.05$) (Figure 6-2D). Similarly, HOMA values were lower (4.2±0.9 vs. 6.0±0.98 vs. 7.1±0.9 (A2 vs. vehicle vs. pair-fed vehicle), $p<0.05$) (Figure 6-3)

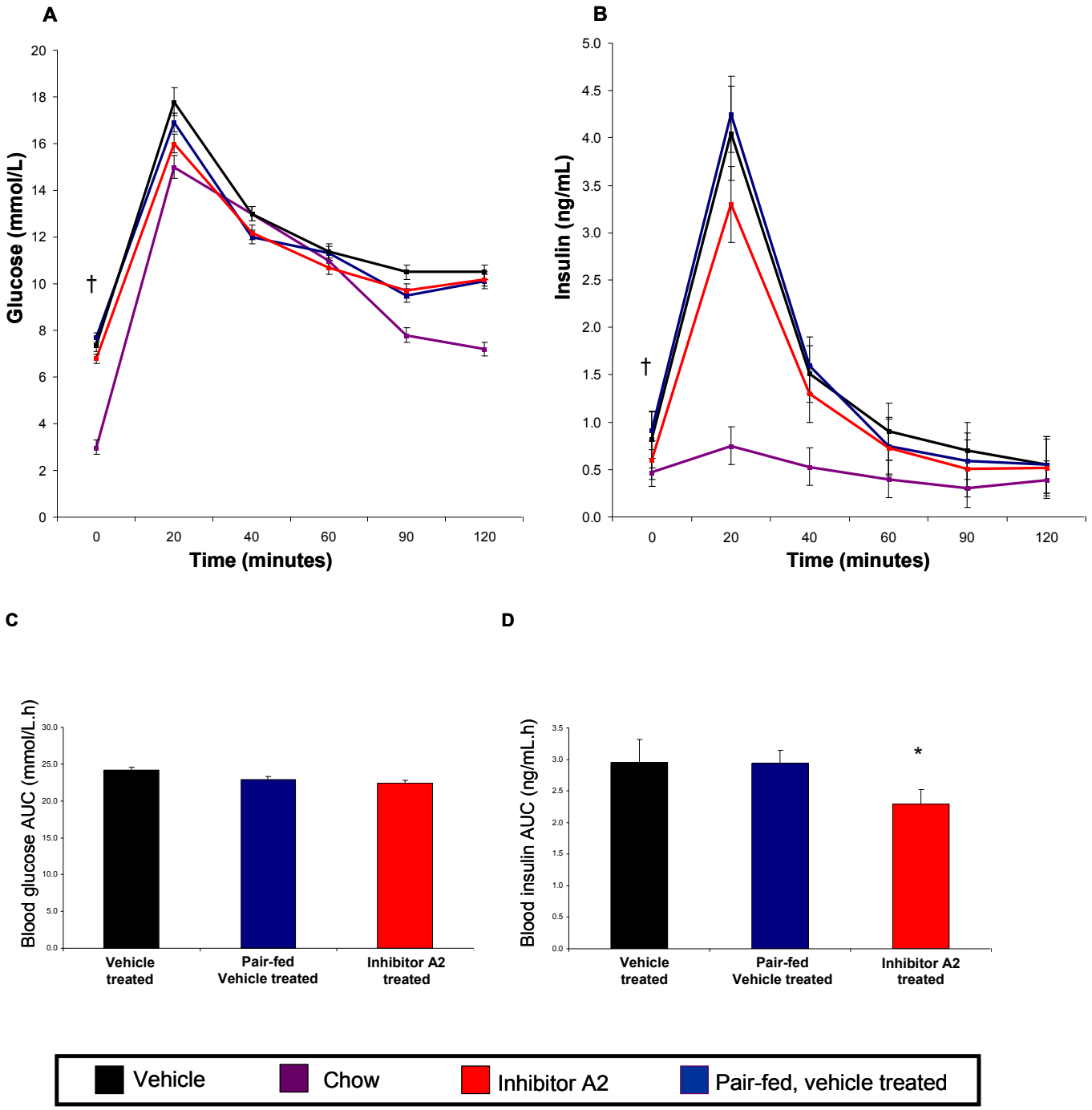

Figure 6-2 Fasting plasma glucose (A) and insulin (B) levels were lower in C57Bl6 mice treated with the selective 11β-HSD1 inhibitor, A2, compared to vehicle treated controls (time 0). († p<0.05 A2 vs. vehicle vs. paid-fed, vehicle treated). Area under curve (AUC) values calculated from (A) and (B) showed no change in plasma glucose levels (C) with A2 treatment compared to vehicle treated controls, by contrast insulin secretion (D) was reduced (p<0.05)*

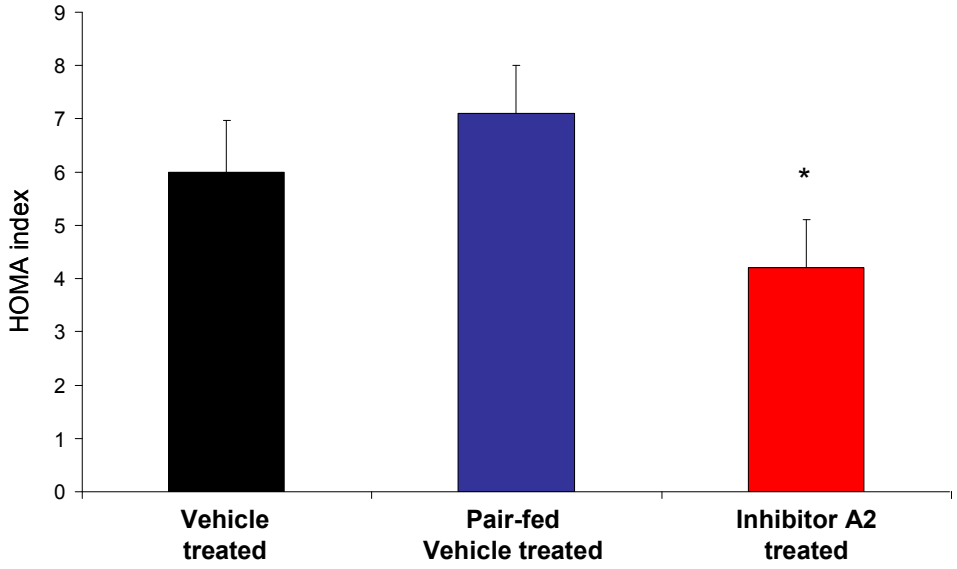

Figure 6-3 C57Bl6 mice treated with the 11β-HSD1 inhibitor, A2, were more insulin sensitive than vehicle treated controls as indicated by HOMA index. (p<0.05)*

Gene and protein expression in skeletal muscle from KK mice: Cortisone pellet implanted KK mice treated with A2 for 4 consecutive days had increased total IRS1 protein expression, decreased inhibitory IRS1 serine-307 phosphorylation and increased activating threonine-308 phosphorylation of PKB/akt in whole tissue quadriceps explants. Activating tyrosine-608 phosphorylation of IRS1 did not change (Figure 6-4).

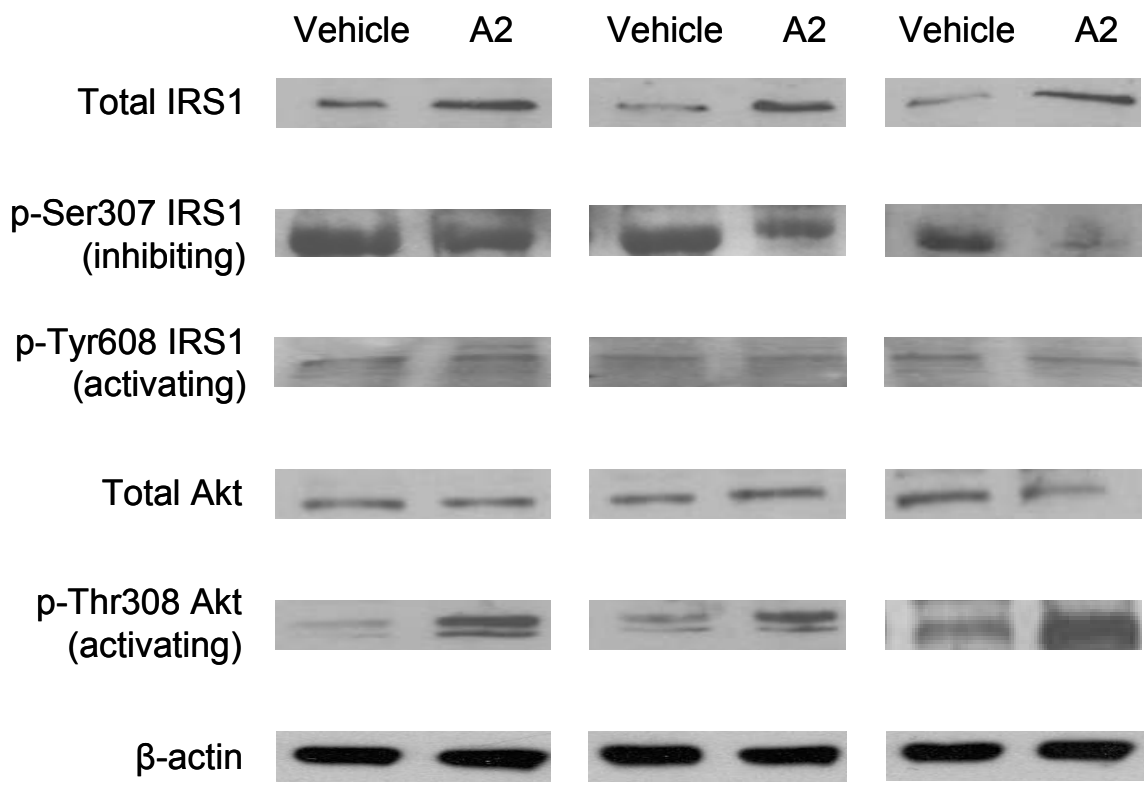

Figure 6-4 In cortisone pellet implanted KK mice, the selective 11β-HSD1 inhibitor, A2, increases IRS1 total protein expression, decreases inactivating IRS1 serine-307 phosphorylation and further downstream enhances insulin stimulated threonine-308 phosphorylation of PKB/akt in quadriceps muscle explants. Representative western blots are shown (A2 vs. vehicle)

Genecard analysis of quadriceps mRNA expression following A2 treatment is shown in Table 6-2. Positive findings were endorsed with real-time PCR (Figure 6-5). A2 decreased 11β-HSD1 expression (0.48-fold) (Table 6-2, Figure 6-5), but was without effect upon GRα or H6PDH expression. In agreement with our protein expression data, IRS1 mRNA expression increased following selective 11β-HSD1 inhibition, whereas IRS2 expression was unchanged (Figure 6-5). mRNA levels of the regulatory subunit of PI3K (p85) decreased 0.25-fold following treatment with A2 with no change in catalytic subunit (p110) expression (Table 6-2, Figure 6-5). A2 decreased expression of key target genes involved in *de novo* lipogenesis (ACC1 0.3-fold, DGAT 0.4-fold,), lipolysis (HSL: 0.3-fold;

ATGL: 0.39-fold) and lipid oxidation (ACC2: 0.6-fold) (Table 6-2, Figure 6-5). In addition, PDK4 increased 1.7-fold following A2 treatment (Figure 6-5).

	Gene of interest	Cortisone + vehicle (mean ΔCt±se)	Cortisone+A2 (mean ΔCt±se)	Fold change in gene
Insulin signalling cascade	Insr	15.9±0.2	16.5±0.2	0.65
	Irs1	16.9±0.1	16.6±0.1	1.27
	Irs2	17.2±0.2	16.3±0.8	1.93
	Pik3r1 (p85α)	14.9±0.2	16.9±0.4	**0.25**
	Pik3cb (p110β)	19.4±0.3	19.8±0.1	0.79
	Pdk1	15.9±0.2	16.9±0.1	**0.49**
	Akt1	16.3±0.1	17.1±0.2	0.59
	Akt2	17.7±0.3	18.2±0.3	0.74
	Prkcz (PKCζ)	19.2±0.3	20.6±0.6	**0.37**
	Prkci (PKCλ)	19.6±0.1	20.2±0.1	0.62
	Tbc1d1	15.7±0.3	16.5±0.1	0.58
	Tbc1d4 (AS160)	17.2±0.3	18.1±0.3	0.53
	Rab10	11.7±0.3	12.3±0.1	0.68
	Slc2a1 (GLUT-1)	16.8±0.2	17.0±0.1	0.91
	Slc2a4 (GLUT-4)	14.1±0.1	14.1±0.1	1.03
	Ptpn1 (PTP-1b)	17.8±0.1	18.8±0.1	0.52
	Ptpn11 (SHP2)	16.1±0.2	16.4±0.1	0.77
	Pten	15.8±0.1	16.6±0.1	0.60
	Ppp2r1a (PP2A)	14.9±0.2	15.2±0.1	0.81
	Socs1	21.5±0.4	21.2±0.4	1.20
	Socs3	19.4±0.2	19.4±0.1	0.98
	Frap1 (mTOR)	16.5±0.2	17.3±0.3	0.55
	Foxo1	16.9±0.2	17.4±0.1	0.75
	Foxo3a	15.9±0.1	16.7±0.5	0.58
	Prkaa2 (AMPK)	14.8±0.1	15.0±0.3	0.91
	Ppargc1a (PGC-1α)	16.9±0.2	17.1±0.1	0.93
Glucocorticoid metabolism and action	H6pd	15.6±0.1	16.2±0.3	0.66
	Hsd11b1 (11β-HSD1)	17.5±0.6	18.5±0.8	**0.48**
	Nr3c1 (GRα)	15.8±0.1	16.3±0.2	0.72
Lipid metabolism	Acaca (ACC1)	15.1±1.0	16.7±0.2	**0.33**
	Acacb (ACC2)	13.6±0.3	14.4±0.2	0.60
	Lpl	12.6±0.2	13.2±0.1	0.68
	Lipe (HSL)	16.4±0.6	18.1±0.1	**0.30**
	Pnpla2 (ATGL)	13.7±0.5	15.1±0.1	**0.39**
	Dgkd (DGKδ)	21.3±0.5	21.4±0.1	0.97
	Pparg (PPARγ)	21.2±0.5	22.4±0.3	**0.43**
Ceramide metabolism	Sptlc1 (SPT1)	17.8±0.1	18.6±0.0	0.59
	Ugcg (Glucosylceramide synthase)	18.8±0.1	19.5±0.1	0.61
	Asah1 (acid ceramidase)	19.0±0.1	19.3±0.1	0.82
	Lass1	16.9±0.1	17.3±0.1	0.77
	Lass6	20.5±0.4	21.1±0.0	0.68
Other genes	Prkca (PKC-α)	16.6±0.2	16.6±0.1	0.94
	Prkcb1 (PKC-β)	22.7±0.3	22.8±0.3	0.96
	Prkcc PKC-γ)	22.6±0.1	23.1±0.7	0.69
	Ppara (PPARα)	18.7±0.3	19.0±0.1	0.85
Internal controls	Ppib (cyclophilin B)	18.1±0.2	18.4±0.1	0.79
	Hprt1	16.5±0.2	17.1±0.0	0.69

Table 6-2 Analysis of 45 pre-selected gene targets implicated in the pathogenesis of insulin resistance. Cortisone pellet implanted KK mice were treated with a selective 11β-HSD1 inhibitor, A2, or vehicle for 4 days prior to animal sacrifice (n=3 per group). Data presented as mean ΔCt±s.e. for both groups of animals relative to 18s as an internal house keeping gene, higher ΔCt values corresponding with lower gene expression. Fold-changes in gene expression were calculated as described in chapter 2. Specific target genes and all changes >2-fold increase or 0.5-fold decrease vs. vehicle (highlighted in bold) were endorsed with real-time PCR (Figure 6-5).

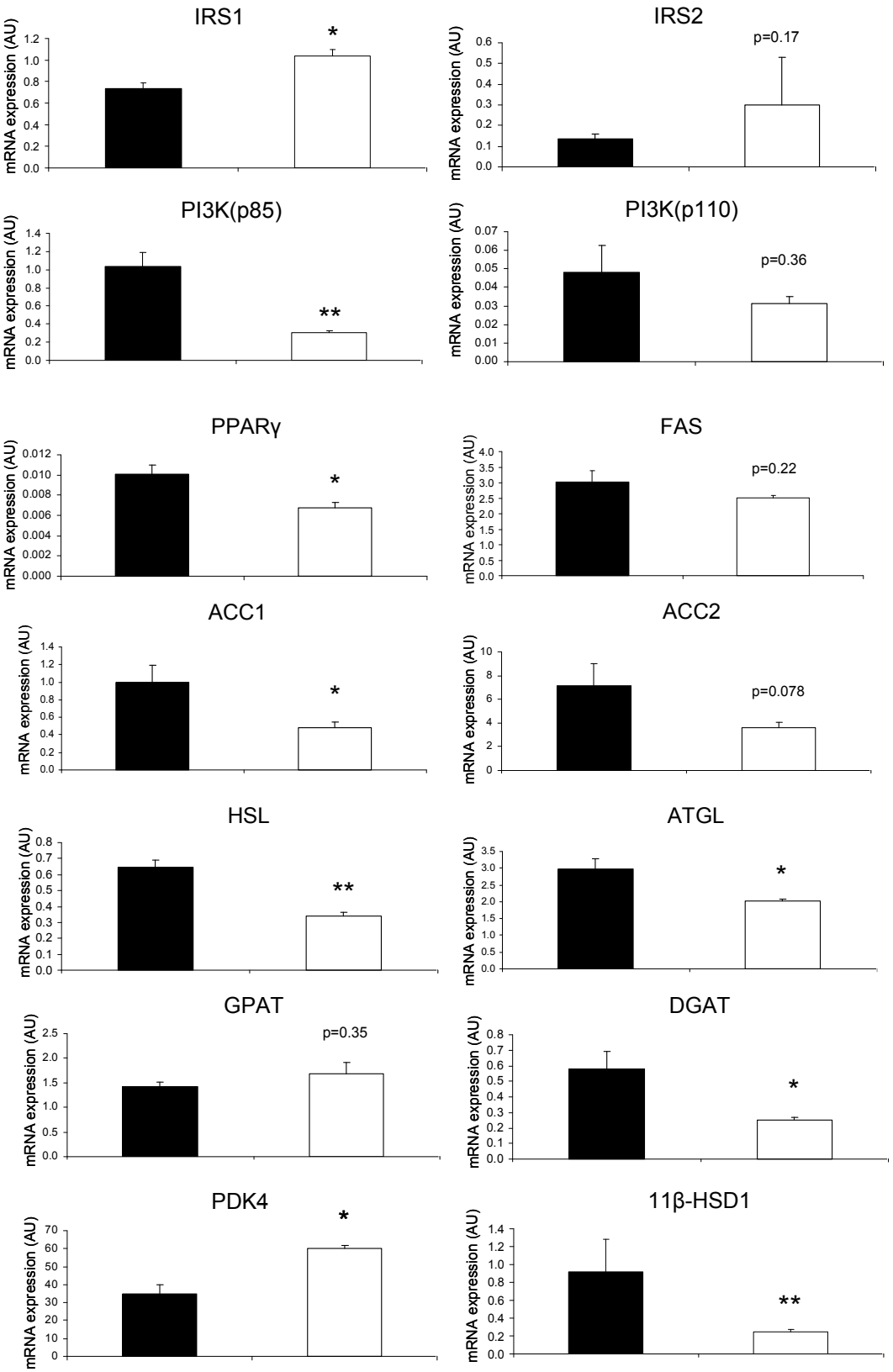

Figure 6-5 Real-time PCR analysis endorsing observations from the genecard analysis presented in Table 6-2. Gene expression from whole tissue quadriceps explants obtained from cortisone pellet implanted KK mice treated for 4 days with the selective 11β-HSD1 inhibitor, A2 (white bars) or vehicle (black bars) (p<0.05, ** p<0.01) (n=3 per group)*

6.5. Discussion

In this chapter, we have shown that selectively inhibiting 11β-HSD1 improves insulin sensitivity *in vivo*, consistent with previously published data (Alberts et al., 2002; Alberts et al., 2003; Berthiaume et al., 2007a; Hermanowski-Vosatka et al., 2005). Furthermore, we have found that 11β-HSD1 inhibitors not only restore IRS1 protein levels to control values, but also decrease inhibitory serine-307 phosphorylation of IRS1 and enhance PKB/akt activation *in vivo*. These findings endorse our results from cell culture models and add more credence to the hypothesis that this may represent an important insulin sensitizing mechanism of these compounds. As reported in both chapters 2 and 3, GC-mediated modulation of PI3K subunit stoichiometry may represent an additional mechanism by which GC modulate the insulin sensitivity of skeletal muscle. The results presented in this chapter also endorse this hypothesis; since mice treated with inhibitor A2 have lower mRNA levels of the regulatory subunit of PI3K (p85) with respect to the catalytic subunit (p110), in contrast to the vehicle treated mice (p85 monomers compete with the catalytically active p85-p110 heterodimer for binding IRS1).

A2 also decreased lipogenic gene expression (ACC1 and DGAT), and increased FFA utilization (decreased ACC2 expression leading to a decrease in the malonyl-CoA mediated inhibition of β-oxidation) in agreement with published observations (Berthiaume et al., 2007b). Furthermore, decreased HSL and ATGL will afford decreases in FFA and DAG generation. Importantly, these mice were not fasted prior to sacrifice, thus some of the gene expression changes observed

here may be a consequence of GCs and insulin working in concert, in a manner analogous to that we demonstrated in cell culture (chapter 4). By contrast, the C2C12 myotube treated with A1 were not exposed to insulin during the 24 h treatment period, mimicking the fasted state. This may offer an explanation for the apparent opposite actions of A1 upon the gene expression of ACC1, FAS and GPAT in the C2C12 myotubes compared with the action of A2 upon the same genes in the cortisone-conditioned mice.

We observed a 1.7-fold increase in PDK4 expression with A2 treatment *in vivo*. PDK4 is a negative regulator of the pyruvate dehydrogenase complex, limiting acetyl CoA generation. Rodents with deletion of PDK4 have increased glucose oxidation (Jeoung & Harris, 2008), and we have shown that DEX increases PDK4 expression in C2C12 myotubes, endorsing published observations in human primary myocytes (Salehzadeh et al., 2009). The discrepancy where A2 increases PDK4 may again reflect the complexities of working with whole animals versus cell culture models (i.e. the concerted action of GC with other factors such as insulin modulating gene expression). Importantly, the increase in PDK4 with selective 11β-HSD1 inhibitors, may further serve to drive lipid oxidation at the expense of glucose oxidation.

The net effect of A2 will be to decrease intramyocellular lipid accumulation, as well as local FFA and DAG generation and, as a consequence, activation of DAG sensitive PKC isoforms will be decreased. This may further explain the reduced IRS1 serine-307 phosphorylation observed in the A2 treated mice.

Intramyocellular accumulation of ceramides has been strongly associated with the onset of insulin resistance in both rodents and humans (Adams et al., 2004; Straczkowski et al., 2004; Turinsky et al., 1990). Recently, GCs have been found to increase *de novo* ceramide synthesis (Holland et al., 2007). However, we observed no regulation of mRNA levels for genes involved in ceramide metabolism in our genecard analysis of A2 treated cortisone-conditioned mice.

The *in vivo* studies presented in this chapter were designed by AstraZeneca for the purpose of measuring the pharmacokinetics of A2. Consequently, we had very little influence over their design. Numerous rodent studies looking into the metabolic impact of selective 11β-HSD1 inhibitors have found that they are most effective in rodent models that are prone to developing insulin resistance / type 2 diabetes. The C57Bl6 mice used in the initial characterisation of the metabolic effect of A2, are prone to developing obesity, but are not the best model for these studies for the reason highlighted above. Consequently, the decision was made (by AstraZeneca) to undertake all additional experiments in KK/Ta Jcl mice, which are genetically predisposed to developing insulin resistance and type 2 diabetes.

In summary, we have demonstrated that selective inhibition of 11β-HSD1 *in vivo* enhances IRS1 expression and reduces inhibitory serine-307 phosphorylation of IRS1, the net result of which is increased downstream activation of AKT leading to increased insulin sensitivity - endorsing our initial cell culture findings. Moreover, the insulin sensitising actions of these compounds may be mediated by reducing intramyocellular lipolysis, *de novo* lipogenesis and perhaps enhancing β-oxidation consistent with other reports (Berthiaume et al., 2007b).

Chapter 7 - Investigating the role of PKC Isoforms in GC-induced Insulin Resistance of Skeletal Muscle

7.1. Introduction

In previous chapters we have demonstrated a clear link between GC exposure, serine-307 of IRS1 and insulin resistance in skeletal muscle, both in cell culture models and *in vivo*. In this chapter we will attempt to identify the mechanism by which GCs mediate these effects.

Numerous kinases have been implicated in phosphorylating IRS1 at inhibitory serine residues, and their dysregulation has been implicated in the pathogenesis of insulin resistance. These include Jun kinase (JNK) (Aguirre et al., 2000), inhibitor of nuclear factor κB (NF-κB) kinase-β (IKKβ) (Gao et al., 2002), p70S6K (S6K1) (Harrington et al., 2004), the mammalian target of rapamycin (mTOR) (Ozes et al., 2001), extracellular signal-regulated kinase (ERK) (Bouzakri et al., 2003) and certain protein kinase C (PKC) isoforms (Yu et al., 2002). As discussed previously, the intramyocellular accumulation of lipid intermediates, such as DAGs, is strongly associated with the activation of DAG-sensitive, novel PKC isoforms (most notably PKCθ), which go on to phosphorylate IRS1 at serine-307 - reducing insulin sensitivity (Yu et al., 2002). Furthermore, other DAG-sensitive PKC isoforms of the conventional subclass (specifically PKCα and β) have also been implicated in inhibiting insulin signal transduction by mediating serine phosphorylation of IRS1 (including serine-307 in the case of PKCα) (Chin, Liu & Roth, 1994; Liberman et al., 2008; Nawaratne et al., 2006). The impact of GCs upon the activation of these kinases in skeletal muscle has not been explored, but DEX has been found to activate conventional PKC isoforms (PKCα, and β) in

rodent adipocytes, and there inhibition (with use of a selective conventional PKC inhibitor) reversed the DEX-induced insulin resistance in these cells (Kajita et al., 2000; Kajita et al., 2001). Since we have shown that GCs regulate intramyocellular lipid metabolism; potentially contributing to enhanced IMTG and DAG levels, we hypothesize that the mechanism of GC-induced insulin resistance is via activation of one or more of these PKC isoforms.

7.2. Strategy of research

Using a myristoylated pseudosubstrate peptide to inhibit PKCθ and an indolocarbazole compound to inhibit the conventional PKC isoforms (Gö6976), the effect of CORT upon the insulin sensitivity of C2C12 myotubes was assessed using western blot analysis (total IRS1 and p-Ser307) and tritiated glucose uptake.

Expression of the conventional PKC isoforms was measured in C2C12 myoblasts, C2C12 myotubes and rodent tissue explants using real-time PCR.

Using siRNA technology to knockdown the mRNA expression of the conventional PKC isoforms in C2C12 myotubes, the effect of CORT upon insulin sensitivity was assessed using western blot analysis (IRS1/pIRS1 and AKT/pAKT) and tritiated glucose uptake.

7.3. Materials and methods

7.3.1. C2C12 cell culture

Proliferating C2C12 myoblasts were cultured in DMEM supplemented with 10% FCS and seeded into 12-well TC plates. At 60-70% confluence, differentiation was initiated by replacing proliferation media with DMEM supplemented with 5% horse serum and differentiated for 8 days. Prior to treatment, cells were incubated in DMEM free from additives for 4 h.

7.3.2. Protein kinase C inhibitors

A cell permeable myristoylated pseudosubstrate of PKCθ (Calbiochem, California, US) was used to selectively inhibit this isoform (Sequence: Myr-Leu-His-Gln-Arg-Arg-Gly-Ala-Ile-Lys-Gln-Ala-Lys-Val-His-His-Val-Lys-Cys-NH_2 (Wang et al., 2009)

The conventional PKC isoforms (α, βI, βII, and γ) were selectively inhibited using an indolocarbazole inhibitor, Gö6976, (Calbiochem, California, US) which is selective for calcium-dependent PKC isoforms (IC_{50}= 7.9nM for rat brain) and does not affect the kinase activity of the calcium-independent PKCδ, ε, or ζ, even at micromolar concentrations (Martiny-Baron et al., 1993).

7.3.3. Cell treatment

In cell culture experiments investigating the protein expression/ phosphorylation status of IRS1, C2C12 myotubes were initially washed out with serum free DMEM media (4 h) before CORT (1μM, 24 h) treatment with or without either a myristoylated PKCθ pseudosubstrate inhibitor (1μM, [highest concentration that did not induce apoptosis]) or a conventional PKC inhibitor (Gö6976) (5μM, 24 h), both added 10 mins prior to the addition of CORT. Media was spiked with human insulin (50nM) for the final 15 mins of the treatment period.

7.3.4. Rodent protocol

Male C57BL/6 mice (6-8 weeks of ages) were housed in standard conditions on a 12 h / 12 h light-dark cycle with access to standard rodent chow and water *ad libitum.* All procedures were carried out in accordance with the UK Animals (Scientific Procedures) Act, 1986. On day of experiment mice were sacrificed by cervical dislocation then femoral quadricept muscles and brain tissue was removed and snap-frozen in liquid nitrogen for characterisation of mRNA expression.

7.3.5. Glucose uptake

Glucose transport was assessed by measuring uptake of a radiolabelled glucose tracer as described previously (Liu et al., 2001), and as described in section 2.3.2. C2C12 myotubes were initially washed with serum free DMEM media (4 h) before the cells were treated with CORT (1μM, 24 h) with or without the

conventional PKC inhibitor (Gö6976) (5μM, 24 h). Gö6976 was incubated on the cells 10 mins prior to the addition of CORT. Cells were washed 3 times with PBS then transferred to 0.9mL of KRB containing same treatments and incubated for 10 mins. Cells were spiked with 0.5μg/mL insulin for 20 mins prior to the addition of 0.1mL KRB containing 6mM glucose combined with 37MBq/L of 2-deoxy-D-[^{3}H-glucose] (GE Healthcare, Bucks, UK) as a tracer. Radioactivity retained by cells was determined by scintillation counting. For all treatments glucose uptake was expressed as radioactivity retained by the cells in presence and absence of insulin.

7.3.6. Immunoblotting

Proteins were extracted from cell lysates and concentration determined as described in section 2.6.2. For both IRS1 and p-IRS1, 40μg of protein was resolved on 8% SDS-PAGE gels. Proteins were transferred to nitrocellulose membranes (both IRS1 and pIRS1 proteins transferred at 140mA for 2 h). Primary (anti-IRS1 and anti-pSer307 were purchased from Upstate, Dundee, UK) and secondary antibodies (Dako, Glostrop, UK) were used at a dilution of 1/1000. Membranes were re-probed for β-actin and primary and secondary antibodies used at a dilution of 1/5000 (Abcam, Cambridge, UK). Bands were visualised using ECL detection kit (GE Healthcare, Bucks, UK) and quantified with Genesnap by Syngene (Cambridge, UK). The ratio of p-IRS1 to β-actin was normalised to the ratio of IRS1 to β-actin.

7.3.7. siGLO- transfection indicator

In order to optimise conditions for most the effective transfection, cells were treated with siGLO - a green fluorescent (6-FAM-labelled), double-stranded oligonucleotide (Thermofisher, Surrey, UK) which localises to the nucleus upon successful transfection. C2C12 myoblasts and myotubes were coincubated with siGLO (50nM) and 0, 1, 2, or 3µL/well of a lipid based transfection reagent (DharmaFECT3, Thermofisher, Surrey, UK), in serum free media, for 24 h after which time the media was removed, cells were fixed with 4% formaldehyde and nucleus stained with Hoechst 33342 (1:5000) (Invitrogen, paisley, UK). The intracellular location of siGLO was visualised using ArrayScan (Thermofisher, Surrey, UK) (Figure 7-1 and 7-2).

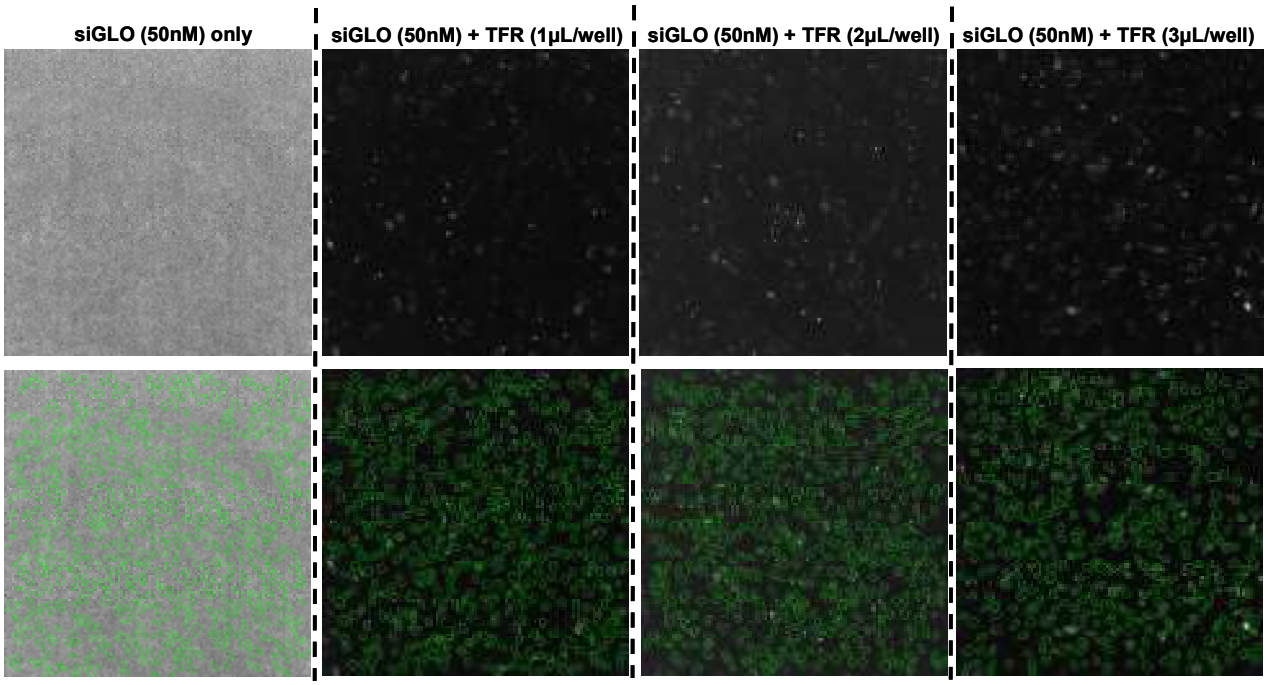

Figure 7-1 Transfection efficiency assessed in C2C12 myoblasts using a range of lipid based transfection reagent concentrations (DharmaFECT3). Top panel: siGLO staining only, bottom panel: siGLO staining superimposed with nuclei positions (green circles). Although there does not appear to be a high degree of colocalisation, cells treated with the highest concentration of DharmaFECT3 had marginally more siGLO localised to the nucleus. (TFR= transfection reagent)

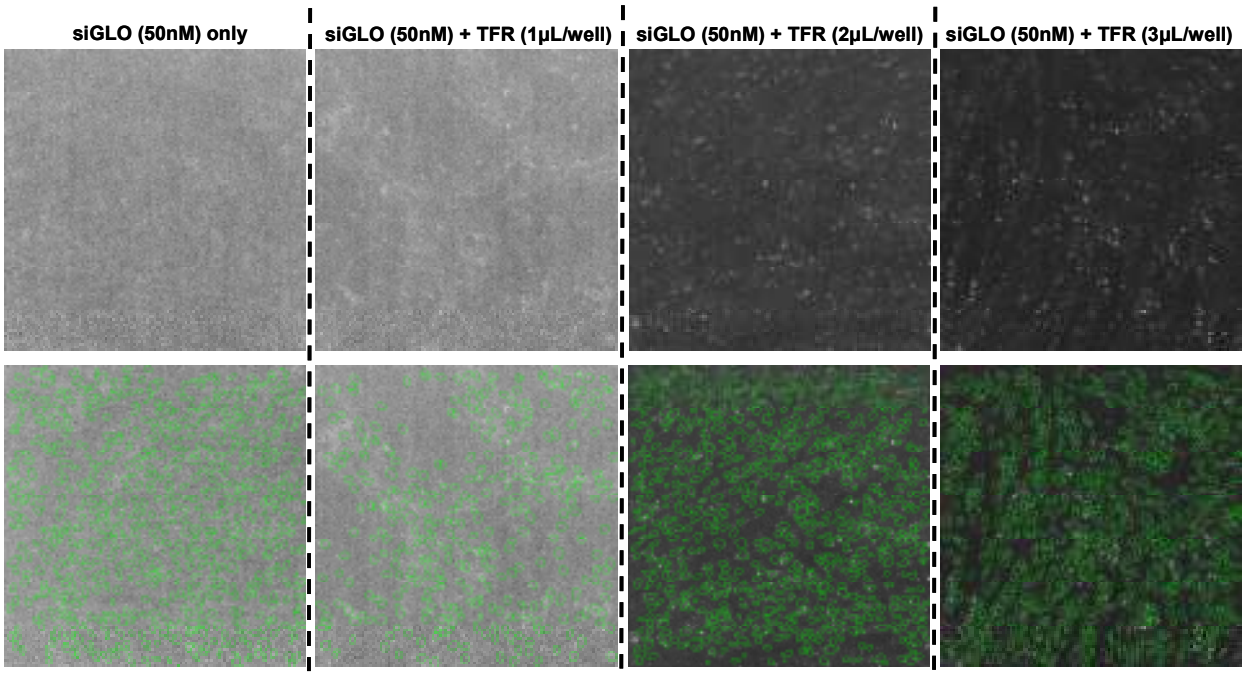

Figure 7-2 Transfection efficiency assessed in differentiated C2C12 myotubes using a range of lipid based transfection reagent concentrations (DharmaFECT3). Top panel: siGLO staining only, bottom panel: siGLO staining superimposed with nuclei positions (green circles). Although there does not appear to be a high degree of colocalisation, cells treated with the highest concentration of DharmaFECT3 had marginally more siGLO localised to the nucleus. (TFR= transfection reagent)

7.3.8. Transient siRNA in C2C12 myoblasts and myotubes

Predesigned short-interfering oligonucleotide (siRNA) sequences directed against mouse PKCα, PKCβ and PKCγ were purchased from Dharmacon (Thermofisher, Surrey, UK), each contains 4 different oligonucleotide sequences directed against separate regions of the target gene (ON-TARGETplus, SMARTpool) – maximising the chances of a high mRNA knockdown. Although, there are two distinct PKCβ isoforms (PKCβI and PKCβII), they are alternative splice products of the same gene (PRKB), thus siRNA directed against the primary transcript should be sufficient to knockdown the expression of both isoforms. In order to facilitate siRNA entry into the cells, a lipid based transfection reagent was used:

DharmaFECT3 (Thermofisher, Surrey, UK) (recommended by the manufacturer as most effective in transfecting C2C12 myoblasts). The optimal DharmaFECT3 concentration that achieved the highest level of transfection was determined by using a fluorescent transfection indicator, as detailed above. C2C12 myoblasts were initially seeded into 12-well plates at $5x10^4$cells/mL and incubated overnight at 37°C with 5% CO_2. The PKC siRNA (100nM) was introduced in normal serum containing media and experimental controls, run in parallel, included: no treatment, negative control (non-targeting siRNA, 100nM), mock transfection (DharmaFECT3 without siRNA) and a positive control (siRNA directed against a highly expressed house keeping gene; cyclophilin B [ON-TARGETplus, SMARTPool, 100nM]). In a separate experiment, trialling a different approach, C2C12 myotubes were treated with siRNA (directed against cyclophilin B) containing novel modifications allowing for their uptake into the cell without the need for a transfection reagent (Accell, SMARTpool siRNA, Thermofisher, Surrey, UK). Here, the siRNA (100nM) was added to the cells using the manufacturers optimized siRNA delivery media (Thermofisher, Surrey, UK) supplemented with 4.5g/L glucose and 3% horse serum. For further details regarding the duration and timing of siRNA treatments see the results section.

7.3.9. RNA extraction

Total RNA was extracted using Tri-reagent system, concentration determined spectrophotometrically at OD_{260} and integrity assessed by agarose gel electrophoresis. For reverse transcription (see section 2.9.2) 1µg of RNA was used.

7.3.10. Real-time PCR

Cyclophilin B, PKCα, PKCβ and PKCγ mRNA levels were determined using an ABI 7500 sequence detection system (Applied Biosystems, Warrington, UK). Reactions were performed in singleplex as described in section 2.11.2, and normalised against the 18s rRNA house keeping gene. Primers and probes and for all genes were supplied by Applied Biosystems as pre-mixed 'assay on demands' (Applied Biosystems, Warrington, UK).

7.3.11. Statistical analysis

Where data were normally distributed, unpaired student t-tests were used to compare single treatments to control using SigmaStat 3.1 (Systat Software, CA, US). If normality tests failed, non-parametric tests were used. One way ANOVA on ranks was used to compare multiple treatments, doses or times using SigmaStat 3.1. Statistical analysis on PCR data was performed on mean ΔCt values.

7.4. Results

Testing the hypothesis that PKC isoforms maybe responsible for GC-induced IRS1 serine-307 phosphorylation, co-incubation of C2C12 myotubes with a myristoylated PKCθ pseudosubstrate peptide inhibitor (PS) (1μM) was without effect upon the CORT (1μM, 24 h) induced IRS1 serine-307 phosphorylation (3.6±0.6 (CORT) vs. 3.2± 0.7 (CORT+PS), p=N.S) (Figure 7-3A). Similarly, the decrease in IRS1 total protein observed following CORT treatment was not recovered with this inhibitor (0.62±0.2 (CORT) vs. 0.60±0.1 (CORT+PS), p=N.S) (Figure 7-3A). By contrast, the conventional PKC inhibitor Gö6976 (5μM), decreased CORT-induced IRS1 serine-307 phosphorylation (3.49±0.5 (CORT) vs. 0.78±0.1 (CORT+Gö6976), $p<0.05$) (Figure 7-3). Total protein levels were not recovered (0.55±0.1 (CORT) vs. 0.55±0.04 (CORT+Gö6976), p=ns) (Figure 7-3B).

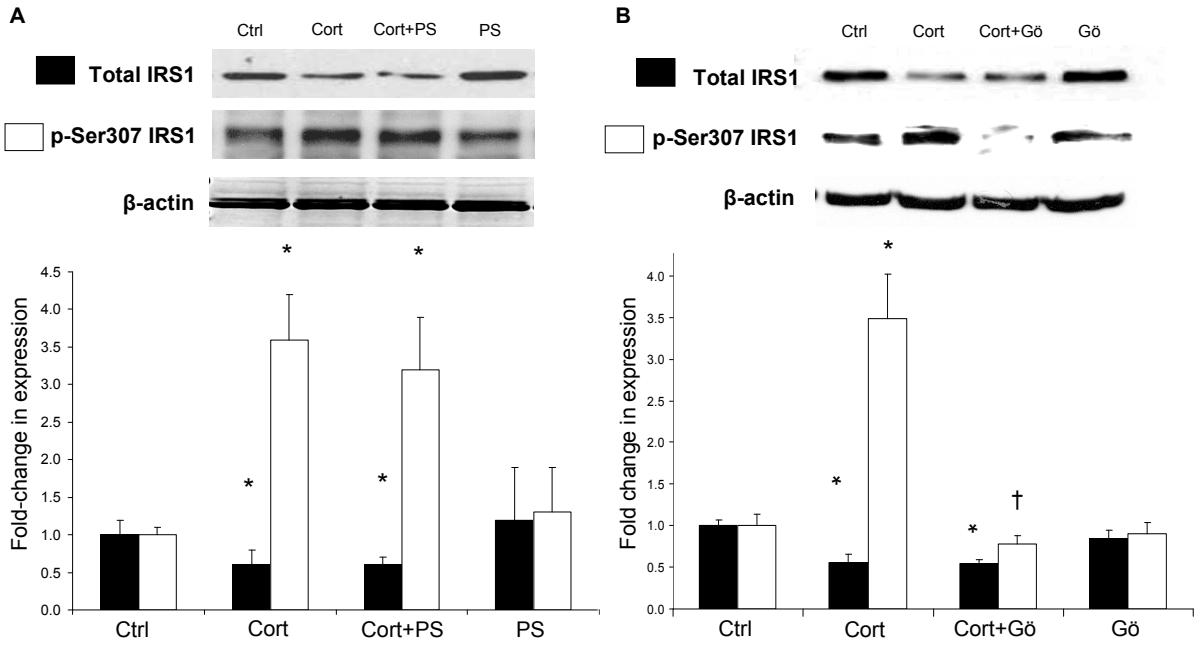

Figure 7-3 The myristoylated PKCθ pseudosubstrate peptide inhibitor (PS) was without effect upon IRS1 serine-307 phosphorylation or IRS1 total protein levels following CORT treatment in C2C12 myotubes (a). By contrast, the conventional PKC inhibitor, Gö6976, blocked the effects of CORT upon IRS1 serine-307 phosphorylation, but had no effect upon IRS1 total protein levels (b). Cells spiked with insulin (50nM) for the last 15 mins of treatment. Data presented are the mean of n=5 experiments with representative western blots inserted above. Bands quantified relative to β-actin as internal loading control and the ratio of p-IRS1 to β-actin was normalised to the ratio of IRS1 to β-actin. (p<0.05 vs. Ctrl, † p<0.05 vs. CORT) (Ctrl=control, CORT=corticosterone, PS=*pseudosubstrate *inhibitor of PKCθ, Gö=Gö6976).*

Importantly, Gö6976 blocked the decrease in both basal glucose uptake (4.9±0.2 (CORT) vs. 6.9±0.4dpmx10^3 (CORT+Gö6976), $p<0.05$) and total insulin-stimulated glucose uptake (5.3±0.6 (CORT) vs. 6.8±0.6dpmx10^3 (CORT+Gö6976), $p<0.05$) following CORT treatment (Figure 7-4), suggesting a critical role of conventional PKC isoforms in GC-induced insulin resistance of skeletal muscle.

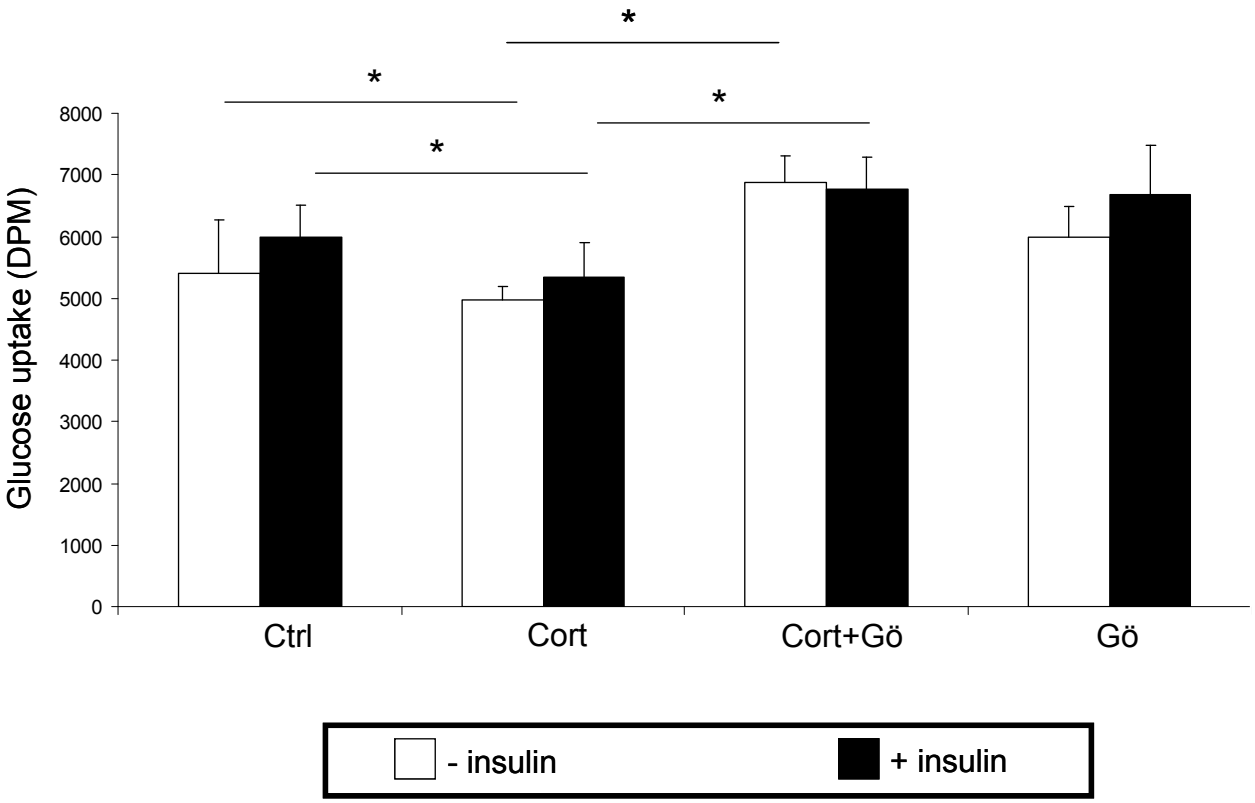

Figure 7-4 CORT decreased both basal and total insulin-stimulated glucose uptake in C2C12 myotubes. Coincubation with the conventional PKC inhibitor, Gö6976, reversed the effects of CORT. Gö6976 treatment alone was without significant effect. (p<0.05) (Ctrl=control, CORT=corticosterone, Gö=Gö6976)*

All conventional PKC isoforms were detected in whole mouse tissue explants of quadricept muscle, with PKCα being the dominant isoform (Table 7-1). Similarly, all isoforms were detected in C2C12 myoblasts, however, following differentiation only PKCα and PKCγ appeared to be expressed (Table 7-1). As with whole tissue quadriceps, PKCα was the most highly expressed isoform in the differentiated cells. Mouse brain was used as a positive control and displayed the highest expression of all three isoforms (Table 7-1).

	mRNA expression (ΔCt ± SE)			
Gene	**C2C12s myoblasts**	**C2C12 myotubes**	**Quadricept**	**Brain**
PKC-α	15.4 ± 0.9	18.2 ± 0.1	16.0 ± 0.3	12.6 ± 0.001
PKC-β	23.0 ± 0.5	Not Expressed	23.1. ± 0.9	9.9 ± 0.08
PKC-γ	15.4 ± 1.0	24.1± 0.5	22.2 ± 0.2	11.4 ± 0.01

Table 7-1 Comparative mRNA expression of the conventional PKC isoforms (α, β and γ). Expression in mouse brain tissue is provided as a quantitative reference. (Data are `expressed as ΔCt±S.E, n=4 experiments)

To identify which specific conventional PKC isoform is involved in GC-induced insulin resistance, we attempted to transiently knockdown the expression of each isoform separately using siRNA. The effectiveness of the siRNA oligos was initially validated in C2C12 myoblasts where, after 24 h incubation, we achieved mRNA expression knockdown of 94% for Cyclophilin B (positive control); 88% for PKCα; 74% for PKCβ and 82% for PKCγ, with minimal off target effects (Figure 7-5).

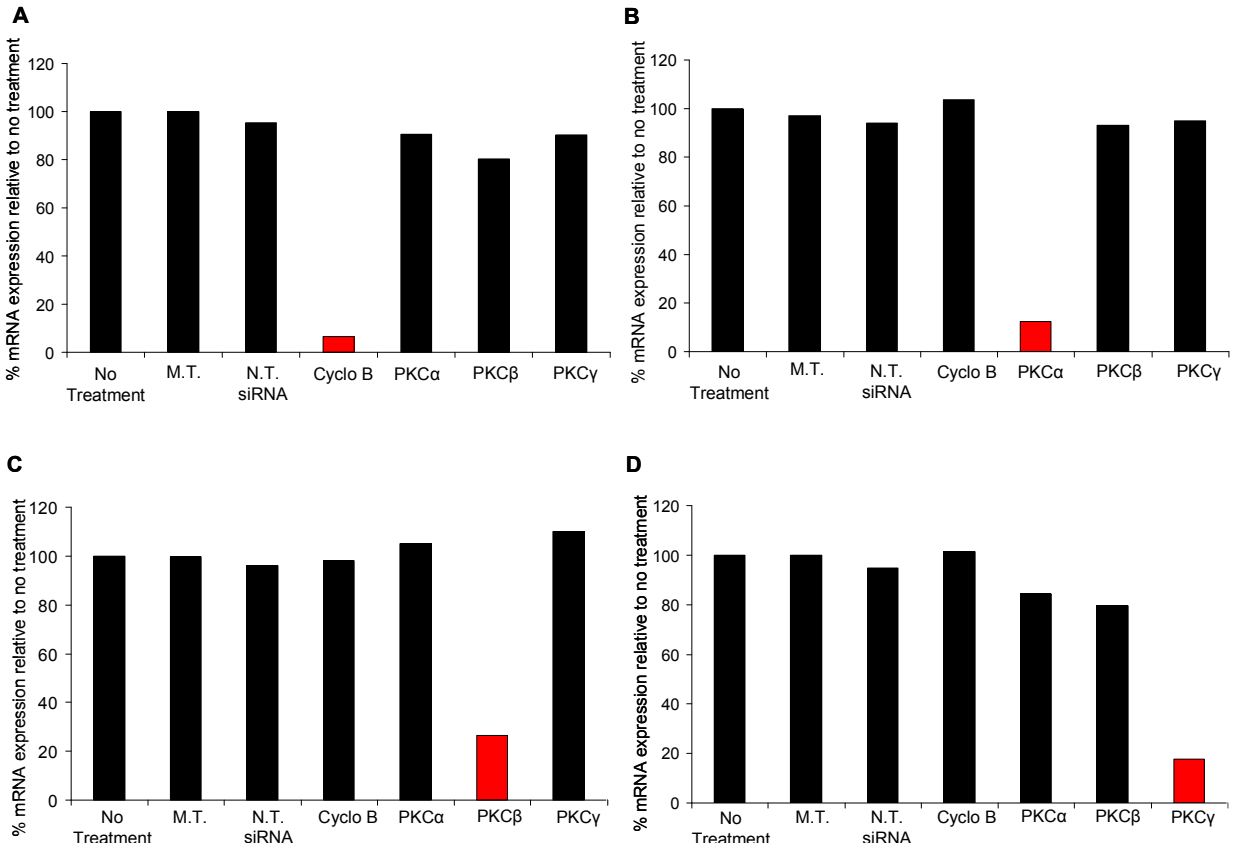

Figure 7-5 siRNA directed against cyclophilin B (positive control) (a), PKCα (b), PKCβ (c) and PKCγ (d) in C2C12 myoblasts. (M.T.= Mock transfection [no siRNA], N.T. = non-targeting siRNA)

In order to knockdown the mRNA expression of these PKC isoforms in differentiated C2C12 myotubes, we employed a variety of strategies: including introducing the siRNA before, during and after myocyte differentiation (summarised in Table 7-2). The highest level of knockdown we achieved was only 21% for Cyclophilin B (positive control); 23% for PKCα and 6.2% for PKCγ, with minimal off target effects (Table 7-2, Figure 7-6) (N.B. PKCβ is not expressed in C2C12 myotubes, Table 7-1). The low mRNA knockdown observed in the differentiated cells is likely due to poor transfection efficiency; consequently, we have been unable to fully explore the precise role that conventional PKC isoforms play in GC-mediated insulin resistance in skeletal muscle.

Protocol	siRNA	% knockdown in mRNA expression relative to no treatment				
		Mock Transfection	Non-targeting siRNA	cyclophilin B	PKCα	PKCγ
siRNA (SmartPool, 100nM) and transfection reagent (3μL/well) introduced at day 0 of differentiation (in differentiation media) and incubated on cells for 24 hours. Media replaced with normal differentiation media on day 1 and cells differentiated as normal until day 8	cyclophilin B	0.1	-0.7	**3.5**	1.1	1.0
	PKCα	0.8.	1.0	1.9	**7.6**	2.2
	PKCγ	0.8	1.2	0.9	3.2	**4.5**
siRNA (SmartPool, 100nM) and transfection reagent (3μL/well) introduced at day 0 of differentiation (in differentiation media) and incubated on cells for 72 hours. Media replaced with normal differentiation media on day 3 and cells differentiated as normal until day 8	cyclophilin B	-1.8	0.6	**21.2**	-6.4	-0.2
	PKCα	0.5	1.0	2.1	**23.3**	3.2
	PKCγ	0.3	-1.1	2.0	3.8	**6.2**
Cells differentiated as normal until day 6 where siRNA (SmartPool, 100nM) and transfection reagent (3μL/well) was introduced (in differentiation media) and incubated on cells until day 8 (48h hours)	cyclophilin B	0.1	-0.3	**8.4**	0.1	1.4
	PKCα	-6.9	-6.3	-9.2	**18.4**	-2.2
	PKCγ	0.1	0.3	0.4	0.3	**3.1**
Cells differentiated as normal until day 8 then siRNA (100nM) and transfection reagent (3μL/well) introduced (in differentiation media) and incubated on cells for 24 hours.	cyclophilin B PKCα PKCγ	Cells were not viable at the end of the treatment				
siRNA (100nM) and transfection reagent (3μL/well) introduced at day 0, 2, 4 and 6 in differentiation media. Cells differentiated for 8 days	cyclophilin B PKCα PKCγ	Myoblasts did not fuse to form myotubes				
siRNA requiring no transfection reagent (Accell, 100nM) introduced at day 0, 2, 4 and 6 in differentiation media. Cells differentiated for 8 days.	cyclophilin B	3.2	4.1	**9.3**		

Table 7-2 siRNA directed against cyclophilin B (positive control), PKCα and PKCγ in C2C12 myotubes, using a variety of different strategies in an attempt to optimise for maximal mRNA knockdown.

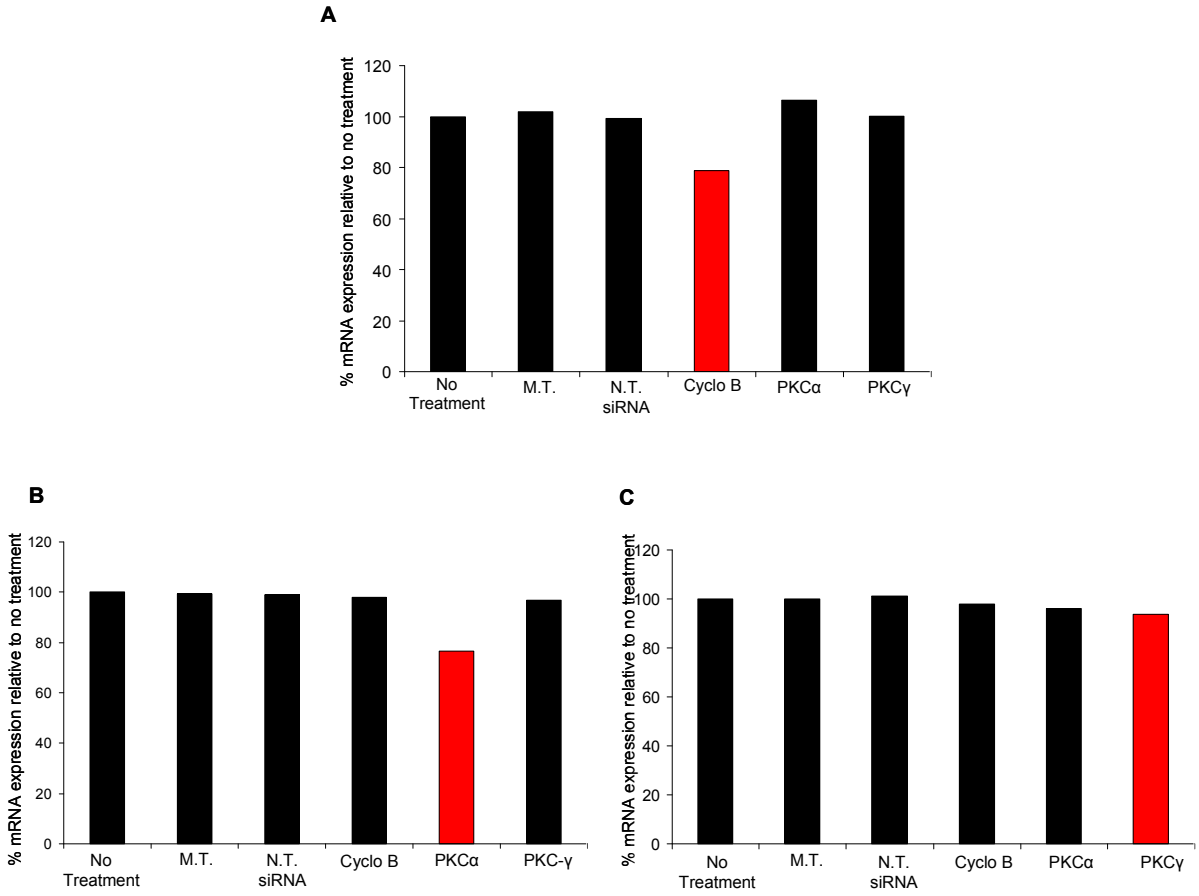

Figure 7-6 siRNA directed against cyclophilin B (positive control) (a), PKCα (b) and PKCγ (c) in C2C12 myotubes (graphical representations of selected results taken from Table 7-2; where highest mRNA knockdown was achieved). (M.T.= Mock transfection [no siRNA], N.T. = non-targeting siRNA)

7.5. Discussion

In this chapter, we have attempted to address the hypothesis that PKC isoforms are implicated in GC-induced insulin resistance of skeletal muscle. From our experiments with PKC inhibitors, we were able to show that PKCθ is unlikely to participate in GC-mediated serine-307 phosphorylation of IRS1. By contrast, inhibition of the conventional PKC isoforms successfully blocks GC-induced IRS1 serine-307 and importantly, restores both basal and total insulin-stimulated glucose uptake. This inhibitor does however fail to restore IRS1 total protein levels. Although serine-307 phosphorylation is known to increase proteosomal degradation of IRS1 (Greene et al., 2003) this result, along with the results of chapters 4 and 6, points towards the possibility that GCs negatively impact upon IRS1 by two separate mechanisms: 1) genomic downregulation, and 2) enhancing serine-307 phosphorylation.

Looking at the relative expression levels of the conventional PKC isoforms in C2C12 myotubes has revealed that PKCα is the most highly expressed, followed by PKCγ, with no detectable expression of PKCβ. Consistent with these findings, an identical pattern of expression has been observed in human primary myocytes (Boczan et al., 2000). PKCα is also the dominant isoform expressed in mouse muscle explants, however, unlike the above there is detectable PKCβ expression.

Interestingly, PKCα has been implicated in GC-induced insulin resistance of adipocytes (Kajita et al., 2001), and in a separate study, this isoform has been shown to have an indirect involvement in IRS1 serine-307 phosphorylation

(Nawaratne et al., 2006). These results taken together suggest that PKCα is the likely candidate mediating the GC-induced insulin resistance of skeletal muscle, however, the possibility that a different PKC isoforms / ser/thr-kinases are responsible cannot be ruled out.

Following on from our results using the conventional PKC inhibitor, we attempted to knockdown the expression of PKCα and PKCγ separately in C2C12 myotubes using siRNA - for the purpose of pinpointing the precise PKC isoform(s) involved in GC-induced insulin resistance. Upon successful knockdown our intention was to then looking at the effect of GCs upon IRS1/pIRS1, akt / p-akt and tritiated glucose uptake. Although we achieved a high level of knockdown for all isoforms in the undifferentiated myoblasts, we were unable to achieve a reasonable level in the differentiated myotubes, using a number of different strategies. Post-mitotic cells, including skeletal myotubes are notoriously difficult to transfect.

In summary, although we have identified DAG-sensitive conventional PKC isoforms as likely candidate kinases mediating GC-induced insulin resistance of skeletal muscle, we have been unable to explore this possibility fully.

Chapter 8 - Discussion and Final Conclusions

8.1. Discussion

The rationale for our interest into the impact of GCs upon the insulin sensitivity of skeletal muscle is based upon the phenotype of GC excess. GC treatment induces whole-body insulin resistance in both rodents and humans (Larsson & Ahren, 1996), and since skeletal muscle takes up the majority of the circulating glucose, under insulin stimulation (DeFronzo et al., 1981), it seemed likely skeletal muscle was the major site of this action of GCs. However, since mechanistic detail regarding how GCs impinge upon the metabolic functions of skeletal muscle were lacking, further investigation was warranted.

The interaction between GC and the insulin signalling cascade in skeletal muscle has only been examined in a limited number of studies, mostly in cultured myocytes. This has provided variable explanations for the induction of insulin resistance, as discussed in section 1.12.3 (Giorgino et al., 1993; Giorgino et al., 1997; Giorgino & Smith, 1995; Rojas et al., 2003; Ruzzin et al., 2005; Saad et al., 1993). We have shown that GCs impact upon the insulin signalling cascade at several critical points (Figure 8-1); firstly, by direct modulation of mRNA gene expression, including: IRS1 downregulation, altered PI3K subunit stoichiometry (although this has not been backed up with protein data and thus robust conclusions cannot be drawn) and increased AS160 expression. Secondly, GCs increase inhibitory serine-307 phosphorylation of IRS1, which is likely to reduce its affinity for the insulin receptor and potentially enhance its proteosomal degradation. Collectively, these gene expression changes / phosphorylation

events act to reduce insulin stimulated glucose uptake into skeletal myocytes (Figure 8-1).

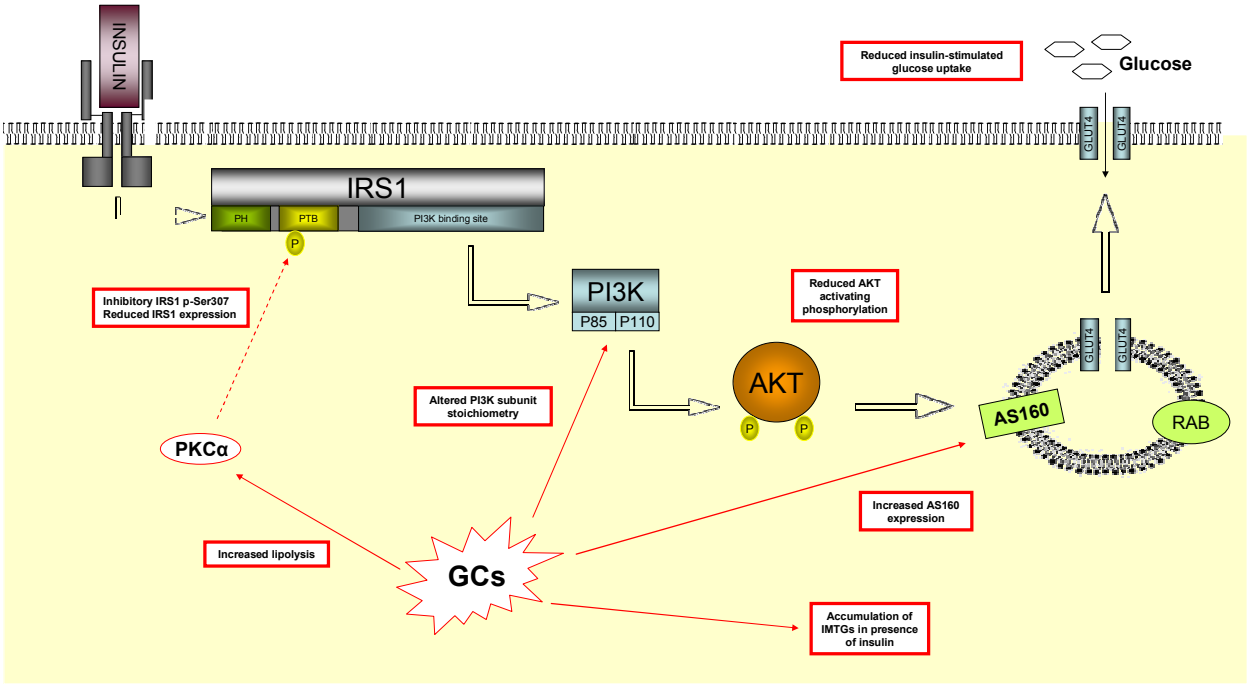

Figure 8-1 The insulin signalling cascade in skeletal muscle and how GCs potentially mediate insulin resistance based on the data presented in this thesis.

Recently, accumulation of intramyocellular lipids have been identified as a marker of reduced insulin sensitivity and type 2 diabetes, in both rodents and humans (Koyama et al., 1997; Pan et al., 1997; van Loon et al., 2004), however, whether this is due to free fatty acid oversupply to skeletal muscle or reduced β-oxidation rates, or a combination of both is unknown. Although increased intracellular TAG is a marker of reduced insulin sensitivity, it is largely agreed that metabolites derived from these lipid stores are responsible for mediating the insulin resistance; these include long-chain fatty acyl-CoAs, DAGs and ceramides.

GCs potently regulate lipid metabolism in adipose tissue and liver, however, their precise role in the regulation of these processes in skeletal muscle has been poorly defined. We have shown that, in conditions mimicking the fasted state (i.e. in the absence of insulin), GCs decrease the rate of intramyocellular lipid accumulation, increase fatty acid release from intramyocellular lipid stores and upregulate the rate of fatty acid oxidation. The latter is vital for maintaining a high ATP/ADP ratio in this highly metabolically active tissue. Importantly, we have shown that some of these catabolic actions may not hold true under conditions mimicking the fed state (i.e. in the presence of insulin), in particular with respect to β-oxidation, where a GC-induced concentration-dependent decrease is observed. This concerted action of GCs and insulin has been reported before, in regulation of *de novo* lipogenesis (Wang et al., 2004) and glycogen metabolism (Lopez, Gomez-Lechon & Castell, 1984). Taking glycogen metabolism as an example, GC have been found to enhance both hepatic glycogen deposition as well as glycogenolysis, whereas insulin stimulates glycogen storage but inhibits glycogenolysis (Baque et al., 1996; Lopez et al., 1984). During fasting adrenal GC secretion increases, and under these conditions, in a low insulin environment, GC allow a more effective release of glucose from glycogen for use as fuel. By contrast, during re-feeding, when recovering from fasting, GC levels remain elevated and work in concert with insulin to promote glycogen re-accumulation (Lopez et al., 1984). In a similar way, the contrasting actions of GCs upon skeletal muscle β-oxidation may be a beneficial mechanism allowing effective generation of ATP from oxidation of free fatty acids during fasting. Conversely, during re-feeding GCs promote recovery from fasting, by enhancing intramyocellular lipid accumulation – replenishing the depleted stores. In this respect it is easy to see

that if GC levels remain elevated over a sustained period of time (e.g. as a consequence of GC therapy or elevated skeletal muscle 11β-HSD1 expression), the resulting reduced rates of β-oxidation may favour the aberrant accumulation of intramyocellular lipids, as is observed in the skeletal muscle of insulin resistant individuals. In addition, since the majority of fatty acids utilised by the skeletal muscle are taken up from the circulation, and insulin resistance is often accompanied by increased circulating free fatty acids levels (Swislocki et al., 1987), then this would only serve to exacerbate the problem.

Elevated intramyocellular DAG is associated with reduced insulin sensitivity in skeletal muscle, by activating PKCθ which goes on to mediate inhibitory serine-307 phosphorylation of IRS1 (Yu et al., 2002). We have shown that GCs may contribute to enhanced intramyocellular DAG accumulation by upregulating the expression of key lipolytic genes. This, in conjunction with the observed increase in serine-307 phosphorylation of IRS1 following GC exposure, lead us to investigate whether activation of DAG-sensitive PKC isoforms underpin GC-induced insulin resistance. Our results indicate that inhibition of the conventional subclass of the PKC isozymes (PKCα, β, γ), rather than PKCθ, protects against GC-induced serine-307 phosphorylation of IRS1, and restore glucose uptake. Unfortunately, we were unable to pinpoint the precise conventional PKC isozyme responsible; although a previous study conducted in adipocytes points towards PKCα as the likely candidate kinase (Kajita et al., 2001). If future studies prove successful in identifying this critical mediator of GC-induced insulin resistance, then its targeted inhibition may offer a novel approach in the treatment of type 2 diabetes.

Although there is unequivocal evidence that elevated circulating GC levels reduce whole-body insulin sensitivity (as demonstrated in Cushing's syndrome), the role of 11β-HSD1 is emerging as a key player in the pathogenesis of insulin resistance and type 2 diabetes, particularly in light of the fact that circulating GC levels are not elevated in these conditions. Importantly, the expression of this enzyme has been found to be increased in myotubes extracted from type 2 diabetic individuals (Abdallah et al., 2005; Whorwood et al., 2002), suggesting that GCs, generated locally within skeletal myocytes, may contribute to the reduced insulin sensitivity.

In this thesis we have confirmed the importance of 11β-HSD1 as a critical regulator of skeletal muscle insulin sensitivity – since its targeted inhibition, using selective compounds, not only reduces inhibitory serine-307 phosphorylation of IRS1 and increases downstream activating AKT phosphorylation, but also has a potentially insulin sensitising impact upon intramyocellular lipid metabolism; by reducing both *de novo* lipogenesis and lipolysis, which may afford decreases in IMTG and DAG levels.

In conclusion, we have described novel mechanisms by which GCs regulate skeletal muscle insulin sensitivity and lipid metabolism. We propose that both increased circulating, and intramyocellularly generated, GCs induce skeletal muscle insulin resistance by impacting upon the insulin cascade at several critical points: IRS1, PI3K and AS160 (Figure 8-1). In addition, we suggest that GC have a direct effect upon intramyocellular *de novo* lipogenesis, lipolysis and β-oxidation, co-ordinating lipid accumulation and loss in conjunction with insulin –

underpinning their insulin resistance-inducing actions. Furthermore, we have identified a critical role for 11β-HSD1 in the regulation of skeletal muscle insulin sensitivity, and have provided new mechanistic detail regarding the known insulin sensitizing actions of selective 11β-HSD1 inhibitors, and thus provide further support for their use in the treatment of type 2 diabetes.

Chapter 9 - Future Directions

The work presented in this thesis has given us a great deal of insight into the role GCs play in the insulin sensitivity of skeletal muscle, however, since this is not an exhaustive study, there remains a number of avenues that warrant further attention in order to gain a greater understanding of this topic. Indeed, our work has raised several interesting questions which we will explore in future studies. In this chapter, we will discuss the future direction we believe this research should follow – preliminary data will be presented where possible.

9.1. Impact of exogenous 11DHC/CORT and 11βHSD1 knockout upon skeletal muscle insulin sensitivity in vivo

In chapter 6, we showed that selective 11β-HSD1 inhibition enhances whole body insulin sensitivity *in vivo,* by reducing inhibitory serine-307 phosphorylation of IRS1 and increasing activating PKB/akt phosphorylation, whilst also impacting upon the expression of numerous genes involved in intramyocellular lipid metabolism. Although these findings have gone some way to elucidating the role that GCs/11β-HSD1 play in the insulin sensitivity of rodent skeletal muscle, further *in vivo* experiments are warranted to include appropriate controls (e.g. none GC treated mice), and to incorporate the 11β-HSD1 knockout mice which, despite previously being shown to be insulin sensitive (Morton et al., 2001), has not been characterised in terms of skeletal muscle insulin sensitivity. Our intention was to undertake these experiments as part of this thesis, but due to the fact that our 11β-HSD1 null colony became infected with pin worm (requiring all mice to undergoing an 8 month an anti-pin worm drug treatment; which

unfortunately had the side effect of inhibiting CYP3A4 activity, and thus interfering with GC metabolism) complete optimisation of these experiments before the submission of this thesis was not possible. We were, however, able to carry out a pilot study which involved exposing wild-type and 11β-HSD1 knockout mice to 11-DHC / placebo for 21 days, by subcutaneous implantation of slow release GC pellets. Aspects of insulin sensitivity were measured using glucose tolerance testing (GTT) and western blot analysis looking at skeletal muscle PKB/akt phosphorylation. In addition, the impact of these treatments upon total body weight, tissue weight and circulating 11DHC/corticosterone levels was also assessed.

9.1.1. Materials and methods

9.1.1.1. Experimental design

Wild-type and 11β-HSD1 null mice (generated in-house by G. G. Lavery) (6-12 weeks of age) had free access to water and irradiated RM3 (E) diet composed of 11.5Kcal% fat, 27Kcal% protein and 62Kcal% carbohydrate (Special Diets Services, Witham, UK). Mice were housed with a standard light cycle (6am on 6pm off). For a schematic representation of this experiment see Figure 9-1. On day 1 of the experiment, slow-release 11DHC / placebo pellets were implanted subcutaneously (see below for specific protocol). Blood was withdrawn from tail vein nicks at 12pm on day 10 - for determination of mid-way 11DHC and CORT plasma concentrations via LC-MS. On day 17, glucose tolerance was assessed via glucose tolerance testing, following a 4 h fast (see below for specific protocol).

On day 21, mice were fasted (4 h) before a standardized dose of insulin (2U/Kg) was administered via intraperitoneal injection to activate the insulin signaling cascade. 10 mins post injection; mice were anaesthetised and humanly sacrificed by exsanguination (cardiac puncture). Blood plasma was snap frozen in liquid nitrogen for determination of circulating CORT and 11DHC levels via LC-MS. Tissue was harvested and weighed before being snap frozen in liquid nitrogen. Short fasting of 4 h (rather then the standard 12 h) was used to avoid the mice becoming so stressed that their endogenous GC levels impinged upon their insulin sensitivity. Mice were weighed at regular intervals throughout the experiment.

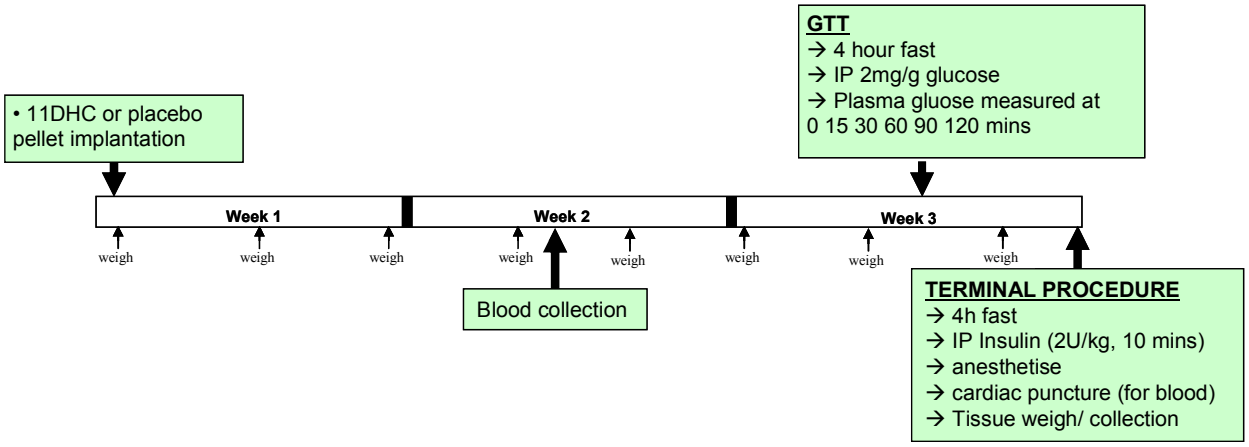

Figure 9-1 Schematic representation of the protocol carried out on both wild-type and 11β-HSD1 knockout mice. (GTT= glucose tolerance test)

9.1.1.2. Slow release GC pellet implantation

We decided upon using slow release GC pellets, implanted subcutaneously, as the method for administering GC to our mice - since this method would provide a controlled and continuous release of the steroids throughout the treatment period, avoiding fluctuations in the circulating levels associated other delivery methods, such as daily injections or spiking drinking water.

Mice were anaesthetised by inhalation of 2-3% v/v isoflurane (vaporised by oxygen at 1.6 litre/minute flow rate) and 5mg slow-release (60-day) 11-DHC/vehicle pellets (approximately 4mg/kg/day in a 20g mouse) were implanted subcutaneously in the lower back (Innovative Research of America, Sarasota, USA). Wounds were closed with staples which were removed after 7 days.

9.1.1.3. Glucose tolerance test (GTT)

Mice were fasted from 8am until 12pm (4 h), before glucose (2g/kg in 0.9% saline) was administered via intraperitoneal injection (IP). Plasma glucose levels were assessed from tail vein nicks using a hand-held glucometer (Roche, Sussex, UK), prior to glucose administration (fasting levels), and at 15, 30, 60, 90 and 120 mins post glucose injection. Plasma glucose levels were plotted against time and the areas under the curves (AUCs) were calculated using trapezoidal integration.

9.1.1.4. Activation of the insulin signalling cascade (terminal procedure)

On day 21 post pellet implantation, mice were fasted for 4 h (from 8am until 12pm) before insulin (2U/Kg in 0.9% saline) was administered via intraperitoneal injection (IP). 10 mins post injection, mice were anaesthetised by inhalation of 2-3% v/v isoflurane (vaporised by oxygen at 1.6 litre/minute flow rate) and were humanly sacrificed by exsanguination (cardiac puncture). Tissue was quickly harvested, weighed then snap frozen with liquid nitrogen.

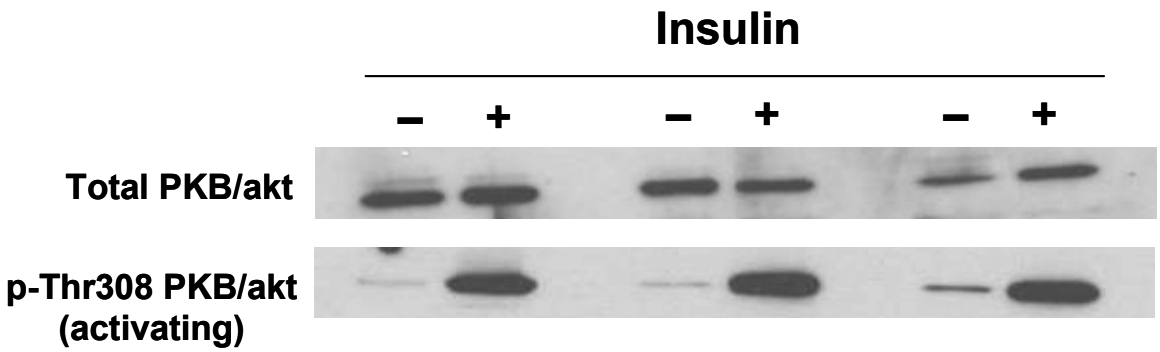

Figure 9-2 To demonstrate that we can activate the insulin signalling cascade in skeletal muscle in vivo: C57Bl6 mice were fasted for 4 h before insulin (2U/Kg in 0.9% saline) or vehicle (0.9% saline) were administered via intraperitoneal injection. 10 mins post injection, mice were humanely sacrificed by cervical dislocation, and femoral quadriceps were removed and quickly snap frozen in liquid nitrogen. Western blot analysis was employed to measure total / activating threonine-308 phosphorylation of PKB/akt.

9.1.1.5. Immunoblotting

Proteins were extracted from femoral quadriceps muscles, and concentration determined as described in section 2.6.2. For PKB/akt and p-PKB/akt, 20µg of protein was resolved on 12.5% SDS-PAGE gels. Proteins were transferred to nitrocellulose membranes (for PKB/akt and p-PKB/akt proteins transferred at 140mA for 1 h). Primary (anti-pThr308 PKB/akt [recognizing isoforms 1 and 2] were purchased from R&D Systems, Abingdon, UK) and secondary antibodies (Dako, Glostrop, UK) were used at a dilution of 1/1000. Secondary antibodies used at a dilution of 1/5000 (Abcam, Cambridge, UK). Bands were visualised using ECL detection kit (GE Healthcare, Bucks, UK).

9.1.1.6. CORT and 11-DHC analysis of mouse plasma and pellets.

The steroids were extracted from 100µL of mouse plasma, by liquid-liquid extraction using MTBE. The mouse plasma was heated at 50°C for 5 mins after which 1mL of MTBE was added. The mixture was then vortexed and centrifuged at 1200rpm for 5 mins. The MTBE layer was removed, evaporated to dryness and reconstituted in 100µL of a 50/50 methanol/water solution.

Pellets were dissolved in 1mL of water. 1ml of MTBE was added and the mixture was then vortexed and centrifuged at 1200rpm for 5 mins. The MTBE layer was removed, evaporated to dryness and reconstituted in 1mL of a 50/50 methanol/water solution, 10µL of this solution was subsequently diluted into 1mL of 50/50 methanol/water before LC/MS/MS analysis.

The steroid extract was analysed using LC/MS/MS (Xevo TQ mass spectrometer combined with an acquity uPLC system) with an electro-spray ionisation source in positive ion mode. The extraction efficiency was >85%. Steroids were eluted from a BEH C_{18} 2.1 x 50mm 1.7µm column using a methanol/water gradient system, solvent A was water 0.1% formic acid, and B was methanol 0.1% formic acid. The flow rate was 0.6mL/min and starting conditions were 45% B increasing linearly to 75% B over 5 mins.

Steroids were quantified via a linear regression method relative to a calibration series, the assay was linear for both corticosterone and 11-dehydrocorticosterone from 200 to 1ng/mL. Intra assay reproducibility RSD was <15%.

Steroids were positively identified by comparison of retention times and mass transitions to steroid standards. Two mass transitions were used to positively identify each steroid (qualifier ion in italics).

Steroid	Mass Transitions	Cone Voltage	Collision Energy
Corticosterone	347.18 > 329.16 *347.18 > 293.184*	26 26	14 16
Dehydrocorticosterone	345.18 > 120.95 345.18 > 242.12	30 30	24 32

9.1.2. Results of pilot study

Glucose tolerance was assessed by glucose tolerance testing (Figure 9-3A). Glucose levels did not change significantly (area under curve, AUC) between wild-type placebo treated and wild-type 11DHC treated mice (1.18±0.01 vs. 1.05±0.02AUCx10^3, p=ns) (Figure 9-3A and B). 11β-HSD1 knockout mice were more insulin sensitive than wild-type mice (0.85±0,01 vs. 1.18±0.01AUCx10^3, p<0.05) (Figure 9-3A and B), consistent with previously published observations (Morton et al., 2001). 11β-HSD1 knockout 11DHC treated mice were unusually more insulin resistant than the placebo treated 11β-HSD1 knockout mice (0.85±0.01 vs. 1.37±0.02AUCx10^3, p<0.05) (Figure 9-3A and B).

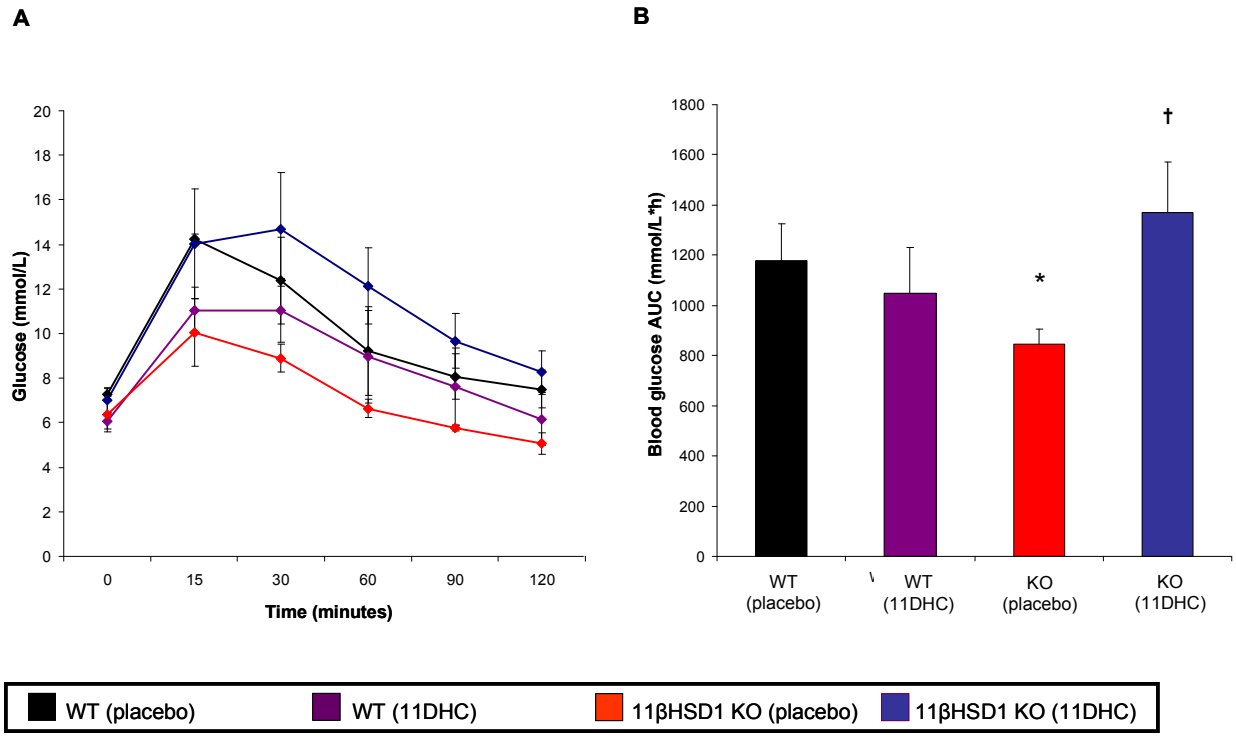

Figure 9-3 Glucose tolerance testing carried out in wild-type and 11β-HSD1 knockout mice treated with either 11DHC or placebo pellets. (A) Plasma glucose levels vs, time plots (B) Calculated AUCs. (p<0.05 WT placebo vs. WT 11DHC, † p<0.05 KO placebo vs, KO 11DHC) (n=4 per treatment group)*

Activation of the insulin signalling cascade in the skeletal muscle was assessed by measuring total PKB/akt levels / activating threonine-308 phosphorylation of PKB/akt, however, no consistent results were obtained (Figure 9-4).

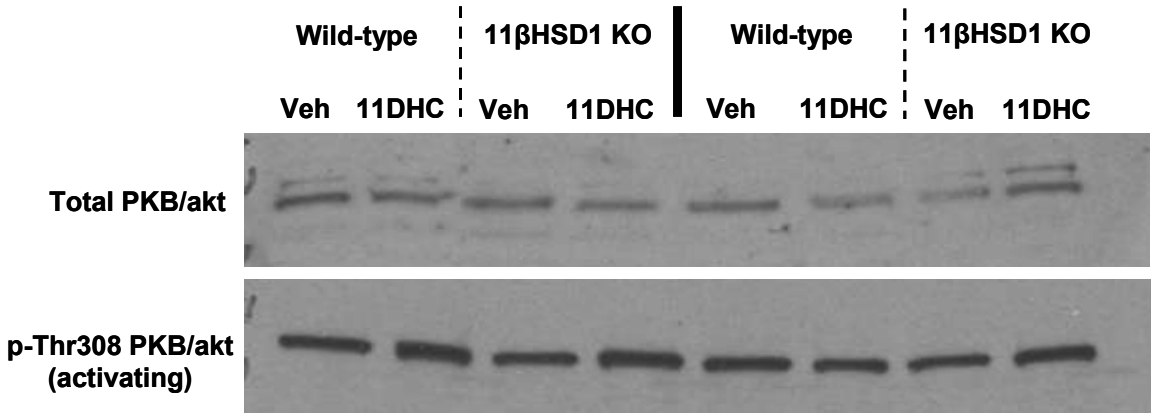

Figure 9-4 Western blot analysis looking at total PKB/akt and activating PKB/akt threonine-308 phosphorylation in the skeletal muscle harvested from wild-type and 11β-HSD1 knockout mice treated with either 11DHC or placebo pellets.

Wild type placebo treated mice steadily gained weight through the treatment period, culminating in a 6% increase overall by day 21 ($p<0.05$) (Figure 9-5). By contrast, the 11DHC treated wild type mice lost weight from day 1 post pellet implantation, and total body weight remained lower than the placebo treated wild type mice throughout the treatment period (Figure 9-5). There was no clear difference in body weights between the placebo treated 11β-HSD1 knockout mice and the11DHC treated11β-HSD1 knockout mice (Figure 9-5).

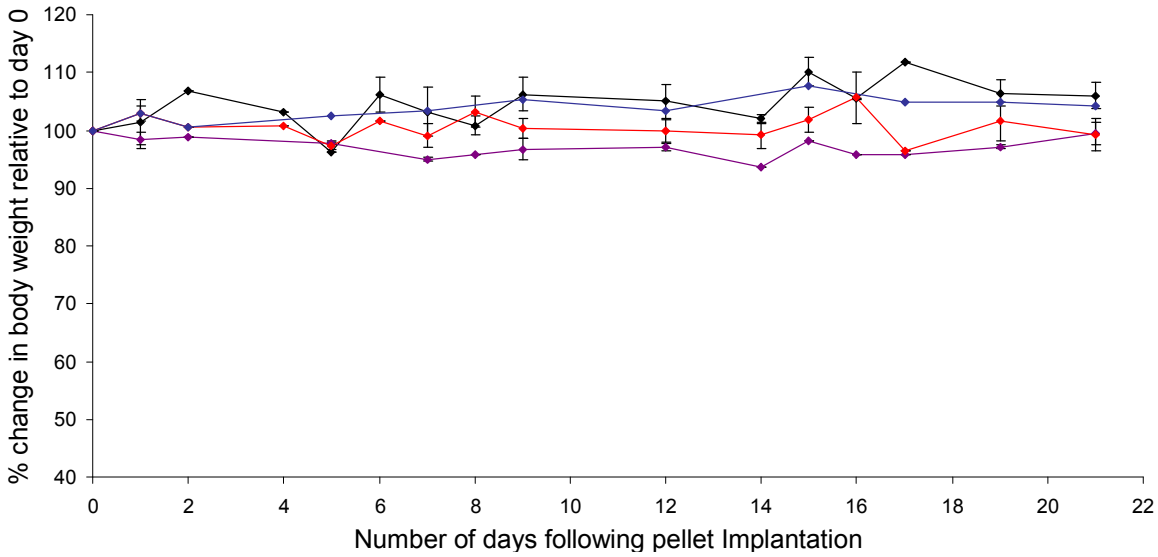

Figure 9-5 Total body weight plotted against time. (n=4 per treatment group)

Between treatment groups, there was no difference in skeletal muscle tissue bed weights (Figure 9-6A), nor in the weights of the liver, kidney or gonadal fat pads (Figure 9-6B).

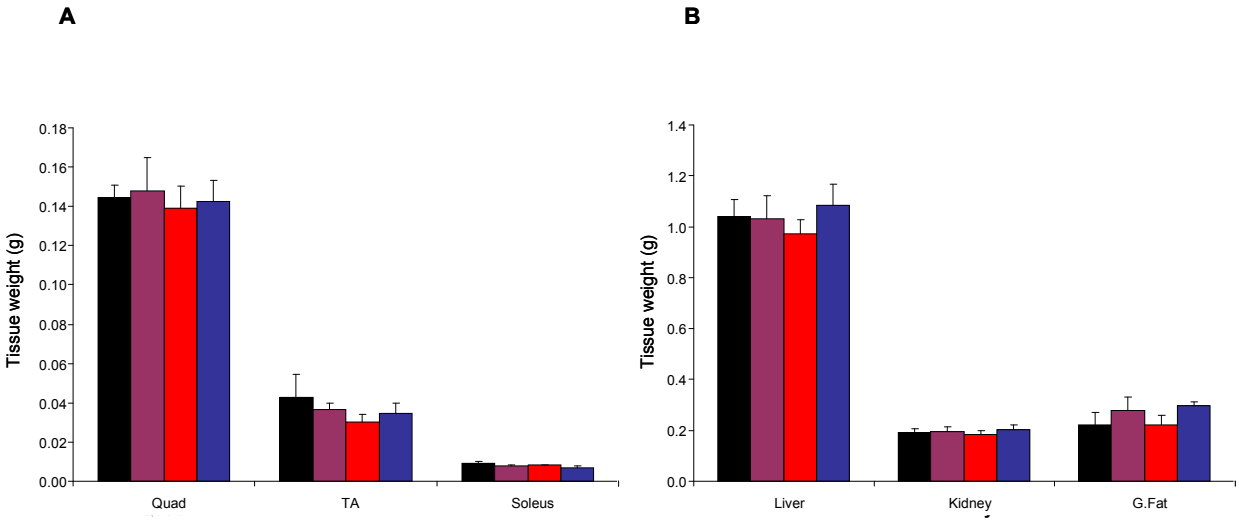

Figure 9-6 Tissue bed weights. (n=4 per treatment group)

To determine whether implantation of 5mg, 60-day release 11DHC pellets was sufficient to elevate circulating 11DHC levels, compared to the placebo treated mice, terminal plasma 11DHC and CORT levels were measured by LC-MS (Figure 9-7 A and B). Although the 11DHC pellets contained significant amounts of the inactive GC (8329±2587nM) compared to the placebo pellets (levels undetectable) (Figure 9-7C), implantation subcutaneously failed to elevate circulating 11DHC levels in both wild-type and 11β-HSD1 knockout mice (Figure 9-7A). Unusually, 11DHC levels appeared to be higher placebo treated mice. Furthermore, CORT levels mirrored that of the 11DHC in these mice (Figure 9-7B).

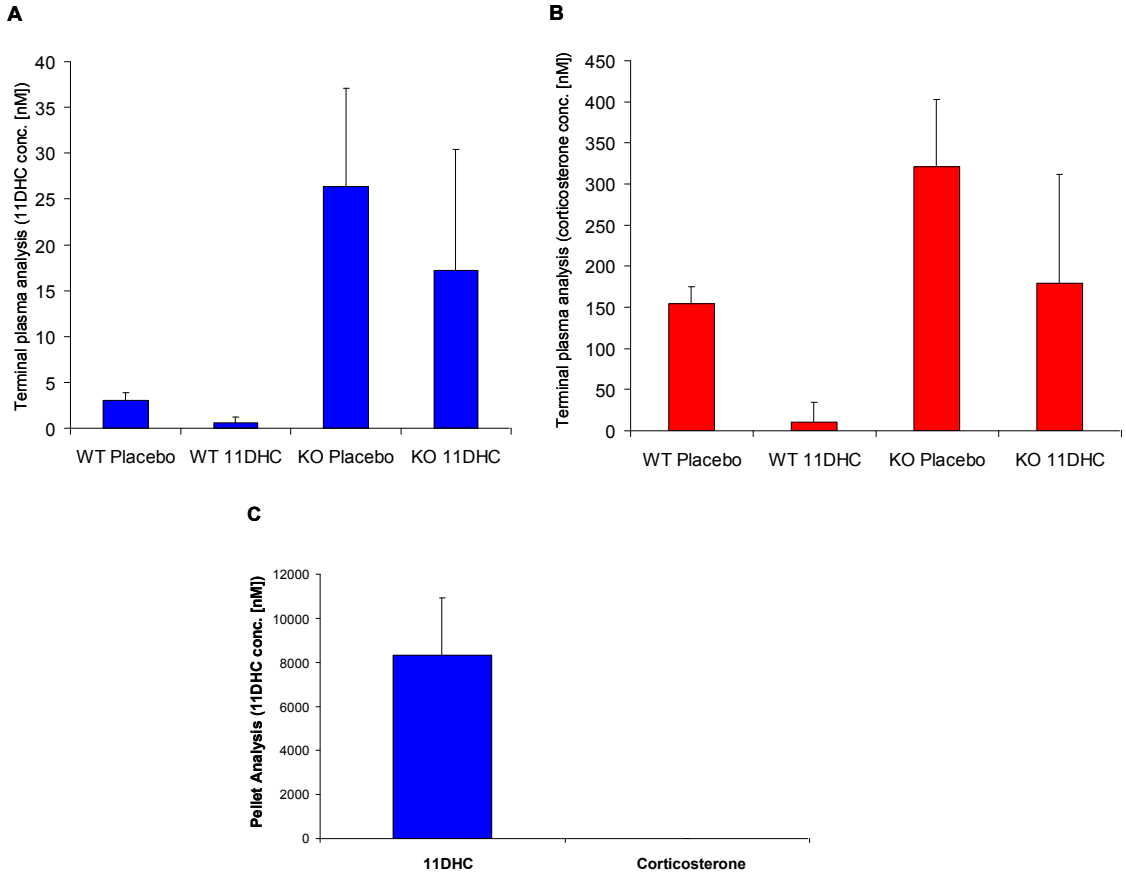

Figure 9-7 LC-MS was used to measure 11DHC levels (A) and CORT levels (B) in the terminal plasma harvested by cardiac puncture on day 21 of the experiment. 11DHC and CORT levels were also assessed in the 5mg, 60-day release 11DHC pellets (C). N.B the placebo pellets were also tested but contained undetectable amounts of 11DHC / CORT.

9.2. Discussion

The results obtained from this pilot study have demonstrated the complexities of working with whole animal models. Clearly, the mice implanted with 11DHC pellets did not have elevated circulating levels as was expected. One possible explanation for this could that the pellets released all their steroids early on during the treatment period, and thus by the 3rd week no impact upon insulin sensitivity or circulating levels was observed. Reassuringly, the 11β-HSD1 knockout, placebo-treated mice were significantly more insulin sensitive than the wild-type, placebo-treated mice, consistent with previously published observations (Morton et al., 2001). Future experiments may benefit from using slow-release GC pellets containing the human GC equivalents; cortisone / cortisol, a longer release half life (~90 days) and shorter treatment duration. Indeed, we have had some success using this strategy, as demonstrated in chapter 6. This would also allow us to distinguish between the circulating endogenous GCs (released by the HPA-axis) and the circulating GCs arising from the treatment. However, this approach is less physiologically relevant. Once we have optimised this protocol, we intend to carry out similar rodent experiments using selective 11β-HSD1 inhibitors.

9.3. Identification of the conventional PKC isoform mediating GC-induced insulin resistance in skeletal muscle

Although we have shown that inhibition of the conventional PKC isoforms blocks GC-induced serine-307 phosphorylation of IRS1, and importantly, restores glucose uptake, identification of the precise PKC isoform responsible for mediating these effects was not possible with the methods employed in this thesis. Future studies may benefit from using a viral transfection method, e.g. lentivirus-mediated siRNA delivery, which allows for a greater transfection efficiency in order to identify which PKC isoform(s) is involved. Alternatively, since PKC translocates to the plasma membrane upon activation, probing membrane fractions with antibodies directed against specific PKC isoforms by western blot may be beneficial. If these methods prove successful, carrying these experiments forward into a rodent model would be the next approach. These could include treating mice with a commercially available PKC inhibitor (such as Go6976, if cell culture results confirm that a conventional PKC isoform is involved) and identifying whether this protects from GC-induced insulin resistance. Alternatively, PKC knockout mice could be employed in similar experiments. Indeed, PKCα knockout mice are known to be insulin sensitive (Leitges et al., 2002), however, whether this protects them from GC-induced insulin resistance remains to be investigated.

9.4. Further investigation into the impact of GC upon intramyocellular lipid metabolism

In chapters 4 and 6 we showed that the actions of GCs upon intramyocellular lipid metabolism vary depending on whether or not insulin is present. For example, in the absence of insulin, GCs appear to increase the rate of β-oxidation, consistent with its known role as a catabolic effector, however, in the presence of insulin GC decreased β-oxidation rates. Although we have shown that GC regulate the mRNA expression of numerous genes involved in intramyocellular lipid metabolism, further investigation is warranted to identify the mechanism by which GC, and the combination of GC and insulin, regulate these metabolic pathways. Specifically, we intend to focus our attention upon measuring total protein levels / phosphorylation status of key enzymes known to regulate lipogenesis (ACC1, FAS); β-oxidation (ACC2, CPT1) and lipolysis (HSL, ATGL) as well as other key enzymes (AMPK, CAMKK). Employing phosphoproteomics might be a useful technique for this.

Importantly, we intend to obtain a functional readout for lipolysis in the C2C12 myotubes, in order for us to fully elucidate the impact of both GC and GCs with insulin on this pathway. Currently, we can measure lipolytic rates in Chub S7 cells, using a colorimetric assay which measures glycerol release, but obtaining consistent meaningful results in C2C12 myotubes has proved problematic thus far.

As we have discussed throughout this thesis, the accumulation of lipid metabolites, such as long-chain fatty acyl-CoAs, DAGs and ceramides are strongly associated with the onset of insulin resistance, and there accumulation may underpin the insulin resistance inducing effects of GCs. Consequently, we will attempt to measure the abundance of these metabolites using liquid chromatography-mass spectroscopy (LC-MS) which we have set up in house.

List of References

AAS, V., KASE, E. T., SOLBERG, R., JENSEN, J. & RUSTAN, A. C. (2004). Chronic hyperglycaemia promotes lipogenesis and triacylglycerol accumulation in human skeletal muscle cells. *Diabetologia* **47,** 1452-61.

ABDALLAH, B. M., BECK-NIELSEN, H. & GASTER, M. (2005). Increased expression of 11beta-hydroxysteroid dehydrogenase type 1 in type 2 diabetic myotubes. *Eur J Clin Invest* **35,** 627-34.

ABU-ELHEIGA, L., MATZUK, M. M., ABO-HASHEMA, K. A. & WAKIL, S. J. (2001). Continuous fatty acid oxidation and reduced fat storage in mice lacking acetyl-CoA carboxylase 2. *Science* **291,** 2613-6.

ADAMS, C. M. (2007). Role of the transcription factor ATF4 in the anabolic actions of insulin and the anti-anabolic actions of glucocorticoids. *J Biol Chem* **282,** 16744-53.

ADAMS, J. M., 2ND, PRATIPANAWATR, T., BERRIA, R., WANG, E., DEFRONZO, R. A., SULLARDS, M. C. & MANDARINO, L. J. (2004). Ceramide content is increased in skeletal muscle from obese insulin-resistant humans. *Diabetes* **53,** 25-31.

ADCOCK, I. M. (2000). Molecular mechanisms of glucocorticosteroid actions. *Pulm Pharmacol Ther* **13,** 115-26.

AGUIRRE, V., UCHIDA, T., YENUSH, L., DAVIS, R. & WHITE, M. F. (2000). The c-Jun NH(2)-terminal kinase promotes insulin resistance during association with insulin receptor substrate-1 and phosphorylation of Ser(307). *J Biol Chem* **275,** 9047-54.

AGUIRRE, V., WERNER, E. D., GIRAUD, J., LEE, Y. H., SHOELSON, S. E. & WHITE, M. F. (2002). Phosphorylation of Ser307 in insulin receptor substrate-1 blocks interactions with the insulin receptor and inhibits insulin action. *J Biol Chem* **277,** 1531-7.

ALBERTI, K. G. & ZIMMET, P. Z. (1998). Definition, diagnosis and classification of diabetes mellitus and its complications. Part 1: diagnosis and classification of diabetes mellitus provisional report of a WHO consultation. *Diabet Med* **15,** 539-53.

ALBERTS, P., ENGBLOM, L., EDLING, N., FORSGREN, M., KLINGSTROM, G., LARSSON, C., RONQUIST-NII, Y., OHMAN, B. & ABRAHMSEN, L. (2002). Selective inhibition of 11beta-hydroxysteroid dehydrogenase type 1 decreases blood glucose concentrations in hyperglycaemic mice. *Diabetologia* **45,** 1528-32.

ALBERTS, P., NILSSON, C., SELEN, G., ENGBLOM, L. O., EDLING, N. H., NORLING, S., KLINGSTROM, G., LARSSON, C., FORSGREN, M., ASHKZARI, M., NILSSON, C. E., FIEDLER, M., BERGQVIST, E., OHMAN, B., BJORKSTRAND, E. & ABRAHMSEN, L. B. (2003). Selective inhibition of 11 beta-hydroxysteroid dehydrogenase type 1 improves hepatic insulin sensitivity in hyperglycemic mice strains. *Endocrinology* **144,** 4755-62.

ALESSI, D. R., JAMES, S. R., DOWNES, C. P., HOLMES, A. B., GAFFNEY, P. R., REESE, C. B. & COHEN, P. (1997). Characterization of a 3-phosphoinositide-dependent protein kinase which phosphorylates and activates protein kinase Balpha. *Curr Biol* **7,** 261-9.

ALESSI, M. C., BASTELICA, D., MORANGE, P., BERTHET, B., LEDUC, I., VERDIER, M., GEEL, O. & JUHAN-VAGUE, I. (2000). Plasminogen activator inhibitor 1,

transforming growth factor-beta1, and BMI are closely associated in human adipose tissue during morbid obesity. *Diabetes* **49,** 1374-80.

ALTSHULER, D., HIRSCHHORN, J. N., KLANNEMARK, M., LINDGREN, C. M., VOHL, M. C., NEMESH, J., LANE, C. R., SCHAFFNER, S. F., BOLK, S., BREWER, C., TUOMI, T., GAUDET, D., HUDSON, T. J., DALY, M., GROOP, L. & LANDER, E. S. (2000). The common PPARgamma Pro12Ala polymorphism is associated with decreased risk of type 2 diabetes. *Nat Genet* **26,** 76-80.

AMTHOR, H., CHRIST, B. & PATEL, K. (1999). A molecular mechanism enabling continuous embryonic muscle growth - a balance between proliferation and differentiation. *Development* **126,** 1041-53.

ANDERSEN, A. S., KJELDSEN, T., WIBERG, F. C., VISSING, H., SCHAFFER, L., RASMUSSEN, J. S., DE MEYTS, P. & MOLLER, N. P. (1992). Identification of determinants that confer ligand specificity on the insulin receptor. *J Biol Chem* **267,** 13681-6.

ANDREWS, R. C., ROOYACKERS, O. & WALKER, B. R. (2003). Effects of the 11 beta-hydroxysteroid dehydrogenase inhibitor carbenoxolone on insulin sensitivity in men with type 2 diabetes. *J Clin Endocrinol Metab* **88,** 285-91.

ARAKI, E., LIPES, M. A., PATTI, M. E., BRUNING, J. C., HAAG, B., 3RD, JOHNSON, R. S. & KAHN, C. R. (1994). Alternative pathway of insulin signalling in mice with targeted disruption of the IRS-1 gene. *Nature* **372,** 186-90.

ARITA, Y., KIHARA, S., OUCHI, N., TAKAHASHI, M., MAEDA, K., MIYAGAWA, J., HOTTA, K., SHIMOMURA, I., NAKAMURA, T., MIYAOKA, K., KURIYAMA, H., NISHIDA, M., YAMASHITA, S., OKUBO, K., MATSUBARA, K., MURAGUCHI, M., OHMOTO, Y., FUNAHASHI, T. & MATSUZAWA, Y. (1999). Paradoxical decrease of an adipose-specific protein, adiponectin, in obesity. *Biochem Biophys Res Commun* **257,** 79-83.

ARIYOSHI, N., KIM, Y. C., ARTEMENKO, I., BHATTACHARYYA, K. K. & JEFCOATE, C. R. (1998). Characterization of the rat Star gene that encodes the predominant 3.5-kilobase pair mRNA. ACTH stimulation of adrenal steroids in vivo precedes elevation of Star mRNA and protein. *J Biol Chem* **273,** 7610-9.

ARLT, W. & STEWART, P. M. (2005). Adrenal corticosteroid biosynthesis, metabolism, and action. *Endocrinol Metab Clin North Am* **34,** 293-313, viii.

ARRIZA, J. L., WEINBERGER, C., CERELLI, G., GLASER, T. M., HANDELIN, B. L., HOUSMAN, D. E. & EVANS, R. M. (1987). Cloning of human mineralocorticoid receptor complementary DNA: structural and functional kinship with the glucocorticoid receptor. *Science* **237,** 268-75.

ASHBY, P. & ROBINSON, D. S. (1980). Effects of insulin, glucocorticoids and adrenaline on the activity of rat adipose-tissue lipoprotein lipids. *Biochem J* **188,** 185-92.

ASHCROFT, F. M. & RORSMAN, P. (1989). Electrophysiology of the pancreatic beta-cell. *Prog Biophys Mol Biol* **54,** 87-143.

ATPIII. (2001). Executive Summary of The Third Report of The National Cholesterol Education Program (NCEP) Expert Panel on Detection, Evaluation, And Treatment of High Blood Cholesterol In Adults (Adult Treatment Panel III). *Jama* **285,** 2486-97.

AUBRY, E. M. & ODERMATT, A. (2009). Retinoic acid reduces glucocorticoid sensitivity in C2C12 myotubes by decreasing 11beta-hydroxysteroid dehydrogenase type 1 and glucocorticoid receptor activities. *Endocrinology* **150,** 2700-8.

BAJAJ, M., WATERFIELD, M. D., SCHLESSINGER, J., TAYLOR, W. R. & BLUNDELL, T.

(1987). On the tertiary structure of the extracellular domains of the epidermal growth factor and insulin receptors. *Biochim Biophys Acta* **916,** 220-6.

BALTZAN, M. A., ANDRES, R., CADER, G. & ZIERLER, K. L. (1962). Heterogeneity of forearm metabolism with special reference to free fatty acids. *J Clin Invest* **41,** 116-25.

BANERJEE, R. R., RANGWALA, S. M., SHAPIRO, J. S., RICH, A. S., RHOADES, B., QI, Y., WANG, J., RAJALA, M. W., POCAI, A., SCHERER, P. E., STEPPAN, C. M., AHIMA, R. S., OBICI, S., ROSSETTI, L. & LAZAR, M. A. (2004). Regulation of fasted blood glucose by resistin. *Science* **303,** 1195-8.

BAQUE, S., ROCA, A., GUINOVART, J. J. & GOMEZ-FOIX, A. M. (1996). Direct activating effects of dexamethasone on glycogen metabolizing enzymes in primary cultured rat hepatocytes. *Eur J Biochem* **236,** 772-7.

BARF, T., VALLGARDA, J., EMOND, R., HAGGSTROM, C., KURZ, G., NYGREN, A., LARWOOD, V., MOSIALOU, E., AXELSSON, K., OLSSON, R., ENGBLOM, L., EDLING, N., RONQUIST-NII, Y., OHMAN, B., ALBERTS, P. & ABRAHMSEN, L. (2002). Arylsulfonamidothiazoles as a new class of potential antidiabetic drugs. Discovery of potent and selective inhibitors of the 11beta-hydroxysteroid dehydrogenase type 1. *J Med Chem* **45,** 3813-5.

BARTHEL, A., SCHMOLL, D., KRUGER, K. D., BAHRENBERG, G., WALTHER, R., ROTH, R. A. & JOOST, H. G. (2001). Differential regulation of endogenous glucose-6-phosphatase and phosphoenolpyruvate carboxykinase gene expression by the forkhead transcription factor FKHR in H4IIE-hepatoma cells. *Biochem Biophys Res Commun* **285,** 897-902.

BASTARD, J. P., JARDEL, C., BRUCKERT, E., BLONDY, P., CAPEAU, J., LAVILLE, M., VIDAL, H. & HAINQUE, B. (2000). Elevated levels of interleukin 6 are reduced in serum and subcutaneous adipose tissue of obese women after weight loss. *J Clin Endocrinol Metab* **85,** 3338-42.

BECKER, K. L., BILEZIKIAN, J. P., BREMNER, W. J. & HUNG, W. (2001). *Principles and Practice of Endocrinology and Metabolism*, 3 edition.

BERTHIAUME, M., LAPLANTE, M., FESTUCCIA, W., GELINAS, Y., POULIN, S., LALONDE, J., JOANISSE, D. R., THIERINGER, R. & DESHAIES, Y. (2007a). Depot-specific modulation of rat intraabdominal adipose tissue lipid metabolism by pharmacological inhibition of 11beta-hydroxysteroid dehydrogenase type 1. *Endocrinology* **148,** 2391-7.

BERTHIAUME, M., LAPLANTE, M., FESTUCCIA, W. T., BERGER, J. P., THIERINGER, R. & DESHAIES, Y. (2009). Additive action of 11beta-HSD1 inhibition and PPAR-gamma agonism on hepatic steatosis and triglyceridemia in diet-induced obese rats. *Int J Obes (Lond)* **33,** 601-4.

BERTHIAUME, M., LAPLANTE, M., FESTUCCIA, W. T., CIANFLONE, K., TURCOTTE, L. P., JOANISSE, D. R., OLIVECRONA, G., THIERINGER, R. & DESHAIES, Y. (2007b). 11beta-HSD1 inhibition improves triglyceridemia through reduced liver VLDL secretion and partitions lipids toward oxidative tissues. *Am J Physiol Endocrinol Metab* **293,** E1045-52.

BHAT, B. G., HOSEA, N., FANJUL, A., HERRERA, J., CHAPMAN, J., THALACKER, F., STEWART, P. M. & REJTO, P. A. (2008). Demonstration of proof of mechanism and pharmacokinetics and pharmacodynamic relationship with 4'-cyano-biphenyl-4-sulfonic acid (6-amino-pyridin-2-yl)-amide (PF-915275), an inhibitor of 11 -hydroxysteroid dehydrogenase type 1, in cynomolgus monkeys. *J Pharmacol Exp Ther* **324,** 299-305.

BICKERTON, A. S., ROBERTS, R., FIELDING, B. A., HODSON, L., BLAAK, E. E., WAGENMAKERS, A. J., GILBERT, M., KARPE, F. & FRAYN, K. N. (2007). Preferential uptake of dietary Fatty acids in adipose tissue and muscle in the postprandial period. *Diabetes* **56,** 168-76.

BINAS, B., HAN, X. X., EROL, E., LUIKEN, J. J., GLATZ, J. F., DYCK, D. J., MOTAZAVI, R., ADIHETTY, P. J., HOOD, D. A. & BONEN, A. (2003). A null mutation in H-FABP only partially inhibits skeletal muscle fatty acid metabolism. *Am J Physiol Endocrinol Metab* **285,** E481-9.

BLAU, H. M., PAVLATH, G. K., HARDEMAN, E. C., CHIU, C. P., SILBERSTEIN, L., WEBSTER, S. G., MILLER, S. C. & WEBSTER, C. (1985). Plasticity of the differentiated state. *Science* **230,** 758-66.

BLOCK, N. E. & BUSE, M. G. (1989). Effects of hypercortisolemia and diabetes on skeletal muscle insulin receptor function in vitro and in vivo. *Am J Physiol* **256,** E39-48.

BOCZAN, J., BOROS, S., MECHLER, F., KOVACS, L. & BIRO, T. (2000). Differential expressions of protein kinase C isozymes during proliferation and differentiation of human skeletal muscle cells in vitro. *Acta Neuropathol* **99,** 96-104.

BODINE, S. C., LATRES, E., BAUMHUETER, S., LAI, V. K., NUNEZ, L., CLARKE, B. A., POUEYMIROU, W. T., PANARO, F. J., NA, E., DHARMARAJAN, K., PAN, Z. Q., VALENZUELA, D. M., DECHIARA, T. M., STITT, T. N., YANCOPOULOS, G. D. & GLASS, D. J. (2001). Identification of ubiquitin ligases required for skeletal muscle atrophy. *Science* **294,** 1704-8.

BOKVIST, K., ELIASSON, L., AMMALA, C., RENSTROM, E. & RORSMAN, P. (1995). Co-localization of L-type Ca2+ channels and insulin-containing secretory granules and its significance for the initiation of exocytosis in mouse pancreatic B-cells. *Embo J* **14,** 50-7.

BONEN, A., LUIKEN, J. J., ARUMUGAM, Y., GLATZ, J. F. & TANDON, N. N. (2000). Acute regulation of fatty acid uptake involves the cellular redistribution of fatty acid translocase. *J Biol Chem* **275,** 14501-8.

BONEN, A., MISKOVIC, D. & KIENS, B. (1999). Fatty acid transporters (FABPpm, FAT, FATP) in human muscle. *Can J Appl Physiol* **24,** 515-23.

BORYCKI, A. G., LI, J., JIN, F., EMERSON, C. P. & EPSTEIN, J. A. (1999). Pax3 functions in cell survival and in pax7 regulation. *Development* **126,** 1665-74.

BOTTINELLI, R. & REGGIANI, C. (2000). Human skeletal muscle fibres: molecular and functional diversity. *Prog Biophys Mol Biol* **73,** 195-262.

BOUZAKRI, K., KARLSSON, H. K., VESTERGAARD, H., MADSBAD, S., CHRISTIANSEN, E. & ZIERATH, J. R. (2006). IRS-1 serine phosphorylation and insulin resistance in skeletal muscle from pancreas transplant recipients. *Diabetes* **55,** 785-91.

BOUZAKRI, K., ROQUES, M., GUAL, P., ESPINOSA, S., GUEBRE-EGZIABHER, F., RIOU, J. P., LAVILLE, M., LE MARCHAND-BRUSTEL, Y., TANTI, J. F. & VIDAL, H. (2003). Reduced activation of phosphatidylinositol-3 kinase and increased serine 636 phosphorylation of insulin receptor substrate-1 in primary culture of skeletal muscle cells from patients with type 2 diabetes. *Diabetes* **52,** 1319-25.

BOYD, G. S. & TRZECIAK, W. H. (1973). Cholesterol metabolism in the adrenal cortex: studies on the mode of action of ACTH. *Ann N Y Acad Sci* **212,** 361-77.

BROOKS, S. V. (2003). Current topics for teaching skeletal muscle physiology. *Adv Physiol Educ* **27,** 171-82.

BROWN, P. D., BADAL, S., MORRISON, S. & RAGOOBIRSINGH, D. (2007). Acute impairment of insulin signalling by dexamethasone in primary cultured rat skeletal myocytes. *Mol Cell Biochem* **297,** 171-7.

BROWN, R. W., DIAZ, R., ROBSON, A. C., KOTELEVTSEV, Y. V., MULLINS, J. J., KAUFMAN, M. H. & SECKL, J. R. (1996). The ontogeny of 11 beta-hydroxysteroid dehydrogenase type 2 and mineralocorticoid receptor gene expression reveal intricate control of glucocorticoid action in development. *Endocrinology* **137,** 794-7.

BUJALSKA, I. J., DRAPER, N., MICHAILIDOU, Z., TOMLINSON, J. W., WHITE, P. C., CHAPMAN, K. E., WALKER, E. A. & STEWART, P. M. (2005). Hexose-6-phosphate dehydrogenase confers oxo-reductase activity upon 11 beta-hydroxysteroid dehydrogenase type 1. *J Mol Endocrinol* **34,** 675-84.

BUJALSKA, I. J., HEWITT, K. N., HAUTON, D., LAVERY, G. G., TOMLINSON, J. W., WALKER, E. A. & STEWART, P. M. (2008). Lack of hexose-6-phosphate dehydrogenase impairs lipid mobilization from mouse adipose tissue. *Endocrinology* **149,** 2584-91.

BUJALSKA, I. J., KUMAR, S. & STEWART, P. M. (1997). Does central obesity reflect "Cushing's disease of the omentum"? *Lancet* **349,** 1210-3.

CAI, D., DHE-PAGANON, S., MELENDEZ, P. A., LEE, J. & SHOELSON, S. E. (2003). Two new substrates in insulin signaling, IRS5/DOK4 and IRS6/DOK5. *J Biol Chem* **278,** 25323-30.

CANN, A. D. & KOHANSKI, R. A. (1997). Cis-autophosphorylation of juxtamembrane tyrosines in the insulin receptor kinase domain. *Biochemistry* **36,** 7681-9.

CARLING, D., CLARKE, P. R., ZAMMIT, V. A. & HARDIE, D. G. (1989). Purification and characterization of the AMP-activated protein kinase. Copurification of acetyl-CoA carboxylase kinase and 3-hydroxy-3-methylglutaryl-CoA reductase kinase activities. *Eur J Biochem* **186,** 129-36.

CARLSON, C. J., WHITE, M. F. & RONDINONE, C. M. (2004). Mammalian target of rapamycin regulates IRS-1 serine 307 phosphorylation. *Biochem Biophys Res Commun* **316,** 533-9.

CATALANO, R. D., STUVE, L. & RAMACHANDRAN, J. (1986). Characterization of corticotropin receptors in human adrenocortical cells. *J Clin Endocrinol Metab* **62,** 300-4.

CHABOWSKI, A., COORT, S. L., CALLES-ESCANDON, J., TANDON, N. N., GLATZ, J. F., LUIKEN, J. J. & BONEN, A. (2004). Insulin stimulates fatty acid transport by regulating expression of FAT/CD36 but not FABPpm. *Am J Physiol Endocrinol Metab* **287,** E781-9.

CHALKLEY, S. M., HETTIARACHCHI, M., CHISHOLM, D. J. & KRAEGEN, E. W. (1998). Five-hour fatty acid elevation increases muscle lipids and impairs glycogen synthesis in the rat. *Metabolism* **47,** 1121-6.

CHEN, F., WATSON, C. S. & GAMETCHU, B. (1999). Association of the glucocorticoid receptor alternatively-spliced transcript 1A with the presence of the high molecular weight membrane glucocorticoid receptor in mouse lymphoma cells. *J Cell Biochem* **74,** 430-46.

CHEN, M. T., KAUFMAN, L. N., SPENNETTA, T. & SHRAGO, E. (1992). Effects of high fat-feeding to rats on the interrelationship of body weight, plasma insulin, and fatty acyl-coenzyme A esters in liver and skeletal muscle. *Metabolism* **41,** 564-9.

CHIASSON, J. L., DIETZ, M. R., SHIKAMA, H., WOOTTEN, M. & EXTON, J. H. (1980). Insulin regulation of skeletal muscle glycogen metabolism. *Am J Physiol* **239,** E69-74.

CHIASSON, J. L., LILJENQUIST, J. E., FINGER, F. E. & LACY, W. W. (1976). Differential sensitivity of glycogenolysis and gluconeogenesis to insulin infusions in dogs. *Diabetes* **25,** 283-91.

CHIBALIN, A. V., LENG, Y., VIEIRA, E., KROOK, A., BJORNHOLM, M., LONG, Y. C., KOTOVA, O., ZHONG, Z., SAKANE, F., STEILER, T., NYLEN, C., WANG, J., LAAKSO, M., TOPHAM, M. K., GILBERT, M., WALLBERG-HENRIKSSON, H. & ZIERATH, J. R. (2008). Downregulation of diacylglycerol kinase delta contributes to hyperglycemia-induced insulin resistance. *Cell* **132,** 375-86.

CHIN, J. E., LIU, F. & ROTH, R. A. (1994). Activation of protein kinase C alpha inhibits insulin-stimulated tyrosine phosphorylation of insulin receptor substrate-1. *Mol Endocrinol* **8,** 51-8.

CHISHOLM, D. J., YOUNG, J. D. & LAZARUS, L. (1969). The gastrointestinal stimulus to insulin release. I. Secretin. *J Clin Invest* **48,** 1453-60.

CHOMCZYNSKI, P. & SACCHI, N. (1987). Single-step method of RNA isolation by acid guanidinium thiocyanate-phenol-chloroform extraction. *Anal Biochem* **162,** 156-9.

CHRIST, B. & ORDAHL, C. P. (1995). Early stages of chick somite development. *Anat Embryol (Berl)* **191,** 381-96.

CHU, J. W. & KIMURA, T. (1973). Studies on adrenal steroid hydroxylases. Molecular and catalytic properties of adrenodoxin reductase (a flavoprotein). *J Biol Chem* **248,** 2089-94.

CINNAMON, Y., KAHANE, N., BACHELET, I. & KALCHEIM, C. (2001). The sub-lip domain--a distinct pathway for myotome precursors that demonstrate rostral-caudal migration. *Development* **128,** 341-51.

CLARK, B. J., RANGANATHAN, V. & COMBS, R. (2000). Post-translational regulation of steroidogenic acute regulatory protein by cAMP-dependent protein kinase A. *Endocr Res* **26,** 681-9.

CLARK, B. J., SOO, S. C., CARON, K. M., IKEDA, Y., PARKER, K. L. & STOCCO, D. M. (1995). Hormonal and developmental regulation of the steroidogenic acute regulatory protein. *Mol Endocrinol* **9,** 1346-55.

CONSITT, L. A., BELL, J. A. & HOUMARD, J. A. (2009). Intramuscular lipid metabolism, insulin action, and obesity. *IUBMB Life* **61,** 47-55.

COOK, K. G., YEAMAN, S. J., STRALFORS, P., FREDRIKSON, G. & BELFRAGE, P. (1982). Direct evidence that cholesterol ester hydrolase from adrenal cortex is the same enzyme as hormone-sensitive lipase from adipose tissue. *Eur J Biochem* **125,** 245-9.

COOKE, B. A. (1999). Signal transduction involving cyclic AMP-dependent and cyclic AMP-independent mechanisms in the control of steroidogenesis. *Mol Cell Endocrinol* **151,** 25-35.

COPPACK, S. W., PERSSON, M., JUDD, R. L. & MILES, J. M. (1999). Glycerol and nonesterified fatty acid metabolism in human muscle and adipose tissue in vivo. *Am J Physiol* **276,** E233-40.

CORBOULD, A., KIM, Y. B., YOUNGREN, J. F., PENDER, C., KAHN, B. B., LEE, A. & DUNAIF, A. (2005). Insulin resistance in the skeletal muscle of women with PCOS involves intrinsic and acquired defects in insulin signaling. *Am J Physiol Endocrinol Metab* **288,** E1047-54.

CORPELEIJN, E., PELSERS, M. M., SOENEN, S., MENSINK, M., BOUWMAN, F. G., KOOI,

M. E., SARIS, W. H., GLATZ, J. F. & BLAAK, E. E. (2008). Insulin acutely upregulates protein expression of the fatty acid transporter CD36 in human skeletal muscle in vivo. *J Physiol Pharmacol* **59,** 77-83.

COURTNEY, R., STEWART, P. M., TOH, M., NDONGO, M. N., CALLE, R. A. & HIRSHBERG, B. (2008). Modulation of 11beta-hydroxysteroid dehydrogenase (11betaHSD) activity biomarkers and pharmacokinetics of PF-00915275, a selective 11betaHSD1 inhibitor. *J Clin Endocrinol Metab* **93,** 550-6.

CROXTALL, J. D., CHOUDHURY, Q. & FLOWER, R. J. (2000). Glucocorticoids act within minutes to inhibit recruitment of signalling factors to activated EGF receptors through a receptor-dependent, transcription-independent mechanism. *Br J Pharmacol* **130,** 289-98.

CROXTALL, J. D., VAN HAL, P. T., CHOUDHURY, Q., GILROY, D. W. & FLOWER, R. J. (2002). Different glucocorticoids vary in their genomic and non-genomic mechanism of action in A549 cells. *Br J Pharmacol* **135,** 511-9.

CRUZ, M. L., WEIGENSBERG, M. J., HUANG, T. T., BALL, G., SHAIBI, G. Q. & GORAN, M. I. (2004). The metabolic syndrome in overweight Hispanic youth and the role of insulin sensitivity. *J Clin Endocrinol Metab* **89,** 108-13.

CURRY, D. L., BENNETT, L. L. & GRODSKY, G. M. (1968). Requirement for calcium ion in insulin secretion by the perfused rat pancreas. *Am J Physiol* **214,** 174-8.

CUSHING, H. (1913). *The Pituitary Body and Its Disorders*.

CZECH, M. P. & CORVERA, S. (1999). Signaling mechanisms that regulate glucose transport. *J Biol Chem* **274,** 1865-8.

CZERWINSKI, S. M., MARTIN, J. M. & BECHTEL, P. J. (1994). Modulation of IGF mRNA abundance during stretch-induced skeletal muscle hypertrophy and regression. *J Appl Physiol* **76,** 2026-30.

D'ALESSANDRIS, C., LAURO, R., PRESTA, I. & SESTI, G. (2007). C-reactive protein induces phosphorylation of insulin receptor substrate-1 on Ser307 and Ser 612 in L6 myocytes, thereby impairing the insulin signalling pathway that promotes glucose transport. *Diabetologia* **50,** 840-9.

DA SILVA XAVIER, G., LODER, M. K., MCDONALD, A., TARASOV, A. I., CARZANIGA, R., KRONENBERGER, K., BARG, S. & RUTTER, G. A. (2009). TCF7L2 regulates late events in insulin secretion from pancreatic islet beta-cells. *Diabetes* **58,** 894-905.

DANIELSSON, A., NYSTROM, F. H. & STRALFORS, P. (2006). Phosphorylation of IRS1 at serine 307 and serine 312 in response to insulin in human adipocytes. *Biochem Biophys Res Commun* **342,** 1183-7.

DASTON, G., LAMAR, E., OLIVIER, M. & GOULDING, M. (1996). Pax-3 is necessary for migration but not differentiation of limb muscle precursors in the mouse. *Development* **122,** 1017-27.

DE ALVARO, C., TERUEL, T., HERNANDEZ, R. & LORENZO, M. (2004). Tumor necrosis factor alpha produces insulin resistance in skeletal muscle by activation of inhibitor kappaB kinase in a p38 MAPK-dependent manner. *J Biol Chem* **279,** 17070-8.

DE MARCO, R., LOCATELLI, F., ZOPPINI, G., VERLATO, G., BONORA, E. & MUGGEO, M. (1999). Cause-specific mortality in type 2 diabetes. The Verona Diabetes Study. *Diabetes Care* **22,** 756-61.

DEFRONZO, R. A., JACOT, E., JEQUIER, E., MAEDER, E., WAHREN, J. & FELBER, J. P. (1981). The effect of insulin on the disposal of intravenous glucose.

Results from indirect calorimetry and hepatic and femoral venous catheterization. *Diabetes* **30,** 1000-7.

DEGERMAN, E., LANDSTROM, T. R., WIJKANDER, J., HOLST, L. S., AHMAD, F., BELFRAGE, P. & MANGANIELLO, V. (1998). Phosphorylation and activation of hormone-sensitive adipocyte phosphodiesterase type 3B. *Methods* **14,** 43-53.

DIABETOLOGIAWAGMAN, A. S. & JENSEN, J. (2005). Glucocorticoid-induced insulin resistance in skeletal muscles: defects in insulin signalling and the effects of a selective glycogen synthase kinase-3 inhibitor. *Diabetologia* **48,** 2119-30.

DIMITRIADIS, G., LEIGHTON, B., PARRY-BILLINGS, M., SASSON, S., YOUNG, M., KRAUSE, U., BEVAN, S., PIVA, T., WEGENER, G. & NEWSHOLME, E. A. (1997). Effects of glucocorticoid excess on the sensitivity of glucose transport and metabolism to insulin in rat skeletal muscle. *Biochem J* **321 (Pt 3),** 707-12.

DIVAKARAN, P. & FRIEDMANN, N. (1976). A fast in vitro effect of glucocorticoids on hepatic lipolysis. *Endocrinology* **98,** 1550-3.

DJURHUUS, C. B., GRAVHOLT, C. H., NIELSEN, S., PEDERSEN, S. B., MOLLER, N. & SCHMITZ, O. (2004). Additive effects of cortisol and growth hormone on regional and systemic lipolysis in humans. *Am J Physiol Endocrinol Metab* **286,** E488-94.

DOLINSKY, V. W., DOUGLAS, D. N., LEHNER, R. & VANCE, D. E. (2004). Regulation of the enzymes of hepatic microsomal triacylglycerol lipolysis and re-esterification by the glucocorticoid dexamethasone. *Biochem J* **378,** 967-74.

DONSMARK, M., LANGFORT, J., HOLM, C., PLOUG, T. & GALBO, H. (2003). Contractions activate hormone-sensitive lipase in rat muscle by protein kinase C and mitogen-activated protein kinase. *J Physiol* **550,** 845-54.

DONSMARK, M., LANGFORT, J., HOLM, C., PLOUG, T. & GALBO, H. (2004). Contractions induce phosphorylation of the AMPK site Ser565 in hormone-sensitive lipase in muscle. *Biochem Biophys Res Commun* **316,** 867-71.

DYCK, D. J., STEINBERG, G. & BONEN, A. (2001). Insulin increases FA uptake and esterification but reduces lipid utilization in isolated contracting muscle. *Am J Physiol Endocrinol Metab* **281,** E600-7.

EDWARDS, C. R., STEWART, P. M., BURT, D., BRETT, L., MCINTYRE, M. A., SUTANTO, W. S., DE KLOET, E. R. & MONDER, C. (1988). Localisation of 11 beta-hydroxysteroid dehydrogenase--tissue specific protector of the mineralocorticoid receptor. *Lancet* **2,** 986-9.

EFENDIC, S., GRILL, V., LUFT, R. & WAJNGOT, A. (1988). Low insulin response: a marker of prediabetes. *Adv Exp Med Biol* **246,** 167-74.

EHTISHAM, S., HATTERSLEY, A. T., DUNGER, D. B. & BARRETT, T. G. (2004). First UK survey of paediatric type 2 diabetes and MODY. *Arch Dis Child* **89,** 526-9.

ELSAS, L. J., ALBRECHT, I. & ROSENBERG, L. E. (1968). Insulin stimulation of amino acid uptake in rat diaphragm. Relationship to protein sythesis. *J Biol Chem* **243,** 1846-53.

ENGERT, J. C., BERGLUND, E. B. & ROSENTHAL, N. (1996). Proliferation precedes differentiation in IGF-I-stimulated myogenesis. *J Cell Biol* **135,** 431-40.

ENOKSSON, S., DEGERMAN, E., HAGSTROM-TOFT, E., LARGE, V. & ARNER, P. (1998). Various phosphodiesterase subtypes mediate the in vivo antilipolytic effect of insulin on adipose tissue and skeletal muscle in man. *Diabetologia* **41,** 560-8.

ESPOSITO, D. L., LI, Y., CAMA, A. & QUON, M. J. (2001). Tyr(612) and Tyr(632) in human insulin receptor substrate-1 are important for full activation of insulin-stimulated phosphatidylinositol 3-kinase activity and translocation of GLUT4 in adipose cells. *Endocrinology* **142,** 2833-40.

ESTEBAN, N. V., LOUGHLIN, T., YERGEY, A. L., ZAWADZKI, J. K., BOOTH, J. D., WINTERER, J. C. & LORIAUX, D. L. (1991). Daily cortisol production rate in man determined by stable isotope dilution/mass spectrometry. *J Clin Endocrinol Metab* **72,** 39-45.

FALDUTO, M. T., HICKSON, R. C. & YOUNG, A. P. (1989). Antagonism by glucocorticoids and exercise on expression of glutamine synthetase in skeletal muscle. *Faseb J* **3,** 2623-8.

FANTIN, V. R., SPARLING, J. D., SLOT, J. W., KELLER, S. R., LIENHARD, G. E. & LAVAN, B. E. (1998). Characterization of insulin receptor substrate 4 in human embryonic kidney 293 cells. *J Biol Chem* **273,** 10726-32.

FANTIN, V. R., WANG, Q., LIENHARD, G. E. & KELLER, S. R. (2000). Mice lacking insulin receptor substrate 4 exhibit mild defects in growth, reproduction, and glucose homeostasis. *Am J Physiol Endocrinol Metab* **278,** E127-33.

FARESE, R. V. (2002). Function and dysfunction of aPKC isoforms for glucose transport in insulin-sensitive and insulin-resistant states. *Am J Physiol Endocrinol Metab* **283,** E1-11.

FERNANDEZ-REAL, J. M., PUGEAT, M., GRASA, M., BROCH, M., VENDRELL, J., BRUN, J. & RICART, W. (2002). Serum corticosteroid-binding globulin concentration and insulin resistance syndrome: a population study. *J Clin Endocrinol Metab* **87,** 4686-90.

FINK, B., THANZAMI, V., SEYDEL, H. & MANNING, J. T. (2006). Digit ratio and hand-grip strength in German and Mizos men: cross-cultural evidence for an organizing effect of prenatal testosterone on strength. *Am J Hum Biol* **18,** 776-82.

FISCHER, H., GUSTAFSSON, T., SUNDBERG, C. J., NORRBOM, J., EKMAN, M., JOHANSSON, O. & JANSSON, E. (2006). Fatty acid binding protein 4 in human skeletal muscle. *Biochem Biophys Res Commun* **346,** 125-30.

FLORINI, J. R., MAGRI, K. A., EWTON, D. Z., JAMES, P. L., GRINDSTAFF, K. & ROTWEIN, P. S. (1991). "Spontaneous" differentiation of skeletal myoblasts is dependent upon autocrine secretion of insulin-like growth factor-II. *J Biol Chem* **266,** 15917-23.

FLOYD, J. C., JR., FAJANS, S. S., CONN, J. W., KNOPF, R. F. & RULL, J. (1966). Stimulation of insulin secretion by amino acids. *J Clin Invest* **45,** 1487-502.

FORD, E. S., GILES, W. H. & DIETZ, W. H. (2002). Prevalence of the metabolic syndrome among US adults: findings from the third National Health and Nutrition Examination Survey. *Jama* **287,** 356-9.

FRIEDMAN, T. C., MASTORAKOS, G., NEWMAN, T. D., MULLEN, N. M., HORTON, E. G., COSTELLO, R., PAPADOPOULOS, N. M. & CHROUSOS, G. P. (1996). Carbohydrate and lipid metabolism in endogenous hypercortisolism: shared features with metabolic syndrome X and NIDDM. *Endocr J* **43,** 645-55.

FRITZ, I. B. & YUE, K. T. (1963). Long-Chain Carnitine Acyltransferase and the Role of Acylcarnitine Derivatives in the Catalytic Increase of Fatty Acid Oxidation Induced by Carnitine. *J Lipid Res* **4,** 279-88.

FRUEBIS, J., TSAO, T. S., JAVORSCHI, S., EBBETS-REED, D., ERICKSON, M. R., YEN, F. T., BIHAIN, B. E. & LODISH, H. F. (2001). Proteolytic cleavage product of 30-

kDa adipocyte complement-related protein increases fatty acid oxidation in muscle and causes weight loss in mice. *Proc Natl Acad Sci U S A* **98,** 2005-10.

GAILLARD, D., WABITSCH, M., PIPY, B. & NEGREL, R. (1991). Control of terminal differentiation of adipose precursor cells by glucocorticoids. *J Lipid Res* **32,** 569-79.

GAMETCHU, B., WATSON, C. S. & WU, S. (1993). Use of receptor antibodies to demonstrate membrane glucocorticoid receptor in cells from human leukemic patients. *Faseb J* **7,** 1283-92.

GAO, T., FURNARI, F. & NEWTON, A. C. (2005). PHLPP: a phosphatase that directly dephosphorylates Akt, promotes apoptosis, and suppresses tumor growth. *Mol Cell* **18,** 13-24.

GAO, Z., HWANG, D., BATAILLE, F., LEFEVRE, M., YORK, D., QUON, M. J. & YE, J. (2002). Serine phosphorylation of insulin receptor substrate 1 by inhibitor kappa B kinase complex. *J Biol Chem* **277,** 48115-21.

GAO, Z., ZHANG, X., ZUBERI, A., HWANG, D., QUON, M. J., LEFEVRE, M. & YE, J. (2004). Inhibition of insulin sensitivity by free fatty acids requires activation of multiple serine kinases in 3T3-L1 adipocytes. *Mol Endocrinol* **18,** 2024-34.

GARCIA-MARTINEZ, C., AGELL, N., LLOVERA, M., LOPEZ-SORIANO, F. J. & ARGILES, J. M. (1993). Tumour necrosis factor-alpha increases the ubiquitinization of rat skeletal muscle proteins. *FEBS Lett* **323,** 211-4.

GASTER, M. & BECK-NIELSEN, H. (2006). Triacylglycerol accumulation is not primarily affected in myotubes established from type 2 diabetic subjects. *Biochim Biophys Acta* **1761,** 100-10.

GATHERCOLE, L. L., BUJALSKA, I. J., STEWART, P. M. & TOMLINSON, J. W. (2007). Glucocorticoid modulation of insulin signaling in human subcutaneous adipose tissue. *J Clin Endocrinol Metab* **92,** 4332-9.

GEEVES, M. A. & HOLMES, K. C. (1999). Structural mechanism of muscle contraction. *Annu Rev Biochem* **68,** 687-728.

GELERNTER-YANIV, L., FENG, N., SEBRING, N. G., HOCHBERG, Z. & YANOVSKI, J. A. (2003). Associations between a polymorphism in the 11 beta hydroxysteroid dehydrogenase type I gene and body composition. *Int J Obes Relat Metab Disord* **27,** 983-6.

GERAGHTY, K. M., CHEN, S., HARTHILL, J. E., IBRAHIM, A. F., TOTH, R., MORRICE, N. A., VANDERMOERE, F., MOORHEAD, G. B., HARDIE, D. G. & MACKINTOSH, C. (2007). Regulation of multisite phosphorylation and 14-3-3 binding of AS160 in response to IGF-1, EGF, PMA and AICAR. *Biochem J* **407,** 231-41.

GERARD, J. (2005). [MODY types of diabetes mellitus]. *Rev Med Liege* **60,** 439-41.

GIBBONS, G. F., WIGGINS, D., BROWN, A. M. & HEBBACHI, A. M. (2004). Synthesis and function of hepatic very-low-density lipoprotein. *Biochem Soc Trans* **32,** 59-64.

GIGUERE, V., HOLLENBERG, S. M., ROSENFELD, M. G. & EVANS, R. M. (1986). Functional domains of the human glucocorticoid receptor. *Cell* **46,** 645-52.

GIORGETTI, S., BALLOTTI, R., KOWALSKI-CHAUVEL, A., TARTARE, S. & VAN OBBERGHEN, E. (1993). The insulin and insulin-like growth factor-I receptor substrate IRS-1 associates with and activates phosphatidylinositol 3-kinase in vitro. *J Biol Chem* **268,** 7358-64.

GIORGINO, F., ALMAHFOUZ, A., GOODYEAR, L. J. & SMITH, R. J. (1993). Glucocorticoid regulation of insulin receptor and substrate IRS-1 tyrosine phosphorylation in rat skeletal muscle in vivo. *J Clin Invest* **91,** 2020-30.

GIORGINO, F., PEDRINI, M. T., MATERA, L. & SMITH, R. J. (1997). Specific increase in p85alpha expression in response to dexamethasone is associated with inhibition of insulin-like growth factor-I stimulated phosphatidylinositol 3-kinase activity in cultured muscle cells. *J Biol Chem* **272,** 7455-63.

GIORGINO, F. & SMITH, R. J. (1995). Dexamethasone enhances insulin-like growth factor-I effects on skeletal muscle cell proliferation. Role of specific intracellular signaling pathways. *J Clin Invest* **96,** 1473-83.

GLOYN, A. L., PEARSON, E. R., ANTCLIFF, J. F., PROKS, P., BRUINING, G. J., SLINGERLAND, A. S., HOWARD, N., SRINIVASAN, S., SILVA, J. M., MOLNES, J., EDGHILL, E. L., FRAYLING, T. M., TEMPLE, I. K., MACKAY, D., SHIELD, J. P., SUMNIK, Z., VAN RHIJN, A., WALES, J. K., CLARK, P., GORMAN, S., AISENBERG, J., ELLARD, S., NJOLSTAD, P. R., ASHCROFT, F. M. & HATTERSLEY, A. T. (2004). Activating mutations in the gene encoding the ATP-sensitive potassium-channel subunit Kir6.2 and permanent neonatal diabetes. *N Engl J Med* **350,** 1838-49.

GLOYN, A. L., WEEDON, M. N., OWEN, K. R., TURNER, M. J., KNIGHT, B. A., HITMAN, G., WALKER, M., LEVY, J. C., SAMPSON, M., HALFORD, S., MCCARTHY, M. I., HATTERSLEY, A. T. & FRAYLING, T. M. (2003). Large-scale association studies of variants in genes encoding the pancreatic beta-cell KATP channel subunits Kir6.2 (KCNJ11) and SUR1 (ABCC8) confirm that the KCNJ11 E23K variant is associated with type 2 diabetes. *Diabetes* **52,** 568-72.

GOMES, M. D., LECKER, S. H., JAGOE, R. T., NAVON, A. & GOLDBERG, A. L. (2001). Atrogin-1, a muscle-specific F-box protein highly expressed during muscle atrophy. *Proc Natl Acad Sci U S A* **98,** 14440-5.

GONZALEZ-BARO, M. R., LEWIN, T. M. & COLEMAN, R. A. (2007). Regulation of Triglyceride Metabolism. II. Function of mitochondrial GPAT1 in the regulation of triacylglycerol biosynthesis and insulin action. *Am J Physiol Gastrointest Liver Physiol* **292,** G1195-9.

GOUNARIDES, J. S., KORACH-ANDRE, M., KILLARY, K., ARGENTIERI, G., TURNER, O. & LAURENT, D. (2008). Effect of dexamethasone on glucose tolerance and fat metabolism in a diet-induced obesity mouse model. *Endocrinology* **149,** 758-66.

GRANT, S. F., THORLEIFSSON, G., REYNISDOTTIR, I., BENEDIKTSSON, R., MANOLESCU, A., SAINZ, J., HELGASON, A., STEFANSSON, H., EMILSSON, V., HELGADOTTIR, A., STYRKARSDOTTIR, U., MAGNUSSON, K. P., WALTERS, G. B., PALSDOTTIR, E., JONSDOTTIR, T., GUDMUNDSDOTTIR, T., GYLFASON, A., SAEMUNDSDOTTIR, J., WILENSKY, R. L., REILLY, M. P., RADER, D. J., BAGGER, Y., CHRISTIANSEN, C., GUDNASON, V., SIGURDSSON, G., THORSTEINSDOTTIR, U., GULCHER, J. R., KONG, A. & STEFANSSON, K. (2006). Variant of transcription factor 7-like 2 (TCF7L2) gene confers risk of type 2 diabetes. *Nat Genet* **38,** 320-3.

GREENE, M. W., SAKAUE, H., WANG, L., ALESSI, D. R. & ROTH, R. A. (2003). Modulation of insulin-stimulated degradation of human insulin receptor substrate-1 by Serine 312 phosphorylation. *J Biol Chem* **278,** 8199-211.

GREIG, C. A., HAMEED, M., YOUNG, A., GOLDSPINK, G. & NOBLE, B. (2006). Skeletal muscle IGF-I isoform expression in healthy women after isometric exercise. *Growth Horm IGF Res* **16,** 373-6.

GROBET, L., MARTIN, L. J., PONCELET, D., PIROTTIN, D., BROUWERS, B., RIQUET, J., SCHOEBERLEIN, A., DUNNER, S., MENISSIER, F., MASSABANDA, J., FRIES, R., HANSET, R. & GEORGES, M. (1997). A deletion in the bovine myostatin gene causes the double-muscled phenotype in cattle. *Nat Genet* **17,** 71-4.

GUAL, P., GREMEAUX, T., GONZALEZ, T., LE MARCHAND-BRUSTEL, Y. & TANTI, J. F. (2003). MAP kinases and mTOR mediate insulin-induced phosphorylation of insulin receptor substrate-1 on serine residues 307, 612 and 632. *Diabetologia* **46,** 1532-42.

GUILLAUME-GENTIL, C., ASSIMACOPOULOS-JEANNET, F. & JEANRENAUD, B. (1993). Involvement of non-esterified fatty acid oxidation in glucocorticoid-induced peripheral insulin resistance in vivo in rats. *Diabetologia* **36,** 899-906.

GUILLET-DENIAU, I., MIEULET, V., LE LAY, S., ACHOURI, Y., CARRE, D., GIRARD, J., FOUFELLE, F. & FERRE, P. (2002). Sterol regulatory element binding protein-1c expression and action in rat muscles: insulin-like effects on the control of glycolytic and lipogenic enzymes and UCP3 gene expression. *Diabetes* **51,** 1722-8.

GUILLET-DENIAU, I., PICHARD, A. L., KONE, A., ESNOUS, C., NIERUCHALSKI, M., GIRARD, J. & PRIP-BUUS, C. (2004). Glucose induces de novo lipogenesis in rat muscle satellite cells through a sterol-regulatory-element-binding-protein-1c-dependent pathway. *J Cell Sci* **117,** 1937-44.

HABER, R. S. & WEINSTEIN, S. P. (1992). Role of glucose transporters in glucocorticoid-induced insulin resistance. GLUT4 isoform in rat skeletal muscle is not decreased by dexamethasone. *Diabetes* **41,** 728-35.

HAEMMERLE, G., ZIMMERMANN, R., HAYN, M., THEUSSL, C., WAEG, G., WAGNER, E., SATTLER, W., MAGIN, T. M., WAGNER, E. F. & ZECHNER, R. (2002). Hormone-sensitive lipase deficiency in mice causes diglyceride accumulation in adipose tissue, muscle, and testis. *J Biol Chem* **277,** 4806-15.

HAFEZI-MOGHADAM, A., SIMONCINI, T., YANG, Z., LIMBOURG, F. P., PLUMIER, J. C., REBSAMEN, M. C., HSIEH, C. M., CHUI, D. S., THOMAS, K. L., PROROCK, A. J., LAUBACH, V. E., MOSKOWITZ, M. A., FRENCH, B. A., LEY, K. & LIAO, J. K. (2002). Acute cardiovascular protective effects of corticosteroids are mediated by non-transcriptional activation of endothelial nitric oxide synthase. *Nat Med* **8,** 473-9.

HAIMOVITZ-FRIEDMAN, A., KOLESNICK, R. N. & FUKS, Z. (1997). Ceramide signaling in apoptosis. *Br Med Bull* **53,** 539-53.

HAJDUCH, E., BALENDRAN, A., BATTY, I. H., LITHERLAND, G. J., BLAIR, A. S., DOWNES, C. P. & HUNDAL, H. S. (2001). Ceramide impairs the insulin-dependent membrane recruitment of protein kinase B leading to a loss in downstream signalling in L6 skeletal muscle cells. *Diabetologia* **44,** 173-83.

HALEVY, O., NOVITCH, B. G., SPICER, D. B., SKAPEK, S. X., RHEE, J., HANNON, G. J., BEACH, D. & LASSAR, A. B. (1995). Correlation of terminal cell cycle arrest of skeletal muscle with induction of p21 by MyoD. *Science* **267,** 1018-21.

HALL, R. K., YAMASAKI, T., KUCERA, T., WALTNER-LAW, M., O'BRIEN, R. & GRANNER, D. K. (2000). Regulation of phosphoenolpyruvate carboxykinase and insulin-like growth factor-binding protein-1 gene expression by insulin. The role of winged helix/forkhead proteins. *J Biol Chem* **275,** 30169-75.

HAMMOND, G. L. (1990). Molecular properties of corticosteroid binding globulin and the sex-steroid binding proteins. *Endocr Rev* **11,** 65-79.

HANADA, M., FENG, J. & HEMMINGS, B. A. (2004). Structure, regulation and function of PKB/AKT--a major therapeutic target. *Biochim Biophys Acta* **1697,** 3-16.

HANNON, K., KUDLA, A. J., MCAVOY, M. J., CLASE, K. L. & OLWIN, B. B. (1996). Differentially expressed fibroblast growth factors regulate skeletal muscle development through autocrine and paracrine mechanisms. *J Cell Biol* **132,** 1151-9.

HANNUN, Y. A. & OBEID, L. M. (2002). The Ceramide-centric universe of lipid-mediated cell regulation: stress encounters of the lipid kind. *J Biol Chem* **277,** 25847-50.

HARALAMBIE, G. (1977). Citrate synthase activity in human skeletal muscle. *Enzyme* **22,** 330-5.

HARD, T., KELLENBACH, E., BOELENS, R., MALER, B. A., DAHLMAN, K., FREEDMAN, L. P., CARLSTEDT-DUKE, J., YAMAMOTO, K. R., GUSTAFSSON, J. A. & KAPTEIN, R. (1990). Solution structure of the glucocorticoid receptor DNA-binding domain. *Science* **249,** 157-60.

HARRINGTON, L. S., FINDLAY, G. M., GRAY, A., TOLKACHEVA, T., WIGFIELD, S., REBHOLZ, H., BARNETT, J., LESLIE, N. R., CHENG, S., SHEPHERD, P. R., GOUT, I., DOWNES, C. P. & LAMB, R. F. (2004). The TSC1-2 tumor suppressor controls insulin-PI3K signaling via regulation of IRS proteins. *J Cell Biol* **166,** 213-23.

HELLER-HARRISON, R. A., MORIN, M. & CZECH, M. P. (1995). Insulin regulation of membrane-associated insulin receptor substrate 1. *J Biol Chem* **270,** 24442-50.

HERMANOWSKI-VOSATKA, A., BALKOVEC, J. M., CHENG, K., CHEN, H. Y., HERNANDEZ, M., KOO, G. C., LE GRAND, C. B., LI, Z., METZGER, J. M., MUNDT, S. S., NOONAN, H., NUNES, C. N., OLSON, S. H., PIKOUNIS, B., REN, N., ROBERTSON, N., SCHAEFFER, J. M., SHAH, K., SPRINGER, M. S., STRACK, A. M., STROWSKI, M., WU, K., WU, T., XIAO, J., ZHANG, B. B., WRIGHT, S. D. & THIERINGER, R. (2005). 11beta-HSD1 inhibition ameliorates metabolic syndrome and prevents progression of atherosclerosis in mice. *J Exp Med* **202,** 517-27.

HEYDRICK, S. J., RUDERMAN, N. B., KUROWSKI, T. G., ADAMS, H. B. & CHEN, K. S. (1991). Enhanced stimulation of diacylglycerol and lipid synthesis by insulin in denervated muscle. Altered protein kinase C activity and possible link to insulin resistance. *Diabetes* **40,** 1707-11.

HIRASHIMA, Y., TSURUZOE, K., KODAMA, S., IGATA, M., TOYONAGA, T., UEKI, K., KAHN, C. R. & ARAKI, E. (2003). Insulin down-regulates insulin receptor substrate-2 expression through the phosphatidylinositol 3-kinase/Akt pathway. *J Endocrinol* **179,** 253-66.

HO, R. C., DAVY, K. P., HICKEY, M. S. & MELBY, C. L. (2005). Circulating tumor necrosis factor alpha is higher in non-obese, non-diabetic Mexican Americans compared to non-Hispanic white adults. *Cytokine* **30,** 14-21.

HOLLAND, W. L., BROZINICK, J. T., WANG, L. P., HAWKINS, E. D., SARGENT, K. M., LIU, Y., NARRA, K., HOEHN, K. L., KNOTTS, T. A., SIESKY, A., NELSON, D. H., KARATHANASIS, S. K., FONTENOT, G. K., BIRNBAUM, M. J. & SUMMERS, S. A. (2007). Inhibition of ceramide synthesis ameliorates glucocorticoid-, saturated-fat-, and obesity-induced insulin resistance. *Cell Metab* **5,** 167-79.

HOTAMISLIGIL, G. S., ARNER, P., CARO, J. F., ATKINSON, R. L. & SPIEGELMAN, B. M. (1995). Increased adipose tissue expression of tumor necrosis factor-alpha in human obesity and insulin resistance. *J Clin Invest* **95,** 2409-15.

HOTAMISLIGIL, G. S., SHARGILL, N. S. & SPIEGELMAN, B. M. (1993). Adipose

expression of tumor necrosis factor-alpha: direct role in obesity-linked insulin resistance. *Science* **259,** 87-91.

HOTTA, K., FUNAHASHI, T., ARITA, Y., TAKAHASHI, M., MATSUDA, M., OKAMOTO, Y., IWAHASHI, H., KURIYAMA, H., OUCHI, N., MAEDA, K., NISHIDA, M., KIHARA, S., SAKAI, N., NAKAJIMA, T., HASEGAWA, K., MURAGUCHI, M., OHMOTO, Y., NAKAMURA, T., YAMASHITA, S., HANAFUSA, T. & MATSUZAWA, Y. (2000). Plasma concentrations of a novel, adipose-specific protein, adiponectin, in type 2 diabetic patients. *Arterioscler Thromb Vasc Biol* **20,** 1595-9.

HU, Z., WANG, H., LEE, I. H., DU, J. & MITCH, W. E. (2009). Endogenous glucocorticoids and impaired insulin signaling are both required to stimulate muscle wasting under pathophysiological conditions in mice. *J Clin Invest* **119,** 3059-69.

HUBBARD, S. R., WEI, L., ELLIS, L. & HENDRICKSON, W. A. (1994). Crystal structure of the tyrosine kinase domain of the human insulin receptor. *Nature* **372,** 746-54.

HUNDERTMARK, S., BUHLER, H., RAGOSCH, V., DINKELBORG, L., ARABIN, B. & WEITZEL, H. K. (1995). Correlation of surfactant phosphatidylcholine synthesis and 11 beta-hydroxysteroid dehydrogenase in the fetal lung. *Endocrinology* **136,** 2573-8.

IKEDA, S., MIYAZAKI, H., NAKATANI, T., KAI, Y., KAMEI, Y., MIURA, S., TSUBOYAMA-KASAOKA, N. & EZAKI, O. (2002). Up-regulation of SREBP-1c and lipogenic genes in skeletal muscles after exercise training. *Biochem Biophys Res Commun* **296,** 395-400.

ITANI, S. I., RUDERMAN, N. B., SCHMIEDER, F. & BODEN, G. (2002). Lipid-induced insulin resistance in human muscle is associated with changes in diacylglycerol, protein kinase C, and IkappaB-alpha. *Diabetes* **51,** 2005-11.

JAMIESON, P. M., CHAPMAN, K. E., EDWARDS, C. R. & SECKL, J. R. (1995). 11 beta-hydroxysteroid dehydrogenase is an exclusive 11 beta- reductase in primary cultures of rat hepatocytes: effect of physicochemical and hormonal manipulations. *Endocrinology* **136,** 4754-61.

JAMIESON, P. M., WALKER, B. R., CHAPMAN, K. E., ANDREW, R., ROSSITER, S. & SECKL, J. R. (2000). 11 beta-hydroxysteroid dehydrogenase type 1 is a predominant 11 beta-reductase in the intact perfused rat liver. *J Endocrinol* **165,** 685-92.

JANG, C., OBEYESEKERE, V. R., DILLEY, R. J., ALFORD, F. P. & INDER, W. J. (2006). 11Beta hydroxysteroid dehydrogenase type 1 is expressed and is biologically active in human skeletal muscle. *Clin Endocrinol (Oxf)* **65,** 800-5.

JANG, C., OBEYESEKERE, V. R., DILLEY, R. J., KROZOWSKI, Z., INDER, W. J. & ALFORD, F. P. (2007). Altered activity of 11beta-hydroxysteroid dehydrogenase types 1 and 2 in skeletal muscle confers metabolic protection in subjects with type 2 diabetes. *J Clin Endocrinol Metab* **92,** 3314-20.

JARVIS, J. C., MOKRUSCH, T., KWENDE, M. M., SUTHERLAND, H. & SALMONS, S. (1996). Fast-to-slow transformation in stimulated rat muscle. *Muscle Nerve* **19,** 1469-75.

JEOUNG, N. H. & HARRIS, R. A. (2008). Pyruvate dehydrogenase kinase-4 deficiency lowers blood glucose and improves glucose tolerance in diet-induced obese mice. *Am J Physiol Endocrinol Metab* **295,** E46-54.

JIANG, G., DALLAS-YANG, Q., LIU, F., MOLLER, D. E. & ZHANG, B. B. (2003). Salicylic

acid reverses phorbol 12-myristate-13-acetate (PMA)- and tumor necrosis factor alpha (TNFalpha)-induced insulin receptor substrate 1 (IRS1) serine 307 phosphorylation and insulin resistance in human embryonic kidney 293 (HEK293) cells. *J Biol Chem* **278,** 180-6.

JOCKEN, J. W., SMIT, E., GOOSSENS, G. H., ESSERS, Y. P., VAN BAAK, M. A., MENSINK, M., SARIS, W. H. & BLAAK, E. E. (2008). Adipose triglyceride lipase (ATGL) expression in human skeletal muscle is type I (oxidative) fiber specific. *Histochem Cell Biol* **129,** 535-8.

JORGENSEN, S. B., HONEYMAN, J., OAKHILL, J. S., FAZAKERLEY, D., STOCKLI, J., KEMP, B. E. & STEINBERG, G. R. (2009). Oligomeric resistin impairs insulin and AICAR-stimulated glucose uptake in mouse skeletal muscle by inhibiting GLUT4 translocation. *Am J Physiol Endocrinol Metab* **297,** E57-66.

KAJITA, K., ISHIZUKA, T., MIURA, A., ISHIZAWA, M., KANOH, Y. & YASUDA, K. (2000). The role of atypical and conventional PKC in dehydroepiandrosterone-induced glucose uptake and dexamethasone-induced insulin resistance. *Biochem Biophys Res Commun* **277,** 361-7.

KAJITA, K., ISHIZUKA, T., MIURA, A., KANOH, Y., ISHIZAWA, M., KIMURA, M., MUTO, N. & YASUDA, K. (2001). Glucocorticoid-induced insulin resistance associates with activation of protein kinase C isoforms. *Cell Signal* **13,** 169-75.

KARLSSON, M., CONTRERAS, J. A., HELLMAN, U., TORNQVIST, H. & HOLM, C. (1997). cDNA cloning, tissue distribution, and identification of the catalytic triad of monoglyceride lipase. Evolutionary relationship to esterases, lysophospholipases, and haloperoxidases. *J Biol Chem* **272,** 27218-23.

KELLEY, D. E., HE, J., MENSHIKOVA, E. V. & RITOV, V. B. (2002). Dysfunction of mitochondria in human skeletal muscle in type 2 diabetes. In *Diabetes*, vol. 51, pp. 2944-50.

KERN, P. A., RANGANATHAN, S., LI, C., WOOD, L. & RANGANATHAN, G. (2001). Adipose tissue tumor necrosis factor and interleukin-6 expression in human obesity and insulin resistance. *Am J Physiol Endocrinol Metab* **280,** E745-51.

KIDO, Y., BURKS, D. J., WITHERS, D., BRUNING, J. C., KAHN, C. R., WHITE, M. F. & ACCILI, D. (2000). Tissue-specific insulin resistance in mice with mutations in the insulin receptor, IRS-1, and IRS-2. *J Clin Invest* **105,** 199-205.

KIELSTEIN, J. T., BECKER, B., GRAF, S., BRABANT, G., HALLER, H. & FLISER, D. (2003). Increased resistin blood levels are not associated with insulin resistance in patients with renal disease. *Am J Kidney Dis* **42,** 62-6.

KIENS, B., LITHELL, H., MIKINES, K. J. & RICHTER, E. A. (1989). Effects of insulin and exercise on muscle lipoprotein lipase activity in man and its relation to insulin action. *J Clin Invest* **84,** 1124-9.

KIENS, B., ROEPSTORFF, C., GLATZ, J. F., BONEN, A., SCHJERLING, P., KNUDSEN, J. & NIELSEN, J. N. (2004). Lipid-binding proteins and lipoprotein lipase activity in human skeletal muscle: influence of physical activity and gender. *J Appl Physiol* **97,** 1209-18.

KIM, J. K., FILLMORE, J. J., SUNSHINE, M. J., ALBRECHT, B., HIGASHIMORI, T., KIM, D. W., LIU, Z. X., SOOS, T. J., CLINE, G. W., O'BRIEN, W. R., LITTMAN, D. R. & SHULMAN, G. I. (2004). PKC-theta knockout mice are protected from fat-induced insulin resistance. *J Clin Invest* **114,** 823-7.

KITAMURA, T., KITAMURA, Y., KURODA, S., HINO, Y., ANDO, M., KOTANI, K., KONISHI, H., MATSUZAKI, H., KIKKAWA, U., OGAWA, W. & KASUGA, M. (1999). Insulin-

induced phosphorylation and activation of cyclic nucleotide phosphodiesterase 3B by the serine-threonine kinase Akt. *Mol Cell Biol* **19,** 6286-96.

KOTELEVTSEV, Y., HOLMES, M. C., BURCHELL, A., HOUSTON, P. M., SCHMOLL, D., JAMIESON, P., BEST, R., BROWN, R., EDWARDS, C. R., SECKL, J. R. & MULLINS, J. J. (1997). 11beta-hydroxysteroid dehydrogenase type 1 knockout mice show attenuated glucocorticoid-inducible responses and resist hyperglycemia on obesity or stress. *Proc Natl Acad Sci U S A* **94,** 14924-9.

KOYAMA, K., CHEN, G., LEE, Y. & UNGER, R. H. (1997). Tissue triglycerides, insulin resistance, and insulin production: implications for hyperinsulinemia of obesity. *Am J Physiol* **273,** E708-13.

KRAUS-FRIEDMANN, N. (1984). Hormonal regulation of hepatic gluconeogenesis. *Physiol Rev* **64,** 170-259.

KUCERA, T., WALTNER-LAW, M., SCOTT, D. K., PRASAD, R. & GRANNER, D. K. (2002). A point mutation of the AF2 transactivation domain of the glucocorticoid receptor disrupts its interaction with steroid receptor coactivator 1. *J Biol Chem* **277,** 26098-102.

KUMAR, R., BETNEY, R., LI, J., THOMPSON, E. B. & MCEWAN, I. J. (2004). Induced alpha-helix structure in AF1 of the androgen receptor upon binding transcription factor TFIIF. *Biochemistry* **43,** 3008-13.

KUMAR, R., SERRETTE, J. M. & THOMPSON, E. B. (2005). Osmolyte-induced folding enhances tryptic enzyme activity. *Arch Biochem Biophys* **436,** 78-82.

KUMAR, R. & THOMPSON, E. B. (2005). Gene regulation by the glucocorticoid receptor: structure:function relationship. *J Steroid Biochem Mol Biol* **94,** 383-94.

LAKSHMI, V. & MONDER, C. (1988). Purification and characterization of the corticosteroid 11 beta-dehydrogenase component of the rat liver 11 beta-hydroxysteroid dehydrogenase complex. *Endocrinology* **123,** 2390-8.

LAMBILLOTTE, C., GILON, P. & HENQUIN, J. C. (1997). Direct glucocorticoid inhibition of insulin secretion. An in vitro study of dexamethasone effects in mouse islets. *J Clin Invest* **99,** 414-23.

LANE, M. D., MOSS, J. & POLAKIS, S. E. (1974). Acetyl coenzyme A carboxylase. *Curr Top Cell Regul* **8,** 139-95.

LANGFORT, J., PLOUG, T., IHLEMANN, J., HOLM, C. & GALBO, H. (2000). Stimulation of hormone-sensitive lipase activity by contractions in rat skeletal muscle. *Biochem J* **351,** 207-14.

LANGFORT, J., PLOUG, T., IHLEMANN, J., SALDO, M., HOLM, C. & GALBO, H. (1999). Expression of hormone-sensitive lipase and its regulation by adrenaline in skeletal muscle. *Biochem J* **340 (Pt 2),** 459-65.

LARANCE, M., RAMM, G., STOCKLI, J., VAN DAM, E. M., WINATA, S., WASINGER, V., SIMPSON, F., GRAHAM, M., JUNUTULA, J. R., GUILHAUS, M. & JAMES, D. E. (2005). Characterization of the role of the Rab GTPase-activating protein AS160 in insulin-regulated GLUT4 trafficking. *J Biol Chem* **280,** 37803-13.

LARSEN, P. R., KRONENBERG, H. M., MELMED, S. & POLONSKY, K. S. (2003). *Williams Textbook of Endocrinology*, 10 edition.

LARSSON, H. & AHREN, B. (1996). Short-term dexamethasone treatment increases plasma leptin independently of changes in insulin sensitivity in healthy women. *J Clin Endocrinol Metab* **81,** 4428-32.

LASSAR, A. B., BUSKIN, J. N., LOCKSHON, D., DAVIS, R. L., APONE, S., HAUSCHKA, S.

D. & WEINTRAUB, H. (1989). MyoD is a sequence-specific DNA binding protein requiring a region of myc homology to bind to the muscle creatine kinase enhancer. *Cell* **58,** 823-31.

LAVAN, B. E., LANE, W. S. & LIENHARD, G. E. (1997). The 60-kDa phosphotyrosine protein in insulin-treated adipocytes is a new member of the insulin receptor substrate family. *J Biol Chem* **272,** 11439-43.

LAVERY, G. G., WALKER, E. A., DRAPER, N., JEYASURIA, P., MARCOS, J., SHACKLETON, C. H., PARKER, K. L., WHITE, P. C. & STEWART, P. M. (2006). Hexose-6-phosphate dehydrogenase knock-out mice lack 11 beta-hydroxysteroid dehydrogenase type 1-mediated glucocorticoid generation. *J Biol Chem* **281,** 6546-51.

LAVERY, G. G., WALKER, E. A., TURAN, N., ROGOFF, D., RYDER, J. W., SHELTON, J. M., RICHARDSON, J. A., FALCIANI, F., WHITE, P. C., STEWART, P. M., PARKER, K. L. & MCMILLAN, D. R. (2008). Deletion of hexose-6-phosphate dehydrogenase activates the unfolded protein response pathway and induces skeletal myopathy. *J Biol Chem* **283,** 8453-61.

LAWLOR, D. A., SMITH, G. D. & EBRAHIM, S. (2006). Does the new International Diabetes Federation definition of the metabolic syndrome predict CHD any more strongly than older definitions? Findings from the British Women's Heart and Health Study. *Diabetologia* **49,** 41-8.

LAWRENCE, J. C., JR., GUINOVART, J. J. & LARNER, J. (1977). Activation of rat adipocyte glycogen synthase by insulins. *J Biol Chem* **252,** 444-50.

LECKER, S. H., JAGOE, R. T., GILBERT, A., GOMES, M., BARACOS, V., BAILEY, J., PRICE, S. R., MITCH, W. E. & GOLDBERG, A. L. (2004). Multiple types of skeletal muscle atrophy involve a common program of changes in gene expression. *Faseb J* **18,** 39-51.

LEIGHTON, B., CHALLISS, R. A., LOZEMAN, F. J. & NEWSHOLME, E. A. (1987). Effects of dexamethasone treatment on insulin-stimulated rates of glycolysis and glycogen synthesis in isolated incubated skeletal muscles of the rat. *Biochem J* **246,** 551-4.

LEITGES, M., PLOMANN, M., STANDAERT, M. L., BANDYOPADHYAY, G., SAJAN, M. P., KANOH, Y. & FARESE, R. V. (2002). Knockout of PKC alpha enhances insulin signaling through PI3K. *Mol Endocrinol* **16,** 847-58.

LETTERON, P., BRAHIMI-BOUROUINA, N., ROBIN, M. A., MOREAU, A., FELDMANN, G. & PESSAYRE, D. (1997). Glucocorticoids inhibit mitochondrial matrix acyl-CoA dehydrogenases and fatty acid beta-oxidation. *Am J Physiol* **272,** G1141-50.

LIBERMAN, Z., PLOTKIN, B., TENNENBAUM, T. & ELDAR-FINKELMAN, H. (2008). Coordinated phosphorylation of insulin receptor substrate-1 by glycogen synthase kinase-3 and protein kinase C betaII in the diabetic fat tissue. *Am J Physiol Endocrinol Metab* **294,** E1169-77.

LIU, F., KIM, J., LI, Y., LIU, X., LI, J. & CHEN, X. (2001). An extract of Lagerstroemia speciosa L. has insulin-like glucose uptake-stimulatory and adipocyte differentiation-inhibitory activities in 3T3-L1 cells. *J Nutr* **131,** 2242-7.

LIU, F., YANG, T., WANG, B., ZHANG, M., GU, N., QIU, J., FAN, H. Q., ZHANG, C. M., FEI, L., PAN, X. Q., GUO, M., CHEN, R. H. & GUO, X. R. (2008). Resistin induces insulin resistance, but does not affect glucose output in rat-derived hepatocytes. *Acta Pharmacol Sin* **29,** 98-104.

LIU, L., WANG, Y. X., ZHOU, J., LONG, F., SUN, H. W., LIU, Y., CHEN, Y. Z. & JIANG, C. L. (2005). Rapid non-genomic inhibitory effects of glucocorticoids on

human neutrophil degranulation. *Inflamm Res* **54,** 37-41.

LIU, S. C., WANG, Q., LIENHARD, G. E. & KELLER, S. R. (1999). Insulin receptor substrate 3 is not essential for growth or glucose homeostasis. *J Biol Chem* **274,** 18093-9.

LOPEZ, M. P., GOMEZ-LECHON, M. J. & CASTELL, J. V. (1984). Glycogen synthesis in serum-free cultured hepatocytes in response to insulin and dexamethasone. *In Vitro* **20,** 923-31.

LU, N. Z. & CIDLOWSKI, J. A. (2004). The origin and functions of multiple human glucocorticoid receptor isoforms. *Ann N Y Acad Sci* **1024,** 102-23.

LUAN, F. L. (2009). Glucose control and vascular complications in type 2 diabetes. *N Engl J Med* **360,** 2031-2; author reply 2032.

LUISI, B. F., XU, W. X., OTWINOWSKI, Z., FREEDMAN, L. P., YAMAMOTO, K. R. & SIGLER, P. B. (1991). Crystallographic analysis of the interaction of the glucocorticoid receptor with DNA. *Nature* **352,** 497-505.

MA, K., MALLIDIS, C., BHASIN, S., MAHABADI, V., ARTAZA, J., GONZALEZ-CADAVID, N., ARIAS, J. & SALEHIAN, B. (2003). Glucocorticoid-induced skeletal muscle atrophy is associated with upregulation of myostatin gene expression. *Am J Physiol Endocrinol Metab* **285,** E363-71.

MA, Y. H., WANG, J., RODD, G. G., BOLAFFI, J. L. & GRODSKY, G. M. (1995). Differences in insulin secretion between the rat and mouse: role of cAMP. *Eur J Endocrinol* **132,** 370-6.

MAEHAMA, T. & DIXON, J. E. (1999). PTEN: a tumour suppressor that functions as a phospholipid phosphatase. *Trends Cell Biol* **9,** 125-8.

MARTINY-BARON, G., KAZANIETZ, M. G., MISCHAK, H., BLUMBERG, P. M., KOCHS, G., HUG, H., MARME, D. & SCHACHTELE, C. (1993). Selective inhibition of protein kinase C isozymes by the indolocarbazole Go 6976. *J Biol Chem* **268,** 9194-7.

MASKE, H. (1954). [Blood sugar-induced insulin secretion.]. *Acta Neuroveg (Wien)* **9,** 307-9.

MATTHEWS, L., BERRY, A., OHANIAN, V., OHANIAN, J., GARSIDE, H. & RAY, D. (2008). Caveolin mediates rapid glucocorticoid effects and couples glucocorticoid action to the antiproliferative program. *Mol Endocrinol* **22,** 1320-30.

MAUVAIS-JARVIS, F., UEKI, K., FRUMAN, D. A., HIRSHMAN, M. F., SAKAMOTO, K., GOODYEAR, L. J., IANNACONE, M., ACCILI, D., CANTLEY, L. C. & KAHN, C. R. (2002). Reduced expression of the murine p85alpha subunit of phosphoinositide 3-kinase improves insulin signaling and ameliorates diabetes. *J Clin Invest* **109,** 141-9.

MAY, R. C., KELLY, R. A. & MITCH, W. E. (1986). Metabolic acidosis stimulates protein degradation in rat muscle by a glucocorticoid-dependent mechanism. *J Clin Invest* **77,** 614-21.

MCCROSKERY, S., THOMAS, M., MAXWELL, L., SHARMA, M. & KAMBADUR, R. (2003). Myostatin negatively regulates satellite cell activation and self-renewal. *J Cell Biol* **162,** 1135-47.

MCFARLAND, D. C., VELLEMAN, S. G., PESALL, J. E. & LIU, C. (2007). The role of myostatin in chicken (Gallus domesticus) myogenic satellite cell proliferation and differentiation. *Gen Comp Endocrinol* **151,** 351-7.

MEHRANI, H. & STOREY, K. B. (1993). Control of glycogenolysis and effects of exercise on phosphorylase kinase and cAMP-dependent protein kinase in rainbow trout organs. *Biochem Cell Biol* **71,** 501-6.

MERRILL, A. H., JR. & JONES, D. D. (1990). An update of the enzymology and

regulation of sphingomyelin metabolism. *Biochim Biophys Acta* **1044,** 1-12.

MILLWARD, T. A., ZOLNIEROWICZ, S. & HEMMINGS, B. A. (1999). Regulation of protein kinase cascades by protein phosphatase 2A. *Trends Biochem Sci* **24,** 186-91.

MIRON, M., LASKO, P. & SONENBERG, N. (2003). Signaling from Akt to FRAP/TOR targets both 4E-BP and S6K in Drosophila melanogaster. *Mol Cell Biol* **23,** 9117-26.

MITCH, W. E., BAILEY, J. L., WANG, X., JURKOVITZ, C., NEWBY, D. & PRICE, S. R. (1999). Evaluation of signals activating ubiquitin-proteasome proteolysis in a model of muscle wasting. *Am J Physiol* **276,** C1132-8.

MOHITI, J., TALEBI, F. & AFKHAMI-ARDEKANI, M. (2009). Circulation free leptin in diabetic patients and its correlation to insulin level. *Pak J Biol Sci* **12,** 397-400.

MONTELL, E., TURINI, M., MAROTTA, M., ROBERTS, M., NOE, V., CIUDAD, C. J., MACE, K. & GOMEZ-FOIX, A. M. (2001). DAG accumulation from saturated fatty acids desensitizes insulin stimulation of glucose uptake in muscle cells. *Am J Physiol Endocrinol Metab* **280,** E229-37.

MOON, B., KWAN, J. J., DUDDY, N., SWEENEY, G. & BEGUM, N. (2003). Resistin inhibits glucose uptake in L6 cells independently of changes in insulin signaling and GLUT4 translocation. *Am J Physiol Endocrinol Metab* **285,** E106-15.

MORTON, N. M., HOLMES, M. C., FIEVET, C., STAELS, B., TAILLEUX, A., MULLINS, J. J. & SECKL, J. R. (2001). Improved lipid and lipoprotein profile, hepatic insulin sensitivity, and glucose tolerance in 11beta-hydroxysteroid dehydrogenase type 1 null mice. *J Biol Chem* **276,** 41293-300.

MORTON, N. M., PATERSON, J. M., MASUZAKI, H., HOLMES, M. C., STAELS, B., FIEVET, C., WALKER, B. R., FLIER, J. S., MULLINS, J. J. & SECKL, J. R. (2004). Novel adipose tissue-mediated resistance to diet-induced visceral obesity in 11 beta-hydroxysteroid dehydrogenase type 1-deficient mice. *Diabetes* **53,** 931-8.

MOSS, F. P. & LEBLOND, C. P. (1971). Satellite cells as the source of nuclei in muscles of growing rats. *Anat Rec* **170,** 421-35.

MOTHE, I. & VAN OBBERGHEN, E. (1996). Phosphorylation of insulin receptor substrate-1 on multiple serine residues, 612, 632, 662, and 731, modulates insulin action. *J Biol Chem* **271,** 11222-7.

MU, H. & HOY, C. E. (2004). The digestion of dietary triacylglycerols. *Prog Lipid Res* **43,** 105-33.

MULNIER, H. E., SEAMAN, H. E., RALEIGH, V. S., SOEDAMAH-MUTHU, S. S., COLHOUN, H. M. & LAWRENSON, R. A. (2006). Mortality in people with type 2 diabetes in the UK. *Diabet Med* **23,** 516-21.

MUOIO, D. M. & KOVES, T. R. (2007). Skeletal muscle adaptation to fatty acid depends on coordinated actions of the PPARs and PGC1 alpha: implications for metabolic disease. *Appl Physiol Nutr Metab* **32,** 874-83.

MUOIO, D. M., SEEFELD, K., WITTERS, L. A. & COLEMAN, R. A. (1999). AMP-activated kinase reciprocally regulates triacylglycerol synthesis and fatty acid oxidation in liver and muscle: evidence that sn-glycerol-3-phosphate acyltransferase is a novel target. *Biochem J* **338 (Pt 3),** 783-91.

MURASE, K., ODAKA, H., SUZUKI, M., TAYUKI, N. & IKEDA, H. (1998). Pioglitazone time-dependently reduces tumour necrosis factor-alpha level in muscle and improves metabolic abnormalities in Wistar fatty rats. *Diabetologia* **41,**

257-64.

MURTHY, M. S. & PANDE, S. V. (1984). Mechanism of carnitine acylcarnitine translocase-catalyzed import of acylcarnitines into mitochondria. *J Biol Chem* **259,** 9082-9.

MUSSIG, K., FIEDLER, H., STAIGER, H., WEIGERT, C., LEHMANN, R., SCHLEICHER, E. D. & HARING, H. U. (2005). Insulin-induced stimulation of JNK and the PI 3-kinase/mTOR pathway leads to phosphorylation of serine 318 of IRS-1 in C2C12 myotubes. *Biochem Biophys Res Commun* **335,** 819-25.

MYERS, M. G., JR., BACKER, J. M., SUN, X. J., SHOELSON, S., HU, P., SCHLESSINGER, J., YOAKIM, M., SCHAFFHAUSEN, B. & WHITE, M. F. (1992). IRS-1 activates phosphatidylinositol 3'-kinase by associating with src homology 2 domains of p85. *Proc Natl Acad Sci U S A* **89,** 10350-4.

MYERS, M. G., JR., MENDEZ, R., SHI, P., PIERCE, J. H., RHOADS, R. & WHITE, M. F. (1998). The COOH-terminal tyrosine phosphorylation sites on IRS-1 bind SHP-2 and negatively regulate insulin signaling. *J Biol Chem* **273,** 26908-14.

NAWARATNE, R., GRAY, A., JORGENSEN, C. H., DOWNES, C. P., SIDDLE, K. & SETHI, J. K. (2006). Regulation of insulin receptor substrate 1 pleckstrin homology domain by protein kinase C: role of serine 24 phosphorylation. *Mol Endocrinol* **20,** 1838-52.

NEWSHOLME, E. A. & TAYLOR, K. (1969). Glycerol kinase activities in muscles from vertebrates and invertebrates. *Biochem J* **112,** 465-74.

NEWTON, A. C. (1995). Protein kinase C: structure, function, and regulation. *J Biol Chem* **270,** 28495-8.

NIELSEN, M. F., CAUMO, A., CHANDRAMOULI, V., SCHUMANN, W. C., COBELLI, C., LANDAU, B. R., VILSTRUP, H., RIZZA, R. A. & SCHMITZ, O. (2004). Impaired basal glucose effectiveness but unaltered fasting glucose release and gluconeogenesis during short-term hypercortisolemia in healthy subjects. *Am J Physiol Endocrinol Metab* **286,** E102-10.

NISHIMURA, M., MIKURA, M., HIRASAKA, K., OKUMURA, Y., NIKAWA, T., KAWANO, Y., NAKAYAMA, M. & IKEDA, M. (2008). Effects of dimethyl sulphoxide and dexamethasone on mRNA expression of myogenesis- and muscle proteolytic system-related genes in mouse myoblastic C2C12 cells. *J Biochem* **144,** 717-24.

NISHIZUKA, Y. (1988). The molecular heterogeneity of protein kinase C and its implications for cellular regulation. *Nature* **334,** 661-5.

NNODIM, J. O. (2001). Testosterone mediates satellite cell activation in denervated rat levator ani muscle. *Anat Rec* **263,** 19-24.

NYE, C. K., HANSON, R. W. & KALHAN, S. C. (2008). Glyceroneogenesis is the dominant pathway for triglyceride glycerol synthesis in vivo in the rat. *J Biol Chem* **283,** 27565-74.

OAKES, N. D., BELL, K. S., FURLER, S. M., CAMILLERI, S., SAHA, A. K., RUDERMAN, N. B., CHISHOLM, D. J. & KRAEGEN, E. W. (1997a). Diet-induced muscle insulin resistance in rats is ameliorated by acute dietary lipid withdrawal or a single bout of exercise: parallel relationship between insulin stimulation of glucose uptake and suppression of long-chain fatty acyl-CoA. *Diabetes* **46,** 2022-8.

OAKES, N. D., COONEY, G. J., CAMILLERI, S., CHISHOLM, D. J. & KRAEGEN, E. W. (1997b). Mechanisms of liver and muscle insulin resistance induced by chronic high-fat feeding. *Diabetes* **46,** 1768-74.

ODERMATT, A., ARNOLD, P., STAUFFER, A., FREY, B. M. & FREY, F. J. (1999). The N-terminal anchor sequences of 11beta-hydroxysteroid dehydrogenases determine their orientation in the endoplasmic reticulum membrane. *J Biol Chem* **274,** 28762-70.

OKUDA, A. & OKUDA, K. (1984). Purification and characterization of delta 4-3-ketosteroid 5 beta-reductase. *J Biol Chem* **259,** 7519-24.

OLSON, E. N. & WILLIAMS, R. S. (2000). Remodeling muscles with calcineurin. *Bioessays* **22,** 510-9.

OLSZANECKA-GLINIANOWICZ, M., ZAHORSKA-MARKIEWICZ, B., JANOWSKA, J. & ZURAKOWSKI, A. (2004). Serum concentrations of nitric oxide, tumor necrosis factor (TNF)-alpha and TNF soluble receptors in women with overweight and obesity. *Metabolism* **53,** 1268-73.

ORDAHL, C. P., BERDOUGO, E., VENTERS, S. J. & DENETCLAW, W. F., JR. (2001). The dermomyotome dorsomedial lip drives growth and morphogenesis of both the primary myotome and dermomyotome epithelium. *Development* **128,** 1731-44.

OSAWA, H., OCHI, M., TABARA, Y., KATO, K., YAMAUCHI, J., TAKATA, Y., NISHIDA, W., ONUMA, H., SHIMIZU, I., FUJII, Y., MIKI, T., OHASHI, J. & MAKINO, H. (2008). Serum resistin is positively correlated with the accumulation of metabolic syndrome factors in type 2 diabetes. *Clin Endocrinol (Oxf)* **69,** 74-80.

OUSOVA, O., GUYONNET-DUPERAT, V., IANNUCCELLI, N., BIDANEL, J. P., MILAN, D., GENET, C., LLAMAS, B., YERLE, M., GELLIN, J., CHARDON, P., EMPTOZ-BONNETON, A., PUGEAT, M., MORMEDE, P. & MOISAN, M. P. (2004). Corticosteroid binding globulin: a new target for cortisol-driven obesity. *Mol Endocrinol* **18,** 1687-96.

OZES, O. N., AKCA, H., MAYO, L. D., GUSTIN, J. A., MAEHAMA, T., DIXON, J. E. & DONNER, D. B. (2001). A phosphatidylinositol 3-kinase/Akt/mTOR pathway mediates and PTEN antagonizes tumor necrosis factor inhibition of insulin signaling through insulin receptor substrate-1. *Proc Natl Acad Sci U S A* **98,** 4640-5.

OZOLS, J. (1995). Lumenal orientation and post-translational modifications of the liver microsomal 11 beta-hydroxysteroid dehydrogenase. *J Biol Chem* **270,** 2305-12.

PALERMO, M., SHACKLETON, C. H., MANTERO, F. & STEWART, P. M. (1996). Urinary free cortisone and the assessment of 11 beta-hydroxysteroid dehydrogenase activity in man. *Clin Endocrinol (Oxf)* **45,** 605-11.

PAN, D. A., LILLIOJA, S., KRIKETOS, A. D., MILNER, M. R., BAUR, L. A., BOGARDUS, C., JENKINS, A. B. & STORLIEN, L. H. (1997). Skeletal muscle triglyceride levels are inversely related to insulin action. *Diabetes* **46,** 983-8.

PARK, E. A., MYNATT, R. L., COOK, G. A. & KASHFI, K. (1995). Insulin regulates enzyme activity, malonyl-CoA sensitivity and mRNA abundance of hepatic carnitine palmitoyltransferase-I. *Biochem J* **310 (Pt 3),** 853-8.

PATZELT, C., LABRECQUE, A. D., DUGUID, J. R., CARROLL, R. J., KEIM, P. S., HEINRIKSON, R. L. & STEINER, D. F. (1978). Detection and kinetic behavior of preproinsulin in pancreatic islets. *Proc Natl Acad Sci U S A* **75,** 1260-4.

PAZ, K., LIU, Y. F., SHORER, H., HEMI, R., LEROITH, D., QUAN, M., KANETY, H., SEGER, R. & ZICK, Y. (1999). Phosphorylation of insulin receptor substrate-1 (IRS-1) by protein kinase B positively regulates IRS-1 function. *J Biol Chem* **274,** 28816-22.

PEAR, W. S., NOLAN, G. P., SCOTT, M. L. & BALTIMORE, D. (1993). Production of

high-titer helper-free retroviruses by transient transfection. *Proc Natl Acad Sci U S A* **90,** 8392-6.

PEARSON, E. R., PRUHOVA, S., TACK, C. J., JOHANSEN, A., CASTLEDEN, H. A., LUMB, P. J., WIERZBICKI, A. S., CLARK, P. M., LEBL, J., PEDERSEN, O., ELLARD, S., HANSEN, T. & HATTERSLEY, A. T. (2005). Molecular genetics and phenotypic characteristics of MODY caused by hepatocyte nuclear factor 4alpha mutations in a large European collection. *Diabetologia* **48,** 878-85.

PERRY, J. R., MCCARTHY, M. I., HATTERSLEY, A. T., ZEGGINI, E., WEEDON, M. N. & FRAYLING, T. M. (2009). Interrogating type 2 diabetes genome-wide association data using a biological pathway-based approach. *Diabetes* **58,** 1463-7.

PETERSON, R. E., WYNGAARDEN, J. B., GUERRA, S. L., BRODIE, B. B. & BUNIM, J. J. (1955). The physiological disposition and metabolic fate of hydrocortisone in man. *J Clin Invest* **34,** 1779-94.

PHIELIX, E. & MENSINK, M. (2008). Type 2 diabetes mellitus and skeletal muscle metabolic function. *Physiol Behav* **94,** 252-8.

PICKERSGILL, L., LITHERLAND, G. J., GREENBERG, A. S., WALKER, M. & YEAMAN, S. J. (2007). Key role for ceramides in mediating insulin resistance in human muscle cells. *J Biol Chem* **282,** 12583-9.

PINKNEY, J. H., STEHOUWER, C. D., COPPACK, S. W. & YUDKIN, J. S. (1997). Endothelial dysfunction: cause of the insulin resistance syndrome. *Diabetes* **46 Suppl 2,** S9-13.

PINNAMANENI, S. K., SOUTHGATE, R. J., FEBBRAIO, M. A. & WATT, M. J. (2006). Stearoyl CoA desaturase 1 is elevated in obesity but protects against fatty acid-induced skeletal muscle insulin resistance in vitro. *Diabetologia* **49,** 3027-37.

POTTER, C. J., PEDRAZA, L. G. & XU, T. (2002). Akt regulates growth by directly phosphorylating Tsc2. *Nat Cell Biol* **4,** 658-65.

POURQUIE, O., FAN, C. M., COLTEY, M., HIRSINGER, E., WATANABE, Y., BREANT, C., FRANCIS-WEST, P., BRICKELL, P., TESSIER-LAVIGNE, M. & LE DOUARIN, N. M. (1996). Lateral and axial signals involved in avian somite patterning: a role for BMP4. *Cell* **84,** 461-71.

POWELL, D. J., HAJDUCH, E., KULAR, G. & HUNDAL, H. S. (2003). Ceramide disables 3-phosphoinositide binding to the pleckstrin homology domain of protein kinase B (PKB)/Akt by a PKCzeta-dependent mechanism. *Mol Cell Biol* **23,** 7794-808.

PRATT, W. B. (1998). The hsp90-based chaperone system: involvement in signal transduction from a variety of hormone and growth factor receptors. *Proc Soc Exp Biol Med* **217,** 420-34.

PRATT, W. B. & TOFT, D. O. (1997). Steroid receptor interactions with heat shock protein and immunophilin chaperones. *Endocr Rev* **18,** 306-60.

PROUD, C. G. & DENTON, R. M. (1997). Molecular mechanisms for the control of translation by insulin. *Biochem J* **328 (Pt 2),** 329-41.

PRUCHNIC, R., KATSIARAS, A., HE, J., KELLEY, D. E., WINTERS, C. & GOODPASTER, B. H. (2004). Exercise training increases intramyocellular lipid and oxidative capacity in older adults. *Am J Physiol Endocrinol Metab* **287,** E857-62.

PUIGSERVER, P., RHEE, J., DONOVAN, J., WALKEY, C. J., YOON, J. C., ORIENTE, F., KITAMURA, Y., ALTOMONTE, J., DONG, H., ACCILI, D. & SPIEGELMAN, B. M. (2003). Insulin-regulated hepatic gluconeogenesis through FOXO1-PGC-1alpha interaction. *Nature* **423,** 550-5.

RAE, P. A., GUTMANN, N. S., TSAO, J. & SCHIMMER, B. P. (1979). Mutations in cyclic AMP-dependent protein kinase and corticotropin (ACTH)-sensitive adenylate cyclase affect adrenal steroidogenesis. *Proc Natl Acad Sci U S A* **76,** 1896-900.

RAJALA, M. W., QI, Y., PATEL, H. R., TAKAHASHI, N., BANERJEE, R., PAJVANI, U. B., SINHA, M. K., GINGERICH, R. L., SCHERER, P. E. & AHIMA, R. S. (2004). Regulation of resistin expression and circulating levels in obesity, diabetes, and fasting. *Diabetes* **53,** 1671-9.

RAMM, G., LARANCE, M., GUILHAUS, M. & JAMES, D. E. (2006). A role for 14-3-3 in insulin-stimulated GLUT4 translocation through its interaction with the RabGAP AS160. *J Biol Chem* **281,** 29174-80.

RASMUSSEN, B. B. & WOLFE, R. R. (1999). Regulation of fatty acid oxidation in skeletal muscle. *Annu Rev Nutr* **19,** 463-84.

REAVEN, G. M. (1988). Banting lecture 1988. Role of insulin resistance in human disease. *Diabetes* **37,** 1595-607.

RELAIX, F., ROCANCOURT, D., MANSOURI, A. & BUCKINGHAM, M. (2005). A Pax3/Pax7-dependent population of skeletal muscle progenitor cells. *Nature* **435,** 948-53.

RICKETTS, M. L., VERHAEG, J. M., BUJALSKA, I., HOWIE, A. J., RAINEY, W. E. & STEWART, P. M. (1998). Immunohistochemical localization of type 1 11beta-hydroxysteroid dehydrogenase in human tissues. *J Clin Endocrinol Metab* **83,** 1325-35.

RIEUSSET, J., BOUZAKRI, K., CHEVILLOTTE, E., RICARD, N., JACQUET, D., BASTARD, J. P., LAVILLE, M. & VIDAL, H. (2004). Suppressor of cytokine signaling 3 expression and insulin resistance in skeletal muscle of obese and type 2 diabetic patients. *Diabetes* **53,** 2232-41.

RINGOLD, G. M., YAMAMOTO, K. R., BISHOP, J. M. & VARMUS, H. E. (1977). Glucocorticoid-stimulated accumulation of mouse mammary tumor virus RNA: increased rate of synthesis of viral RNA. *Proc Natl Acad Sci U S A* **74,** 2879-83.

RIZZA, R. A., MANDARINO, L. J. & GERICH, J. E. (1982). Cortisol-induced insulin resistance in man: impaired suppression of glucose production and stimulation of glucose utilization due to a postreceptor detect of insulin action. *J Clin Endocrinol Metab* **54,** 131-8.

ROBERTSON, R. P., OLSON, L. K. & ZHANG, H. J. (1994). Differentiating glucose toxicity from glucose desensitization: a new message from the insulin gene. *Diabetes* **43,** 1085-9.

ROGATSKY, I., WANG, J. C., DERYNCK, M. K., NONAKA, D. F., KHODABAKHSH, D. B., HAQQ, C. M., DARIMONT, B. D., GARABEDIAN, M. J. & YAMAMOTO, K. R. (2003). Target-specific utilization of transcriptional regulatory surfaces by the glucocorticoid receptor. *Proc Natl Acad Sci U S A* **100,** 13845-50.

ROGOFF, D., RYDER, J. W., BLACK, K., YAN, Z., BURGESS, S. C., MCMILLAN, D. R. & WHITE, P. C. (2007). Abnormalities of glucose homeostasis and the hypothalamic-pituitary-adrenal axis in mice lacking hexose-6-phosphate dehydrogenase. *Endocrinology* **148,** 5072-80.

ROJAS, F. A., HIRATA, A. E. & SAAD, M. J. (2003). Regulation of insulin receptor substrate-2 tyrosine phosphorylation in animal models of insulin resistance. *Endocrine* **21,** 115-22.

RUI, L., YUAN, M., FRANTZ, D., SHOELSON, S. & WHITE, M. F. (2002). SOCS-1 and SOCS-3 block insulin signaling by ubiquitin-mediated degradation of IRS1

and IRS2. *J Biol Chem* **277,** 42394-8.

RUSSELL, D. W. & WILSON, J. D. (1994). Steroid 5 alpha-reductase: two genes/two enzymes. *Annu Rev Biochem* **63,** 25-61.

RUZZIN, J., WAGMAN, A. S. & JENSEN, J. (2005). Glucocorticoid-induced insulin resistance in skeletal muscles: defects in insulin signalling and the effects of a selective glycogen synthase kinase-3 inhibitor. *Diabetologia* **48,** 2119-30.

SAAD, M. J., FOLLI, F., KAHN, J. A. & KAHN, C. R. (1993). Modulation of insulin receptor, insulin receptor substrate-1, and phosphatidylinositol 3-kinase in liver and muscle of dexamethasone-treated rats. *J Clin Invest* **92,** 2065-72.

SAHA, A. K., KUROWSKI, T. G., COLCA, J. R. & RUDERMAN, N. B. (1994). Lipid abnormalities in tissues of the KKAy mouse: effects of pioglitazone on malonyl-CoA and diacylglycerol. *Am J Physiol* **267,** E95-101.

SAKODA, H., OGIHARA, T., ANAI, M., FUNAKI, M., INUKAI, K., KATAGIRI, H., FUKUSHIMA, Y., ONISHI, Y., ONO, H., FUJISHIRO, M., KIKUCHI, M., OKA, Y. & ASANO, T. (2000). Dexamethasone-induced insulin resistance in 3T3-L1 adipocytes is due to inhibition of glucose transport rather than insulin signal transduction. *Diabetes* **49,** 1700-8.

SALEHZADEH, F., AL-KHALILI, L., KULKARNI, S. S., WANG, M., LONNQVIST, F. & KROOK, A. (2009). Glucocorticoid-mediated effects on metabolism are reversed by targeting 11 beta hydroxysteroid dehydrogenase type 1 in human skeletal muscle. *Diabetes Metab Res Rev* **25,** 250-8.

SAMRA, J. S., CLARK, M. L., HUMPHREYS, S. M., MACDONALD, I. A., BANNISTER, P. A. & FRAYN, K. N. (1998). Effects of physiological hypercortisolemia on the regulation of lipolysis in subcutaneous adipose tissue. *J Clin Endocrinol Metab* **83,** 626-31.

SANDRI, M., SANDRI, C., GILBERT, A., SKURK, C., CALABRIA, E., PICARD, A., WALSH, K., SCHIAFFINO, S., LECKER, S. H. & GOLDBERG, A. L. (2004). Foxo transcription factors induce the atrophy-related ubiquitin ligase atrogin-1 and cause skeletal muscle atrophy. *Cell* **117,** 399-412.

SANGER, F. (1959). Chemistry of insulin; determination of the structure of insulin opens the way to greater understanding of life processes. *Science* **129,** 1340-4.

SANO, H., KANE, S., SANO, E., MIINEA, C. P., ASARA, J. M., LANE, W. S., GARNER, C. W. & LIENHARD, G. E. (2003). Insulin-stimulated phosphorylation of a Rab GTPase-activating protein regulates GLUT4 translocation. *J Biol Chem* **278,** 14599-602.

SARBASSOV, D. D., GUERTIN, D. A., ALI, S. M. & SABATINI, D. M. (2005). Phosphorylation and regulation of Akt/PKB by the rictor-mTOR complex. *Science* **307,** 1098-101.

SATOH, H., NGUYEN, M. T., MILES, P. D., IMAMURA, T., USUI, I. & OLEFSKY, J. M. (2004). Adenovirus-mediated chronic "hyper-resistinemia" leads to in vivo insulin resistance in normal rats. *J Clin Invest* **114,** 224-31.

SAVAGE, D. B., SEWTER, C. P., KLENK, E. S., SEGAL, D. G., VIDAL-PUIG, A., CONSIDINE, R. V. & O'RAHILLY, S. (2001). Resistin / Fizz3 expression in relation to obesity and peroxisome proliferator-activated receptor-gamma action in humans. *Diabetes* **50,** 2199-202.

SCHAAF, M. J. & CIDLOWSKI, J. A. (2002). Molecular mechanisms of glucocorticoid action and resistance. *J Steroid Biochem Mol Biol* **83,** 37-48.

SCHACKE, H., DOCKE, W. D. & ASADULLAH, K. (2002). Mechanisms involved in the

side effects of glucocorticoids. *Pharmacol Ther* **96,** 23-43.

SCOW, R. O., BLANCHETTE-MACKIE, E. J. & SMITH, L. C. (1976). Role of capillary endothelium in the clearance of chylomicrons. A model for lipid transport from blood by lateral diffusion in cell membranes. *Circ Res* **39,** 149-62.

SELTZER, W. K., ANGELINI, C., DHARIWAL, G., RINGEL, S. P. & MCCABE, E. R. (1989). Muscle glycerol kinase in Duchenne dystrophy and glycerol kinase deficiency. *Muscle Nerve* **12,** 307-13.

SENFT, G., SCHULTZ, G., MUNSKE, K. & HOFFMANN, M. (1968). Effects of glucocorticoids and insulin on 3',5'-AMP phosphodiesterase activity in adrenalectomized rats. *Diabetologia* **4,** 330-5.

SEOW, K. M., JUAN, C. C., HSU, Y. P., HWANG, J. L., HUANG, L. W. & HO, L. T. (2007). Amelioration of insulin resistance in women with PCOS via reduced insulin receptor substrate-1 Ser312 phosphorylation following laparoscopic ovarian electrocautery. *Hum Reprod* **22,** 1003-10.

SEWARD, D. J., HANEY, J. C., RUDNICKI, M. A. & SWOAP, S. J. (2001). bHLH transcription factor MyoD affects myosin heavy chain expression pattern in a muscle-specific fashion. *Am J Physiol Cell Physiol* **280,** C408-13.

SHACKLETON, C. H. (1993). Mass spectrometry in the diagnosis of steroid-related disorders and in hypertension research. *J Steroid Biochem Mol Biol* **45,** 127-40.

SHAMS, M., KILBY, M. D., SOMERSET, D. A., HOWIE, A. J., GUPTA, A., WOOD, P. J., AFNAN, M. & STEWART, P. M. (1998). 11Beta-hydroxysteroid dehydrogenase type 2 in human pregnancy and reduced expression in intrauterine growth restriction. *Hum Reprod* **13,** 799-804.

SIMPSON, E. R. & WATERMAN, M. R. (1988). Regulation of the synthesis of steroidogenic enzymes in adrenal cortical cells by ACTH. *Annu Rev Physiol* **50,** 427-40.

SIPILA, S. & POUTAMO, J. (2003). Muscle performance, sex hormones and training in peri-menopausal and post-menopausal women. *Scand J Med Sci Sports* **13,** 19-25.

SLAVIN, B. G., ONG, J. M. & KERN, P. A. (1994). Hormonal regulation of hormone-sensitive lipase activity and mRNA levels in isolated rat adipocytes. *J Lipid Res* **35,** 1535-41.

SMITH, S., WITKOWSKI, A. & JOSHI, A. K. (2003). Structural and functional organization of the animal fatty acid synthase. *Prog Lipid Res* **42,** 289-317.

SPRANGER, J., KROKE, A., MOHLIG, M., HOFFMANN, K., BERGMANN, M. M., RISTOW, M., BOEING, H. & PFEIFFER, A. F. (2003). Inflammatory cytokines and the risk to develop type 2 diabetes: results of the prospective population-based European Prospective Investigation into Cancer and Nutrition (EPIC)-Potsdam Study. *Diabetes* **52,** 812-7.

STANCATO, L. F., SILVERSTEIN, A. M., GITLER, C., GRONER, B. & PRATT, W. B. (1996). Use of the thiol-specific derivatizing agent N-iodoacetyl-3-[125I]iodotyrosine to demonstrate conformational differences between the unbound and hsp90-bound glucocorticoid receptor hormone binding domain. *J Biol Chem* **271,** 8831-6.

STANDAERT, M. L., BANDYOPADHYAY, G., KANOH, Y., SAJAN, M. P. & FARESE, R. V. (2001). Insulin and PIP3 activate PKC-zeta by mechanisms that are both dependent and independent of phosphorylation of activation loop (T410) and autophosphorylation (T560) sites. *Biochemistry* **40,** 249-55.

STEINER, D., RAUDA, V. & WILLIAMS, H. (1961). Effects of Insulin, Glucagon, and

Glucocorticoids upon Hepatic Glycogen Synthesis from Uridine Diphosphate Glucose. *J Biol Chem* **236**

STEPHENS, L., ANDERSON, K., STOKOE, D., ERDJUMENT-BROMAGE, H., PAINTER, G. F., HOLMES, A. B., GAFFNEY, P. R., REESE, C. B., MCCORMICK, F., TEMPST, P., COADWELL, J. & HAWKINS, P. T. (1998). Protein kinase B kinases that mediate phosphatidylinositol 3,4,5-trisphosphate-dependent activation of protein kinase B. *Science* **279,** 710-4.

STEPPAN, C. M., WANG, J., WHITEMAN, E. L., BIRNBAUM, M. J. & LAZAR, M. A. (2005). Activation of SOCS-3 by resistin. *Mol Cell Biol* **25,** 1569-75.

STEWART, P. M., KROZOWSKI, Z. S., GUPTA, A., MILFORD, D. V., HOWIE, A. J., SHEPPARD, M. C. & WHORWOOD, C. B. (1996). Hypertension in the syndrome of apparent mineralocorticoid excess due to mutation of the 11 beta-hydroxysteroid dehydrogenase type 2 gene. *Lancet* **347,** 88-91.

STEWART, P. M., MURRY, B. A. & MASON, J. I. (1994). Human kidney 11 beta-hydroxysteroid dehydrogenase is a high affinity nicotinamide adenine dinucleotide-dependent enzyme and differs from the cloned type I isoform. *J Clin Endocrinol Metab* **79,** 480-4.

STRACZKOWSKI, M., KOWALSKA, I., NIKOLAJUK, A., DZIENIS-STRACZKOWSKA, S., KINALSKA, I., BARANOWSKI, M., ZENDZIAN-PIOTROWSKA, M., BRZEZINSKA, Z. & GORSKI, J. (2004). Relationship between insulin sensitivity and sphingomyelin signaling pathway in human skeletal muscle. *Diabetes* **53,** 1215-21.

STRATFORD, S., HOEHN, K. L., LIU, F. & SUMMERS, S. A. (2004). Regulation of insulin action by ceramide: dual mechanisms linking ceramide accumulation to the inhibition of Akt/protein kinase B. *J Biol Chem* **279,** 36608-15.

SUN, X. J., ROTHENBERG, P., KAHN, C. R., BACKER, J. M., ARAKI, E., WILDEN, P. A., CAHILL, D. A., GOLDSTEIN, B. J. & WHITE, M. F. (1991). Structure of the insulin receptor substrate IRS-1 defines a unique signal transduction protein. *Nature* **352,** 73-7.

SUNDBOM, M., KAISER, C., BJORKSTRAND, E., CASTRO, V. M., LARSSON, C., SELEN, G., NYHEM, C. S. & JAMES, S. R. (2008). Inhibition of 11betaHSD1 with the S-phenylethylaminothiazolone BVT116429 increases adiponectin concentrations and improves glucose homeostasis in diabetic KKAy mice. *BMC Pharmacol* **8,** 3.

SUTHERLAND, C., LEIGHTON, I. A. & COHEN, P. (1993). Inactivation of glycogen synthase kinase-3 beta by phosphorylation: new kinase connections in insulin and growth-factor signalling. *Biochem J* **296 (Pt 1),** 15-9.

SWISLOCKI, A. L., CHEN, Y. D., GOLAY, A., CHANG, M. O. & REAVEN, G. M. (1987). Insulin suppression of plasma-free fatty acid concentration in normal individuals and patients with type 2 (non-insulin-dependent) diabetes. *Diabetologia* **30,** 622-6.

SZALAY, K., RAZGA, Z. & DUDA, E. (1997). TNF inhibits myogenesis and downregulates the expression of myogenic regulatory factors myoD and myogenin. *Eur J Cell Biol* **74,** 391-8.

TAJBAKHSH, S., ROCANCOURT, D., COSSU, G. & BUCKINGHAM, M. (1997). Redefining the genetic hierarchies controlling skeletal myogenesis: Pax-3 and Myf-5 act upstream of MyoD. *Cell* **89,** 127-38.

TARNOPOLSKY, M. A., RENNIE, C. D., ROBERTSHAW, H. A., FEDAK-TARNOPOLSKY, S. N., DEVRIES, M. C. & HAMADEH, M. J. (2007). Influence of endurance

exercise training and sex on intramyocellular lipid and mitochondrial ultrastructure, substrate use, and mitochondrial enzyme activity. *Am J Physiol Regul Integr Comp Physiol* **292,** R1271-8.

TASKINEN, M. R., NIKKILA, E. A., PELKONEN, R. & SANE, T. (1983). Plasma lipoproteins, lipolytic enzymes, and very low density lipoprotein triglyceride turnover in Cushing's syndrome. *J Clin Endocrinol Metab* **57,** 619-26.

TATSUMI, R. & ALLEN, R. E. (2004). Active hepatocyte growth factor is present in skeletal muscle extracellular matrix. *Muscle Nerve* **30,** 654-8.

TATSUMI, R., ANDERSON, J. E., NEVORET, C. J., HALEVY, O. & ALLEN, R. E. (1998). HGF/SF is present in normal adult skeletal muscle and is capable of activating satellite cells. *Dev Biol* **194,** 114-28.

THAMER, C., MACHANN, J., TSCHRITTER, O., HAAP, M., WIETEK, B., DAHL, D., BACHMANN, O., FRITSCHE, A., JACOB, S., STUMVOLL, M., SCHICK, F. & HARING, H. U. (2002). Relationship between serum adiponectin concentration and intramyocellular lipid stores in humans. *Horm Metab Res* **34,** 646-9.

THELER, J. M., MOLLARD, P., GUERINEAU, N., VACHER, P., PRALONG, W. F., SCHLEGEL, W. & WOLLHEIM, C. B. (1992). Video imaging of cytosolic Ca2+ in pancreatic beta-cells stimulated by glucose, carbachol, and ATP. *J Biol Chem* **267,** 18110-7.

THOMPSON, A. L., LIM-FRASER, M. Y., KRAEGEN, E. W. & COONEY, G. J. (2000). Effects of individual fatty acids on glucose uptake and glycogen synthesis in soleus muscle in vitro. *Am J Physiol Endocrinol Metab* **279,** E577-84.

THORENS, B., SARKAR, H. K., KABACK, H. R. & LODISH, H. F. (1988). Cloning and functional expression in bacteria of a novel glucose transporter present in liver, intestine, kidney, and beta-pancreatic islet cells. *Cell* **55,** 281-90.

TIPPETT, P. S. & NEET, K. E. (1982). Specific inhibition of glucokinase by long chain acyl coenzymes A below the critical micelle concentration. *J Biol Chem* **257,** 12839-45.

TISCHLER, M. E., SATARUG, S., AANNESTAD, A., MUNOZ, K. A. & HENRIKSEN, E. J. (1997). Insulin attenuates atrophy of unweighted soleus muscle by amplified inhibition of protein degradation. *Metabolism* **46,** 673-9.

TOMLINSON, J. W., SHERLOCK, M., HUGHES, B., HUGHES, S. V., KILVINGTON, F., BARTLETT, W., COURTNEY, R., REJTO, P., CARLEY, W. & STEWART, P. M. (2007). Inhibition of 11beta-hydroxysteroid dehydrogenase type 1 activity in vivo limits glucocorticoid exposure to human adipose tissue and decreases lipolysis. *J Clin Endocrinol Metab* **92,** 857-64.

TOMLINSON, J. W., WALKER, E. A., BUJALSKA, I. J., DRAPER, N., LAVERY, G. G., COOPER, M. S., HEWISON, M. & STEWART, P. M. (2004). 11beta-hydroxysteroid dehydrogenase type 1: a tissue-specific regulator of glucocorticoid response. *Endocr Rev* **25,** 831-66.

TOWBIN, H., STAEHELIN, T. & GORDON, J. (1979). Electrophoretic transfer of proteins from polyacrylamide gels to nitrocellulose sheets: procedure and some applications. *Proc Natl Acad Sci U S A* **76,** 4350-4.

TRAN, H., BRUNET, A., GRIFFITH, E. C. & GREENBERG, M. E. (2003). The many forks in FOXO's road. *Sci STKE* **2003,** RE5.

TREMBLAY, P., DIETRICH, S., MERICSKAY, M., SCHUBERT, F. R., LI, Z. & PAULIN, D. (1998). A crucial role for Pax3 in the development of the hypaxial musculature and the long-range migration of muscle precursors. *Dev Biol* **203,** 49-61.

TURINSKY, J., O'SULLIVAN, D. M. & BAYLY, B. P. (1990). 1,2-Diacylglycerol and ceramide levels in insulin-resistant tissues of the rat in vivo. *J Biol Chem* **265,** 16880-5.

VAN LOON, L. J., KOOPMAN, R., MANDERS, R., VAN DER WEEGEN, W., VAN KRANENBURG, G. P. & KEIZER, H. A. (2004). Intramyocellular lipid content in type 2 diabetes patients compared with overweight sedentary men and highly trained endurance athletes. *Am J Physiol Endocrinol Metab* **287,** E558-65.

VAN STAA, T. P., LEUFKENS, H. G., ABENHAIM, L., BEGAUD, B., ZHANG, B. & COOPER, C. (2000). Use of oral corticosteroids in the United Kingdom. *Qjm* **93,** 105-11.

VELHO, G., VAXILLAIRE, M., BOCCIO, V., CHARPENTIER, G. & FROGUEL, P. (1996). Diabetes complications in NIDDM kindreds linked to the MODY3 locus on chromosome 12q. *Diabetes Care* **19,** 915-9.

VENKATESAN, N., LIM, J., BOUCH, C., MARCIANO, D. & DAVIDSON, M. B. (1996). Dexamethasone-induced impairment in skeletal muscle glucose transport is not reversed by inhibition of free fatty acid oxidation. *Metabolism* **45,** 92-100.

VILLENA, J. A., ROY, S., SARKADI-NAGY, E., KIM, K. H. & SUL, H. S. (2004). Desnutrin, an adipocyte gene encoding a novel patatin domain-containing protein, is induced by fasting and glucocorticoids: ectopic expression of desnutrin increases triglyceride hydrolysis. *J Biol Chem* **279,** 47066-75.

WADDELL, D. S., BAEHR, L. M., VAN DEN BRANDT, J., JOHNSEN, S. A., REICHARDT, H. M., FURLOW, J. D. & BODINE, S. C. (2008). The glucocorticoid receptor and FOXO1 synergistically activate the skeletal muscle atrophy-associated MuRF1 gene. *Am J Physiol Endocrinol Metab* **295,** E785-97.

WAJCHENBERG, B. L., LEME, C. E., LERARIO, A. C., TOLEDO E SOUZA, I. T., RODBARD, H. W. & RODBARD, D. (1984). Insulin resistance in Cushing's disease. Evaluation by studies of insulin binding to erythrocytes. *Diabetes* **33,** 455-9.

WALKER, B. R., CONNACHER, A. A., LINDSAY, R. M., WEBB, D. J. & EDWARDS, C. R. (1995). Carbenoxolone increases hepatic insulin sensitivity in man: a novel role for 11-oxosteroid reductase in enhancing glucocorticoid receptor activation. *J Clin Endocrinol Metab* **80,** 3155-9.

WALTER, P. & JOHNSON, A. E. (1994). Signal sequence recognition and protein targeting to the endoplasmic reticulum membrane. *Annu Rev Cell Biol* **10,** 87-119.

WANG, C., LIU, M., RIOJAS, R. A., XIN, X., GAO, Z., ZENG, R., WU, J., DONG, L. Q. & LIU, F. (2009). Protein kinase C theta (PKCtheta)-dependent phosphorylation of PDK1 at Ser504 and Ser532 contributes to palmitate-induced insulin resistance. *J Biol Chem* **284,** 2038-44.

WANG, Y., JONES VOY, B., URS, S., KIM, S., SOLTANI-BEJNOOD, M., QUIGLEY, N., HEO, Y. R., STANDRIDGE, M., ANDERSEN, B., DHAR, M., JOSHI, R., WORTMAN, P., TAYLOR, J. W., CHUN, J., LEUZE, M., CLAYCOMBE, K., SAXTON, A. M. & MOUSTAID-MOUSSA, N. (2004). The human fatty acid synthase gene and de novo lipogenesis are coordinately regulated in human adipose tissue. *J Nutr* **134,** 1032-8.

WARAICH, R. S., WEIGERT, C., KALBACHER, H., HENNIGE, A. M., LUTZ, S. Z., HARING, H. U., SCHLEICHER, E. D., VOELTER, W. & LEHMANN, R. (2008). Phosphorylation of Ser357 of rat insulin receptor substrate-1 mediates

adverse effects of protein kinase C-delta on insulin action in skeletal muscle cells. *J Biol Chem* **283,** 11226-33.

WATERMAN, M. R. & BISCHOF, L. J. (1997). Cytochromes P450 12: diversity of ACTH (cAMP)-dependent transcription of bovine steroid hydroxylase genes. *Faseb J* **11,** 419-27.

WATT, M. J., HEIGENHAUSER, G. J. & SPRIET, L. L. (2003). Effects of dynamic exercise intensity on the activation of hormone-sensitive lipase in human skeletal muscle. *J Physiol* **547,** 301-8.

WATT, M. J., HOLMES, A. G., PINNAMANENI, S. K., GARNHAM, A. P., STEINBERG, G. R., KEMP, B. E. & FEBBRAIO, M. A. (2006). Regulation of HSL serine phosphorylation in skeletal muscle and adipose tissue. *Am J Physiol Endocrinol Metab* **290,** E500-8.

WATT, M. J., STEINBERG, G. R., CHAN, S., GARNHAM, A., KEMP, B. E. & FEBBRAIO, M. A. (2004). Beta-adrenergic stimulation of skeletal muscle HSL can be overridden by AMPK signaling. *Faseb J* **18,** 1445-6.

WELSH, G. I. & PROUD, C. G. (1993). Glycogen synthase kinase-3 is rapidly inactivated in response to insulin and phosphorylates eukaryotic initiation factor eIF-2B. *Biochem J* **294 (Pt 3),** 625-9.

WERNER, E. D., LEE, J., HANSEN, L., YUAN, M. & SHOELSON, S. E. (2004). Insulin resistance due to phosphorylation of insulin receptor substrate-1 at serine 302. *J Biol Chem* **279,** 35298-305.

WHITE, M. F., MARON, R. & KAHN, C. R. (1985). Insulin rapidly stimulates tyrosine phosphorylation of a Mr-185,000 protein in intact cells. *Nature* **318,** 183-6.

WHITEHEAD, J. P., RICHARDS, A. A., HICKMAN, I. J., MACDONALD, G. A. & PRINS, J. B. (2006). Adiponectin--a key adipokine in the metabolic syndrome. *Diabetes Obes Metab* **8,** 264-80.

WHORWOOD, C. B., DONOVAN, S. J., FLANAGAN, D., PHILLIPS, D. I. & BYRNE, C. D. (2002). Increased glucocorticoid receptor expression in human skeletal muscle cells may contribute to the pathogenesis of the metabolic syndrome. *Diabetes* **51,** 1066-75.

WHORWOOD, C. B., DONOVAN, S. J., WOOD, P. J. & PHILLIPS, D. I. (2001). Regulation of glucocorticoid receptor alpha and beta isoforms and type I 11beta-hydroxysteroid dehydrogenase expression in human skeletal muscle cells: a key role in the pathogenesis of insulin resistance? *J Clin Endocrinol Metab* **86,** 2296-308.

WHORWOOD, C. B., MASON, J. I., RICKETTS, M. L., HOWIE, A. J. & STEWART, P. M. (1995). Detection of human 11 beta-hydroxysteroid dehydrogenase isoforms using reverse-transcriptase-polymerase chain reaction and localization of the type 2 isoform to renal collecting ducts. *Mol Cell Endocrinol* **110,** R7-12.

WHORWOOD, C. B., RICKETTS, M. L. & STEWART, P. M. (1994). Epithelial cell localization of type 2 11 beta-hydroxysteroid dehydrogenase in rat and human colon. *Endocrinology* **135,** 2533-41.

WILD, S., ROGLIC, G., GREEN, A., SICREE, R. & KING, H. (2004). Global prevalence of diabetes: estimates for the year 2000 and projections for 2030. *Diabetes Care* **27,** 1047-53.

WILLIAMS, B. H. & BERDANIER, C. D. (1982). Effects of diet composition and adrenalectomy on the lipogenic responses of rats to starvation-refeeding. *J Nutr* **112,** 534-41.

WING, S. S. & GOLDBERG, A. L. (1993). Glucocorticoids activate the ATP-ubiquitin-

dependent proteolytic system in skeletal muscle during fasting. *Am J Physiol* **264,** E668-76.

WITHERS, D. J., GUTIERREZ, J. S., TOWERY, H., BURKS, D. J., REN, J. M., PREVIS, S., ZHANG, Y., BERNAL, D., PONS, S., SHULMAN, G. I., BONNER-WEIR, S. & WHITE, M. F. (1998). Disruption of IRS-2 causes type 2 diabetes in mice. *Nature* **391,** 900-4.

WOLFRUM, C., ASILMAZ, E., LUCA, E., FRIEDMAN, J. M. & STOFFEL, M. (2004). Foxa2 regulates lipid metabolism and ketogenesis in the liver during fasting and in diabetes. *Nature* **432,** 1027-32.

WU, A., CHEN, J. & BASERGA, R. (2008). Nuclear insulin receptor substrate-1 activates promoters of cell cycle progression genes. *Oncogene* **27,** 397-403.

XU, C., HE, J., JIANG, H., ZU, L., ZHAI, W., PU, S. & XU, G. (2009). Direct effect of glucocorticoids on lipolysis in adipocytes. *Mol Endocrinol* **23,** 1161-70.

YAFFE, D. & SAXEL, O. (1977). Serial passaging and differentiation of myogenic cells isolated from dystrophic mouse muscle. *Nature* **270,** 725-7.

YALOW, R. S. & BERSON, S. A. (1960). Immunoassay of endogenous plasma insulin in man. *J Clin Invest* **39,** 1157-75.

YAMAZAKI, S., KATADA, T. & UI, M. (1982). Alpha 2-adrenergic inhibition of insulin secretion via interference with cyclic AMP generation in rat pancreatic islets. *Mol Pharmacol* **21,** 648-53.

YEH, L. A., LEE, K. H. & KIM, K. H. (1980). Regulation of rat liver acetyl-CoA carboxylase. Regulation of phosphorylation and inactivation of acetyl-CoA carboxylase by the adenylate energy charge. *J Biol Chem* **255,** 2308-14.

YOON, M. J., LEE, G. Y., CHUNG, J. J., AHN, Y. H., HONG, S. H. & KIM, J. B. (2006). Adiponectin increases fatty acid oxidation in skeletal muscle cells by sequential activation of AMP-activated protein kinase, p38 mitogen-activated protein kinase, and peroxisome proliferator-activated receptor alpha. *Diabetes* **55,** 2562-70.

YOUN, B. S., KLOTING, N., KRATZSCH, J., LEE, N., PARK, J. W., SONG, E. S., RUSCHKE, K., OBERBACH, A., FASSHAUER, M., STUMVOLL, M. & BLUHER, M. (2008). Serum vaspin concentrations in human obesity and type 2 diabetes. *Diabetes* **57,** 372-7.

YU, C., CHEN, Y., CLINE, G. W., ZHANG, D., ZONG, H., WANG, Y., BERGERON, R., KIM, J. K., CUSHMAN, S. W., COONEY, G. J., ATCHESON, B., WHITE, M. F., KRAEGEN, E. W. & SHULMAN, G. I. (2002). Mechanism by which fatty acids inhibit insulin activation of insulin receptor substrate-1 (IRS-1)-associated phosphatidylinositol 3-kinase activity in muscle. *J Biol Chem* **277,** 50230-6.

YU, J., ZHANG, Y., MCILROY, J., RORDORF-NIKOLIC, T., ORR, G. A. & BACKER, J. M. (1998). Regulation of the p85/p110 phosphatidylinositol 3'-kinase: stabilization and inhibition of the p110alpha catalytic subunit by the p85 regulatory subunit. *Mol Cell Biol* **18,** 1379-87.

YUDKIN, J. S., STEHOUWER, C. D., EMEIS, J. J. & COPPACK, S. W. (1999). C-reactive protein in healthy subjects: associations with obesity, insulin resistance, and endothelial dysfunction: a potential role for cytokines originating from adipose tissue? *Arterioscler Thromb Vasc Biol* **19,** 972-8.

ZHANG, M., LV, X. Y., LI, J., XU, Z. G. & CHEN, L. (2009). Alteration of 11beta-hydroxysteroid dehydrogenase type 1 in skeletal muscle in a rat model of type 2 diabetes. *Mol Cell Biochem* **324,** 147-55.

ZHANG, Y., YIN, L. & HILLGARTNER, F. B. (2003). SREBP-1 integrates the actions of

thyroid hormone, insulin, cAMP, and medium-chain fatty acids on ACCalpha transcription in hepatocytes. *J Lipid Res* **44,** 356-68.

ZHAO, J., BRAULT, J. J., SCHILD, A. & GOLDBERG, A. L. (2008). Coordinate activation of autophagy and the proteasome pathway by FoxO transcription factor. *Autophagy* **4,** 378-80.

ZICK, Y. (2005). Ser/Thr phosphorylation of IRS proteins: a molecular basis for insulin resistance. *Sci STKE* **2005,** pe4.

ZINMAN, B., HANLEY, A. J., HARRIS, S. B., KWAN, J. & FANTUS, I. G. (1999). Circulating tumor necrosis factor-alpha concentrations in a native Canadian population with high rates of type 2 diabetes mellitus. *J Clin Endocrinol Metab* **84,** 272-8.

Publications

Conference Proceedings

Morgan SA, Gathercole LL, Bujalska IJ, Stewart PM, Smith DM, Tomlinson JW. Regulation of insulin signalling across differentiation and following glucocorticoid treatment in human skeletal myocytes. British Endocrine Society's Annual Scientific Meeting 2007. Poster Presentation

Morgan SA, Gathercole LL, Bujalska IJ, Lenaghan C, sherlock M, Lavery GG, Hegyi K, Sethi JK, Stewart PM, Smith DM, Tomlinson JW. Selective inhibition of 11β-hydroxysteroid dehydrogenase type 1 improves insulin sensitivity in skeletal muscle through modulation of IRS1 serine phosphorylation. British Endocrine Society's Annual Scientific Meeting 2009. Oral Communication

Morgan SA, Gathercole LL, Bujalska IJ, Stewart PM, Smith DM, Tomlinson JW. Serine phosphorylation of IRS-1 by conventional PKC as a mechanism of glucocorticoid induced insulin resistance in skeletal muscle. Endocrine Society's 90th Annual Meeting 2008. Poster Presentation

Morgan SA, Gathercole LL, Bujalska IJ, Stewart PM, Smith DM, Tomlinson JW. Serine phosphorylation of IRS-1 as a mechanism of glucocorticoid induced insulin resistance in mouse C2C12 myotubes. British Endocrine Society's Annual Scientific Meeting 2008. Poster Presentation

Morgan SA, Gathercole LL, Bujalska IJ, Lenaghan C, sherlock M, Lavery GG, Hegyi K, Sethi JK, Stewart PM, Smith DM, Tomlinson JW. Selective inhibition of 11β-hydroxysteroid dehydrogenase type 1 improves insulin sensitivity in skeletal muscle. Endocrine Society's 91st Annual Meeting 2009. Poster Presentation